METHODS IN MOLECULAR BIOLOGY™

Series Editor
John M. Walker
School of Life Sciences
University of Hertfordshire
Hatfield, Hertfordshire, AL10 9AB, UK

For other titles published in this series, go to
www.springer.com/series/7651

The Plant Cell Wall

Methods and Protocols

Edited by

Zoë A. Popper

Botany and Plant Science, School of Natural Sciences,
National University of Ireland, Galway,
Galway, Ireland

Humana Press

Editor
Zoë A. Popper, Ph.D.
Botany and Plant Science
School of Natural Sciences
National University of Ireland, Galway
Galway,
Ireland
zoe.popper@nuigalway.ie

ISSN 1064-3745 e-ISSN 1940-6029
ISBN 978-1-61779-007-2 e-ISBN 978-1-61779-008-9
DOI 10.1007/978-1-61779-008-9
Springer New York Dordrecht Heidelberg London

Humana Press is part of Springer Science+Business Media (www.springer.com)

Preface

When they got home to dinner they met the Hemulen on the steps. He was beaming with happiness. "Well?" said Moomintroll. "What is it?" "Nature study!" shouted the Hemulen. "I shall botanize …"

Tove Jansson

Plants are essential to life on earth, and, while some readers of this book may not be entirely familiar with the cell wall *per se*, they will have come across it in many forms. Cellulose, a major plant cell wall polysaccharide, is also the most abundantly occurring natural biopolymer, with many other plant cell wall components being among the next most abundant. Some ways in which people may be familiar with the cell wall and/or cell wall components are as; textiles (many, such as cotton, are cellulose); paper; timber; pectin, which is the gelling agent used in jams and other foods; dietary fiber; and cell wall characteristics and metabolism control, for example, fruit ripening and texture. We are therefore dependent on plant cell walls for health, food, and clothing, and a major current area of research is their use as biofuels.

Plant cells are surrounded by a cell wall which is fundamental to their function and survival. The cell wall and its constituent polysaccharides and proteins control nearly all plant-based biological and biophysical processes including expansive plant cell growth, plant development, cell shape and size, cell–cell communication, and interactions with, and defence against pathogens. Understanding the cell wall is therefore not only fundamental to the plant sciences but it is also pertinent to aspects of human and animal nutrition and health as well as plant–microbe and plant–animal interactions. Furthermore, advanced cell wall analysis is the key to developing novel or improving current uses of the wall and plants.

Comprehensive analysis of the plant cell wall demands a multidisciplinary approach and employs a multitude of tools and techniques. This volume describes some of the methods which are currently applied to investigate the many aspects of the plant cell wall including its structure, biochemical composition, and metabolism, to name but a few. Each chapter is written by leading experts in cell wall research and is written with the aim that the protocol(s) can be carried out by someone without previous experience in that particular method or specifically in cell wall research. The techniques included in this volume range from plant tissue culture techniques, which can be applied to investigating cell wall structure and metabolism, to methods directed towards structural analysis and occurrence of carbohydrates, to the development and use of microscopy-based tools and techniques, to those which measure the physical properties of the wall, to methods based on the application of molecular genetic approaches. Many of the methods have been recently developed or are becoming more widely used with the development of advanced instrumentation and technology, and several are high throughput and/or *in situ* techniques which facilitate powerful new insights into cell wall biochemistry and metabolism.

While this volume aims to describe a wide-range of cell wall-directed protocols that can be used to investigate the cell wall, there are other resources which the reader is also likely to find extremely useful. *The Growing Plant Cell Wall: Chemical and Metabolic*

Analysis [1] provides detailed and user-friendly descriptions of cell wall-directed methods, the majority of which are not contained in this volume, and which are widely used and fundamental to research in the field. Furthermore, it also provides a comprehensive and accessible introduction to the cell wall. The reader may also find helpful the video-based explanations of protocols which are available from companies such as Megazyme in addition to recent JoVE publications [2–4].

I would like to wish the reader every success with their plant-based conjectures, hypotheses, and experiments (Fig. 1). Finally, I would like to thank all members of the cell wall community and colleagues at NUI Galway who have supported and enabled this project.

Zoë A. Popper

Fig. 1. Simon Popper. Copyright: The artist (Courtesy: Rachmaninoff's, London and the artist).

References

1. Fry SC (2000) The growing plant cell wall: chemical and metabolic analysis. Reprint Edition, Blackburn, Caldwell, NJ. [ISBN 1-930665-08-3]
2. Foster CE, Martin TM, Pauly M (2010) Comprehensive analysis of plant cell walls (lignocellulosic biomass). Part I: lignin. JoVE. 37. http://www.jove.com/index/details.stp?id=1745, doi: 10.3791/1745
3. Foster CE, Martin TM, Pauly M (2010) Comprehensive compositional analysis of plant cell walls (lignocellulosic biomass). Part II: carbohydrates. JoVE. 37. http://www.jove.com/index/details.stp?id=1837, doi: 10.3791/1837
4. Durachko DM, Cosgrove DJ (2009) Measuring plant cell wall extension (creep) induced by acidic pH and alpha-expansin. JoVE 25. http://www.jove.com/index/details.stp?id=1263, doi: 10.3791/1263

Acknowledgment

This publication was grant-aided by the Publications Fund of National University of Ireland, Galway.

Contents

Contributors

Clauda Blaukopf • *Department of Applied Genetics and Cell Biology, University of Natural Resources and Applied Life Sciences, Vienna, Austria*

Tracey J. Bootten • *School of Biological Sciences, The University of Auckland, Auckland, New Zealand; Industrial Research Limited, Lower Hutt, New Zealand*

Michael J. Budziszek, Jr. • *Department of Biological Sciences, Center for Biotechnology and Life Sciences, University of Rhode Island, Kingston, RI, USA*

Daniel J. Cosgrove • *Department of Biology, Penn State University, University Park, PA, USA*

Seth DeBolt • *Department of Horticulture, University of Kentucky, Lexington, KY, USA*

Christos S. Dimos • *Department of Biological Sciences, Center for Biotechnology and Life Sciences, University of Rhode Island, Kingston, RI, USA*

Paul Dupree • *Department of Biochemistry, University of Cambridge, Cambridge, UK*

Alfred D. French • *Southern Regional Research Center, U. S. Department of Agriculture, New Orleans, LA, USA*

Stephen C. Fry • *The Edinburgh Cell Wall Group, Institute of Molecular Plant Sciences, School of Biological Sciences, University of Edinburgh, Edinburgh, UK*

Hiroo Fukuda • *Department of Biological Sciences, Graduate School of Science, University of Tokyo, Tokyo, Japan*

Michael J. Gidley • *ARC Centre of Excellence in Plant Cell Walls, Centre for Nutrition and Food Sciences, The University of Queensland, Brisbane, Queensland, Australia*

Chessa A. Goss • *Department of Biological Sciences, Center for Biotechnology and Life Sciences, University of Rhode Island, Kingston, RI, USA*

Florence Goubet • *Bayer BioScience NV, Ghent, Belgium*

Markus Günl • *Energy Biosciences Institute, University of California, Berkeley, CA, USA*

Philip J. Harris • *School of Biological Sciences, The University of Auckland, Auckland, New Zealand*

Cécile Hervé • *Station Biologique de Roscoff, UMR7139 Marine Plants and Biomolecules, Roscoff, France*

Kuninori Iwamoto • *Department of Biological Sciences, Graduate School of Science, University of Tokyo, Tokyo, Japan*

Katja Salomon Johansen • *Novozymes A/S, Bagsvaerd, Denmark*

Glenn P. Johnson • *Southern Regional Research Center, U. S. Department of Agriculture, New Orleans, LA, USA*

Anna Kärkönen • *Department of Agricultural Sciences, University of Helsinki, Helsinki, Finland; Department of Agricultural Sciences, MTT Agrifood Research Finland, University of Helsinki, Helsinki, Finland*

Marcia J. Kieliszewski • *Department of Chemistry and Biochemistry, Biochemistry Research Facility, Ohio University, Athens, OH, USA*
Andrew R. Kirby • *Institute of Food Research, Colney, Norwich, Norfolk, UK*
J. Paul Knox • *Centre for Plant Sciences, Faculty of Biological Sciences, University of Leeds, Leeds, UK*
Florian Kraemer • *Energy Biosciences Institute, University of California, Berkeley, CA, USA*
Matthäus Z. Krol • *Department of Applied Genetics and Cell Biology, University of Natural Resources and Applied Life Sciences, Vienna, Austria; University of Applied Sciences, Wiener Neustadt, Austria*
Virginia Lai • *Department of Biological Sciences, Center for Biotechnology and Life Sciences, University of Rhode Island, Kingston, RI, USA*
Derek T.A. Lamport • *School of Life Sciences, University of Sussex, Falmer, Brighton, UK*
Sang-Jik Lee • *Department of Plant Biology, Cornell University, Ithaca, NY, USA*
Susan E. Marcus • *Centre for Plant Sciences, Faculty of Biological Sciences, University of Leeds, Leeds, UK*
Laurence D. Melton • *Food Science, Chemistry Department, The University of Auckland, Auckland, New Zealand*
Deirdre Mikkelsen • *Centre of Excellence in Plant Cell Walls, Centre for Nutrition and Food Sciences, The University of Queensland, Brisbane, Queensland, Australia*
Andrew Mort • *Department of Biochemistry and Molecular Biology, Oklahoma State University, Stillwater, OK, USA*
Meera Nair • *Department of Horticulture, University of Kentucky, Lexington, KY, USA*
Roger H. Newman • *Industrial Research Limited, Lower Hutt, New Zealand; Scion, Rotorua, New Zealand*
Morten H.H. Nørholm • *The Department of Plant Biology and Biotechnology, University of Copenhagen, Copenhagen, Denmark*
Marisa S. Otegui • *Department of Botany, University of Wisconsin, Madison, WI, USA*
Markus Pauly • *Energy Biosciences Institute, University of California, Berkeley, CA, USA*
Zoë A. Popper • *Botany and Plant Science, School of Natural Sciences, National University of Ireland, Galway, Galway, Ireland*
Alison W. Roberts • *Department of Biological Sciences, Center for Biotechnology and Life Sciences, University of Rhode Island, Kingston, RI, USA*
Jocelyn K.C. Rose • *Department of Plant Biology, Cornell University, Ithaca, NY, USA*
Yumiko Sakuragi • *The Department of Plant Biology and Biotechnology, University of Copenhagen, Copenhagen, Denmark*
Arja Santanen • *Department of Agricultural Sciences, University of Helsinki, Helsinki, Finland*
Henrik V. Scheller • *Joint Bioenergy Institution, Feedstocks Division, Lawrence Berkeley National Laboratory, Emeryville, CA, USA*
Georg J. Seifert • *Department of Applied Genetics and Cell Biology, University of Natural Resources and Applied Life Sciences, Vienna, Austria*

Iben Sørensen • *Department of Biology, University of Copenhagen, Copenhagen, Denmark*
Li Tan • *Complex Carbohydrate Research Center, University of Georgia, Athens, GA, USA*
William G.T. Willats • *Department of Biology, University of Copenhagen, Copenhagen, Denmark*
Xiangmei Wu • *Department of Biochemistry and Molecular Biology, Oklahoma State University, Stillwater, OK, USA*

Chapter 1

Plant Tissue Cultures

Anna Kärkönen, Arja Santanen, Kuninori Iwamoto, and Hiroo Fukuda

Abstract

Plant tissue cultures are an efficient system to study cell wall biosynthesis in living cells *in vivo*. Tissue cultures also provide cells and culture medium where enzymes and cell wall polymers can easily be separated for further studies. Tissue cultures with tracheary element differentiation or extracellular lignin formation have provided useful information related to several aspects of xylem and lignin formation. In this chapter, methods for nutrient medium preparation, callus culture initiation, and its maintenance, as well as those for protoplast isolation and viability observation, are described. As a case study, we describe the establishment of a xylogenic culture of *Zinnia elegans* mesophyll cells.

Key words: Callus culture, Initiation, Maintenance, Nutrient medium, Protoplast, Tracheary element

1. Introduction

Plant cells and organs can be cultivated *in vitro* in aseptic conditions (1). Plant tissue cultures are an efficient system to study cell wall biosynthesis in living cells *in vivo*. Tissue cultures also provide cells and culture medium where enzymes and cell wall polymers can easily be separated for further studies. *In vitro* cultures allow investigations to be conducted in controlled conditions independent of seasons. Factors related to cell wall formation can be studied, for example, by adding the compound of interest into the culture medium, and after incubation, the cells and the medium are collected for further analysis. The culture medium can be considered as a continuum of the plant cell wall as it contains the proteins and the cell wall polymers that are sloughed off from the cell wall. In callus culture, cells grow mainly as a mass of undifferentiated cells, but there exist also some differentiated cells making the callus an inhomogeneous mixture of cells. With certain growth regulators, organogenesis (shoots or roots) or somatic

Zoë A. Popper (ed.), *The Plant Cell Wall: Methods and Protocols*, Methods in Molecular Biology, vol. 715,
DOI 10.1007/978-1-61779-008-9_1,

embryo formation may be induced. In the latter case, callus is embryogenic. Tissue cultures with tracheary element (TE) differentiation (2) and cell wall or extracellular lignin formation (3–6) have provided useful information related to several aspects of xylem and lignin formation. One of the most famous xylogenic cultures is that of *Zinnia elegans* (2). *Zinnia* system is useful for studying the sequence of events during xylem differentiation largely because the differentiation is highly frequent and synchronous, and all processes can be followed in single cells. Systematic gene expression analysis and molecular markers have revealed that many processes are common between *in vitro* and *in situ* TE formation (7, 8). Studies using this system have clarified numbers of physiological, biochemical, cell biological, and molecular biological events underlying TE differentiation (9–11).

This chapter describes the procedures for surface sterilisation, callus culture initiation, and maintenance, as well as for protoplast preparation and viability observations. Finally, we describe the basic method for the establishment of a xylogenic culture of isolated *Zinnia* mesophyll cells.

2. Materials

2.1. Nutrient Medium

Nutrient medium is a source of nutrients that plant normally obtains from the soil. The medium also contains a carbon source (often 1–4% w/v sucrose) and growth regulators the plant needs for cell division and growth *in vitro*. Gelling agent can be added to make the medium solid (1). As various species (even genotypes) have different nutritional requirements for optimum growth, a wide variety of nutrient media have been developed for *in vitro* cultured plants. In order to select a medium for the species of interest, it is useful to make a literature search. In Table 1 we show some widely used media that can be the choices to start with (see Note 1). Also, the explants with successful callus initiation are listed, since the developmental stage of the plant has a great effect on the success of culture initiation.

Table 2 shows the nutrient salt composition of the various media. Various macro- and microelement mixtures can be purchased commercially or the stock solutions can be prepared from the nutrient salts. A mixture of macroelements can be prepared as 10 times concentrated (10×) stock solution, whereas those of microelements, vitamins, and growth regulators can be made as 100–1,000× stock solutions (see Notes 2–5). After combining all components of the medium except the gelling agent, adjust the pH, adjust to the final volume, add the gelling agent (e.g. agar), and autoclave the medium at 121°C for 20 min. Let the medium cool to ca. 60°C. In a laminar air-flow cabinet, filter-sterilise the

Table 1
Types of explants, some widely used nutrient media, and growth regulator concentrations used for successful callus culture initiation

Plant group	Explant	Medium	Growth regulators
Monocotyledonous plants	Immature and mature embryos Leaf, or root segments of aseptically germinated seedlings	MS (14), N6 (24)	Auxin (2,4-D) 1.0–18 µM
Dicotyledonous plants	Young leaf, roots Stem segments Leaf, root, and stem segments of aseptically germinated seedlings	MS, WPM (25)	Cytokinin (BA, 2iP, kinetin, zeatin) 0.1–40 µM + auxin (NAA, 2,4-D) 0.5–10 µM
Gymnosperms	Cambial/xylem strips Shoot tips Zygotic embryos	MS Mod. Brown and Lawrence (3) Mod. N6 (12)	Cytokinin (BA, kinetin) 2–5 µM + auxin (2, 4-D, NAA) 9–16 µM 2.4-D alone: 11 µM (3)

heat-labile compounds (if any, see Note 6) and pour the medium into Petri dishes (ca. 25 mL medium/Petri dish with a diameter of 9 cm) (see Note 7).

2.2. Surface Sterilisation

1. 70% (v/v) ethanol.
2. Diluted Na-hypochlorite: NaClO, 1–2% (v/v) active chlorine, supplemented with a couple of drops of Tween 20.
3. Sterile distilled water.
4. 96% (v/v) ethanol for flaming.
5. Forceps.
6. Scalpels.
7. Sterile Petri dishes.
8. Parafilm®.

2.3. Maintenance

1. Fresh nutrient medium with a gelling agent or, alternatively, without the gelling agent.
2. 96% (v/v) ethanol for flaming.
3. Forceps.
4. Parafilm®.
5. Sterile 5 mL pipette tips with cut tips.
6. Sterile measuring cylinders (e.g. 25 mL in volume).
7. Orbital shaker (in the case of liquid cultures).
8. Temperature- and light-adjusted growth chamber.

Table 2
Nutrient media constituents for plant tissue culture basal media (26)

	B5 (15)		Mod. Brown and Lawrence (3)		MS (14)		N6 (24)		WPM (25)	
Macronutrients	mg/L	mM	mg/L	mM	mg/L	mM	mg/L	mM	mg/L	mM
NH_4NO_3			1,650	20.6	1,650	20.6			400	5
$(NH_4)_2SO_4$	134	1.0					463	3.5		
$Ca(NO_3)_2 \cdot 4H_2O$									556	2.4
KNO_3	2,528	25	1,900	18.8	1,900	18.8	2,830	28		
$MgSO_4 \cdot 7H_2O$	246	1.0	1,900	7.7	370	1.5	185	0.75	370	1.5
KH_2PO_4			340	2.5	170	1.25	400	2.94	170	1.25
$NaH_2PO_4 \cdot H_2O$	150	1.1								
$CaCl_2 \cdot 2H_2O$	150	1.0	22	0.15	440	3.0	166	1.1	96	0.65
K_2SO_4									990	5.7
Micronutrients		µM		µM		µM		µM		µM
H_3BO_3	3.0	49	30.9	500	6.2	100	1.6	26	6.2	100
KI	0.75	4.5	4.15	25	0.83	5.0	0.8	4.8		
$MnSO_4 \cdot 4H_2O$	13.2	59.2	31.2	140	22.3	100	4.4	19.7	22.3	100
$ZnSO_4 \cdot 7H_2O$	2.0	7.0	43.1	150	8.6	30	1.5	5.2	8.6	30
$CuSO_4 \cdot 5H_2O$	0.025	0.1	1.0	4.0[a]	0.025	0.1			0.25	1.0
$Na_2MoO_4 \cdot 2H_2O$	0.25	1.0	1.2	5.0	0.25	1.0			0.25	1.0
$CoCl_2 \cdot 6H_2O$	0.025	0.1	0.13	0.55	0.025	0.1				
$FeSO_4 \cdot 7H_2O$	27.8	100	27.8	100	27.8	100	27.8	100	27.8	100
$Na_2EDTA \cdot 2H_2O$	37.2	100	37.2	100	37.2	100	37.2	100	37.2	100
Organic constituents										
Myo-inositol	100	560	20	111	100	560	100	560	100	560
Nicotinic acid	1.0	8.1	0.5	4.1	0.5	4.1	0.5	4.1	0.5	4.1
Pyridoxine-HCl	1.0	4.9	0.1	0.49	0.5	2.4	0.5	2.4	0.5	2.4
Thiamine-HCl	10	30	0.1	0.3	0.1	0.3	1.0	3.0	1.0	3.0
Glycine					2.0	26.6	2.0	26.6	2.0	26.6
	g/L	mM	g/L	mM	g/L	mM	g/L	mM	g/L	mM
Sucrose	20	58.4	30	87.6	30	87.6	20	58.4	20	58.4
pH	5.7		5.5		5.7		5.7		5.7	

[a]L.B., Davin, personal communication

2.4. Protoplasts

1. Preplasmolysis solution, enzyme solution, and nutrient medium for protoplast cultivation according to Table 3.
2. Syringes.
3. Syringe filters (0.2 µm pore size).
4. Forceps.
5. Scalpels.
6. 96% (v/v) ethanol for flaming.

Table 3
Solutions for protoplast preparation and cultivation

Preplasmolysis solution	
B5/MS macroelements	
B5/MS Microelements	
sucrose	60 mM
Mannitol/sorbitol	0.3–0.5 M
pH 5.7 (see Note 33)	
Sterilise in autoclave.	
Enzyme solution (make fresh each time)	
0.5% (w/v) Cellulase and 0.2% (w/v) Macerase or 0.1–4% (w/v) Cellulase, 0.05–2% (w/v) Pectolyase/Macerase and 0.1–2% (w/v) Hemicellulase in the preplasmolysis solution	
Mix gently for 15–30 min to dissolve, filter-sterilise through syringe filters (0.2 μm pore size)	
Nutrient medium for protoplast cultivation	
B5/MS macroelements	
B5/MS microelements	
NaFe-EDTA	100 μM
B5/MS vitamins	
Sucrose	60 mM
Mannitol/sorbitol	0.3–0.5 M
Myo-inositol	100 mg/L
Plant growth regulators	
Auxin (2,4-D/NAA/IAA)	1–10 μM
Cytokinin (BA/2iP/kinetin/zeatin)	0.5–2.5 μM
pH 5.7 (see Note 33)	
Sterilise in autoclave	

See Table 2 for B5/MS medium constituents

7. Sterile nylon or steel sieves (70–100 μm pore size), screw-cap centrifuge tubes.
8. 20% (w/v) sucrose solution (autoclaved).
9. Fuchs-Rosenthal modified haemocytometer.
10. Microscopic slides.
11. Cover glasses.
12. Agars with low melting point (m.p.) specifically designed for protoplast culturing (e.g. A8678 Agar washed, m.p. 25–27°C; A7921 Agar purified, m.p. 30–35°C, Sigma).
13. Sterile pipette tips.
14. Petri dishes.
15. Parafilm®.

Viability stains:

16. 5–10 mg/mL fluorescein diacetate (FDA) in acetone (stock solution). This is then diluted immediately prior to use by adding 20 μL of the stock solution to 1 mL of 0.65 M mannitol.

17. 0.025–0.25% (w/v) Evans blue (EVB) in 0.65 M mannitol.
18. 0.025–0.25% (w/v) Methanol blue in 0.65 M mannitol.
19. 0.1% (w/v) Phenosafranine in 0.65 M mannitol.
20. 0.01–0.1% (w/v) Tinopal CBS-X (disodium 4,4′-bis[2-sulfostyryl)biphenyl) in 0.65 M mannitol.

2.5. Zinnia Cultures

2.5.1. Germination of Zinnia Seeds

1. 0.25% Na-hypochlorite.
2. Mesh strainer.
3. Vermiculite.
4. Plastic trays.
5. Growth chamber.
6. Liquid fertiliser: e.g. HYPONeX; N:P:K = 6:10:5 (HYPONeX Japan, Osaka). Dilute 1:100 before use.

2.5.2. Isolation and Culture of Mesophyll Cells

1. Table 4 shows the composition of the nutrient medium (see Note 8). Frequency of TE differentiation is optimal when the nutrient medium is supplemented with 0.89 μM 6-benzyladenine (BA) and 0.54 μM 1-naphtalene acetic acid (NAA). Medium without BA and/or NAA can be used for control cultures in which TE differentiation does not occur.
2. 0.1% Na-hypochlorite with 0.001% (w/v) Triton X-100.
3. Sterile distilled water.
4. Sterile labware: Waring-type blender, stainless-steel cups, nylon mesh (50–80 μm pore size), screw-cap centrifuge tubes, pipette tips, culture tubes (30 mm internal diameter (i.d.) × 200 mm, 18 mm i.d. × 180 mm or 12 mm i.d. × 105 mm) capped with aluminium foil.
5. Revolving drum.
6. Growth chamber.

2.5.3. Observations of Zinnia Cells

1. Glutaraldehyde.
2. 0.2 mg/mL 4′,6-diamidino-2-phenylindole (DAPI), 1 mM SYTO16 in DMSO (Molecular Probes).
3. Microscopic slides.
4. Cover glasses.
5. Haemocytometer.

3. Methods

3.1. Surface Sterilisation

The idea of surface sterilisation is to selectively kill micro-organisms on the plant material without killing the plant tissue. For culture

Table 4
Medium for xylogenic culture of *Zinnia* mesophyll cells

Constituents	Concentration (mg/L)	Molarity
Macroelements		mM
KNO_3	2,020	20
$MgSO_4 \cdot 7H_2O$	247	1
$CaCl_2 \cdot 2H_2O$	147	1
KH_2PO_4	68	0.5
NH_4Cl	54	1
Microelements I		µM
$MnSO_4 \cdot 4H_2O$	25	110
H_3BO_3	10	60
$ZnSO_4\ 7H_2O$	10	35
$Na_2MoO_4 \cdot 2H_2O$	0.25	1
$CuSO_4 \cdot 5H_2O$	0.025	0.1
Microelements II		µM
$Na_2EDTA \cdot 2H_2O$	37	100
$FeSO_4 \cdot 7H_2O$	28	100
Organic growth factors I		µM
Myo-inositol	100	560
Nicotinic acid	5	41
Glycine	2	27
Pyridoxine-HCl	0.5	2.4
Thiamine-HCl	0.5	1.5
Biotin	0.05	0.2
Organic growth factors II		µM
Folic acid	0.5	1.1
Growth regulators		µM
NAA	0.1	0.54
BA	0.2	0.89
	g/L	mM
Sucrose	10	29.2
D-Mannitol	36.4	200
pH	5.5	

initiation, it is important to select a healthy plant tissue as an explant. If necessary, wash the plant organ with tap water and cut it to ca. 1 cm pieces. Seeds are surface-sterilised intact. Carry out the procedures aseptically in the laminar air-flow cabinet.

1. Pretreat the explants for 30–60 sec in 70% (v/v) ethanol.
2. Transfer the pieces into a diluted 1–2% (v/v) Na-hypochlorite solution supplemented with couple of drops of Tween 20. Incubate for 5–30 min (see Note 9) with occasional shaking.

3. Rinse the explants carefully with sterile distilled water (three times with at least 1 min incubation in each rinse to wash all surface sterilants away). Use alcohol-flamed forceps to transfer the pieces from one solution into the other (see Note 10).
4. As cut surfaces of the plant material are injured by contact with the surface sterilising agent, cut the surfaces fresh with a sterile scalpel by using a half of a sterile Petri dish as a cutting board.
5. Aseptically dissect the tissue of interest (e.g. embryo, cambial strips) out of the seed/plant organ and place it onto the surface of the initiation medium. Use a stereomicroscope in the laminar air-flow cabinet if needed. Seal the dish by using a strip of Parafilm®.

3.2. Growth Conditions

The temperature and light requirements depend on the plant species. If no information exists in literature in relation to *in vitro* growth conditions of the species (or related species) of your interest, it might be useful to choose the light and temperature conditions in which the plant grows *in vivo*. Usually, a constant temperature (e.g. +25°C) is used; alternatively, the temperature is reduced for night (+25°C during day, +20°C during night). The quality of light is obtained by selection of lamps. Some species, like Norway spruce, prefer fluorescent warm white lamps (5, 12).

The intensity of light and its rhythm are very important. It is basically by trial and error you can estimate these values unless some information is available in literature. In general, light intensities of 20–200 μmol/m^2/s are used. Some *in vitro* cultures, however, are cultivated in the dark.

3.3. Maintenance

After 2–6 weeks in culture, callus growth becomes visible at the edges of the explant (Fig. 1). You have to subculture callus in order to supplement the cells with fresh nutrients and growth regulators. Subculture cells in 1- to 4-week intervals depending on the growth of callus. You might need to modify the nutrient medium at this stage in relation to nutrient and growth regulator concentrations and types (see Notes 1 and 11).

1. Subculture callus by transferring the freshest cells (usually at the edges of callus) onto the fresh medium with flamed forceps (see Note 10). The size of the inoculum should be kept in a constant size (ca. $0.9 \times 0.9 \times 0.5$ cm; see Note 12). Do not transfer inoculums which are too small in size because it takes longer for cells to start dividing when they are subcultured. Alternatively, if you subculture inoculums that are too big, the cells divide very fast and enter the stationary phase early (they also fill the growth container). This means more frequent subculturing.

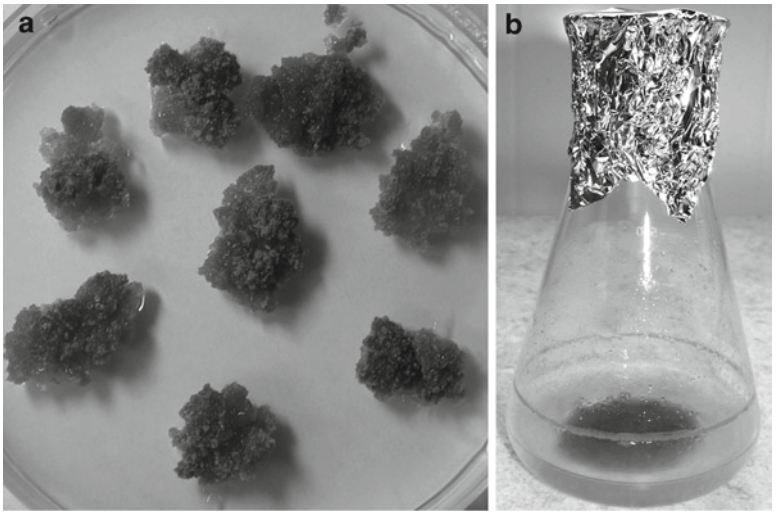

Fig. 1. (**a**) Callus culture of Norway spruce (*Picea abies*). (**b**) Cell suspension culture of Norway spruce composed of single cells and small cell aggregates.

2. You can also transfer callus into liquid culture (Fig. 1b). For this, make the nutrient medium without the gelling agent, aliquot it in 25 mL aliquots in 100 mL flasks (see Note 13), close the flask with a double layer of aluminium foil, and autoclave. Inoculate the most friable callus cells into the liquid medium (ca. 0.5 g of cells into 25 mL medium). It depends on the type of callus whether you will get a fine cell suspension with single cells and small cell aggregates or whether the callus grows in big clumps with no cell detachment.
3. For aeration, keep the cultures on an orbital shaker (100 rpm) in the same growth conditions as cultures on solid medium.
4. Subculture at regular intervals into fresh medium (see above) by letting cells to settle down to the bottom of the flask. Decant some culture medium off. Transfer ca. 5 mL cells into 20 mL of fresh medium, for example, with the help of a 5-mL cut, autoclaved pipette tip or with a measuring cylinder.

3.4. Protoplasts

Protoplasts are plant cells that have their cell wall removed by digestion with plant cell wall-degrading enzymes pectinases, hemicellulases, and cellulases (Table 5). Protoplasts can be isolated enzymatically in two different ways. In a two-step method, the cells are first separated to cell suspension with pectinases that digest the pectinous middle lamella between cells. Then the remaining cell walls are digested with cellulases and hemicellulases. The one-step method uses a mixture of pectinases and cellulases simultaneously for cell wall digestion (13).

Protoplasts can be produced from intact plant parts such as root tips and leaves, or from suspension-cultured and callus cells.

Table 5
Some commercially available cell wall-digesting enzymes utilised in protoplast isolation

Enzyme	Source	Supplier
Pectin-digesting enzymes		
Macerozyme R-10	*Rhizopus* sp.	Yakult Honsha, Japan
Macerase	*Rhizopus* sp.	Calbiochem
Pectinase	*Aspergillus niger*	Sigma
Pectolyase	*Aspergillus japonicus*	Sigma
Hemicellulose-digesting enzymes		
Hemicellulase	*A. niger*	Sigma
Viscozyme	*Aspergillus* sp.	Novozymes Corp.
Cellulose-digesting enzymes		
Onozuka R-10	*Trichoderma viride*	Yakult Honsha, Japan
Cellulysin	*T. viride*	Calbiochem
Driselase	*Basidiomycetes* sp.	Sigma

Having no cell wall, protoplasts are very sensitive to osmotic stress and must be handled in an isotonic/slightly hypertonic solution to prevent rupture. Nutrient medium requirements of protoplasts are quite similar to those of cultured plant cells. Extra calcium is supplemented to stabilise plasma membranes, and optimisation of commonly used MS (14) and B5 (15) medium for different species is often essential.

Protoplasts can be used in plant breeding either through protoplast fusion of related species or in transformation. After cell wall development, regenerable cells can be induced to plant formation. Protoplasts are also an excellent model to study cell wall synthesis or transport through cell membranes. Cell wall develops in protoplasts normally during 24–36 h incubation after which cells are capable of division. Protoplasts lose their characteristic spherical shape once the wall formation is complete (Fig. 2).

3.4.1. Protoplast Isolation

Prepare the preplasmolysis and enzyme solutions according to Table 3. Then continue as described below.
Leaves:

1. Surface sterilise young, fully expanded leaves as described in Subheading 3.1.
2. Cut the leaf into narrow sections with a sharp scalpel in a Petri dish that contains a small volume (10 mL) of the preplasmolysis solution. Peeling of abaxial epidermis accelerates cell wall digestion by the enzymes as they enter the intracellular spaces more easily (see Note 14).

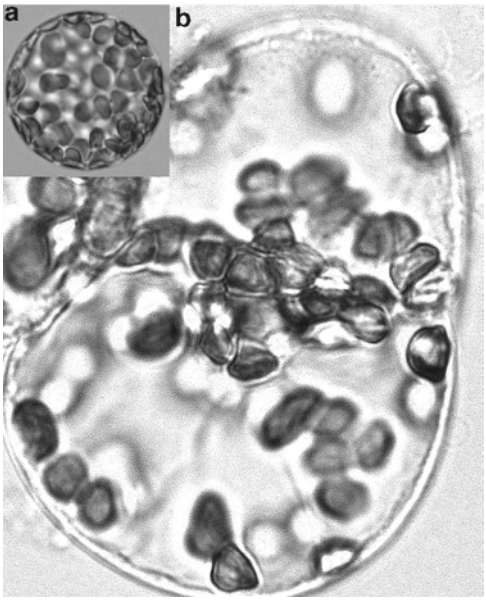

Fig. 2. (**a**) Protoplasts made of *Nicotiana tabacum* leaves. (**b**) After a couple of days in culture, the cell wall has regenerated and the cell has divided. (Photograph courtesy of Enni Väisänen, University of Helsinki).

Suspension-cultured cells:

3. Centrifuge actively growing cell suspension culture (10 mL) in the early logarithmic or exponential stage of growth for 5–10 min at 50–100 × *g* to separate the cells from the culture medium.
4. Decant medium after centrifugation and transfer the cells into a Petri dish with the preplasmolysis solution (see above).

Callus culture:

5. Transfer actively growing callus cells (from the edges of callus pieces) into a Petri dish containing the preplasmolysis solution.
6. Incubate plant material in the preplasmolysis solution. After 30 min, replace the preplasmolysis solution with the enzyme solution. Incubate for 0.5–20 h (see Note 15) in the dark at room temperature.
7. After incubation, shake the Petri dish gently to see that the tissue is digested; if not, incubate for 1–2 more hours.
8. To remove cell debris, pipette protoplasts through a nylon or a steel sieve (70–100 μm pore size) into a sterile screw-cap centrifuge tube. Centrifuge for 5–10 min at 50–100 × *g*.
9. Resuspend the protoplast pellet in the preplasmolysis solution. Alternatively, fractionate protoplasts from the cell debris by pipetting the protoplast suspension on top of a 20% (w/v) sucrose solution.

10. Centrifuge for 5–10 min at 50–100 × *g*. Cell debris sediments to the bottom of the tube and protoplasts float at the interface of the sugar layer and the enzyme solution. Transfer protoplast on top of a fresh sucrose solution by pipetting, repeat washing for three times (see Note 16). Resuspend protoplasts in the nutrient medium at an appropriate density (see Notes 17 and 18).

3.4.2. Protoplast Viability Tests

Protoplast viability can be detected with different dyes which indicate viable or non-viable cells. Appropriate osmoticum has to be added to the staining solution to avoid protoplast bursting. EVB is excluded from living cells and only dead cells are stained blue. Methanol blue (MB) enters both living and dead cells, but in living cells the dye is reduced to a colourless compound. Phenosafranine (PS) enters to dead protoplasts staining them red.

Fluorescent dyes: FDA accumulates inside protoplasts. In viable cells FDA is cleaved to fluorescent fluorescein by an esterase. Tinopal CBS-X is capable of permeating only dead cells (16, 17).

1. Select the dye you will use in your viability staining. Prepare it as described in Subheading 2.4.
2. On a microscopic slide, mix equal volumes of staining solution and the protoplast suspension and overlay with a cover glass.
3. Observe EVB, MB, or PS in a light microscope and count the number of dead protoplasts per all protoplasts in some fields (see Note 19).
4. Observe FDA in a fluorescent microscope with the excitation and emission of 440–490 nm and 510 nm, respectively (FITC, fluorescein isothiocyanate filter combination). Living protoplasts have bright fluorescence (see Note 20).
5. Use excitation and emission of 334–385 nm and 420 nm, respectively, for Tinopal CBS-X. Viable protoplasts have blue fluorescence (see Note 21).

3.4.3. Culturing of Protoplasts

Protoplasts are usually cultured on semi-solid agar-containing medium or in liquid medium. The salts of MS (14) or B5 (15) medium supplemented with an extra osmoticum, sorbitol, mannitol, sucrose, or glucose are usually suitable (Table 3) (see Note 17).

1. Mix double density protoplast suspension with molten agar (see Note 22), at a double concentration as required in the final culture. Make sure that the agar is not too warm since this kills your protoplasts (agar should be just above its melting point, ca. ≥30°C).
2. Pipette quickly as small droplets (100–200 µL) or plate evenly onto Petri dish.
3. Seal plates with Parafilm® and incubate in diffuse light (5–10 µmol/m^2/s) at room temperature.

3.5. Special Case: Zinnia Cultures

Fukuda and Komamine established an *in vitro* experimental system in which single mesophyll cells of *Z. elegans* redifferentiate directly into TEs independently of cell division (Fig. 3) (2). During TE formation, cell wall structures undergo dynamic changes, such as localised thickenings and lignification of secondary cell walls, partial degradation of primary cell walls, and perforation at the longitudinal end(s). In *Zinnia* xylogenic culture, concurrently with the secondary cell wall formation in developing TEs, active cell wall degradation takes place; pectin is one of the most actively degraded substances (18). Thus, taking advantage of *in vitro* xylogenic culture system, mechanisms concerning the structural changes of cell walls can also be studied.

3.5.1. Germination of Zinnia seeds

The first true leaves of 14-day-old seedlings of *Z. elegans* are used for the *in vitro* xylogenic culture. Mesophyll cells should be prepared from healthy leaves carefully grown under optimal conditions.

1. Surface sterilise seeds of *Z. elegans* cv. Canary bird or Envy in 0.25% Na-hypochlorite solution for 10 min with occasional shaking.
2. Wash the seeds with running water for 10 min in a mesh strainer (see Note 23).
3. Sow seeds in moistened vermiculite (0.1 g of seeds/100 cm^2) in plastic trays (see Note 24).

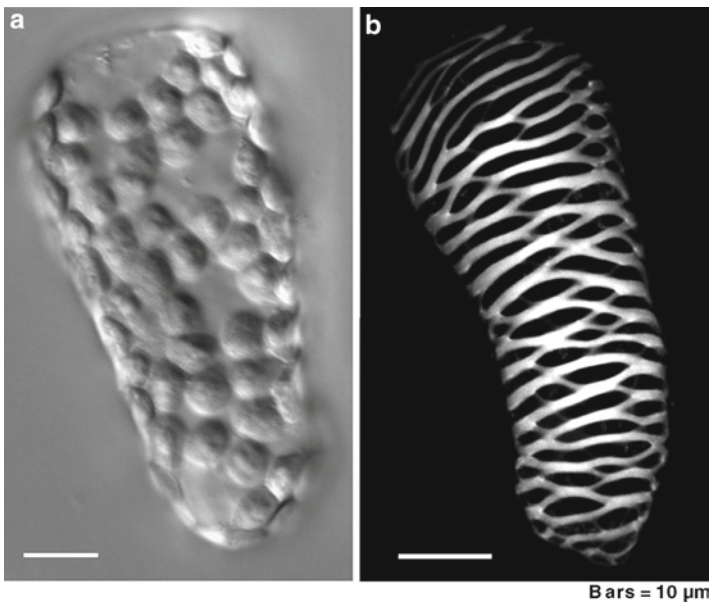

Fig. 3. A mesophyll cell and a TE formed in *in vitro Zinnia* xylogenic culture. (**a**) A single mesophyll cell just after isolation. (**b**) A TE with a thickened secondary cell wall.

4. Grow seedlings at 25° C for 14 days under a cycle of 14 h light (approx. 100 μmol/m²/s, white light from fluorescent lamps) and 10 h dark. Humidity in the growth chamber should be kept under 45%. Water when surface of vermiculite is dry (see Note 25). Feed 100-fold diluted liquid fertiliser (HYPONeX; N:P:K = 6:10:5; HYPONeX Japan, Osaka) once at the fourth day after sowing.

3.5.2. Isolation and Culture of Mesophyll Cells

Because of weak attachment between mesophyll cells of *Z. elegans*, single mesophyll cells can be isolated by mechanical maceration using a Waring-type blender. Epidermal and vascular cells are removed by filtration of the cell homogenate through a nylon mesh because of their strong adhesion to each other. Steps of isolation and culture of mesophyll cells are described below.

1. Harvest first true leaves (80–120 leaves) that are 3–4 cm in length (see Note 26).
2. Surface sterilise leaves for 10 min in 0.1% Na-hypochlorite solution supplemented with 0.001% (w/v) Triton X-100 with occasional stirring (see Note 27).
3. Rinse the leaves with autoclaved water three times (see Notes 23 and 28).
4. Transfer the leaves into a 100-mL stainless-steel cup containing 60 mL of nutrient medium.
5. Macerate the leaves at 10,000 rpm for 40 s using a Waring-type blender (Fig. 4a, b, see Note 29).
6. Filter the homogenate through a nylon mesh (Fig. 4c, pore size 50–80 μm) by pipetting using a large-bore pipette. Wash the homogenate that remains on the nylon mesh with 40 mL of additional nutrient medium (see Note 30).
7. Centrifuge the filtrate at 200 × *g* for 1 min.
8. Remove and discard the supernatant with a pipette or by decantation. Suspend the pelleted cells in 80 mL of nutrient medium by gentle shaking.
9. Centrifuge again at 200 × *g* for 1 min.
10. Resuspend the pelleted cells in nutrient medium at a cell density of ca. 8×10^4 cells/mL (see Note 18).
11. Distribute the cell suspension into culture tubes (20 mL for a tube of 30 mm i.d. × 200 mm, 3 mL for a tube of 18 mm i.d. × 180 mm, and 1 mL for a tube of 12 mm i.d. × 105 mm) capped with aluminium foil.
12. Incubate cultures in darkness at 25–27°C on a revolving drum at 10 rpm at an angle of elevation of 8° (Fig. 4d, see Note 31).

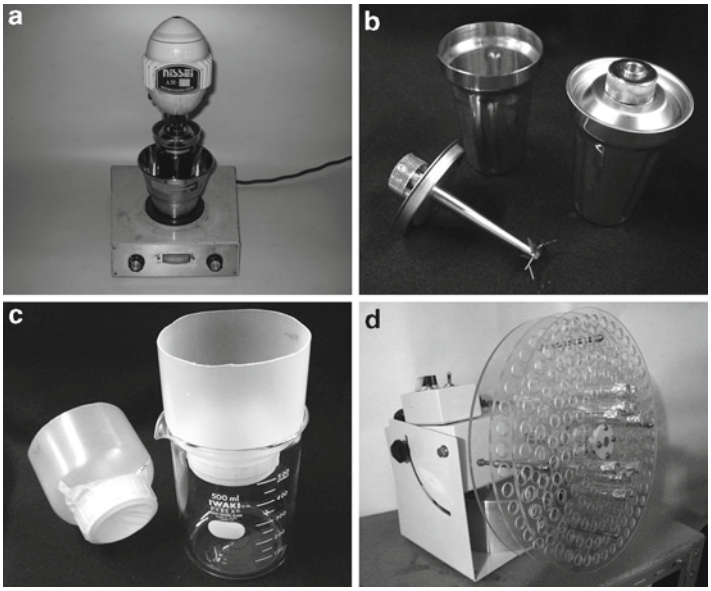

Fig. 4. Experimental apparatus used for the culture of *Zinnia* mesophyll cells. (**a**) A Waring-type blender (**b**) Two sets of the stainless-steel cup and a blade used with the blender (**c**) A nylon mesh is attached to a cylinder and set on a glass beaker for use (**d**) A revolving drum, which is placed in a temperature-controlled incubator or room.

3.5.3. Determination of Frequencies of TE Differentiation and Cell Division

At 72 h of culture, 30–50% of cells synchronously differentiate into TEs. These can be easily identified by characteristic patterns of secondary cell walls, which are observed even under a light microscope (see Note 32). Therefore, the number of TEs formed can be counted using haemocytometer without any pre-treatment. The frequency of TE formation is determined as the number of TEs per number of living cells plus TEs. The frequency of cell division can be estimated from the number of septa, since initially all mesophyll cells are single.

3.5.4. Observation of Zinnia Cells

TEs are distinguishable from other cells by their peculiar cell wall thickenings seen under a light microscope as described above. TEs can also be detected by staining of lignified secondary cell walls with phloroglucinol-HCl (19) or fluorochrome-conjugated wheat germ agglutinin (20). Isolated cells of *Z. elegans* are suitable for observation under a fluorescence microscope and a confocal laser scanning microscope as well.

Upon maturation of TEs, intracellular components including nuclei are lysed autonomously. This stage of differentiation can be monitored by staining of nuclei with a DNA-specific fluorochrome, DAPI.

1. Fix the cells by adding glutaraldehyde to a final concentration of 2% (v/v).

2. Add 1/100 volume of 0.2 mg/mL DAPI and incubate briefly in dark. Observe the nuclei under ultraviolet light using a fluorescence microscope.
3. To visualise the nuclei in living TEs, add 1/1,000 volume of 1 mM SYTO16 and incubate for 10 min. Detect using a fluorescent microscope. The dye is excited at 488-nm and the fluorescence is detected at 515–545 nm (21).

4. Notes

1. Sometimes it is useful to include an undefined mixture of organic substances (e.g. casein hydrolysate (0.1–1 g/L), coconut milk (3–10%, v/v)) to the nutrient medium for culture initiation. During the maintenance growth this is gradually omitted, if possible, as the exact composition of the mixture is not known and varies according to the lot.
2. Cytokinins (e.g. 6-benzyladenine (BA), 6-(γ,γ-dimethylallylamino)purine (2iP), kinetin, zeatin) are usually dissolved in a few drops of alkali (1 M NaOH), then filled with water to the final volume. Auxins (e.g. 2,4-dichlorophenoxyacetic acid (2,4-D), 3-indoleacetic acid (IAA), 1-naphthalene acetic acid (NAA)) are dissolved in a few drops of absolute ethanol. Boiling water (warmed in a water-bath) is poured over to let the ethanol evaporate. After the solution has cooled, adjust the final volume. Store at +4°C.
3. Store stock solutions of macroelements and microelements at +4°C. Stock solutions of many macroelements (10×) can be autoclaved to increase their storage time.
4. Iron can be supplied as NaFe(III)EDTA chelate. Make a separate stock solution (100×) out of this. Store at +4°C.
5. Mixtures of organic compounds, like vitamins, are prepared as 1,000× stock solutions. Aliquot the stock solution (e.g. 1 mL aliquots) and store in –20°C freezer.
6. Heat-labile compounds (e.g. certain growth regulators, some amino acids) are added to the autoclaved medium (when cooled to ca. 60°C) by filter-sterilisation through syringe filters (0.2 μm pore size).
7. Depending on the nutrient medium, you may be able to store the ready-made dishes for some time. After plating the agar-containing medium onto Petri dishes, let the medium solidify. Pack the dishes into clean plastic bags (the ones that contained the empty dishes) in a laminar air-flow cabinet, close the bag with tape. Store at room temperature, in the dark, agar-side down.

8. A mixture of macroelements can be stored as a 50× stock solution. Microelements I, microelements II, organic growth factors I, and organic growth factors II can be stored separately as 400× stock solutions. Microelements II should be autoclaved to form a chelate. Folic acid should be dissolved by adding a small amount of NaOH.
9. For leaf material, 5–10 min in Na-hypochlorite may be enough. For stem fragments and seeds, 20–30 min will be necessary.
10. After flaming, let the forceps cool down before touching the explants. Cooling can be done, for example, by dipping into sterile water or by pressing into the agar.
11. Sometimes the growth of callus ceases on nutrient medium where the callus has previously grown well. It might help if you transfer the cells onto a medium where either cytokinin or auxin is depleted. If the growth continues, the cells have started to produce the growth hormone by themselves. This phenomenon is called habituation (22, 23).
12. At the beginning, especially if there is only little callus growth, it is good to transfer the whole explant with the new growth onto the fresh nutrient medium. Only when you have enough callus, separate it from the explant for subculturing.
13. You can use different volumes of liquid cultures, but make sure that the medium to flask ratio is similar to 25 mL culture per 100 mL flask. This is to make sure that enough air space exists in the culture flask for gas exchange.
14. Epidermis can be easily removed from surface-sterilised leaves with the help of forceps and a scalpel. It is also possible to make protoplasts separately from the epidermal cell layer and mesophyll cells.
15. Duration of incubation has to be determined for each plant material.
16. Alternatively, protoplasts can be fractionated with Ficoll (10% in 0.6 M mannitol) or with Percoll (20% with 0.25 M mannitol and 0.1 M $CaCl_2$).
17. Some plant species prefer glucose (100–200 mM) to sucrose.
18. Protoplast/cell density can be determined by Fuchs-Rosenthal modified haemocytometer. For many species, protoplast density of 1×10^3–1×10^5 is suitable.
19. Notice that most dyes are quite toxic and prolonged incubation of protoplasts in staining solution may kill cells.
20. With FDA, you have to count the number of all protoplasts in the bright field since only the viable ones are detectable in the dark field.

21. Tinopal CBS-X-stained protoplasts can be counted by simultaneous illumination with UV and visible light.
22. Specifically designed agars for protoplast culture remain liquid down to their melting point, which is ca. ≥30°C. Plating into agar facilitates further observations of protoplasts as they become stationary. Agar concentration should be low enough (0.6%, w/v) to give a soft medium. Agars with low melting point are recommended for temperature-sensitive protoplasts not successful in liquid culture.
23. Na-hypochlorite should be thoroughly removed after surface sterilisation of seeds and leaves.
24. The size of the plastic trays we routinely use is 40 × 30 × 6.5 cm, and the depth of vermiculite is about 4 cm. Seeds should be covered with a little vermiculite after sowing. Seeds and liquid fertiliser should be equally distributed in a plastic tray so that seedlings grow uniformly.
25. Since too much watering of seedlings often causes serious diseases, water only when the surface of soil is dry. During watering, leaves should be kept dry. Use of leaves with splashes often leads to bacterial contamination in the subsequent cell culture.
26. During harvesting, healthy leaves without withered area and rough surface should be cut off with a pair of scissors sterilised with 70% (v/v) ethanol. Leaves harvested should be kept in water in a plastic container until the next step.
27. Leaves are damaged when they are soaked in Na-hypochlorite solution for longer than 10 min.
28. All steps between rinse of sterilised leaves and distribution of cell suspension to tubes must be done under aseptic conditions.
29. The optimal condition for maceration of leaves depends on the plant materials and the type of the blender used. Speed and time of maceration should be adjusted to keep the number of dead cells low and the number of living cells collected high. Single mesophyll cells can also be isolated using mortar and pestle with gentle maceration in the nutrient medium.
30. Application of filtrated cell suspension onto remaining homogenates on the nylon mesh increases the number of cells collected (optional step).
31. Alternatively, 25 mL of cell suspension can be incubated in a 100-mL flask using a rotary shaker at 40 rpm.
32. *Zinnia* cells fixed with 0.25% (v/v) glutaraldehyde can be stored at 4°C for at least a few months without significant visual change.
33. pH can be adjusted to 5.7 with KOH. Alternatively, pH can be buffered to 5.7 with 0.5% (w/v) MES (2-[*N*-Morpholino] ethanesulfonic acid)-KOH.

Acknowledgements

We thank University of Helsinki and the Academy of Finland for the financial support of the work (A.K., A.S.). We also thank Teresa Pehkonen (University of Helsinki) for useful comments and Enni Väisänen (University of Helsinki) for allowing us to include the protoplast figures.

References

1. Pierik, R.L.M. (1997) In vitro culture of higher plants. 4th ed. Kluwer, Dordrecht. 348 p.
2. Fukuda, H., and Komamine, A. (1980) Establishment of an experimental system for the tracheary element differentiation from single cells isolated from the mesophyll of *Zinnia elegans*. *Plant Physiol* **65,** 57–60.
3. Eberhardt, T. L., Bernards, M. A., He, L., Davin, L. B., Wooten, J. B., and Lewis, N. G. (1993) Lignification in cell suspension cultures of *Pinus taeda*. In situ characterization of a gymnosperm lignin. *J Biol Chem* **268,** 21088–21096.
4. Brunow, G., Ämmälahti, E., Niemi, T., Sipilä, J., Simola, L. K., and Kilpeläinen, I. (1998) Labelling of a lignin from suspension cultures of *Picea abies*. *Phytochemistry* **47,** 1495–1500.
5. Kärkönen, A., Koutaniemi, S., Mustonen, M., Syrjänen, K., Brunow, G., Kilpeläinen, I., Teeri, T.H., and Simola, L. K. (2002) Lignification related enzymes in *Picea abies* suspension cultures. *Physiol Plant* **114,** 343–353.
6. Kärkönen, A., and Koutaniemi, S. (2010) Lignin biosynthesis studies in plant tissue cultures. *J Integr Plant Biol* **52,** 176-185.
7. Fukuda, H. (1997) Tracheary element differentiation. *Plant Cell* **9,** 1147–1156.
8. Demura, T., Tashiro, G., Horiguchi, G., Kishimoto, N., Kubo, M., Matsuoka, N., Minami, A., Nagata-Hiwatashi, M., Nakamura, K., Okamura, Y., Sassa, N., Suzuki, S., Yazaki, J., Kikuchi, S., and Fukuda, H. (2002) Visualization by comprehensive microarray analysis of gene expression programs during transdifferentition of mesophyll cells into xylem cells. *Proc Natl Acad Sci USA* **99,** 15794–15799.
9. Fukuda, H. (2004) Signals that govern plant vascular cell differentiation. *Nat Rev Mol Cell Biol* **5,** 379–391.
10. Motose, H., Sugiyama, M., and Fukuda, H. (2004) A proteoglycan mediates inductive interaction during plant vascular development. *Nature* **429,** 873–878.
11. Ito, Y., Nakanomyo, I., Motose, H., Iwamoto, K., Sawa, S., Dohmae, N., and Fukuda, H. (2006) Dodeca-CLE peptides as suppressors of plant stem cell. *Science* **313,** 842–845.
12. Simola, L.K., and Santanen, A. (1990) Improvement of nutrient medium for growth and embryogenesis of megagametophyte and embryo callus lines of *Picea abies Physiol. Plant* **80,** 27–35.
13. Bajaj, Y.P.S. (1996) Plant protoplasts and genetic engineering VII. Springer, Berlin. 317 p. ISBN 3-540-60876-1.
14. Murashige, T., and Skoog, F. (1962) A revised medium for rapid growth and bio assays with tobacco tissue cultures. *Physiol Plant* **15,** 473–497.
15. Gamborg, O. L., Miller, R. A., and Ojima, K. (1968) Nutrient requirements of suspension cultures of soybean root cells. *Exp Cell Res* **50,** 151–158.
16. Widholm, J. M. (1972) The use of fluorescein diacetate and phenosafranine for determining viability of cultured plant cells. *Stain Technol* **47,** 189–194.
17. Huang, C. N., Cornejo, M. J., Bush, D. S., and Jones, R. L. (1986) Estimating viability of plant protoplasts using double and single staining. *Protoplasma* **135,** 80–87.
18. Ohdaira, Y., Kakegawa, K., Amino, S., Sugiyama, M., and Fukuda, H. (2002) Activity of cell-wall degradation associated with differentiation of isolated mesophyll cells of *Zinnia elegans* into tracheary elements. *Planta* **215,** 177–184.
19. Siegel, S. M. (1953) On the biosynthesis of lignin. *Physiol Plant* **6,** 134–139.
20. Hogetsu, T. (1990) Detection of hemicelluloses specific to the cell wall of tracheary elements and phloem cells by fluorescein-conjugated lectins. *Protoplasma* **156,** 67–73.
21. Obara, K., Kuriyama, H., and Fukuda, H. (2001) Direct evidence of active and rapid nuclear degradation triggered by vacuole

rupture during programmed cell death in *Zinnia*. *Plant Physiol* **125,** 615–626.

22. Christou, P. (1988) Habituation in in vitro soybean cultures. *Plant Physiol* **87,** 809–812.
23. Piscke, M. S., Huttlin, E.L., Hegeman, A. D., and Sussman, M. R. (2006) A transcriptome-based characterization of habituation in plant tissue culture *Plant Physiol* **140,** 1255–1278.
24. Chu, C. C., Wang, C. C., Sun, C. S., Hsu, C., Yin, K. C., Chu, C. Y., and Bi, B. Y. (1975) Establishment of an efficient medium for anther culture of rice through comparative experiments on the nitrogen sources *Sci Sin* **18,** 659–668.
25. Lloyd, G. and McCown, B. (1980) Commercially-feasible micropropagation of mountain laurel, *Kalmia latifolia*, by use of shoot-tip culture. *Comb Proc Internat Plant Prop Soc* **30,** 421–427.
26. Owen, H. R., Miller, A. R. (1992) An examination and correction of plant tissue culture basal medium formulations. *Plant Cell Tiss Org Cult* **28,** 147–150.

Chapter 2

Computerized Molecular Modeling of Carbohydrates

Alfred D. French and Glenn P. Johnson

Abstract

Computerized molecular modeling continues to increase in capability and applicability to carbohydrates. This chapter covers nomenclature and conformational aspects of carbohydrates, perhaps of greater use to carbohydrate-inexperienced computational chemists. Its comments on various methods and studies might be of more use to computation-inexperienced carbohydrate chemists. New work on intrinsic variability of glucose, an overall theme, is described.

Key words: Carbohydrate, Disaccharide, Conformation, Puckering, Modeling, Quantum mechanics, Molecular mechanics

1. Introduction

Various computer modeling software systems provide a graphical user interface with a drawing function that lets the user start without any information other than a vision in their head and a knowledge of the pattern of atom connectivity. Such software "knows" about atomic diameters, usual bond lengths, angles, etc., so it will assist the user in creating a structure that may highly resemble the actual molecule as represented by balls and/or sticks. Different display options for the molecules provide a sense of artistic accomplishment and better convey information and may even enhance the appeal of a particular research program. Still, the validity of such pictures of typical carbohydrate molecules is questionable because there are many alternative structures (conformations or shapes) that can be formed by mostly changing the torsion angles. Figure 1 shows the three staggered conformations of *n*-butane and

Zoë A. Popper (ed.), *The Plant Cell Wall: Methods and Protocols*, Methods in Molecular Biology, vol. 715,
DOI 10.1007/978-1-61779-008-9_2,

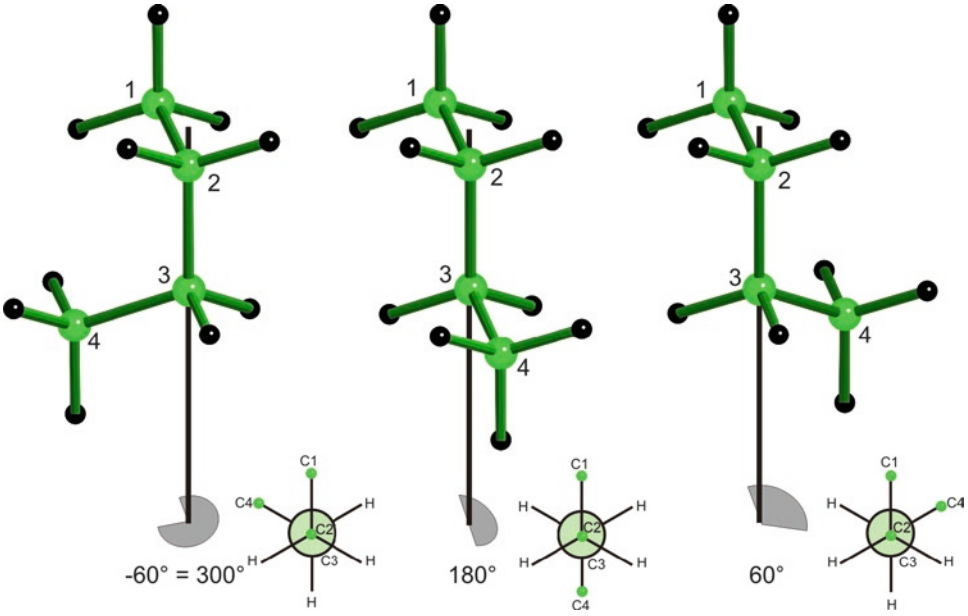

Fig. 1. Staggered conformations of butane, with their C1–C2–C3–C4 torsion angles indicated. Newman projections are also shown. The angles refer to the angle of the C1–C2 bond relative to the C3–C4 bond, when viewed down the C2–C3 bond. The C1–C2–C3–C4 torsion angle is 0° when all four atoms are in a plane and C1 and C4 are *cis*. The *vertical rods* indicate the axes about which the C4 groups rotate. All three conformations (*–gauche, trans*, and *+gauche*) correspond to minima in the energy, but the 180° conformer has the lowest energy, i.e., it is the global minimum. The *gauche* forms are also called *syn*, and the *trans* form is also called *anti*.

their torsion angles. Deciding which conformer best represents the "real" population of molecules requires a measure of the relative free energy of each alternative. That may seem simple, but for a carbohydrate there are actually two complicated issues. One is how to calculate the energy, and the other is to decide which alternative structures to consider and which to ignore. Both issues are typically approached with assumptions and approximations that are being reduced as computer power and software sophistication increase.

Regarding alternative structures, the pyranosyl ring of aldohexose sugars is often assumed to be in a chair form, even though there are alternatives. In fact, idopyranose appears to have significant populations for both chairs and a skew form of the ring in solution (1). Even glucose has conformational ambiguity, as some methylated or acylated cyclodextrin molecules have glucose residues that take alternative chair or skew forms in their experimentally determined crystal structures (2, 3).

Energy can be calculated in many ways, starting historically with a simple scan for short distances between atoms that are not bonded to each other. If such contacts exist, that kind of analysis would assign a potential energy of infinity, reflecting complete

improbability. One mainstream approach is Molecular Mechanics (MM). The energy terms of these empirical force-field models arise from our useful "cartoons" of molecular structure, with potential functions for bond stretching, angle bending, and charge–charge interactions. Quantum mechanics (QM) calculations consider distributions and interactions among individual electrons. Thus, QM is also called electronic structure theory. QM calculations are so expensive in terms of computer time and memory that trisaccharides (4) are about the largest molecules to consider. Also, explicit treatments of neighbor molecules such as solvent or adjacent molecules in a crystal are rarely included in QM calculations, nor are most of the alternative structures, all because of the time required.

Sometimes errors in calculated energy cancel each other. When comparing two different molecular shapes, the same errors may affect both forms. Even if the absolute energy values are not correct, the relative energies could still be useful. Also, there is a useful but ultimately unreliable compensation for the lack of explicit treatment of electron correlation in the Hartree–Fock (HF) QM method. That error can often be countered by errors from using a small basis set such as 6-31G*. Combining the HF method and the 6-31G* basis set gives HF/6-31G*, a "magic" level of theory (5).

To some extent, the present chapter follows up on proceedings from a symposium on carbohydrates in 1989 (*ACS Symposium Series 430*). Besides many articles in chemical and carbohydrate journals, special issues have been at least partly dedicated to carbohydrate modeling (*Molecular Simulation* (vol. 4, issue 4); *THEOCHEM* (vol. 395–397), *Carbohydrate Research* (vol. 340, issue 5), *ACS Symposium Series 930*). Some of the issues treated herein are covered in more detail in a recent review (6).

2. Structural Descriptors of Carbohydrates

2.1. Nomenclature

Because most carbohydrates have numerous asymmetric centers, they have kept their traditional nomenclature (7). β-D-Glucopyranose should be easier to remember than (*2R, 3R, 4S, 5S, 6R*) 2,3,4,5 tetrahydroxy, 6 methoxy oxacyclohexane. Another point is that the first carbon atom in the parent acyclic sugar is number 1 instead of the heteroatom in the sugar ring as would be the case if standard organic chemistry nomenclature were used. Suppose a disaccharide is composed of two D-glucopyranose residues, linked at the 1′ and 4 positions. The particulars of the linkage between the glucose residues define the compound, i.e., whether it is maltose or cellobiose. The configuration at C1, the reducing end anomeric center, defines whether it is the α- or β-anomer. Thus, β-maltose

and α-cellobiose both exist, despite the opposite configurations at the anomeric centers of their linkages. Rules for carbohydrates composed of more than two monosaccharides are covered by publications cited in (7).

2.2. Drawings

To aid recognizability of ring compounds, the anomeric center (the carbon bound to both the ring oxygen and a hydroxyl in the native sugar) is drawn on the far right, and the bond between the ring oxygen and the nonanomeric carbon is parallel to the plane of the paper and indicated as being at the back of the ring. The ring oxygen of five-membered (furanosyl) rings is shown at the back.

2.3. Ring Puckering

Carbohydrate rings are puckered, not flat. An extensive analysis of both furanose and pyranose ring shapes is presented in a study of the conformationally and configurationally ambiguous sugar, psicose (8). Furanose rings can be envelopes, with four coplanar atoms and one atom out-of-plane. For example, a ring with its oxygen atom out of plane is a characteristic form, denoted ^{O}E if the oxygen is above the ring and E_O if below. Otherwise, they are twists, with three coplanar atoms and one atom above the plane and one below (see Fig. 2 for $^{3}T_2$ and E_2 examples based

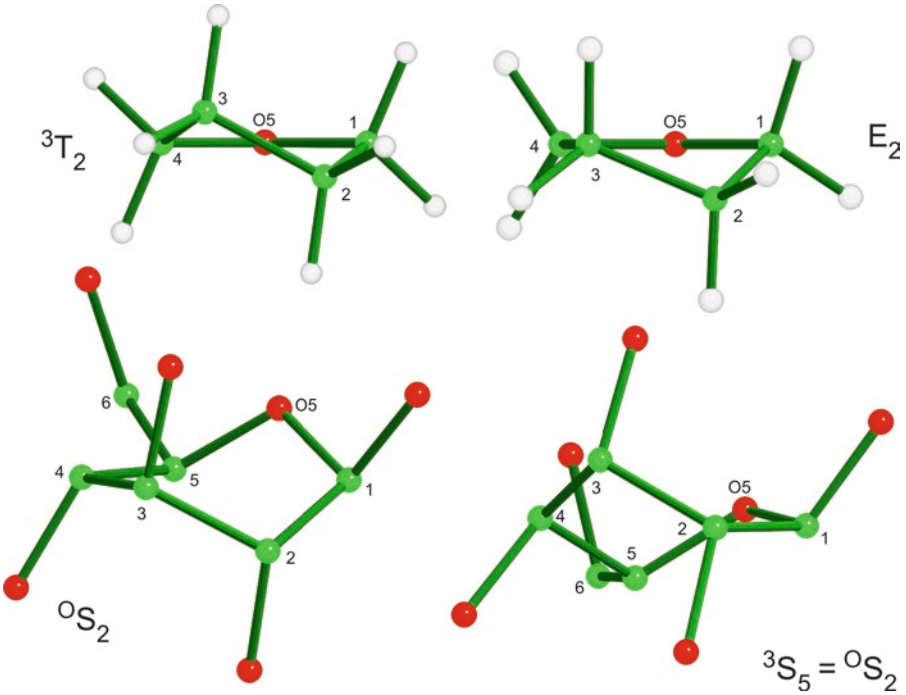

Fig. 2. Sample furanosyl rings with C1, O5, and C4 all coplanar. The $^{3}T_2$ drawing has C3 above the plane, and C2 below, where the E_2 drawing has only C2 out of plane. Both of the β-D-glucopyranosyl rings (hydrogen atoms not shown) are exactly the same structures, correctly described as $^{0}S_2$ rings. The ring on the *right* has been rotated about a line between C1 and C4. *Convention* dictates that the ring is described as $^{0}S_2$ instead of $^{3}S_5$. There are two planes that contain four of the atoms. One contains C1, C3, C4, and C5, and the other contains C1, C2, C4, and O5.

on tetrahydrofuran). Each individual envelope (E) or twist (T) is a "characteristic form." Ten E forms of furanose rings exist, as well as ten T forms, such as $^{4}T_{3}$, a favored form for β-D-fructofuranose. Facile transitions known as pseudorotation are permitted between the adjacent alternating E and T forms, such as ^{4}E, $^{4}T_{3}$, and E_{3}. The characteristic forms do not necessarily correspond to energy minima but are merely markers in ring-shape hyperspace for understanding the shape of a particular ring.

Characteristic pyranosyl forms include two chairs, six boats, and six skews (twist-boats, see Fig. 2). Also, there are 12 envelopes and 12 half-chairs, and Boyen described 12 additional (screw-boat) characteristic forms (9). For ordinary sugars, these latter forms correspond to intermediates or transition states during conversions and are not stable. There are only two unique chairs, with convention dictating use of the lowest-numbered ring atoms. For example, the same glucopyranosyl chair could be described as $^{4}C_{1}$, $^{2}C_{5}$, or $^{O}C_{3}$ but only $^{4}C_{1}$ is used. The other form is $^{1}C_{4}$. Similarly, each skew form could be described in two ways (Fig. 2), but convention dictates the use of the lower-numbered atoms.

Because experimental and computational sugar rings usually do not correspond exactly to a characteristic conformation, it is useful to specify the shape quantitatively. That is the job of puckering parameters. The 15 *x, y, z* coordinates of the five atoms of a furanosyl ring are reduced to two puckering parameters, and three for the positions of the six atoms of a pyranosyl ring. Just as variations in bond lengths and angles are ignored in ordinary conformational analysis based on torsion angles, puckering parameters are intended as overall descriptors, not a completely detailed description. Any computed puckering from an experimental or computed structure can be translated to a phrase such as "a conformation that is nearest in puckering space to $^{O}S_{2}$" (a skew form, with the ring oxygen above the plane and C2 below the plane that includes C1, C3, C4, and C5). Even when the shape is obvious, such as the frequently found $^{4}C_{1}$ (chair) form, assessment of puckering parameters allows the degree of distortion from the normal shape to be described to learn the effects of being packed in a crystal or complexed with an enzyme. In another example, the degree of puckering for glucose could be compared with that of tetrahydropyran to learn the effects of substituents on the ring shape.

Cremer–Pople puckering parameters (10) work well in most circumstances but in cases where bond lengths are quite different, the translation from the computed parameters to a characteristic conformer may not meet expectations based on a visual assessment. Besides the Cremer–Pople puckering parameters, which apply to all sizes of rings, there are the Altoona–Sundaralingam puckering parameters for furanosyl rings (11). Ring puckering conformations also have descriptors that are derived from endocyclic torsion angles (12–15) or flap angles (16, 17).

Other measures of the ring shape are useful, especially when they are interrelated with the conformation of polysaccharides. For example, the distance between O1 and O4 of α-D-glucopyranose varies between 3.88 and 4.84 Å (see below) in crystals of mono- and oligosaccharides, despite a basic $^4C_1$ shape. If those residues are used to make models of the amylose polysaccharide, the resulting helix shape will vary widely. Recently, we observed a twist of the glucose ring, i.e., the O1–C1…C4–O4 virtual torsion angle ranges over about 25° (18). Again, this parameter governs the location of the adjacent residue in model polymers.

2.4. Exocyclic Group Orientation

The orientation of primary alcohol groups is often an interesting variable. Most often the three staggered rotamers are described as *gg (gauche–gauche)*, *gt (gauche–trans)*, and *tg (trans–gauche)*. These different conformers are shown below in Fig. 2. The first of the two letters corresponds, in D-glucose, to O5–C5–C6–O6 torsion angles (ω) of −60° (−*g*), 60° (+*g*), and 180° (*t*) (see Fig. 1). The second letter corresponds to C4–C5–C6–O6 torsion angles of 60°, 180°, and −60°. Other authors prefer −*g*, +*g*, and *t* for the O5–C5–C6–O6 angle. Because C5 is sp^3 hybridized, the use of two letters could be considered redundant, but it avoids needing to remember the sign of the torsion angle. If considering L-glucopyranose, the signs of *gauche* forms must be reversed for the single-letter notation, but with the two-letter notation the mirror image of D-glucose with O6 *gt* is L-glucose with O6 *gt*. The *tg* conformation has been described as "forbidden" because it was not observed in early crystal structure studies of molecules having the *gluco* configuration at C4 (O4 equatorial), and some NMR-based analyses of sugars have yielded a sum of the *gt* and *gg* conformations slightly greater than 100%, implying negative amounts of *tg*. More recent experimental work has found examples, especially in native cellulose I. The *galacto* configuration, with O4 axial, has a low population of *gg* conformations (6).

Secondary alcohol (hydroxyl) orientations are important to the calculated energy. They are often described in terms of clockwise and counter-clockwise (reverse clockwise) systems of intra-residue hydrogen bonds that provide maximum stabilization for isolated molecules. Despite the significant lowering of the energy due to having all of the secondary hydroxyl groups appearing to participate in a continuous donor–acceptor–donor–acceptor network, the resulting long H…O distances and small O–H…O angles would yield weak attractions. According to Bader's Atoms-In-Molecules (AIM) theory (19) ("electron density gradient vector field analysis"), these energy-lowering orientations do not result in the bond paths and bond critical points (20–22) needed for true hydrogen bonds (23). The primary alcohol can form a hydrogen bond with O4, and two axial hydroxyl groups with 1,3 spacing (such as in $^1C_4$ glucose) can form better hydrogen bonds (21).

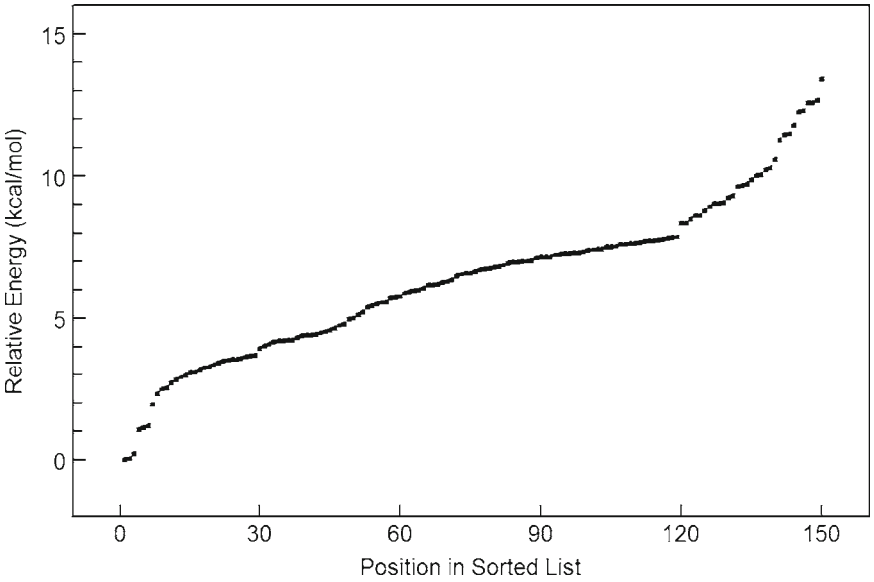

Fig. 3. Energy distribution for stationary shapes of glucose at the B3LYP/6-31+G** level. Twenty-five of the energies above 4.3 kcal/mol correspond to "saddle-point" or "transition state" structures.

All staggered rotamers for glucose can be studied by fairly good QM. Putting each of the six rotatable groups into all three orientations, there are 3^6 (=729) combinations. The Jaguar program (24) was used with B3LYP/6-31+G** energy minimization on each of the conformers as isolated (gas phase) molecules. Most of the 729 combinations were unstable and one or more of their exocyclic groups rotated to a different staggered orientation. Still, there were 150 unique stationary structures, and their energy range (13.4 kcal/mol) is considerable. Figure 3 shows their nearly continuous distribution of energies. Figure 4 shows the six lowest-energy and the six highest-energy forms. The six lowest-energy structures included the *gt*, *gg*, and *tg* conformations of O6 and both reverse-clockwise and clockwise secondary hydroxyl groups. This would seem to support the notion of cooperative rings of hydrogen bonds, for which there is some experimental support (25), despite the above AIM studies. Four of the six highest-energy structures have the hydroxyl hydrogen on O1 located underneath the pyranose ring, a sterically disadvantageous orientation, and the rings of OH interactions are absent.

The exocyclic group orientations have a substantial effect on the molecular geometry, including the O1…O4 distance. Figure 5 shows answers to three different questions about this distance. The top curve shows the probability distribution predicted by $p_i = e^{-\Delta E/RT}$ for a glucose residue stretched and compressed with MM3 (26) calculations. The underlying energy curve obeys Hooke's Law almost perfectly. The middle graph presents the

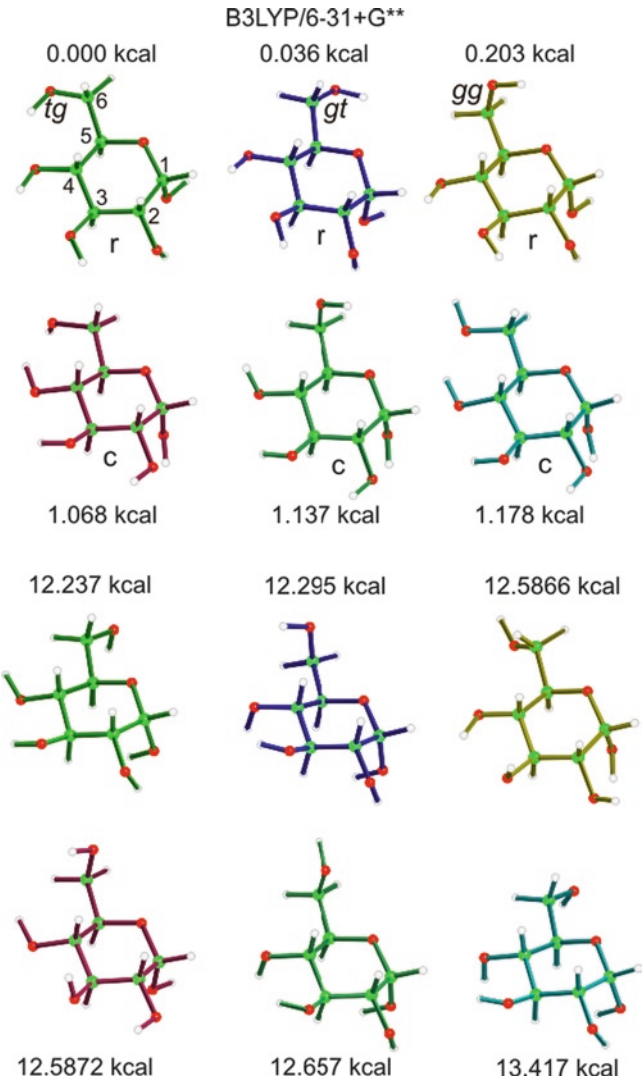

Fig. 4. Six lowest energy and six highest-energy stationary forms of α-D-glucopyranose. Of these structures, only the *lower left* is in a transition state according to frequency calculations.

O1…O4 distances in 2,582 experimental examples of α-D-glucose and its derivatives having $^4C_1$ rings, obtained from a scan of the Cambridge Structural Database (27). The lowest graph shows the O1…O4 distances within the 150 stable structures discussed above. The top and bottom theoretical analyses indicate, respectively, the elasticity of glucose and the intrinsic variability based on the exocyclic group orientations. The experimental data combine both these factors, with the elasticity corresponding to deformations from random crystal packing and strain from being part of larger molecules, including macrocycles. The mean MM3 distance

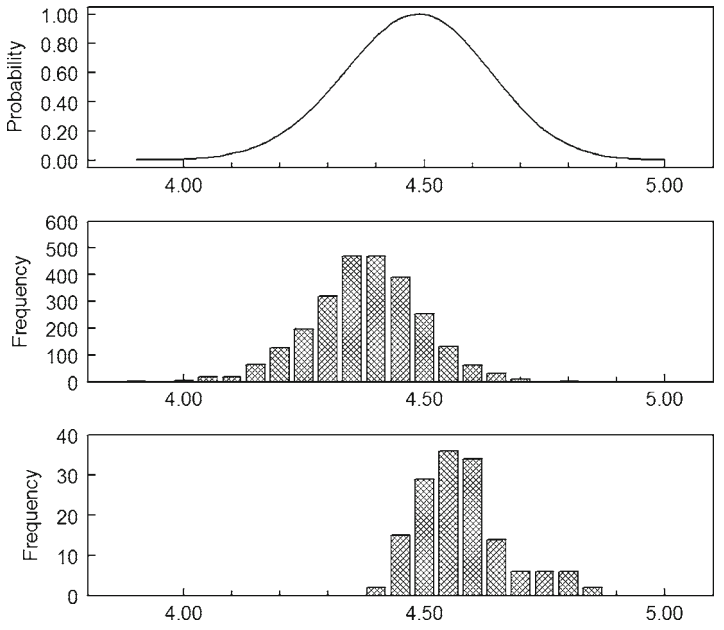

Fig. 5. *Upper*: Probabilities calculated by MM3 for stretched and compressed α-D-glucopyranose for different O1–O4 distances. *Center*: Frequencies of experimental O1–O4 distances in 2,582 α-D-glucopyranose rings from a scan of the Cambridge Structural Database. The mean value is 4.356 Å. *Lower*: Frequencies of intrinsic O1–O4 distances in 150 stationary B3LYP/6-31+G** structures of α-D-glucopyranose.

is longer than the mean experimental value, as is the shortest B3LYP/6-31+G** result.

Other methods for calculating the energy of the 729 conformers will give different numbers of final structures as well as energy values. All of these 150 structures have the $^4C_1$ shape; many more stationary points would be found for other ring shapes. Some of those alternatives will give energies lower than the higher-energy $^4C_1$ shapes.

2.5. Anomeric Centers

In aqueous solution, a single enantiomer such as D-glucose is five compounds: acyclic, and α- and β-pyranoses and furanoses. The populations of the furanose and acyclic forms are minimal for glucose, but must be considered for sugars such as the ketohexose, psicose is a ketohexose (8). Opening and re-closing the ring allows the configuration of glucose to change at C1, and the resulting forms, α- and β-glucopyranose, are "anomers." Experimental data for reducing sugars are affected by this interconversion, which is known as mutarotation. It can be avoided by substituting the hydroxyl hydrogen on the glycosidic oxygen with a methyl group.

2.6. Di-, Oligo-, and Polysaccharides

Atom numbers in the nonreducing residue of disaccharides are primed, while longer molecules have increasing values of Roman numerals for residues further from the reducing end. Linkages

between monomeric units of larger molecules consist of either two or three bonds, typically with the oxygen atom attached to the anomeric carbon (the glycosidic oxygen) leaving during synthesis. Thus, in the formation of cellobiose, O4 remains. Disaccharide conformations are specified by the values of the torsion angles for the glycosidic (C1′–On) (ϕ) and aglycon (On–Cn) (ψ) bonds ($n = 4$ for cellobiose). Three-bond linkages involve a primary alcohol group. Its conformation is described with letters, sometimes upper case, e.g., *GG*, *GT*, and *TG*, or by the ω torsion angle. The central bond is specified by ψ, and ϕ is for rotation about the glycosidic bond. Polysaccharides have disaccharide linkages so the same descriptors apply. For polysaccharides composed of regular repeating units, helix nomenclature applies. Helices are described by the number of units per turn (n), and the rise, or advance, (h) along the helix axis.

Along with C1′, O4, and C4, the four-atom definition of the torsion angle ϕ in maltose or cellobiose could involve any of the three atoms H1′, O5′, or C2′. Many workers have used H1′, especially if they have a background in NMR and are thinking of using nuclear Overhauser effects to solve the structure. Others, mindful of the difficulties in accurately locating hydrogen atoms by X-ray crystallography, have opted for O5′. No examples of C2′ come to mind. The ψ torsion angle has been defined by all three possible atoms. For cellobiose, they would be H4, C3 or C5. The above reasons for favoring a hydrogen atom or a heavier atom also apply, but the above-cited nomenclature (7) uses the lower-numbered carbon atom. Thus, the standard definition of ψ for cellobiose is C1′–O4–C4–C3, along with the standard ϕ of O5′–C1′–O4–C4. Greek letter descriptors are italicized.

Standardization of the ends of the 360° ranges of ϕ and ψ on plots of energies, experimental points and molecular dynamics (MD) trajectories would allow quick visual comparisons of different plots. We argue for plots that are equivalent to ϕ_H and ψ_H (e.g., H1′–C1′–O4–C4 and C1′–O4–C4–H4) values from −180° to +180° for two reasons. Firstly, experimentally determined points for many reducing disaccharides are mostly in minima that have ϕ_H and ψ_H near 0° and therefore will fall in the center of the map. If the ranges were 0–360°, the major populations could be separated into as many as four visual groups despite close structural similarity. Secondly, on such plots for maltose and cellobiose the diagonal line from the lower right to the upper left corresponds to helices with no chirality, separating right- and left-handed forms. For maltose, the diagonal line corresponds to polymers with $h = 0$. Long molecules having maltose-type linkages and ϕ,ψ values on the diagonal line would self-intersect, but molecules with six, seven or eight glucose residues could form cyclodextrins. Cellulose polymers with ϕ,ψ values on the diagonal line are helices with $n = 2$. By adding or subtracting 120° as appropriate, the

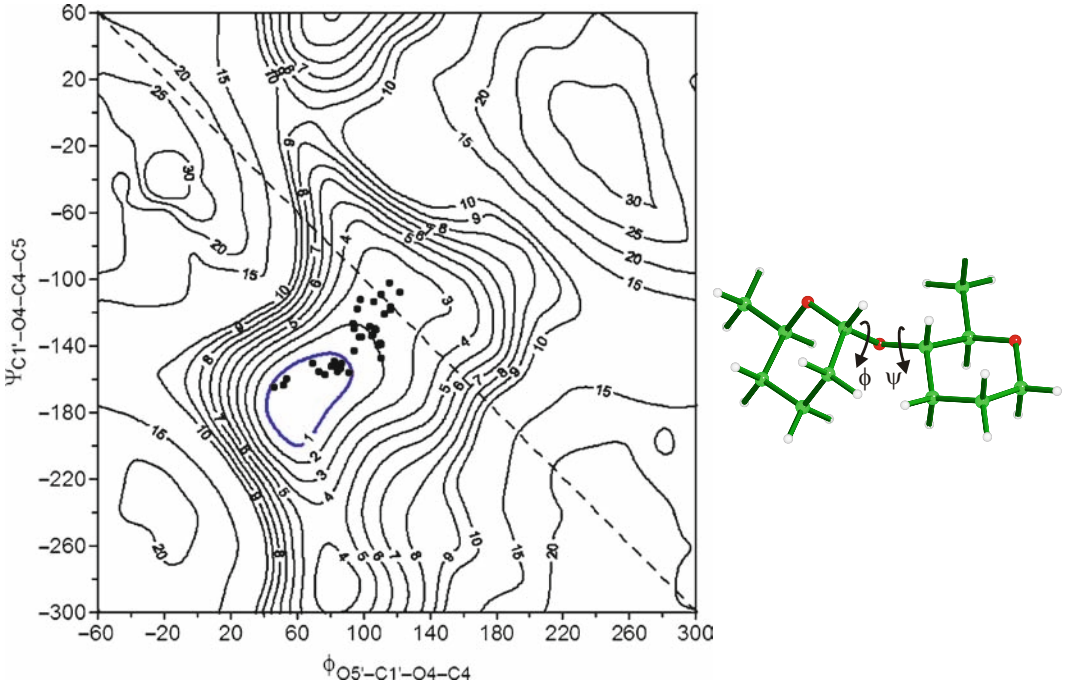

Fig. 6. HF/6-31G* energies from the depicted methylated maltose analog. Observed conformations in experimental crystal structures of maltose and related structures are shown as *points*. Structures within the 1 kcal/mol contour do not possess the O2–O3′ hydrogen bond that is found for all other observed experimental structures. Axes correspond to ϕ_H and ψ_H (e.g., H1′–C1′–O4–C4 and C1′–O4–C4–H4) values from −180° to +180°. Note that a copy of this map can be placed on each edge to test for periodicity.

ranges of ϕ and ψ defined according to the nonhydrogen atoms can cover the structures and retain the central location of most experimental structures and the desirable diagonal line (see Fig. 6, above).

3. Special Problems of Carbohydrates

Because of their many hydroxyl groups and substantial flexibility, carbohydrates exaggerate many of the problems experienced in modeling other molecules. Also, while some other molecules such as dimethoxymethane (DMM) have sequences of atoms that correspond to anomeric centers, such centers are relentlessly prevalent in carbohydrates. The following gives an overview of ways to cope with these problems.

3.1. Sampling

With all of the rotatable exocyclic substituents, it is necessary to ascertain that the modeling results are based on a sufficient exploration of the possible different states. How can one be certain that the final results depend only on the energy calculations of a

particular modeling method and not on a failure to consider the best possible arrangements of these exocyclic groups? As seen above, there are 729 combinations of staggered exocyclic orientations for glucose, and cellobiose has 59,049. Again, most will not be stable, but many will and their stabilities are dependent on ϕ and ψ. This leaves a large conformation space to sample. One approach is to use simulated annealing (28).

Two examples come from our recent work. In one (29), we developed ϕ,ψ energy maps to provide energies of distortion for conformations of substrates in complexes with hydrolyzing enzymes. The goal was to learn whether ϕ,ψ distortion might be part of the catalytic function. To sufficiently sample conformation space, we use different "starting structures," each with a particular combination of orientations of the exocyclic groups. The energy is computed for each of these starting structures at each ϕ,ψ location. The ϕ and ψ values were fixed at grid points in 20° intervals for a total of ($18\times18=$) 324 unique ϕ,ψ points. Initial studies, using Monte Carlo methods (30) and the OPLS-2005 (31) force field in MacroModel (24) identified 1,863 stable starting structures for cellobiose when both rings were in the normal chair forms, 3,485 when the reducing ring had the $^{2}S_{O}$ conformation, and 2,871 when the reducing ring had the $^{3}S_{1}$ shape. Thiocellobiose (where sulfur replaces the interresidue oxygen) yielded 2,277 different structures to test at each ϕ,ψ point.

In another project (32), methyl cellobioside, -tetraoside, and-hexaoside were investigated with Replica Exchange Molecular Dynamics studies in explicit TIP3P water. (Ref. (33) has a tutorial study on replica exchange MD of disaccharides in vacuum). Depending on the size of the carbohydrate, 714–3,741 molecules of water were included in the AMBER (34) calculations, using the GLYCAM-04 force field (35). To assure complete sampling for the hexamer, replicas had temperatures of 297–557° in 42 increments, with each simulation lasting more than 16 ns.

To make Ramachandran surfaces, the ϕ and ψ torsion angles of a disaccharide conformation are adjusted in increments of perhaps 10° or 20° and the energy calculated. Over the past 20 years, the energy has often been minimized for each ϕ,ψ conformation, holding ϕ and ψ constant but allowing all other parameters to find their nearest local minimum. Such studies are called "relaxed-residue" analyses. Their primary rationale is that they avoid collisions that would occur if the rings were kept rigid. (On one rigid-residue map, the crystallographic conformation of the sucrose moiety in raffinose corresponded to an unreasonable 100 kcal/mol (36)). Modeling software often provides for these calculations to step through ϕ,ψ space, using a tool called "dihedral driver" or "scan." Because the monosaccharide units of the disaccharide are flexible, there is the strong likelihood that an inelastic deformation of the molecule will occur during the scan.

For example, a hydroxyl group may simply rotate to a new staggered form, or the ring might lose its chair form. If that deformed structure is used to start the subsequent minimization, the energy at –180° will be different from the one at +180°. This is a sampling issue because the points after the deformation occurs will not be tested with the intended starting structure. Our procedure for avoiding this problem is to use the same starting geometry at each ϕ,ψ point, with only rigid rotations to the point in question.

Our approach is not without problems. Not having energy-minimized structures at each preceding point can lead to an interpenetration of the two monosaccharide residues in regions of high energy. The interpenetration causes much higher calculated energies or failure of minimization altogether but can be partially avoided by increasing the glycosidic bond angle to 150° for each starting structure. A similar sampling problem is a concern during MD simulations because simulations may be too short. At least with MD, the deformed structures could recover if the simulation runs long enough.

3.2. Hydrogen Bonding

Hydrogen bonding is especially important for most carbohydrates because of the high density of hydroxyl groups. If the stabilization from a typical moderate to weak hydrogen bond is 5.0 kcal/mol (37), model structures that have them would completely dominate those with otherwise similar structures. Further, the various acceptor oxygen atoms do not appear to accept hydrogen bonds with equal eagerness. The oxygen atom of the glycosidic linkage is a poor acceptor, and donations to the ring oxygen are less stabilizing than to hydroxyl groups. Further, there are cooperative effects. These effects are found in continuous donor–acceptor–donor–acceptor chains. Such sequences are more stable than an equal number of discontinuous hydrogen bonds and their H…O distances are shortened (38). In modeling hydrogen bonds, some workers find that no further consideration is needed after the charges are assigned to the atoms in their empirical models. Other modelers have devised elaborate schemes to provide calculated energies whenever hydrogen bonding is present. With QM, most workers are finding that reliable calculation of hydrogen-bonding geometries and energies requires fairly sophisticated techniques, such as post-Hartree–Fock theory or Density Functional Theory (DFT) and correction for Basis Set Superposition Error. Bader's AIM theory (see above) has been employed extensively in hydrogen bond studies (39).

Paradoxically, we have found that ϕ,ψ conformations in carbohydrate crystal structures can be predicted by isolated models with an elevated dielectric constant (e.g., 4.0–8.0) rather than the prescribed value of 1.0 for CHARMM and AMBER calculations or 1.5 for MM3 or MM4. Elevated dielectric constants reduce the

strengths of interactions between charged atoms, including those in hydrogen bonds. This work-around appears to provide a potential of mean force similar to what might otherwise have been obtained by MD with explicit solvent. This approach is not appropriate for investigation of specific molecule–molecule interactions such as might be found in modeling an entire crystal, for example. It seems to work only for modeling condensed-phase systems when the rest of the condensed phase is not explicitly present.

Less clear is the impact of C–H…O hydrogen bonds. Geometric criteria identified 14 such bonds in the crystal structure of dicyclohexyl cellobioside (40). These fairly weak interactions have typically been emphasized less when developing empirical force fields.

3.3. Anomeric Effects

The anomeric effect was the unexpected finding that the experimental α:β ratio for compounds such as D-glucopyranose favored the α-anomeric form more than would have been expected for an axial substituent on a cyclohexane ring (6). The exoanomeric effect was named for the preference of the substituent in methyl glucopyranoside to take an orientation *gauche* to the ring oxygen. This increased stabilization affects ϕ_{O5} directly, favoring –60° and +60° angles but not the *trans*, 180° angle. An external anomeric torsional effect has also been proposed that affects ψ (41). The term "general anomeric effect" covers the *gauche* preference for any R–X–C–Y atom sequence in organic chemistry where X denotes O, N, or S, and Y denotes any atom having lone pairs of electrons. Thus, DMM, which has a C–O–C–O–C sequence, prefers the *gg* conformation, while *n*-pentane prefers the all-*trans* form. The analogy between small molecules and the C5–O5–C1–O1–C_{Mc} sequence in methyl glucosides was noted many years ago (42, 43).

Besides conformational preferences, anomeric effects cause differences in bond lengths and angles. In the very accurate multipole refinement of crystalline sucrose at 20 K (44), the bonds from the anomeric carbons to the ring oxygens are 1.4192 and 1.4146 Å for the pyranosyl and furanosyl rings, respectively, whereas the distances between the ring oxygens and the other carbon atoms (C5 and C5′) are 1.4477 and 1.4543 Å, with standard deviations of 0.0005.

Often overlooked is the effect of an anomeric center, regardless of conformational details. It results in extra stability of the compound, as discussed by Tvaroška and Bleha (45). A "bond and group enthalpy increment scheme" can be used to calculate heats of formation (46), either by QM or MM. The increment in MM3 for O–C–O is 6.62 kcal, much larger than the corrections for QM (0.505 kcal/mol for HF/6-31G* and –0.351 kcal/mol for B3LYP/6-31G*). MM3 steric energies do not consider anomeric centers, so a large adjustment is needed. Fairly simple

QM does calculate most of this enthalpy, but some correction is still needed.

Earlier, we used this method to calculate heats of formation for analogs of some disaccharides (47). The analogs were based on the native sugars but all exocyclic groups were replaced by hydrogen. We also joined two tetrahydropyran molecules with an ether oxygen at the 4 positions (organic nomenclature), making isomeric pseudodisaccharide analogs with di-axial, axial-equatorial, and di-equatorial linkages. Analogs of α,α-, α,β-, and β,β-trehalose had enthalpies of –149.9, –147.4, and –147.5 kcal/mol, respectively. The analogs of nigerose, laminarabiose, maltose, cellobiose, and galabiose gave –142.6, –141.7, –141.3, –140.6, and –140.4 kcal/mol, and the di-axial, axial-equatorial, and di-equatorial pseudosugar analogs had values of –135.1, –135.4, and –135.8 kcal/mol. These were the B3LYP/6-31G* values, but quite similar results were computed by MM3 and HF/6-31G*. The trehalose analogs had two anomeric centers and roughly 12 kcal of stabilization, and the analogs of the other disaccharides had one center and 6 kcal, relative to the pseudosugar analogs with no centers.

Anomeric effects are likely to have several different causes and are affected by different factors. Magnitudes vary in different solvents, suggesting that there is an electrostatic component, and considerable effort has been directed to analyses of the changes in electronic structure (6). One group suggested that *gauche* conformers for anomeric sequences are stabilized by C–H…O hydrogen bonds and carried out Natural Bond Order calculations to confirm that result (48).

4. Quantum Mechanics Approaches

Empirical force fields (MM) summarize our knowledge of molecular structure and energy relationships for application to other molecules. On the other hand, electronic structure theory calculations (QM) are closer to experiment, with the possibility of increasing the resolution by using more computer time and memory. There are two other important concepts: balance between method and basis set, and DFT. Perdew *et al.* (49) has introduced a "Jacob's Ladder" to rate the various DFT methods, and Csonka *et al.* (50) evaluated various DFT methods for applicability to carbohydrates. The importance of choosing a QM method and basis set cannot be exaggerated. Consider the calculations of energy for four conformers of β-D-glucopyranose (5). Some levels of theory favored the seldom-observed chair ($^1C_4$) by as much as 17 kcal/mol while others favored the dominant $^4C_1$ form by that same amount.

The analogs described above in the studies of the anomeric effect are much less demanding of a particular level of QM theory. We have made relaxed ϕ,ψ surfaces for the cellobiose analog at HF/6-31G*, B3LYP/6-31G*, MP2/6-31+G**, and MP2/6-311+G** levels of theory, as well as B3LYP/6-311++G** calculations based on the B3LYP/6-31G* geometries. All of these maps are very similar, with the B3LYP maps being slightly flatter than the HF (51) and unpublished MP2 maps. Although it makes little difference for these analogs, the diffuse function (indicated by the +) is needed to avoid substantial overestimation of hydrogen bond energies for the native saccharides with the B3LYP and MP2 methods and Pople basis sets.

Another lesson from those analogs was that QM maps are fairly predictive of conformations of the native disaccharides in crystals. The addition of methyl groups at C5 to complete the carbon backbone improved predictions for cellobiose by reducing the size of the 1 kcal/mol region (51). Figure 6 shows a map for the methylated maltose analog with the crystalline maltose linkages (except cyclodextrins). (This energy map was shown earlier with conformations from cyclodextrins (18).) Structures inside the 1.0 kcal/mol contour are in accord with the exoanomeric effect and do not have intramolecular hydrogen bonds in the crystals. Their hydroxyl groups are either acylated and cannot form hydrogen bonds or they form intermolecular linkages. All other observed maltose-type structures have intramolecular, interresidue hydrogen bonds between O2′ and O3 that presumably compensate for the higher energy of the analog "backbone." The diagonal line corresponding to the helical parameter value of $h=0$ is also shown. To its left are conformations that lead to left-handed helices, with right-handed ones on the right. The secondary minimum at $\phi=80°$, $\psi=-280°$ is populated by some linkages in larger cycloamyloses, and is also compatible with the exoanomeric effect.

In at least one instance, the global minimum structure for the fully hydroxylated native disaccharide is not in the region of the crystal structures. That global minimum, for cellobiose, is stabilized by an exceptional hydrogen bonding network (52). In an important validation of that computational finding with QM, that structure, and the global minimum for the closely related lactose molecule have been observed experimentally in the gas phase at very low temperature (53).

As might be expected because of the time required, there are only a few molecular dynamics simulations based on QM energies. The Car–Parinello method has been applied in a study of the distortion energies of glucopyranose (54). The metadynamics approach was applied to force the ring into different puckering arrangements in a short time (44.4 ps). Our energy-minimization approach to mapping the energy of cellobiose

against the linkage torsion angles was also computationally expensive, with 181 different starting geometries, and only a quarter of the entire ϕ,ψ space was covered (55).

5. Empirical Force Fields and Some Applications

Empirical, or MM, force fields can be used with either energy minimization methods or MD. A minute's worth of MM time can be equivalent to a month or more of QM time. Therefore, many more issues can be evaluated with MM, making a more complete study possible. Even if it is desired to ultimately study the problem with QM, it can be worthwhile to study it first with MM.

Development of force fields that are "carbohydrate aware" continues. Besides the generally applicable MM3 and MM4 (56) programs, the GLYCAM-06 (57) force field primarily for AMBER is also intended for carbohydrates as well as proteins and lipids. Refinements of GLYCAM continue with the addition of explicit lone pairs on oxygen and nitrogen (58). The CHARMM (59) program also has had carbohydrate force fields available, e.g., the Ha *et al.* (60) parameterization and the CSFF parameters (61). New parameterizations for CHARMM that include carbohydrates are being released (62, 63). Some of the GROMOS parameter sets also consider carbohydrates (64). Force fields that incorporate these parameterizations were recently compared, as well as some older force fields (65). There are still substantial variations among the various systems. One factor is that some force fields have been parameterized so that aqueous solution data can be reproduced with MD using explicit water molecules, especially TIP3P (66).

DeMarco and Woods (67) reviewed several state-of-the-art simulations and studies pertaining to carbohydrate–protein interactions, both conformational and energetic. That paper then advocates a new carbohydrate nomenclature that is more useful for glycomics and integration with the Protein Data Bank protocols and data formats.

Tvaroška has used a hybrid method for studying enzymatic action on carbohydrates, in which the substrate is systematically deformed in the protein. In that work, the active site atoms and ligand are represented by QM and the rest of the protein and water are represented by MM (68). Schramm's group has a similar approach (69).

In our nonintegral hybrid method, QM maps for the analog furnish the conformational energy for the backbone of the disaccharide, while the hydrogen bonding and other steric considerations result from MM. The MM backbone map is subtracted

from the MM disaccharide map and the QM map is added. This approach is useful when the torsional energies of a particular linkage are not well parameterized. Originally, the method was developed for studying sucrose (70), which has two adjacent anomeric centers. More recently, similar hybrid studies of acarviosinde and thiocellobiose compensated for incomplete parameters involving the nitrogen and sulfur atoms, respectively (29).

6. Conclusions

It is not possible to completely understand the plant cell wall without understanding the structures of the various carbohydrates that compose it. Cellulose is, of course, the main component of many cell walls, and other cell wall polysaccharides are closely related to it in regard to their backbone structures. In this chapter, we have of course cited some of our papers on cellulose, and we have presented brief studies of the monomer and dimer of starch, α-D-glucose, and maltose, as examples of different but chemically similar materials. Without attempting to be intimidating, the examples are intended to illustrate the magnitude of the problems in modeling carbohydrates as well as some ways to surmount the problems. A checklist to be considered in a carbohydrate modeling study could be developed from the section headings above, along with the specific issues that instigated the research in the first place.

As early as the 1920s, ball-and-stick molecular modeling was applied to help understand the structure of cellulose, and Jones applied computerized modeling to cellulose in the late 1950s (see Zugenmaier's review (71)). The use of modeling to augment the limited experimental data available from cellulose is well established, but modeling has matured enough that it was able to make fairly bold predictions for the lowest energy conformation of cellobiose (52) that were subsequently confirmed by exotic experiments (53).

Cell walls are of course much more complicated than the small components that have been modeled so far. As computers become even faster, larger assemblies of molecules can be studied, along with physical and chemical processes. For example, current studies include models of cellulose crystallites in water (72) and dynamic conversions of such crystallites (73) and models composed of up to a hundred thousand atoms are being studied. Thus, the future of carbohydrate modeling will include the study of previously undetermined structures, repeat studies of familiar structures but with ever-improving methods, and ever-larger and more complete representations of complex structures such as the plant cell wall.

Numerous resources are available online, and at least two should be mentioned. The Centre de Recherches sur les Macromolécules Végétales (CERMAV) in Grenoble, France maintains a site (http://www.cermav.cnrs.fr/glyco3d/index.php) that has a library of disaccharide maps as well as a general tutorial on carbohydrate modeling. Interactive views of various mono- and oligosaccharides are also available. The GLYCAM (http://www.glycam.com) site at the Complex Carbohydrate Research Center at the University of Georgia in Athens provides several interactive tools for the carbohydrate modeler, including a builder for different structures.

References

1. Kurihara, Y. and Ueda, K. (2006) An investigation of the pyranose ring interconversion path of α-L-idose calculated using density functional theory. *Carbohydr Res* **341,** 2565–2574.
2. Steiner, T. and Saenger, W. (1998) Closure of the cavity in permethylated cyclodextrins through glucose inversion, flipping, and kinking. *Angew Chem Int Ed* **37,** 3404–3407.
3. Añibarro, M., Gessler, K., Usón, I., Sheldrick, G. M., Harata, K., Hirayama, K., Abe, Y. and Saenger, W. (2001) Effect of peracylation of β-cyclodextrin on the molecular structure and on the formation of inclusion complexes: an X-ray study. *J Am Chem Soc* **123,** 11854–11862.
4. Gould, I. R., Bettley, H. A.-A. and Bryce, R. A. (2007) Correlated ab initio quantum chemical calculations of di- and trisaccharide conformations. *J Comput Chem* **28,** 1965–1973.
5. Barrows, S. E., Dulles, F. J., Cramer, C. J., French, A. D. and Truhlar, D. G. (1995) Relative stability of alternative chair forms and hydroxymethyl conformations of β-glucopyranose. *Carbohydr Res* **276,** 219–251.
6. Grindley, T. B. (2008) Structure and conformation of carbohydrates. In: Fraser-Reid, B. O., Tatsuta, K. and Thiem, J. eds., Glycosciences. Springer, Berlin, pp. 3–55.
7. McNaught, A. D. (1996) Nomenclature of carbohydrates (IUPAC Recommendations 1996). *Pure Appl Chem* **68,** 1919–2008. http://www.chem.qmul.ac.uk/iupac/2carb/00n01.html#00.
8. French, A. D. and Dowd, M. K. (1994) Analysis of the ring-form tautomers of psicose with MM3 (92). *J Comput Chem* **15,** 561–570.
9. Boeyens, J.C.A. (1978) The conformation of six-membered rings. *J Cryst Mol Struct* **8,** 317–320.
10. Cremer, D. and Pople, J. A. (1975) A general definition of ring puckering coordinates. *J Am Chem Soc* **97,** 1354–1358.
11. Altona, C. and Sundaralingam, M. (1972) Conformational analysis of the sugar ring in nucleosides and nucleotides. A new description using the concept of pseudorotation. *J Am Chem Soc* **94,** 8205–8212.
12. Haasnoot, C. A. G. (1992) The conformation of six-membered rings described by puckering coordinates derived from endocyclic torsion angles. *J Am Chem Soc* **114,** 882–887.
13. Zotov, A. Y., Palyulin, V. A. and Zefirov, N. S. (1997) RICON – the computer program for the quantitative investigations of cyclic organic molecule conformations. *J Chem Inf Comput Sci* **37,** 766–773.
14. Geremia, S., Vicentini, L. and Calligaris, M. (1998) Stereochemistry of ruthenium bischelate disulfoxide complexes. A molecular mechanics investigation. *Inorg Chem* **37,** 4094–4103.
15. Bérces, A., Whitfield, D. M. and Nukada, T. (2001) Quantitative description of six-membered ring conformations following the IUPAC conformational nomenclature. *Tetrahedron* **57,** 477–491.
16. Joshi, N. V. and Rao, V. S. R. (1979) Flexibility of the pyranose ring in α- and β-D-glucoses. *Biopolymers* **18,** 2993–3004.
17. Hill, D. and Reilly, P. J. (2007) Puckering coordinates of monocyclic rings by triangular decomposition. *J Chem Inf Model* **47,** 1031–1035.
18. French, A. D. and Johnson, G. P. (2007) Linkage and pyranosyl ring twisting in cyclodextrins. *Carbohydr Res* **342,** 1223–1237.
19. Bader, R. F. W. (1990) Atoms in Molecules – A Quantum Theory. Oxford University Press, Oxford.

20. Csonka, G. I., Kolossváry, I., Császár, P., Éliás, K. and Csizmadia, I. G. (1997) The conformational space of selected aldo-pyrano-hexoses *J Mol Struct: THEOCHEM* **395–396,** 29–40.
21. Klein, R. A. (2002) Electron density topological analysis of hydrogen bonding in glucopyranose and hydrated glucopyranose. *J Am Chem Soc* **124,** 13931–19937.
22. Klein, R. A. (2006) Lack of intramolecular hydrogen bonding in glucopyranose: vicinal hydroxyl groups exhibit negative cooperativity. *Chem Phys Lett* **433,** 165–169.
23. Koch, U. and Popelier, P. (1995) Characterization of C–H–O hydrogen bonds on the basis of the charge density. *J Phys Chem* **99,** 9747–9754.
24. Schrodinger, Portland, Oregon. http://www.schrodinger.com.
25. Çarçabal, P., Jockusch, R. A., Hunig, I., Snoek, L. C., Kroemer, R. T., Davis, B. G., Gamblin, D. P., Compagnon, I., Oomens, J. and Simons, J. P. (2005) Hydrogen bonding and cooperativity in isolated and hydrated sugars: mannose, galactose, glucose, and lactose. *J Am Chem Soc* **127,** 11414–11425.
26. Allinger, N. L., Yuh, Y. H. and Lii, J.-H. (1989) Molecular mechanics. The MM3 force field for hydrocarbons. 1. *J Am Chem Soc* **111,** 8551–8567.
27. Allen, F. H. (2002) The Cambridge Structural Database: a quarter of a million crystal structures and rising. *Acta Crystallogr B: Struct Sci* **58,** 380–388.
28. Naidoo, K. J. and Brady, J. W. (1997) The application of simulated annealing to the conformational analysis of disaccharides. *Chem Phys* **224,** 263–273.
29. Johnson, G. P., Petersen, L., French, A. D. and Reilly, P. J. (2009) Twisting of glycosidic bonds by hydrolases. *Carbohydr Res* **344,** 2157–2166.
30. Mohamadi, F., Richards, N. G. J., Guida, W. C., Liskamp, R., Lipton, M., Caufield, C., Chang, G., Hendrikson, T. and Still, W. C. (1990) Macromodel – an integrated software system for modeling organic and bioorganic molecules using molecular mechanics. *J Comput Chem* **11,** 440–467.
31. Kaminski, G. A., Friesner, R. A., Tirado-Rives, J. and Jorgensen, W. J. (2001) Evaluation and reparametrization of the OPLS-AA force field for proteins via comparison with accurate quantum chemical calculations on peptides. *J Phys Chem B* **105,** 6474–6487.
32. Shen, T., Langan, P., French, A. D., Johnson, G. P. and Gnanakaran, S. (2009) Conformational flexibility of soluble cellulose oligomers: chain length and temperature dependence. *J Amer Chem Soc* **131,** 14786–14794.
33. Campen, R. K., Verde, A. V. and Kubicki, J. D. (2007) Influence of glycosidic linkage neighbors on disaccharide conformation in vacuum. *J Phys Chem B* **111,** 13775–13785.
34. Weiner, S. J., Kollman, P. A., Case, D. A., Singh, U. C., Ghio, C., Alagona, G., Profeta, S., Jr. and Weiner, P. (1984) A new force field for molecular mechanical simulation of nucleic acids and proteins. *J Am Chem Soc* **106,** 765–784.
35. Woods, R. J., Dwek, R. A., Edge, C. J. and Fraser-Reid, B. (1995) Molecular mechanical and molecular dynamic simulations of glycoproteins and oligosaccharides. 1. GLYCAM_93 parameter development. *J Phys Chem* **99,** 3832–3846.
36. Ferretti, V., Bertolasi, V. and Gilli, G. (1984) Structure of 6-kestose monohydrate, $C_{18}H_{31}O_{16}.H_2O$. *Acta Crystallogr C* **40,** 531–535.
37. Jeffrey, G. A. (1997) Introduction to Hydrogen Bonding. Oxford University Press, New York, p. 12.
38. Parthasarathi, R., Elango, M., Subramanian, V. and Sathyamurthy, N. (2009) Structure and stability of water chains $(H_2O)_n$, n = 5–20. *J Phys Chem A* **113,** 3744–3749.
39. Grabowski, S. J. (2006) Hydrogen Bonding – New Insights. Springer, Dordrecht, The Netherlands, 519pp.
40. Yoneda, Y., Mereiter, K., Jaeger, C., Brecker, L., Kosma, P., Rosenau, T. and French, A. (2008) van der Waals versus hydrogen-bonding forces in a crystalline analog of cellotetraose: cyclohexyl 4′-o-cyclohexyl β-D-cellobioside cyclohexane solvate. *J Am Chem Soc* **130,** 16678–16690.
41. Lii, J.-H., Chen, K.-H., Johnson, G. P., French, A. D. and Allinger, N. L. (2005) The external-anomeric torsional effect. *Carbohydr Res* **340,** 853–862.
42. Jeffrey, G. A., Pople, J. A. and Radom, L. (1972) The application of ab initio molecular orbital theory to the anomeric effect. A comparison of theoretical predictions and experimental data on conformations and bond lengths in some pyranoses and methyl pyranosides. *Carbohydr Res* **25,** 117–131.
43. Jeffrey, G. A., Pople, J. A. and Radom, L. (1974) The application of ab initio molecular orbital theory to structural moieties of carbohydrates. *Carbohydr Res* **38,** 81–95.
44. Jaradat, D. M. M., Mebs, S., Chęcińska, L. and Luger, P. (2007) Experimental charge density of sucrose at 20 K: bond topological, atomic, and intermolecular quantitative properties. *Carbohydr Res* **342,** 1480–1489.

45. Tvaroška, I. and Bleha, T. (1979) Lone pair interactions in dimethoxymethane and anomeric effect. *Can J Chem* **57,** 424–435.
46. Allinger, N. L., Schmitz, L. R., Motoc, I., Bender, C. and Labanowski, J. K. (1992) Heats of formation of organic molecules. 2. The basis for calculations using either ab initio or molecular mechanics methods. Alcohols and ethers. *J Am Chem Soc* **114,** 2880–2883.
47. French, A. D., Kelterer, A.-M., Johnson, G. P. and Dowd, M. K. (2000) B3LYP/6-31G*, RHF/6-31G* and MM3 heats of formation of disaccharide analogs. *J Mol Struct* **556,** 303–313.
48. Takahashia, O., Yamasakia, K., Kohnob, Y., Uedab, K., Suezawac, H. and Nishio, M. (2009) The origin of the generalized anomeric effect: possibility of CH/n and CH/π hydrogen bonds. *Carbohydr Res* **344,** 1225–1229.
49. Perdew, J. P., Ruzsinszky, A., Constantin, L. A., Sun, J. and Csonka, G. I. (2009) Some fundamental issues in ground-state density functional theory: a guide for the perplexed. *J Chem Theory Comput* **5,** 902–908.
50. Csonka, G. I., French, A. D., Johnson, G. P. and Stortz, C. A. (2009) Evaluation of density functionals and basis sets for carbohydrates. *J Chem Theory Comput* **5,** 679–692.
51. French, A. D. and Johnson, G. P. (2004) Advanced conformational energy surfaces for cellobiose. *Cellulose* **11,** 449–462.
52. Strati, G. L., Willett, J. L. and Momany, F. A. (2002) Ab initio computational study of β-cellobiose conformers using B3LYP/6-311++G**. *Carbohydr Res* **337,** 1851–1859.
53. Cocinero, E. J., Gamblin, D. P., Davis, B. G. and Simons, J. P. (2009) The building blocks of cellulose: the intrinsic conformational structures of cellobiose, its epimer, lactose, and their singly hydrated complexes. *J Am Chem Soc* **131,** 11117–11123.
54. Biarnés, X., Ardèvol, A., Planas, A., Rovira, C., Laio, A. and Parrinello, M. (2007) The conformational free energy landscape of β-D-glucopyranose. Implications for substrate preactivation in β-glucoside hydrolases. *J Am Chem Soc* **129,** 10686–10693.
55. French, A. D. and Johnson, G. P. (2006) Quantum mechanics studies of cellobiose conformations. *Can J Chem* **84,** 603–612.
56. Lii, J.-H., Chen, K.-H. and Allinger, N. L. (2003) Alcohols, ethers, carbohydrates, and related compounds. IV. Carbohydrates. *J Comput Chem* **24,** 1504–1513.
57. Kirschner, K. N., Yongye, A. B., Tschampel, S. M., González-Outeriño, J., Daniels, C. R., Foley, B. L. and Woods, R. J. (2008) GLYCAM06: a generalizable biomolecular force field. Carbohydrates. *J Comput Chem* **29,** 622–655.
58. Tschampel, S. M., Kennerty, M. R. and Woods, R. J. (2007) TIP5P-consistent treatment of electrostatics for biomolecular simulations. *J Chem Theory Comput* **3**, 1721–1733.
59. Brooks, B. R., Bruccoleri, R. E., Olafson, B. D., States, D. J., Swaminathan, S. and Karplus, M. (1983) CHARMM: a program for macromolecular energy, minimization, and dynamics calculations. *J Comput Chem* **4,** 187–217.
60. Ha, S. N., Giammona, A., Field, M. and Brady, J. W. (1988) A revised potential-energy surface for molecular mechanics studies of carbohydrates. *Carbohydr Res* **180,** 207–221.
61. Kuttel, M., Brady, J. W. and Naidoo, K. J. (2002) Carbohydrate solution simulations: producing a force field with experimentally consistent primary alcohol rotational frequencies and populations. *J Comput Chem* **23,** 1236–1243.
62. Guvench, O., Greene, S. N., Kamath, G., Brady, J. W., Venable, R. M., Pastor, R. W. and Mackerell, Jr., A. D. (2008) Additive empirical force field for hexopyranose monosaccharides. *J Comput Chem* **29,** 2543–2564.
63. Hatcher, E. R., Guvench, O. and MacKerell, Jr., A. D. (2009) CHARMM additive all-atom force field for acyclic polyalcohols, acyclic carbohydrates, and inositol. *J Chem Theory Comput* **5,** 1315–1327.
64. Oostenbrink, C., Soares, T. A., van der Vegt, N. F. A. and van Gusteren, W. F. (2005) Validation of the 53A6 GROMOS force field. *Eur Biophys J* **34,** 273–284.
65. Stortz, C. A., Johnson, G. P., French, A. D. and Csonka, G. I. (2009) Comparison of different force fields for the study of disaccharides. *Carbohydr Res* **344,** 2217–2228.
66. Jorgensen, W. L., Chandrasekhar, J., Madura, J. D., Impey, R. W. and Klein, M. L. (1983) Comparison of simple potential functions for simulating liquid water. *J Chem Phys* **79**, 926–935.
67. DeMarco, M. L. and Woods, R. J. (2008) Structural glycobiology: a game of snakes and ladders. *Glycobiology* **18,** 426–440.
68. Krupička, M. and Tvaroška, I. (2009) Hybrid quantum mechanical/molecular mechanical investigation of the β-1,4-galactosyltransferase-I mechanism. *J Phys Chem B* **113,** (32), 11314–11319.
69. Zhang, Y., Luo, M. and Schramm, V. L. (2009) Transition states of *Plasmodium falciparum*

and human orotate phosphoribosyltransferases. *J Am Chem Soc* **131,** 4685–4694.

70. French, A. D., Kelterer, A.-M., Cramer, C. J., Johnson, G. P. and Dowd, M. K. (2000) A QM/MM analysis of the conformations of crystalline sucrose moieties. *Carbohydr Res* **326,** 305–322.
71. Zugenmaier, P. (2008) Crystalline Cellulose and Derivatives. Characterization and Structrures. Springer, Berlin, pp. 8 and 38.
72. Matthews, J. F., Skopec, C. E., Mason, P. E., Zuccato, P., Torget, R. W., Sugiyama, J., Himmel, M. E. and Brady, J. W. (2006). Computer simulation studies of microcrystalline cellulose Iβ. *Carbohydr Res* **341,** 138–152.
73. Yui, T. and Hayashi, S. (2009) Structural stability of the solvated cellulose III_I crystal models: a molecular dynamics study. *Cellulose* **16,** 151–165.

Chapter 3

Oligosaccharide Mass Profiling (OLIMP) of Cell Wall Polysaccharides by MALDI-TOF/MS

Markus Günl, Florian Kraemer, and Markus Pauly

Abstract

In today's field of plant cell wall research, insights into the structure of wall components are obtained using many different techniques, ranging from spectroscopic and microscopic to chemical and biochemical. In this chapter, we describe one method: oligosaccharide mass profiling (OLIMP). Using OLIMP, we can harness the selective power of a specific wall hydrolase together with the speed and sensitivity of mass spectrometry to provide highly reproducible structural and compositional information about the wall molecule of interest.

Key words: Mass spectrometry, Matrix polysaccharides, Oligosaccharides, Glycosylhydrolases, Xyloglucan, Xylan, Pectins

1. Introduction

Oligosaccharide mass profiling (OLIMP) is a useful, rapid, and sensitive tool to reveal structural properties of cell wall polysaccharides (1, 2). The sample preparation and analysis of wall polysaccharides by OLIMP is simple and quick, as shown in Fig. 1. It comprises three steps: (1) the preparation of wall material from plant tissues, (2) enzymatic release of specific oligosaccharides from the wall materials, followed by (3) mass spectrometry on the solubilised oligosaccharides. Based on the observed ions and the known specificity of the enzymes used, specific structures can be assigned to the ions. Hence, OLIMP is capable of giving valuable insights into the diversity and substitution patterns of wall polysaccharides. The analysis of oligosaccharide composition with matrix-assisted laser desorption/ionisation time-of-flight mass spectrometry (MALDI-TOF/MS) is furthermore a method that does not involve strong acid or base treatments, which allows a

Zoë A. Popper (ed.), *The Plant Cell Wall: Methods and Protocols*, Methods in Molecular Biology, vol. 715,
DOI 10.1007/978-1-61779-008-9_3,

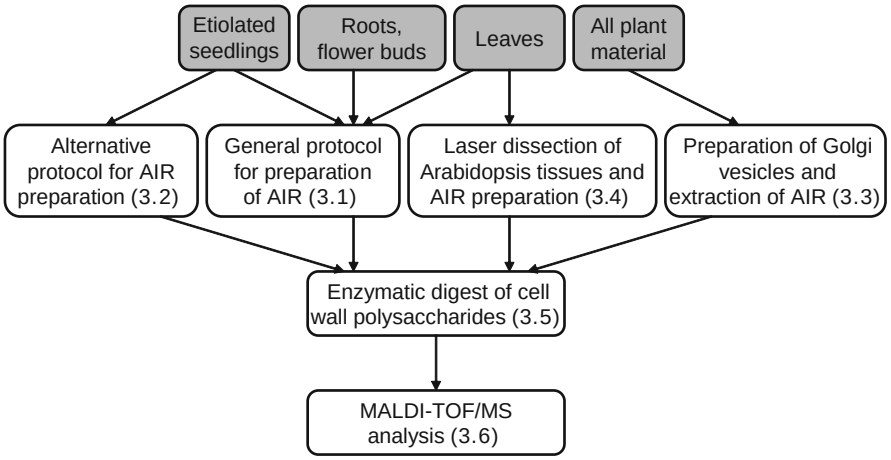

Fig. 1. Flow chart for OLIMP procedure using MALDI-TOF/MS. The first step encompasses preparation of AIR from plant material. AIR can be extracted from a variety of plant tissues, and the preparation method can be modified according to the wall material to be analysed (see Subheadings 1–4). Oligosaccharides can be released from AIR with enzymes specific for various polysaccharides (see Subheading 5) and subsequently analysed by MALDI-TOF/MS (see Subheading 6).

comprehensive analysis of the polysaccharide structure including *O*-acetylation and methylesterification substitution levels. OLIMP is very sensitive, requiring walls of only 5,000 cells for a complete analysis (3). In addition, a rapid analysis of the samples allows high-throughput experiments as shown by Lerouxel *et al.* (1) and Mouille *et al.* (4). However, structural isomers cannot be distinguished with OLIMP unless further structural information is obtained by mass fragmentation methods such as post-source decay (PSD). This procedure will generate several smaller fragments of a single oligosaccharide, which are further analysed by mass spectrometry (5, 6). This information can also be helpful for the analysis of polysaccharides for which limited structural information is available. Another limitation of OLIMP is its non-quantitative nature. Although the relative abundance of the oligosaccharide ions can be delineated from the spectra, the absolute amount present in the sample cannot, because the enzyme might not solubilise the polymer in its entirety from the wall (7), or because of ion suppression of the mass spectrometer at high concentrations or salt contaminants.

OLIMP can be used on a wide range of wall materials; it has been successfully used for the analysis of various *Arabidopsis* tissues such as leaves, roots, and flower buds. Because only very small samples are required for OLIMP analysis, it is possible to analyse specific cell types, cell compartments, or single etiolated seedlings (3).

OLIMP can be used to analyse a variety of wall polymers, limited only by the type of enzymes available (Fig. 2). A wide variety of commercially available hydrolases are suitable for use in OLIMP.

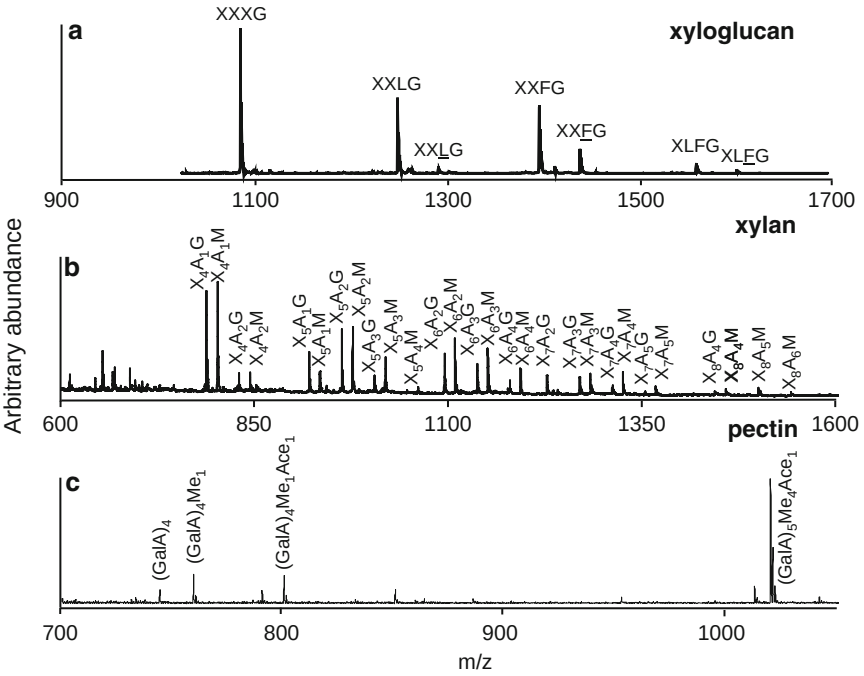

Fig. 2. OLIMP spectra of solubilised oligosaccharides (see Note 10). (**a**) Xyloglucan OLIMP spectrum from an *Arabidopsis* hypocotyl using a xyloglucan-specific endoglucanase. Nomenclature of oligosaccharide structures is according to Fry *et al.* (26), whereby the single letter indicates the reducing end sugar of the side-chain: e.g. *G* non-substituted glucosyl-residue; *X* xylosyl; *L* galactosyl; *F* fucosyl-residue. Underlined structures indicate galactosyl *O*-acetylation. (**b**) Xylan OLIMP spectrum derived from rice leaves using a xylanase M6 (Megazyme). Nomenclature for putative structures from Lee *et al.* (14). X_n number of pentoses, *G* glucuronic acid, and *M* methylated glucuronic acid. (**c**) Pectin OLIMP spectrum from *Arabidopsis* leaf walls using *endo*PG and pectin methylesterase. $(GalA)_n$ number of galacturonic acid; Me_n number of methylester; Ac_n number of *o*-acetyl substituents.

For example, for xyloglucan OLIMP, *endo*-β-(1–4)-glucanases are commonly used (8–12); these enzymes can be specific for xyloglucan (10–12). Similarly, for the analysis of xylan and pectin, *endo*-β-(1–4)-xylanases (13, 14) and *endo*-polygalacturonases (endoPG) (3, 15) are utilised, respectively. For the analysis of the pectic polysaccharides, a pectin methylesterase (PME) is added to the digestion to increase the susceptibility of pectin to hydrolysis by *endo*PG (3, 15). A large number of other enzymes have been recently cloned and are available to the public (16) with a potential to expand the wall components that can be assessed by OLIMP. For instance, digestion of cell wall material with lichenase leads to the release of mixed-linkage glucan-derived oligosaccharides that can be analysed with MALDI-TOF/MS (17, 18). Furthermore, with slightly altered experimental set-ups, glycosyltransferase and glycoside hydrolase activities can be assayed (19–23). For this purpose, purified enzymes or plant extracts are incubated with suitable substrates, and the product released is analysed by mass spectrometry.

2. Materials

2.1. Preparation of Alcohol-Insoluble Residue (AIR) from Arabidopsis Plant Materials

1. 2 mL Microcentrifuge tubes (Eppendorf, Hamburg, Germany) (see Note 1).
2. 70% (v/v) Aqueous ethanol.
3. 1:1 (v/v) Chloroform:methanol.
4. Acetone, pure.

2.2. Alternative Protocol for Preparation of AIR from Dark-Grown Seedlings

1. 2 mL microcentrifuge tubes (Eppendorf, Hamburg, Germany) (see Note 1).
2. Methanol, pure.
3. 1:1 (v/v) Chloroform:methanol.

2.3. Preparation of Golgi Vesicles and Extraction of AIR

1. Sucrose buffers: 0.1 M KH_2PO_4 buffer (pH 6.65), 10 mM $MgCl_2$, 8, 16, 33, 36, and 38% (w/v) sucrose.
2. STM buffer: 0.25 M sucrose, 1 mM $MgCl_2$, 10 mM Tris–HCl (pH 8.0).
3. Ethanol, pure.
4. 80% (v/v) Aqueous ethanol.
5. 1:1 (v/v) Chloroform:methanol.

2.4. Laser Dissection and AIR Extraction from Arabidopsis Leaf Tissue

1. Ethanol dilution series for dehydration of leaf tissue: 20, 30, 40, 50, 60, 70, 80, 90% (v/v) aqueous ethanol, and pure ethanol.
2. Pure xylene and 1:1 ethanol/xylene (v/v) solution.
3. Paraffin solutions for embedding: 30, 50, and 80% paraffin in xylene (v/v) and pure paraffin.

2.5. Enzymatic Digest of Cell Wall Polysaccharides

1. Enzymes: Xyloglucan-specific *endo*-glucanase (XEG) (EC 3.2.1.151, (24)), PME (Novozymes, Bagsvaerd, Denmark) *endo*-polygalacturonase M2 (*endo*PG), and xylanase M6 (Megazyme, Bray, Ireland).
2. 1 M ammonium formate stock solution (pH 4.5).
3. 4 M sodium hydroxide.
4. 1 M hydrochloric acid.
5. Float-A-Lyzer G2 dialysis devices (MWCO 8–10 kDa; Spectrum Labs, Greensboro, NC, USA).
6. 1 M sodium acetate stock solution (pH 6.0).

2.6. MALDI-TOF MS Analysis

1. 2,5-dihydroxybenzoic acid 10 mg/mL in water (see Note 2).
2. Bio-Rad MSZ-501 (D) cation exchange resin beads (see Note 3).

3. Methods

3.1. General Procedure for Preparation of Alcohol-Insoluble Residue (AIR) from Arabidopsis Plant Material

1. 0.1–10 mg plant material is placed in a 2 mL microcentrifuge tube and snap frozen in liquid nitrogen (see Note 4).
2. The plant tissue is ground using a Retsch ball mixer mill MM301 for 1 min at 25 Hz with a single steel ball (3 mm).
3. After the tissue has been ground, the steel ball is removed from the tube via a magnet.
4. 1 mL 70% Ethanol is added to the ground material; the microcentrifuge tube is vortexed briefly and centrifuged for 10 min at 20,000 × *g* in a tabletop centrifuge.
5. The supernatant is removed and the pellet is washed with 1 mL chloroform:methanol and vortexed briefly; the plant tissue is spun down for 10 min at 20,000 × *g* in a tabletop centrifuge.
6. The supernatant is discarded and the pellet dried under a stream of air. The dried tissue can be directly used for enzyme digestion (see Subheading 3.5; Note 5).

3.2. Alternative Protocol for Preparation of AIR from Dark-Grown Arabidopsis Seedlings

1. Approximately 10 seedlings (3–7 days old) are placed in a 2 mL microcentrifuge tube and 1 mL of methanol is added (see Note 4).
2. The tissue is homogenised using a Retsch ball mixer mill MM301 for 1 min at 25 Hz with a 5-mm stainless steel ball.
3. After the tissue has been homogenised, the metal ball is removed from the tube using a magnet.
4. The macerated material is centrifuged for 15 min at 20,000 × *g* and the supernatant is discarded.
5. The pellet is resuspended in 1 mL chloroform:methanol and centrifuged for 15 min at 20,000 × *g*.
6. The supernatant is discarded and the pellet air dried. Alternatively, the material can be dried under vacuum.
7. The dried tissue is ready for enzyme digestion (see Subheading 3.5).

3.3. Preparation of Golgi Vesicles and Extraction of AIR

The method described here is based on Muñoz *et al.* (25). Ultracentrifugation was performed using a Beckman Coulter SW 32 Ti rotor and 38.5 mL thin-wall rotor tubes. To prevent degradation, all preparation steps are performed in the cold room or on ice.

1. 5–10 mg of fresh plant material is transferred into a cold Petri dish and the material is finely chopped (1–2 mm sections) with a razor blade.

2. The chopped material is added to a cold mortar and 8 mL of cold 16% sucrose buffer is added.
3. The material is homogenised for 3 min with a pestle by rotation, applying only light pressure.
4. The suspension is filtered through a nylon mesh (diameter 30 μm) into a 50 mL Falcon tube, and the filtrate is centrifuged for 10 min at 2,000 × *g* and 4°C.
5. The ultracentrifugation tube is prepared by adding 8 mL of cold 38% sucrose buffer.
6. Add the supernatant of step 4 on top of the sucrose layer, trying not to disturb the sucrose solution. This can be accomplished by transferring the supernatant with a Pasteur pipette onto the side of the centrifuge tube walls. The sample is centrifuged for 100 min at 100,000 × *g*. The microsomal fraction will form as a milky layer on top of the 38% sucrose cushion with the microsome free cell extract layer above.
7. The microsome free cell extract (top layer) is removed with a Pasteur pipette.
8. 8 mL of cold 36% sucrose buffer is carefully added on top of the microsomal layer. Be careful not to disturb the layer. Then, 8 mL of cold 33% sucrose buffer is added on top of this layer, with care not to disturb the layer.
9. The tube is filled up to 3.5 mL with cold 8% sucrose buffer and centrifuged for 90 min at 100,000 × *g*. During this centrifugation step, the microsomal fraction (on top of the 36% sucrose layer) will separate and float on top, resulting in an enriched ER and Golgi fraction.
10. The fraction above the 33% cushion is the Golgi-enriched fraction. This fraction is transferred with a Pasteur pipette into a new ultracentrifuge tube and the fraction is diluted 1:2 with water.
11. The diluted fraction is centrifuged for 60 min at 100,000 × *g*.
12. The supernatant is discarded, and the pellet is washed twice with STM buffer to remove inorganic phosphate.
13. The pellet is resuspended in 1 mL STM buffer and stored at –80°C until needed.
14. To prepare AIR for OLIMP using MALDI-TOF/MS analysis, a portion of the solution containing 100 μg protein equivalent is used. The protein content can be determined (e.g. by Bradford assay).
15. Pure ethanol is added to the sample to reach a final concentration of 80% (v/v), and then the sample is filled up with 80% ethanol to a final volume of 1 mL.

16. The sample is centrifuged for 10 min at 20,000 × *g* and the supernatant is discarded.
17. 1 mL of chloroform:methanol is added to the pellet and the pellet is vortexed gently.
18. The sample is centrifuged for 10 min at 20,000 × *g*, the supernatant is discarded and the sample is air dried for 30 min.
19. The sample is now ready for enzyme digestion (see Subheading 3.5).

3.4. Laser Dissection of Arabidopsis Tissues and Their AIR Preparation

1. A leaf from a 5-week-old plant is harvested, directly transferred to a 2 mL microcentrifuge tube containing 1 mL 20% ethanol, and incubated at room temperature.
2. After 6 h, the 20% ethanol is removed and the procedure is repeated with increasing ethanol concentrations in 10% incrementals, each 6 h long, until incubation with pure ethanol is achieved. Incubation with pure ethanol is carried out twice. The pure ethanol is removed and ethanol:xylene (1:1, v/v) is added. The ethanol:xylene incubation is followed by three incubations with pure xylene. All incubations are carried out for at least 6 h with 1 mL of solvent.
3. After removal of pure xylene, the leaf tissue is incubated in 1 mL 30% paraffin xylene solution for 8 h at 42°C, followed by sequential incubation in 50 and 80% paraffin for 8 h at 52 and 58°C, respectively. Then, the tissue is transferred to pure paraffin and incubated for 7 h at 64°C. This step is repeated once.
4. The tissue is then placed in aluminium tray (3 mL) containing melted paraffin. After the paraffin solidifies at room temperature, the leaf is excised and mounted on a cutting block.
5. Sections of 20–40 μm are made and placed on glass microscope slides. The paraffin is removed by adding xylene dropwise onto the tissue, and soaking up the solubilised paraffin with a paper tissue from the side.
6. Tissues of interest are dissected using a laser dissector, according to the guidelines of the manufacturer. To analyse oligosaccharide composition, the equivalent of approximately 5,000 cells must be collected.
7. The collected cells (fragments) are transferred to a 0.5 mL microcentrifuge tube, washed with 200 μL xylene, and spun down at 20,000 × *g* in a tabletop centrifuge. After decanting the supernatant, 200 μL methanol:chloroform is added and the sample is briefly vortexed and centrifuged at 20,000 × *g* in a tabletop centrifuge.
8. Discard the supernatant and air dry the pellet. The dried cell fragments can be directly used for enzyme digestion (see Subheading 3.5; Note 5).

3.5. Enzymatic Digest of Cell Wall Polysaccharides

1. Depending on the polysaccharide to be investigated, the following digests can be carried out.
   (a) *Xyloglucan-specific endoglucanase (XEG) digest for analysis of the cross-linking glycan xyloglucan*: 50 µL of 50 mM ammonium formate (made with 2.5 µL ammonium formate stock solution) containing 0.2 U XEG (1 U of XEG releases 1 µmol xyloglucan oligosaccharides per min) are added to previously prepared AIR from plant material (see Subheadings 3.1–3.4) and incubated overnight (16 h) at 37°C and shaking at 120 rpm.
   (b) *Pectin digest with endo-polygalacturonase M2 (endoPG)*: 50 µL of 100 mM ammonium formate (prepared with 5 µL ammonium formate stock solution) containing 0.15 U *endo*PG (1 U of *endo*PG releases 1 µmol polygalacturonic acid oligosaccharides per min) and 0.08 U PME (1 U of PME releases 1 µmol methanol per min) are added to previously prepared AIR from plant material and incubated overnight (16 h) at 37°C, shaking at 120 rpm.
   (c) *Xylan digest*: 200 µL of 4 M sodium hydroxide is added to the previously prepared AIR and incubated for 1 h at 37°C under shaking (500 rpm). The samples are neutralised by adding 800 µL of 1 M hydrochloric acid and spun at 20,000 × *g* for 10 min in a tabletop centrifuge. The supernatant is transferred into a Float-A-Lyzer G2 dialysis device (MWCO 8–10 kDa), and dialysis is performed against ultrapure water with at least one change of water. After dialysis, the sample is transferred into a microcentrifuge tube and dried down in a speed vac. The dried material is digested overnight (16 h) in 200 µL 50 mM sodium acetate (prepared with 10 µL sodium acetate stock solution) containing 8 U xylanase M6 (1 U of xylanase releases 1 µmol arabinoxylan oligosaccharides) per min at 40°C and 120 rpm.
2. The digest is spun down for 10 min at 20,000 × *g* in a tabletop centrifuge, and the supernatant containing the released oligosaccharide fragments is transferred to a new microcentrifuge tube (see Note 6).

3.6. MALDI-TOF/MS Analysis

The analysis can be performed on a Kratos AXIMA CFR MALDI-TOF/MS instrument using a stainless steel MALDI target type DE1580TA (Kratos).

1. Prepare the MALDI-TOF/MS sample target by adding a layer of matrix. Use 2 µL of 2,5-dihydroxybenzoic acid per sample, spot and dry the matrix under vacuum (see Note 7).
2. Transfer 10 µL digest into a fresh 1.5 mL or 0.5 mL microcentrifuge tube.

3. Add approximately 5–10 cation exchange beads to each sample and incubate at room temperature for 15 min. (see Notes 3 and 8).
4. Transfer the desalted remaining liquid into a new microcentrifuge tube.
5. Spot as many samples as possible within a 3 min time frame (2 μL of the desalted oligosaccharide sample solutions) onto the target plate mesas containing the dried matrix spot (step 1). This time limit ensures that the first spot is not fully air-dried. Wait another 2 min and dry the target under vacuum. Repeat these steps until all your samples are spotted (see Note 9).
6. The mono- and oligosaccharides are detected by the MS as their sodium $[M+Na]^+$ and to a lesser degree potassium $[M+K]^+$ adducts. Therefore, the molecular mass detected will be 23 or 39 m/z larger than that of your analyte.

4. Notes

1. Testing different microcentrifuge brands and sizes showed that the Eppendorf 2 mL tubes are best suited to withstand milling with the ball mixer at very low temperatures. Of course, once in a while plastic pieces break or crack.
2. You can prepare a stock solution of the matrix chemical and store aliquots at –20°C for as long as 6 months. Thaw the aliquot 30 min before use and vortex vigorously several times. Make sure that the matrix is completely dissolved. Other solvents than water can be used, such as acetone, acetonitrile, methanol, or chloroform. However, in our experience water is the most effective solvent to achieve good spectra of oligosaccharides.
3. The MSZ501 (D) resin comes as a mixture of anion and cation resin beads, and the two forms can be distinguished visually. We use only the cation exchange resin beads. The anion exchange beads are lighter than the cation beads and have a blue indicator dye irreversibly bound, whereas the cation exchange beads are of a golden brown colour. To prepare the cation exchange resin you have to separate the brown and blue beads. For this purpose, transfer several spoonfuls of Bio-Rad MSZ-501 (D) resin beads into a 50 mL Falcon tube and fill with water. Swirl the tube a few times and decant the lighter, blue cation beads into a second 50 mL Falcon tube. Repeat until you have reached separation. The beads can be stored at room temperature for 6 months in water. However, before use, wash the beads several times with fresh water.

4. In our experience, a wide range of plant material and tissues can be used, but there are some limitations. Tissues that work very well are 4-day-old dark-grown seedlings and flower buds, and leaves of 2–3-week-old plants. In many cases, weighing of material may not be necessary, and we have found that the following amounts work well: 1–20 four-day-old dark-grown seedlings, flower buds of 1 inflorescence, 1 leaf of a 2–3-week-old plant.
5. To dry samples more quickly, an additional washing step with 1 mL acetone is recommended.
6. For samples that contain very small amounts of material, it is advisable to dry the supernatant containing the solubilised oligosaccharides using a vacuum centrifuge followed by re-dissolving the pellet in 10 μL water to increase the oligosaccharide concentration.
7. Prepare about 20 sample spots at a time with the matrix. Preparation of too many sample spots at a time can lead to longer drying times under vacuum, which can lead to poor quality of the matrix crystals. Prepare more sample spots than you have samples to provide some leeway in case some samples mix and you have to re-spot.
8. To add the ion exchange beads, use a small spoon-shaped spatula to hold a small amount of beads. With a second tapered spatula, move a small quantity of beads over the edge of the spoon. The beads will stick to the tapered spatula. Tap the tapered spatula on the rim of the microcentrifuge tube to transfer the beads into the tube.
9. As a quality control and to simplify troubleshooting, it is advisable to include a sample that is known to produce good spectra on each target that you prepare. If possible, use a previous sample derived from plant material rather than a pure standard.
10. Ionised oligosaccharides will be analysed as their sodium or potassium adducts; therefore, you should not expect to find masses that exactly match the predicted oligosaccharide masses, but with an additional +23 or +39 m/z.

Acknowledgements

The authors would like to thank Kirk Schorr (Novozymes) for providing the enzymes XEG and PME. Karen Bird, DOE-Plant Research Lab, Michigan State University, is thanked for editing the text.

References

1. Lerouxel, O., Choo, T. S., Seveno, M., Usadel, B., Faye, L., Lerouge, P., and Pauly, M. (2002) Rapid structural phenotyping of plant cell wall mutants by enzymatic oligosaccharide fingerprinting. *Plant Physiology* **130**, 1754–1763.
2. Günl, M., Gille, S., and Pauly, M. (2010) OLIigo Mass Profiling (OLIMP) of extracellular polysaccharides. *Journal of Visualized Experiments*. http://jove.com/index/details.stp?id=2046:doi: 10.3791/2046.
3. Obel, N., Erben, V., Schwarz, T., Kühnel, S., Fodor, A., and Pauly, M. (2009) Microanalysis of plant cell wall polysaccharides. *Molecular Plant* **2**, 922–923.
4. Mouille, G., Witucka-Wall, H., Bruyant, M. P., Loudet, O., Pelletier, S., Rihouey, C., Lerouxel, O., Lerouge, P., Höfte, H., and Pauly, M. (2006) Quantitative trait loci analysis of primary cell wall composition in Arabidopsis. *Plant Physiology* **141**, 1035–1044.
5. Ray, B., Loutelier-Bourhis, C., Lange, C., Condamine, E., Driouich, A., and Lerouge, P. (2004) Structural investigation of hemicellulosic polysaccharides from *Argania spinosa*: characterisation of a novel xyloglucan motif. *Carbohydrate Research* **339**, 201–208.
6. Yamagaki, T., Mitsuishi, Y., and Nakanishi, H. (1997) Structural analyses of xyloglucan heptasaccharide by the post-source decay fragment method using matrix-assisted laser desorption/ionization time-of-flight mass spectrometry. *Bioscience Biotechnology and Biochemistry* **61**, 1411–1414.
7. Pauly, M., Albersheim, P., Darvill, A., and York, W. S. (1999) Molecular domains of the cellulose/xyloglucan network in the cell walls of higher plants. *The Plant Journal* **20**, 629–639.
8. Aboughe-Angone, S., Nguerna-Ona, E., Ghosh, P., Lerouge, P., Ishii, T., Rayb, B., and Driouich, A. (2008) Cell wall carbohydrates from fruit pulp of *Argania spinosa*: structural analysis of pectin and xyloglucan polysaccharides. *Carbohydrate Research* **343**, 67–72.
9. Vanzin, G. F., Madson, M., Carpita, N. C., Raikhel, N. V., Keegstra, K., and Reiter, W. D. (2002) The *mur2* mutant of *Arabidopsis thaliana* lacks fucosylated xyloglucan because of a lesion in fucosyltransferase AtFUT1. *Proceedings of National Academy of Sciences of the United States of America* **99**, 3340–3345.
10. Cavalier, D. M., Lerouxel, O., Neumetzler, L., Yamauchi, K., Reinecke, A., Freshour, G., Zabotina, O. A., Hahn, M. G., Burgert, I., Pauly, M., Raikhel, N. V., and Keegstra, K. (2008) Disrupting two *Arabidopsis thaliana* xylosyltransferase genes results in plants deficient in xyloglucan, a major primary cell wall component. *Plant Cell* **20**, 1519–1537.
11. Hilz, H., de Jong, L. E., Kabel, M. A., Schols, H. A., and Voragen, A. G. (2006) A comparison of liquid chromatography, capillary electrophoresis, and mass spectrometry methods to determine xyloglucan structures in black currants. *Journal of Chromatography A* **1133**, 275–286.
12. Pauly, M., Eberhard, S., Albersheim, P., Darvill, A., and York, W. S. (2001) Effects of the *mur1* mutation on xyloglucans produced by suspension-cultured *Arabidopsis thaliana* cells. *Planta* **214**, 67–74.
13. Brown, D. M., Goubet, F., Wong, V. W., Goodacre, R., Stephens, E., Dupree, P., and Turner, S. R. (2007) Comparison of five xylan synthesis mutants reveals new insight into the mechanisms of xylan synthesis. *Plant Journal* **52**, 1154–1168.
14. Lee, C., Zhong, R., Richardson, E A., Himmelsbach, D.S., McPhail, B.T., and Ye, Z. -H. (2007) The PARVUS gene is expressed in cells undergoing secondary wall thickening and is essential for glucuronoxylan biosynthesis. *Plant and Cell Physiology* **48**, 1659–1672.
15. Egelund, J., Obel, N., Ulvskov, P., Geshi, N., Pauly, M., Bacic, A., and Petersen, B. L. (2007) Molecular characterization of two *Arabidopsis thaliana* glycosyltransferase mutants, *rra1* and *rra2*, which have a reduced residual arabinose content in a polymer tightly associated with the cellulosic wall residue. *Plant Molecular Biology* **64**, 439–451.
16. Bauer, S., Vasu, P., Persson, S., Mort, A. J., and Somerville, C. R. (2006) Development and application of a suite of polysaccharide-degrading enzymes for analyzing plant cell walls. *Proceedings of National Academy of Sciences of the United States of America* **103**, 11417–11422.
17. Sørensen, I., Pettolino, F. A., Wilson, S. M., Doblin, M. S., Johansen, B., Bacic, A., and Willats, W. G. T. (2008) Mixed-linkage (1 → 3), (1 → 4)-beta-D-glucan is not unique to the Poales and is an abundant component of *Equisetum arvense* cell walls. *Plant Journal* **54**, 510–521.
18. Doblin, M. S., Pettolino, F. A., Wilson, S. M., Campbell, R., Burton, R. A., Fincher, G. B., Newbigin, E., and Bacic, A. (2009) A barley *cellulose synthase-like CSLH* gene mediates (1,3; 1,4)-beta-D-glucan synthesis in transgenic *Arabidopsis*. *Proceedings of National Academy of Sciences of the United States of* America **106**, 5996–6001.

19. Cavalier, D. M., and Keegstra, K. (2006) Two xyloglucan xylosyltransferases catalyze the addition of multiple xylosyl residues to cellohexaose. *Journal of Biological Chemistry* **281**, 34197–34207.
20. Leonard, R., Pabst, M., Bondili, J. S., Chambat, G., Veit, C., Strasser, R., and Altmann, F. (2008) Identification of an Arabidopsis gene encoding a GH95 alpha1, 2-fucosidase active on xyloglucan oligo- and polysaccharides. *Phytochemistry* **69**, 1983–1988.
21. Lee, C. H., O'Neill, M. A., Tsumuraya, Y., Darvill, A. G., and Ye, Z. -H. (2007) The *irregular xylem9* mutant is deficient in xylan xylosyltransferase activity. *Plant and Cell Physiology* **48**, 1624–1634.
22. Iglesias, N., Abelenda, J. A., Rodino, M., Sampedro, J., Revilla, G., and Zarra, I. (2006) Apoplastic glycosidases active against xyloglucan oligosaccharides of *Arabidopsis thaliana*. *Plant and Cell Physiology* **47**, 55–63.
23. Leboeuf, E., Immerzeel, P., Gibon, Y., Steup, M., and Pauly, M. (2008) High throughput functional assessment of polysaccharide-active enzymes using MALDI-TOF mass spectrometry as exemplified on plant cell wall polysaccharides. *Analytical Biochemistry* **373**, 9–17.
24. Pauly, M., Andersen, L. N., Kauppinen, S., Kofod, L. V., York, W. S., Albersheim, P., and Darvill, A. (1999) A xyloglucan-specific endo-beta-1,4-glucanase from *Aspergillus aculeatus*: expression cloning in yeast, purification and characterization of the recombinant enzyme. *Glycobiology* **9**, 93–100.
25. Muñoz, P., Norambuena, L., and Orellana, A. (1996) Evidence for a UDP-glucose transporter in golgi apparatus-derived vesicles from pea and its possible role in polysaccharide biosynthesis. *Plant Physiology* **112**, 1585–1594.
26. Fry, S. C., York, W. S., Albersheim, P., Darvill, A., Hayashi, T., Joseleau, J. P., Kato, Y., Pārez Lorences, E., Maclachlan, G. A., McNeil, M., Mort, A. J., Grant Reid, J. S., Seitz, H. U., Selvendran, R. R., Voragen, A.G. J., and White, A. R. (1993) An unambiguous nomenclature for xyloglucan-derived oligosaccharides. *Physiologia Plantarum* **89**, 1–3.

Chapter 4

High-Voltage Paper Electrophoresis (HVPE) of Cell-Wall Building Blocks and Their Metabolic Precursors

Stephen C. Fry

Abstract

HVPE is an excellent and often overlooked method for obtaining objective and meaningful information about cell-wall "building blocks" and their metabolic precursors. It provides not only a means of analysis of known compounds but also an insight into the charge and/or mass of any unfamiliar compounds that may be encountered. It can be used preparatively or analytically. It can achieve either "class separations" (e.g. delivering all hexose monophosphates into a single pool) or the resolution of different compounds within a given class (e.g. ADP-Glc from UDP-Glc; or GlcA from GalA).

All information from HVPE about charge and mass can be obtained on minute traces of analytes, especially those that have been radiolabelled, e.g. by *in-vivo* feeding of a ^{3}H- or ^{14}C-labelled precursor. HVPE does not usually damage the substance under investigation (unless staining is used), so samples of interest can be eluted intact from the paper ready for further analysis. Although HVPE is a technique that has been available for several decades, recently it has tended to be sidelined, possibly because the apparatus is not widely available. Interested scientists are invited to contact the author about the possibility of accessing the Edinburgh apparatus.

Key words: Charge:mass ratio, Electrophoresis, Hydroxyproline oligoarabinosides, Ionisation, Monosaccharides, Nucleotide-sugars, Oligosaccharides, Radiolabelling, Sugar-phosphates, Uronic acids

1. Introduction

High-voltage paper electrophoresis (HVPE) is a seriously undervalued method for the analysis of small (<2,500 Da), hydrophilic, charged compounds such as uronic acids, amino sugars, sugar phosphates, sugar sulphates, sugar nucleotides, ascorbate metabolites and Krebs-cycle intermediates. In addition, it can be useful for normally uncharged compounds, such as neutral sugars, that can be given a charge by complexing with ions such as borate or

Zoë A. Popper (ed.), *The Plant Cell Wall: Methods and Protocols*, Methods in Molecular Biology, vol. 715,
DOI 10.1007/978-1-61779-008-9_4,

molybdate. HVPE is a very rapid separation method, typical run-times being 30–60 min with 10–20 samples typically being run simultaneously.

The electrophoretic mobilities of compounds on HVPE are *not* simply random values that need to be determined empirically. On the contrary, a compound's electrophoretic mobility is governed by a definable property, related to its charge:mass ratio, in a highly predictable way, discussed below (1).

Ion-exchange chromatography is in some ways comparable to HVPE and is an alternative method for analysis of charged compounds. For example, an anion-exchange matrix will bind anions, which can subsequently be released from the chromatography column by a gradient of increasing ionic strength or changing pH. This provides some evidence that the compound thus obtained had a negative charge. However, there is the potential pitfall that a compound might adsorb to an anion-exchange resin by some means *other than* electrostatic bonding, such as hydrophobic interaction. In contrast, a compound can migrate towards the anode on HVPE (relative to a neutral marker) *only* if it possesses a negative charge.

HVPE can be used analytically (e.g. 20 small samples on thin paper) or preparatively (a single large sample "streak-loaded" on a sheet of thick paper). The separated compounds can be detected either by staining (which is usually destructive) or by fluorescence, autoradiography (for ^{14}C, ^{35}S or ^{32}P) or fluorography (for ^{3}H), after which the sample can usually be recovered for further work. Alternatively, the compounds can be eluted from a preparative paper ready for further analysis, e.g. by MS, NMR or bioassay. Most of the recommended electrophoresis buffers are volatile, so the eluted compounds simply need to be dried, not specially desalted, prior to further analysis. Another advantage of HVPE is that – like paper chromatography – it provides a very convenient means of archiving samples that have been separated but not yet analysed: what you are storing is a dried paper with zones of potentially interesting compounds on it; this is much more convenient than column chromatography separations in which liquid fractions need to be stored.

2. Materials

2.1. HVPE Apparatus

The basic principle of HVPE, a form of zone electrophoresis, is that the sample is dried on a sheet of paper, which is then wetted with an aqueous buffer and subjected to a voltage gradient. The compounds in the sample migrate as zones towards the anode or cathode according to their net charge. The higher the voltage applied, the faster the compounds migrate; fast migration minimises

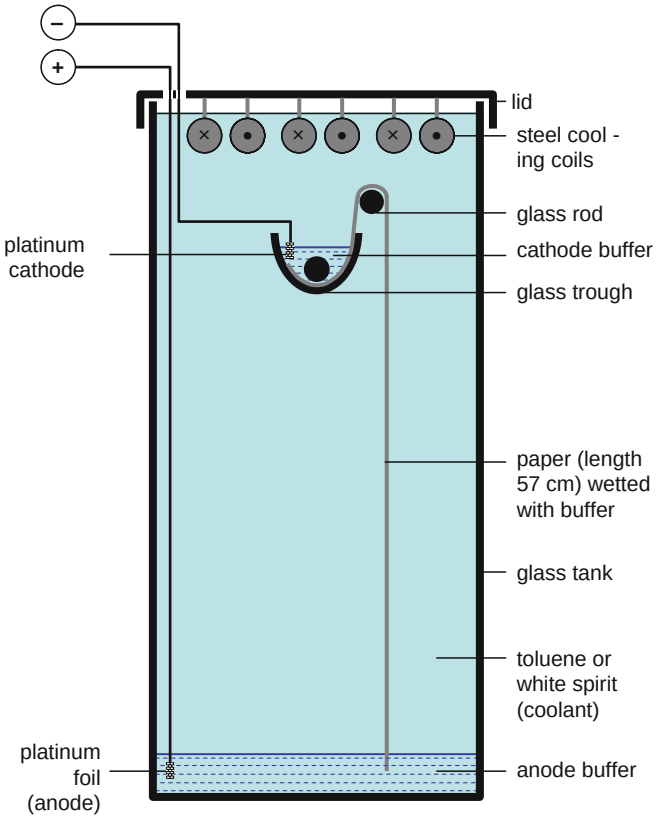

Fig. 1. Apparatus for high-voltage paper electrophoresis using a liquid coolant such as white spirit or toluene. This type of apparatus is available at the University of Edinburgh but not widely elsewhere; interested scientists are invited to contact the author about the possibility of accessing the Edinburgh apparatus. The tank is shown in cross-section. *Filled circle* = glass rod, *plus* = anode, *minus* = cathode, ⊗⊙⊗⊙⊗⊙ = cooling coil (suspended from the lid). Cold tap-water flows through the coil to cool the white spirit or toluene. The anode and cathode are platinum wires encased in glass tubes and connected at the tips to platinum foil.

diffusion of the spots. However, an excessively high voltage would overheat the wet paper and possibly degrade the compounds of interest. A cooling system must therefore also be used.

1. HVPE equipment: apparatus set up as shown in Fig. 1 (see Note 1).
2. 42×57-cm Sheets of filter paper (see Note 2): two types of paper are commonly used: Whatman No. 1 and the thicker Whatman 3CHR (formerly called 3MM) (see Notes 3 and 4).
3. Coolant for wet paper: white spirit, toluene, or 20:1 (v/v) toluene:pyridine. Cooling of the wet paper is best provided by a large volume of a water-immiscible liquid (see Notes 5 and 6).
4. Glass trough: capable of containing ~350 mL.

5. Glass bar for holding the wet paper in the glass trough.
6. Aqueous running buffer: ~350 mL in the glass trough at the cathode end and 1–2 L of identical running buffer at the bottom of the tank and into which the platinum anode dips (see Subheading 2.3).
7. Platinum cathode.
8. Platinum anode.
9. Steel cooling coils in the top 1–2 cm of the coolant to keep its temperature below about 30°C.
10. Lid.

2.2. HVPE Apparatus: Flat-Bed System

If the use of water-immiscible coolant liquids is not feasible, e.g. because hydrophobic compounds are of interest, HVPE can also be performed on a flat-bed system. The paper is laid on a polythene-insulated metal plate (containing cooling coils) with the ends of the paper dipping into troughs containing buffer and electrodes. An insulated and padded lid is tightly clamped on top of the paper to maximise uniform contact with the cooling plate (see Note 7).

1. 30 × 57-cm sheets of filter paper.
2. Polythene-insulated metal plate (containing cooling coils).
3. Insulated and padded lid to maximise uniform contact with the cooling plate.
4. Troughs containing buffer (see Subheading 2.3).

2.3. Recommended Buffers and Coolants

Whenever possible, volatile buffers are used so that after the run the electrophoretograms can be freed of buffer salts simply by drying. The three volatile buffers routinely used in our laboratory are listed in Table 1. The buffer concentrations recommended are a compromise between the need to provide adequate buffering capacity (the higher the better) and the need to avoid excessive heating during the run (a concentrated buffer has a higher conductivity and thus draws a higher current, giving excessive heating). Approximate p*K*a values of the compounds employed in the buffers are H_2SO_4, 2.0 (second ionisation); formic acid, 3.7; acetic acid, 4.7; pyridine, 5.3; borate, 9.2; molybdate, 6.0. White spirit (painters' turpentine substitute) is used as the coolant for HVPE at pH 2.0 or 3.5. A toluene/pyridine mixture is used for cooling the pH 6.5 buffer because pure toluene or white spirit would extract a high proportion of the pyridine (which is largely in its unionised form at pH 6.5) from the wet paper into the coolant, thus decreasing the pH of the buffer during the run.

Sodium borate and sodium molybdate are not volatile, so compounds that have been purified by HVPE in these buffers and eluted from the paper with water require de-salting, e.g. by re-electrophoresis in a volatile buffer such as at pH 2.0.

Table 1
Recommended HVPE buffer/coolant/marker combinations[a]

Buffer[b]	Composition	Coolant	Suitable coloured negative markers	Suitable coloured positive markers
Volatile buffers				
pH 2.0	Formic acid/acetic acid/H_2O (1:4:45 by vol.)	White spirit	Orange G [picrate would be lost into the white spirit]	N^{ε}-2,4-dinitrophenyl-lysine, methyl green, methyl violet
pH 3.5	Acetic acid/pyridine/H_2O (10:1:189 by vol.)[c]	White spirit	Orange G, picrate	Methyl green
pH 6.5[d]	Acetic acid/pyridine/H_2O (10:1:189 by vol.)	Toluene/pyridine (20:1)	Orange G, picrate	Methyl green
Sugar-complexing buffers				
Borate, pH 9.4	1.9% w/v Borax ($Na_2B_4O_7 \cdot 10H_2O$), pH adjusted with NaOH	White spirit	Orange G, picrate	[Not required]
Molybdate, pH 3–5	2.0% w/v $Na_2MoO_4 \cdot 2H_2O$, pH adjusted with formic acid or H_2SO_4	White spirit	Orange G, bromophenol blue, picrate	[Not required]

[a] In most buffer systems, a suitable neutral marker is glucose, which is revealed by staining. A better alternative is a non-ionic fluorescent compound, such as feruloyl-arabinose (20), which can be used at trace concentrations as an internal marker and visualised by its autofluorescence without staining. On HVPE in borate or molybdate buffers, glucose is unsuitable as a neutral marker since it may bind oxyanions; non-binding alternatives include 2,3,4,6-tetra-*O*-methylglucose

[b] Except for pH 3.5, the buffer specified is used both at the electrodes and for wetting the paper

[c] The composition of the electrode buffer is given; it should be diluted with an equal volume of water for wetting the paper

[d] For quantitatively accurate conclusions about charge:mass ratio to be drawn, the effective pH of the buffer in the paper *during electrophoresis* must be known. In the case of the pH 6.5 buffer, it sometimes happens that insufficient pyridine is added to the coolant (toluene), so that although the buffer used for wetting the paper had been accurately adjusted to pH 6.5 the pH of the buffer within the paper gradually falls during the run because some of the pyridine partitions from the paper into the toluene. A good test compound with which to show whether the pH in the paper during the run was correct is histidine, whose imido group has a p*K*a of 6.0. At pH 6.5, histidine has a net charge of +0.24, increasing strongly at slightly lower pHs. On the other hand, lysine has a constant net charge of approximately +1.00 at all pH values between 4.5 and 7.5. At pH 6.5, His should move towards the cathode at about 0.23× the rate of Lys. If His runs almost as fast as Lys, more pyridine should be added to the toluene

2.4. Buffers Used in Sample Preparation Prior to Electrophoresis

Since non-volatile salts (including buffers) can interfere in electrophoresis, these should be avoided during sample preparation. Any buffer used, e.g. to control the pH of an enzyme, should preferably be *volatile*. For the pH range 2–6, this can be similar to one of the mixtures given in Table 1 – if necessary diluted so that pyridine, which at high concentrations may inhibit enzymes, does not exceed ~2% v/v. For pHs in the 6–8 range, 1% v/v methylpyridines (adjusted to the desired pH with acetic acid) form useful volatile buffers e.g. 2,6-dimethylpyridine (lutidine; pKa ≈ 6.7) or 2,4,6-trimethylpyridine (collidine; pKa ≈ 7.4).

2.5. Wetting the Paper

1. Tissue paper.
2. Pipette.
3. Two glass rods.
4. Neutral marker: examples include glucose, [^{14}C]glucose, or 5-*O*-feruloyl arabinose.
5. Mobile marker: typically orange G (Table 1).
6. Glass plate: this should be slightly larger than the paper to be loaded.
7. Wash-bottle.
8. Buffer (see Subheading 2.4).

2.6. Detection of Analytes

1. Aniline hydrogen phthalate stain: 16 g phthalic acid in 490 mL acetone, 490 mL diethyl ether and 20 mL dH_2O is used to prepare a stock solution. 0.5 mL of aniline is added to 100 mL of stock solution immediately before use (2).
2. $AgNO_3$ stain (2) solution A: 0.8 g $AgNO_3$ is dissolved in 1.6 mL water, then diluted into in 104 mL acetone; if necessary, a little extra water added dropwise to redissolve the $AgNO_3$.
3. $AgNO_3$ stain solution B: 100 mL ethanol + 1.25 mL 10 M NaOH.
4. $AgNO_3$ stain solution C: 10% w/v sodium thiosulphate.
5. NH_3 solution.
6. Folin–Ciocalteu reagent.
7. Ninhydrin stain containing isatin: 270 mg ninhydrin, 130 mg isatin, 2 mL triethylamine in 100 mL acetone (2).
8. –80°C freezer.
9. Fluor: 7% (w/v) PPO in ether.
10. Autoradiography film.
11. Film for fluorography: autoradiography film pre-flashed with a photographic flash gun at such a distance that the background of the film will be slightly fogged when developed.

12. pH indicator: 0.04% (w/v) bromophenol blue in 10 mM NaOH.
13. Solution for removing pyridine: acetic acid/toluene 1:20 (v/v).
14. Solution for removing acetic acid: diethyl ether/methanol 3:1 (v/v).

3. Methods

3.1. Layout of Electrophoretogram

1. If it is known that all compounds of interest in the samples are neutral or negatively charged, the samples are loaded 12 cm from the cathode end of the paper. Conversely, if all compounds of interest are neutral or positively charged, they are loaded 9 cm from the anode end. If anions and cations are both of interest, the samples are loaded near the middle of the paper.
2. For analytical HVPE, the solutions are typically loaded at up to 12 and 30 μL per sample on Whatman No. 1 and 3CHR papers respectively. If necessary, multiple 12- or 30-μL portions are applied, with drying between each application.
3. A small amount of a visible mobile marker (e.g. 5 μg orange G; Table 1) is either pre-mixed with the sample (i.e. used as an internal marker) or loaded as a series of spots alternating with the samples (i.e. as an external marker).
4. A neutral marker: preferably internal (e.g. glucose, [^{14}C]glucose, or 5-*O*-feruloyl-arabinose; revealed by staining, autoradiography or autofluorescence, respectively), should also be included so that the extent of electro-endo-osmosis (see Subheading 3.3 below) can be monitored.

3.2. Wetting and Running the Electrophoretogram

1. The paper, with samples loaded, is laid on a large glass plate and wetted with electrophoresis buffer (Fig. 2a). The majority of the paper area can be wetted quite quickly, e.g. by use of a wash-bottle.
2. Any excess buffer is very lightly blotted from the electrophoretogram with dry tissue paper; care must be taken not to crease the wet paper during this process.
3. Wetting in the vicinity of the samples should be done last, and very carefully, with a pipette so that the samples do not diffuse excessively. This can be achieved if the area of the paper that includes the origin line is suspended between two glass rods; the wetting of this part of the paper is left until last. With practice, the wetting of this part of the paper can be made to focus the sample spots into narrow bands, instead of discs, along the origin line (Fig. 2b).

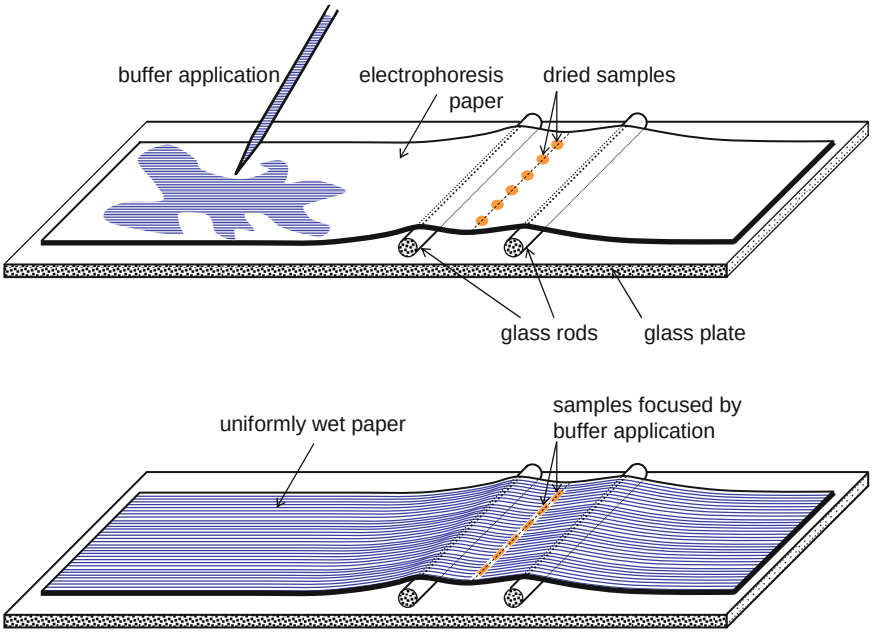

Fig. 2. Method for wetting the electrophoretogram with running buffer.

4. With the apparatus shown in Fig. 1, and with the samples loaded near the end of the paper, we typically perform HVPE at 4.5 kV for ~30 min (see Note 8). With a full-size sheet of Whatman No. 1 paper (57×42 cm), appropriately wetted, 4.5 kV delivers a current of about 150 mA (pH 2.0 buffer), 80 mA (pH 3.5) or 130 mA (pH 6.5) (see Note 9).
5. It should be noted that the pH of the buffer has an effect on the charge of the analytes (see Note 10, Tables 2 and 3).

3.3. Reporting the Electrophoretic Mobility of an Analyte

The mobility (m) of a substance in HVPE is often quoted relative to an easily detectable mobile marker, e.g. orange G, and a neutral one, e.g. glucose. The neutral marker is important since neutral compounds often move slightly away from the origin by electro-endo-osmosis. If orange G is used, the electrophoretic mobility is quoted as m_{OG}, where:

$$m_{OG} = \frac{(\text{distance moved by compound}) - (\text{distance moved by glucose})}{(\text{distance moved by orange G}) - (\text{distance moved by glucose})}.$$

A compound that remains at or near the origin while the neutral marker moves towards the anode should therefore usually be recorded as having electrophoretic mobility towards the cathode, as exemplified by AMP on HVPE at pH 2.0 (Fig. 3a). This is based on the assumption that a compound remaining at the origin has not been insolubilised there (as would happen for example with cellohexaose, which hydrogen-bonds strongly to the cellulose

Table 2
Typical pK_a values of some functional groups involved in plant cell-wall and apoplast biochemistry

Functional group	Q[a]	pK_a value(s)	Examples of compounds in the stated pK_a range[b]
–COOH	–	1.3	Oxalic acid (1st ionisation)
		1.8–2.5	α-Carboxy group of amino acids, oxaloacetic (1st), pyruvic, diketogulonic
		3.0–5.2	Most typical carboxylic acids, e.g. acetic, gluconic, glucuronic, glucaric (both), tartaric (both), malic (both), ferulic, side-chain of glutamic and aspartic, oxalic (2nd), citric (1st & 2nd)
		5.0–6.5	Tri- and a few di-carboxylic acids e.g. citric (3rd), succinic (2nd)
–SO_3H	–	1.3	Cysteic acid
Φ–OH[c]	–	8.5–10.5	Phenolic –OH of tyrosine, isodityrosine, dityrosine (2nd), feruloyl esters, ferulate, coumarate
		6.7	Phenolic –OH of dityrosine (1st)
Amino	+	10–11	Most typical amino groups, e.g. of methylamine, lysine (side-chain), putrescine (2nd); also imino group of proline
		8.5–10	α-Amino group of amino acids; amino group of putrescine (1st); also imino group of hydroxyproline
		7–8	Amino group of amino-sugars
Phosphate ester	–	1–2	Phosphate group of Glc-6-P, dihydroxyacetone phosphate etc. (1st)
	2–	6–6.5	Phosphate group of Glc-6-P, dihydroxyacetone phosphate etc. (2nd)
Imidazole	+	6.0	Imidazole ring of histidine

[a] Q = sign of charge when ionised
[b] 1st, 2nd, both etc., refer to compounds possessing more than one of the functional group mentioned
[c] Φ = benzene ring

of paper) — an assumption that can easily be tested by rinsing in water if there is any doubt. m_{OG} values estimated from Fig. 3a, with fructose as the neutral marker, are: ATP, 0.57; ADP, 0.36; AMP, –0.05; and (by definition) fructose, 0.00; orange G, 1.00.

Table 3
Behaviour of the principal ionisable groups present in cell-wall components and precursors (amino, carboxy and phosphate) on HVPE at pH 2.0 and 6.5

Observed net charge	Positive at pH 2.0	Little or no net charge at pH 2.0	Negative at pH 2.0
Positive at pH 6.5	$-NH_2$ group(s) present. Fewer or no acidic groups. *Lysine, putrescine*	n/a[a]	n/a[a]
Little or no net charge at pH 6.5	$-NH_2$ group(s) present. Equal –COOH groups. *Serine, isodityrosine*	No –COOH, $-NH_2$, phosphate or sulphate groups. *Glucose, glucitol*	n/a[a]
Negative at pH 6.5	$-NH_2$ group(s) present. More –COOH groups. *Aspartate, glutamate*	Weak acid group(s) present e.g. –COOH. *Galacturonate, malate, ascorbate, tartrate, citrate*	Strong acid group(s) present e.g. phosphate, sulphate, or a low-pK_a –COOH. Few or no $-NH_2$ groups. *Glucose 6-phosphate, oxalate*

The sample is run by HVPE at pH 2.0 and 6.5, and the direction of migration (if any) at these two pHs leads to the conclusions entered in the table. Specific examples of compounds in each category are given in italics
[a]Would be an implausible result

3.4. Calibrating with Electrophoretic Mobilities of "Knowns"

As mentioned above, the mobility of a compound during HVPE is decided by its charge and mass. More precisely, mobility is proportional to the $Q{:}M_r^{2/3}$ ratio, where Q is the net charge and M_r to the power of 2/3 is an indication of the molecule's relative surface area (1). It is useful to prepare a calibration curve of the relationship between m_{OG} and $Q{:}M_r^{2/3}$ ratio for a few "knowns" run as markers. The M_r of an authentic marker is usually given by the suppliers (but subtract any contribution due to a counter-ion such as the Cl in glucosamine hydrochloride, or any water of crystallisation).

If the pK_a of the "known" has been published (for example, see http://research.chem.psu.edu/brpgroup/pK$_a$_compilation.pdf), then its Q can be calculated. The pK_a is the pH at which 50% of the molecules are ionised (at the group under consideration) and 50% are not. For example, glyceric acid has a pK_a of 3.5; therefore, if a dilute solution of this compound is present in pH 3.5 electrophoresis buffer, 50% of the molecules at any moment are glycerate anions ($CH_2OH–CHOH–COO^-$, represented as A^-), while the other 50% are un-ionised

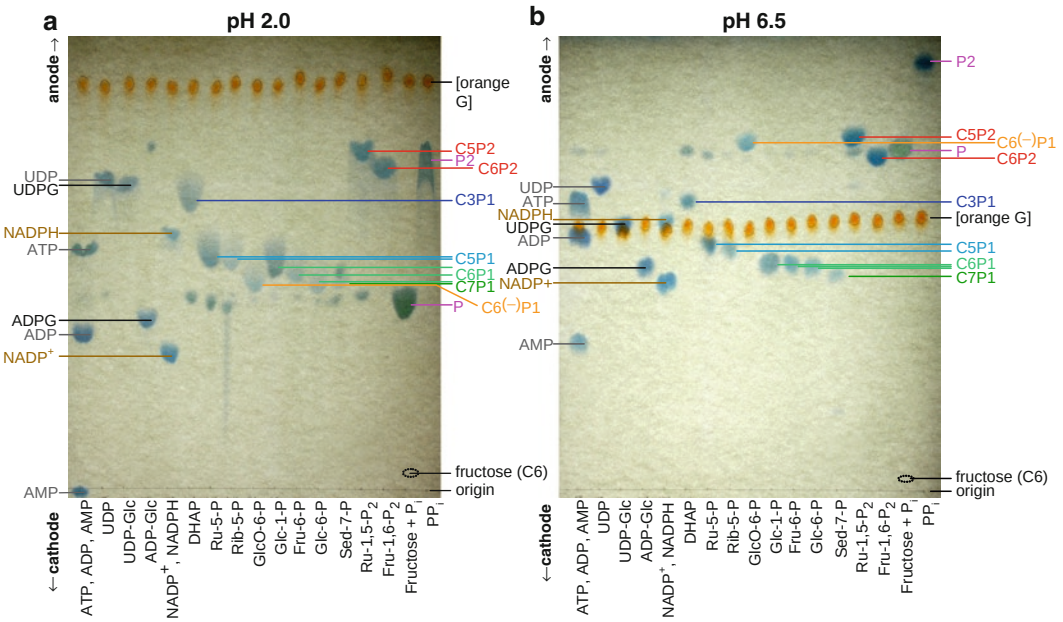

Fig. 3. HVPE at pH 2.0 and 6.5 used for separating *classes* of phosphorylated metabolites involved in cell-wall biosynthesis. Here, we are aiming not to resolve all possible phosphorylated metabolites, but to place them into classes of related compounds (sharing approximately the same charge:mass ratio) prior to more detailed analysis. For example, the hexose monophosphate pool can later be eluted from the electrophoretogram and hydrolysed to determine whether the sugar present is Glc, Gal, Man, Fru etc. Specific compounds run are listed along the origin of each electrophoretogram; classes of compounds are listed along the right-hand edge: for example, "C5P2" indicates a compound (ribulose 1,5-bisphosphate) with five carbon atoms and two phosphate groups. "$C6^{(-)}P1$" is gluconate 6-phosphate: note that its carboxy group is strongly ionised at pH 6.5 but not 2.0, causing it to migrate very differently on the two electrophoretograms. Nucleotides are listed along the left edge. Orange G, a coloured marker, was added into each sample before electrophoresis. Some of the standard solutions used contained P_i as a contaminant. Each compound was loaded at 50 μg per spot except dihydroxyacetone phosphate (DHAP; 25 μg), and P_i and PP_i (15 μg each). Electrophoresis was conducted on Whatman no. 1 paper at 4.5 kV for 30 min (**a**, pH 2.0) or 35 min (**b**, pH 6.5), and the spots were stained with molybdate reagent (2). Fructose (C6) is not phosphorylated and is therefore not immediately revealed by the molybdate reagent; its position (*dotted outline*) gradually becomes visible when the electrophoretogram is stored. Neutral compounds such as fructose (C6) migrate slightly towards the anode owing to electro-endo-osmosis. At pH 2.0, AMP has a small net positive charge and therefore moves slightly towards the cathode (relative to the neutral marker, fructose).

($CH_2OH–CHOH–COOH$, represented as HA). In other words, at pH 3.5, the reaction

$$H^+ + A^- \leftrightarrow HA$$

is precisely balanced with half the molecules on the left and half on the right. If a buffer of pH 2.0 had been used (i.e. with a 32-fold higher concentration of H^+ than at pH 3.5), then the equilibrium would have been pushed towards the right and there would have been much more HA and much less A^-. Conversely, if a buffer of pH 6.5 had been used, then the vast majority of the

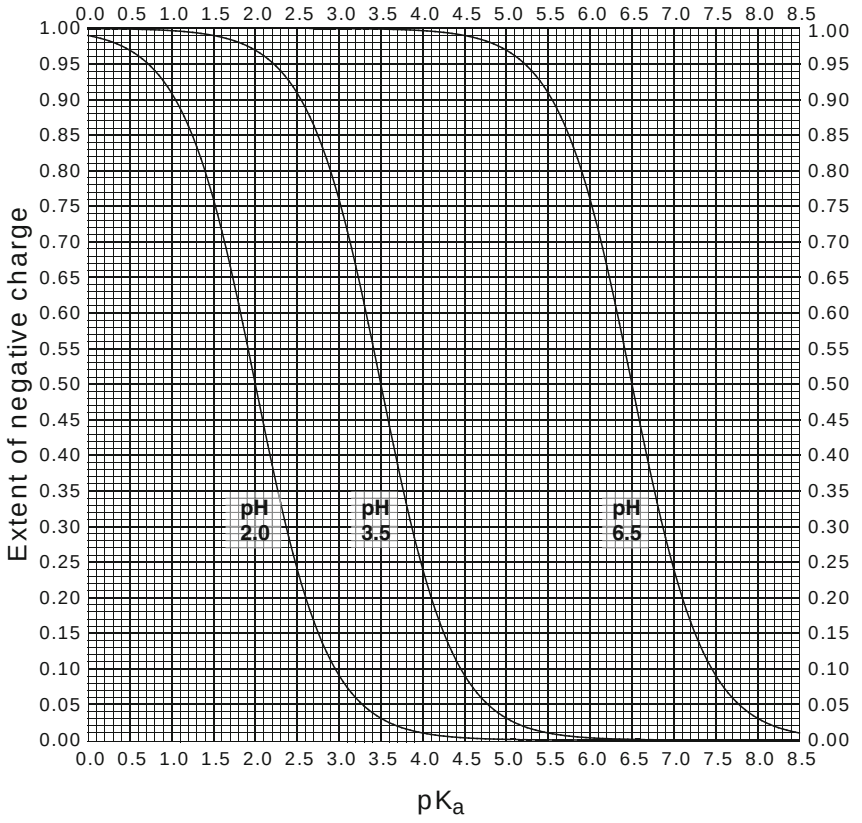

Fig. 4. Relationship between pH and pK_a. The degree of ionisation of any anionic group with a pK_a between 0.0 and 8.5 at each of the three recommended pH values for routine HVPE. For example, the graph shows that a carboxy group with pK_a = 6.0 has a charge of –0.76 in pH 6.5 buffer. The graph can also be used for cationic groups, but an amino group with pK_a = 6.0 has a charge of 1.00–0.76 = +0.24 in pH 6.5 buffer.

molecules would have been in the form A^-. The ratio of $[A^-]$ to [HA] at any given pH is given by the equation

$$\log\{[A^-]/[HA]\} = pH - pK_a.$$

Thus, with glucuronic acid (pK_a = 3.2) in pH 3.5 buffer, $\log\{[A^-]/[HA]\} = 0.3$, so $[A^-]/[HA] \approx 2.0$, and therefore 67% is present as the glucuronate anion and 33% as uncharged glucuronic acid. This can conveniently be described as GlcA having a net charge $Q = -0.67$ at pH 3.5. This and similar values can be read off in Fig. 4.

With weak *bases* such as glucosamine (Glc–NH_2), similar rules apply, but raising the pH *decreases* the % ionisation, e.g.

$$Glc{-}NH_3^+ \leftrightarrow H^+ + Glc{-}NH_2.$$

The equation for weak bases is:

$$\log\{[B]/[BH^+]\} = pH - pK_a,$$

where, in this example, B is Glc–NH_2 and BH^+ is Glc–NH_3^+.

In compounds with two or more ionisable groups, each group must be treated separately, and the net charge for the whole molecule is then calculated by addition of the individual charges. For example, with fumaric acid [which has two carboxy (–COOH) groups, with pK_a values of 3.0 and 4.4 respectively] in an electrophoresis buffer of pH 3.5, it is calculated that the "first" and "second" carboxy groups contribute partial charges of –0.76 and –0.11 respectively, and thus the compound has *net* charge $Q = -0.87$ at this pH. As a second example, leucine has a carboxy group with p$K_a = 2.3$ and an amino ($-NH_2$) group with p$K_a = 9.7$; thus in a buffer at pH 2.0 these two ionisable groups contribute partial charges of –0.33 and very nearly +1.00 respectively, giving leucine a net charge $Q = +0.67$.

3.5. Interpreting Electrophoretic Mobilities of "Unknowns"

Armed with a graph plotting m_{OG} against $Q{:}M_r^{2/3}$ for several "knowns", we can interpret the m_{OG} values of unknown compounds, run under the same conditions, in terms of their $Q{:}M_r^{2/3}$ ratios. If either of the parameters, Q or M_r, can be assumed, then we can estimate the other. For example, if the charge is known to be –1 at the pH of the electrophoresis buffer, then the compound's M_r can be estimated. Likewise, if the M_r is known (e.g. because we know it is a hexuronic acid), then we can estimate the p*K*a, which may identify which specific uronic acid it is.

On electrophoresis at pH 2.0, amino groups are fully positively charged. Therefore, a compound with a single amino group, and no groups that possess an appreciable negative charge at that pH, can be estimated for size by HVPE if we have a calibration curve. An example of a calibration curve is given in Fig. 5. The compounds tested here were reductively aminated sugars [oligosaccharidyl-1-amino-1-deoxyalditols (OADs), prepared from glucose and various authentic oligosaccharides of DP 2–9], which can be assumed to have $Q = +1.00$ at pH 2.0. The reference compounds were glucose and glucosamine, so the *y*-axis on this occasion reports m_{GlcN} rather than m_{OG}. The graph exhibits a good approximation to a straight line, so this calibration curve can be used to estimate the size of other OADs, prepared from unknown oligosaccharides.

At pH 6.5, most carboxy groups are almost fully negatively ionised, so each carboxy group can be assumed to have $Q \approx -1$. Again, then, if the approximate M_r is known, a suitable calibration curve allows us to "count" the carboxy groups. Thus, for example, the C_4 compound tartaric acid (with two COOH groups) is readily distinguished from threonic acid (also a C_4 compound but with one COOH group). Likewise, if the number of carboxy groups is known, then the M_r can be roughly estimated. These approaches have proved useful in characterising novel apoplastic metabolites of ascorbate by HVPE at pH 6.5 (3).

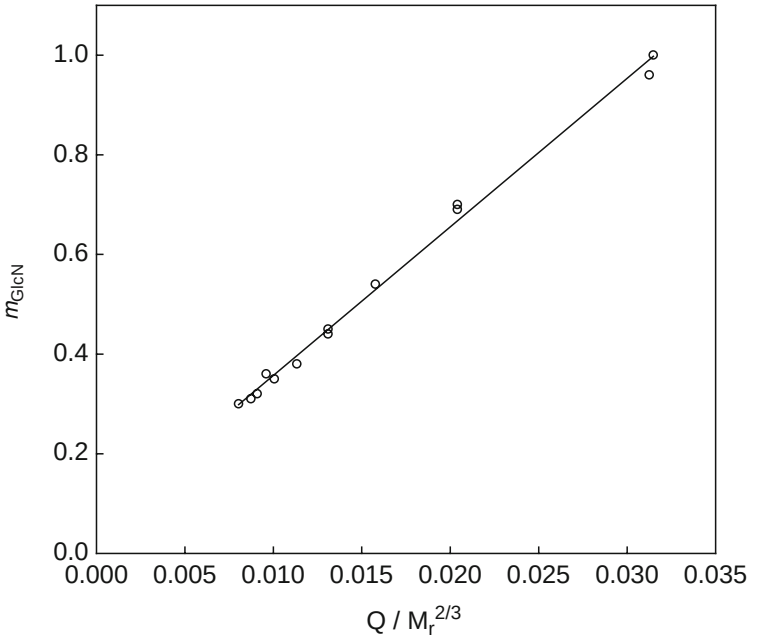

Fig. 5. A calibration curve plotting electrophoretic mobility against the $Q{:}M_r^{2/3}$ ratio for several "knowns" (reductively aminated sugars). 1-Amino-1-deoxyalditols were obtained by reaction of glucose or an oligosaccharide in the presence of $NaCNBH_3 + NH_4HCO_3$. The *x*-axis shows the $Q{:}M_r^{2/3}$ ratio calculated on the basis that $Q = +1.00$; the *y*-axis plots the observed electrophoretic mobility (as m_{GlcN}) at pH 2.0. The top data-point is for glucosamine itself ($m_{GlcN} = 1.00$, by definition). Other data-points refer to (in order of decreasing m_{GlcN}) reductively aminated glucose, maltose, cellobiose, maltotriose, maltotetraose, isomaltotetraose, maltopentaose, maltohexaose, XXXG, maltoheptaose, XXLG and XLLG (21).

3.6. Detection of Analytes: Staining

Staining can be used after HVPE to detect many cell-wall components with reasonable sensitivity, though usually destructively. Several methods are described in detail by Fry (2).

3.6.1. Staining for Sugars

Sugars are readily detected by staining with aniline hydrogen-phthalate or $AgNO_3$. The former is quicker, distinguishes different classes of sugar by colour differences, and is compatible with the subsequent detection of radioactivity, but fails to detect non-reducing sugars and is less sensitive than $AgNO_3$. $AgNO_3$ also detects non-reducing sugars e.g. trehalose and sucrose as well as "sugar-like" compounds such as glycerol, galactonate, threonate, tartrate, ascorbate and dehydroascorbate. $AgNO_3$ can detect down to about 0.1 µg of arabinose; aniline hydrogen-phthalate down to about 0.4 µg. Borate may interfere with $AgNO_3$ staining (see Note 11).

1. Aniline hydrogen-phthalate
   (a) Dip the paper through the aniline hydrogen-phthalate stain (see Subheading 2.6.1).

(b) Allow the paper to dry.

(c) Heat the paper in an oven at 105°C for 5 min.

2. $AgNO_3$ staining

(a) Work in subdued light throughout. Dip the electrophoretogram through solution A (see Subheading 2.6.2).

(b) Dry for ~15 min.

(c) Dip the electrophoretogram with a smooth continuous motion through solution B (see Subheading 2.6.3).

(d) Dry ~15 min.

(e) Repeat steps 3 and 4 until the spots can be seen clearly.

(f) Dip the paper through solution C (see Subheading 2.6.4) and then wash in tap water for 1–2 h.

(g) Dry the paper.

3.6.2. Staining for Phosphates

Phosphates, including sugar-phosphates and NDP-sugars, are detected by molybdate reagent (2) (Fig. 3), although this is relatively insensitive (down to 2 µg of Glc-6-P) and is mainly used for localisation of markers run alongside (or mixed with) radioactive samples of interest.

3.6.3. Staining for Phenolics

Phenolics can often be visualised by their autofluorescence, sometimes intensified by exposure of the paper to NH_3 vapour, or less sensitively by spraying with commercially available Folin–Ciocalteu phenol reagent followed by exposure of the paper to NH_3 vapour until the yellow background is decolourised.

3.6.4. Staining for Amino Acids

Amino acids can be detected very sensitively with ninhydrin, which is rendered more specific for hydroxyproline by inclusion of isatin (2).

3.6.5. Staining Acidic Compounds

Acidic compounds such as oxalic or citric acids, that are not phosphates or carbohydrate-related, and therefore cannot be stained with molybdate or $AgNO_3$, can be detected if the paper is sprayed with an aqueous solution of a pH indicator (0.04% bromophenol blue in 10 mM NaOH). Acidic analytes show up as yellow spots on a blue background. Before use of a pH indicator, the electrophoretogram should be freed of any traces of pyridine (by dipping through acetic acid/toluene 1:20 and re-drying) and then thoroughly freed of acetic acid; this can be promoted by repeated dipping of the paper through diethyl ether/methanol (3:1) and re-drying. After the paper has been sprayed with the pH indicator, the contrast between non-volatile acidic analytes and the background colour can be adjusted if the paper is lightly exposed to NH_3 vapour. The spots may be transient and should be recorded as soon as they appear.

3.7. Detection of Radioactivity

Radioactivity is often detected on paper electrophoretograms by autoradiography (for ^{14}C, ^{32}P, ^{33}P and ^{35}S) or fluorography (^{3}H).

3.7.1. Autoradiography

1. Expose the electrophoretogram to film.
2. After incubating in the dark develop the film in a darkroom.

3.7.2. Fluorography

1. The paper is dipped through a fluor (7% w/v PPO in ether) and dried.
2. The film is pre-flashed (see Subheading 2.6.8).
3. The electrophoretogram is exposed to the film at a low temperature e.g. –80°C (see Note 12).

3.8. Detection of Analytes: Bioassay

Substances separated on the electrophoretogram can be eluted for further analysis (see Subheading 3.9) – including bio-assays (for oligosaccharins), in which case the paper should be carefully freed of all traces of the liquids used during electrophoresis (acetic acid, pyridine, trace contaminants from the white spirit, etc.). Anionic analytes on the paper (e.g. oligogalacturonides) will be present as their pyridinium salts; thus, after electrophoresis, the dried paper is dipped in toluene/acetic acid (20:1 v/v) and re-dried to remove the pyridine, then dipped in diethyl ether/methanol (3:1 v/v) and re-dried to remove the acetic acid. If necessary, the paper can be very thoroughly washed in pure toluene (e.g. by descending paper chromatography with the toluene as the solvent) to remove contaminants picked up from the coolant (white spirit or practical-grade toluene).

3.9. Elution Method

Substances separated on the electrophoretogram can be eluted, usually in water, for further analysis. Elution is achieved in a minimal volume of eluent by the syringe-barrel method (4).

1. The relevant zone of the electrophoretogram is cut out with scissors and tightly packed into a plastic syringe barrel, which is then suspended in a plastic centrifuge tube (Fig. 6).
2. The paper is wetted with just enough water to moisten it.
3. The assembly is bench-centrifuged (e.g. $4{,}000 \times g$), causing the eluate to collect in the bottom of the centrifuge tube.
4. Moistening and centrifugation are repeated, typically 4–5 times, until the analyte of interest has been eluted. Simultaneously eluting an orange G marker spot can indicate when elution is complete.

3.10. Specific Examples

3.10.1. Monomeric Sugar Acids and Related Metabolites

Monomeric uronic acids, aldonic acids, aldaric acids, Krebs-cycle intermediates and many ascorbate metabolites possess 1–3 ionisable carboxy groups. At pH 6.5, most carboxy groups are almost fully ionised: any carboxy group with a pK_a less than 5.2 will be >95% fully ionised (Fig. 4). Thus, the advantage of HVPE at pH 6.5 is that it can be used to "count" the compound's carboxy

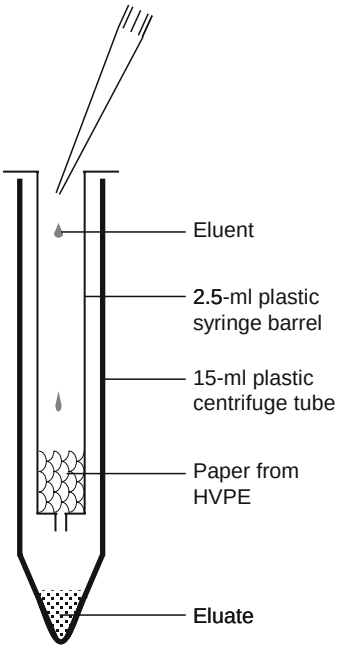

Fig. 6. Method for the elution of analytes from electrophoresis paper.

groups if its approximate M_r is known, or to estimate its M_r if the number of carboxy groups is known. If neither is known (as was the case with novel metabolites of ascorbate e.g. 4-*O*-oxalyl-L-threonate and a corresponding cyclic oxalyl ester; (3)), useful information can still be obtained, for example that the compound is either a (C_6 2–)[1] compound such as oxalyl-threonate or a (C_3 1–) compound such as glyceric acid.

At pH 6.5 there is little resolution between different members of a given class e.g. hexuronic acids, which all have the same M_r and a single carboxy group and are thus grouped together into a tight zone on the electrophoretogram. On the other hand, pH 3.5 is reasonably close to the pK_a of many carboxy groups. Therefore, small differences in pK_a, such as exist between isomeric uronic acids (e.g. GalA, GlcA, ManA and GulA), enable their separation from each other (Fig. 7) (5).

3.10.2. Acidic Oligosaccharides

HVPE at pH 6.5, at which uronic acid carboxy groups are almost fully ionised, is valuable for determining whether an acidic oligosaccharide of known size (degree of polymerisation, as estimated for example by gel-permeation or paper chromatography) consists only of acidic residues (e.g. galacturonobiose) or of a mixture of neutral and acidic residues (e.g. α-D-glucuronosyl-(1→3)-L-galactose (6)). As above, the charge:mass ratio is obtained.

[1]i.e. a compound with 6 carbon atoms and two negative charges.

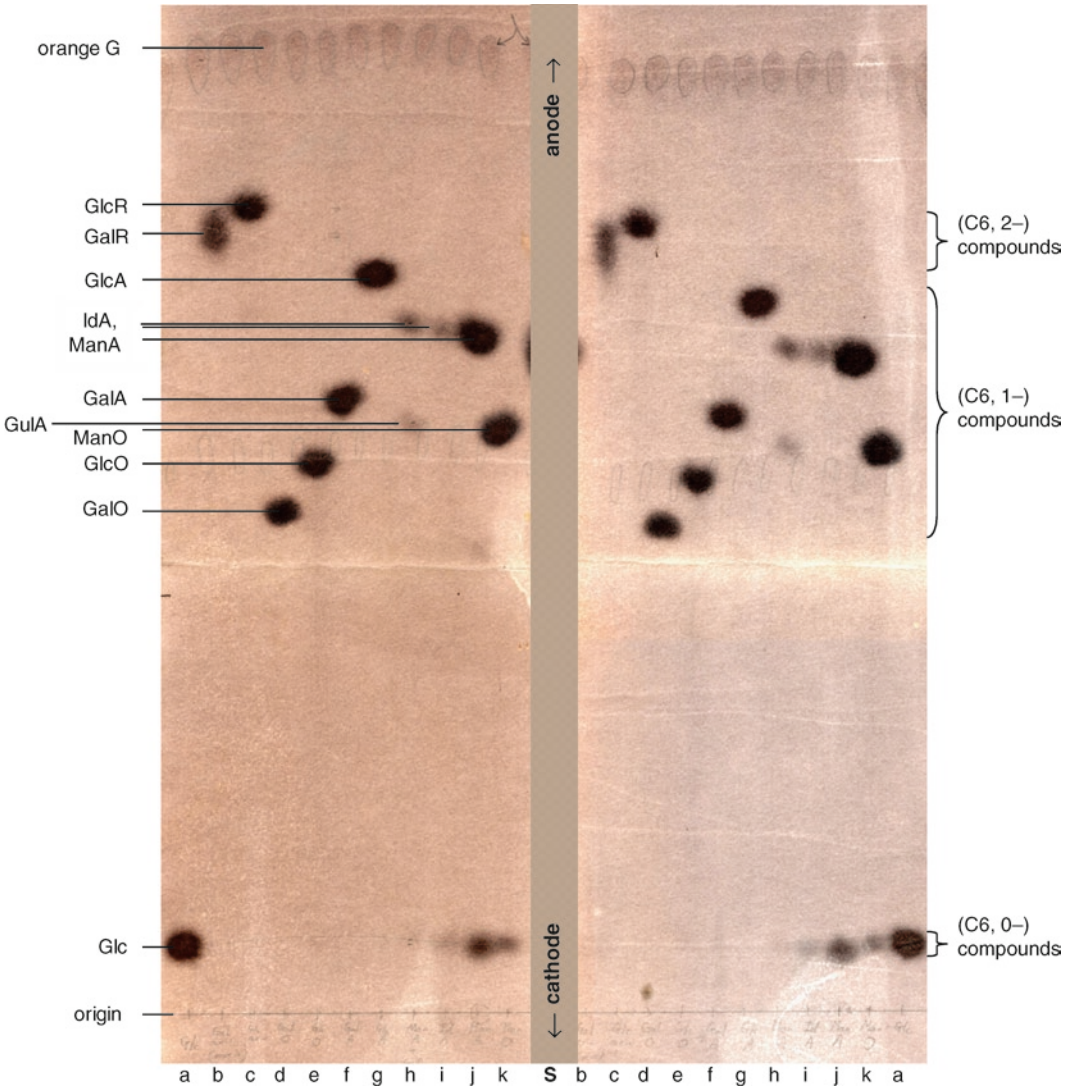

Fig. 7. HVPE at pH 3.5 used for separating specific sugar-acids, differing subtly in their p*K*a values. The specific compounds are listed along the *left edge*; classes of compounds are listed on the *right*: for example, ("C6, 1–)" indicates a compound (e.g. galacturonic acid) with six carbon atoms and one negatively ionised group. Orange G, a coloured marker, was loaded between each sample. Each compound was loaded at 10 μg per spot except h and i, which were crude preparations of unknown concentration; h is a mixture of ManA and GulA. Electrophoresis was conducted on Whatman 3CHR paper at 4.5 kV for 50 min, and the spots were stained with $AgNO_3$. Several of the sugar-acids are accompanied by neutral lactones, co-migrating with glucose. The suffixes -A, -O and -R indicate -uronic acids, -onic acids and -aric acids: for example, *GalA* galacturonic acid; *GalO* galactonic acid; *GalR* galactaric acid. The *left* and *right halves* are from a single, wide electrophoretogram, illustrating the good reproducibility of m_{0G} values; the compounds shown acted as external markers for a radioactive experimental sample (central band "S"; not shown in full).

3.10.3. Sugar Phosphates and Sulphates

Since phosphate and sulphate are strongly acidic groups, they remain appreciably ionised during HVPE at pH 2.0 (Fig. 3a), unlike most of the carboxylic acid groups present in carbohydrates. Thus, it is possible to obtain an excellent class-separation of sugar phosphates from non-phosphorylated sugars at this pH (7). Here,

we are aiming not to resolve all possible phosphorylated metabolites from each other, but to place them into classes of related compounds (sharing approximately the same charge:mass ratio) prior to more detailed analysis. For example, the hexose monophosphate pool can later be eluted from the electrophoretogram and hydrolysed; this will reveal whether the sugar present is Glc, Gal, Man, Fru etc. At pH 2.0, all the sugar phosphates are tightly clustered, though, as expected, the tendency is for some resolution to occur on the basis of size: in order of decreasing mobility towards the anode, we have triose-phosphates, tetrose-phosphates, pentose-phosphates, hexose-phosphates and heptose-phosphates (Fig. 3a). Gluconic acid 6-phosphate co-migrates with glucose 6-phosphate because the carboxy group of the former is not appreciably ionised at pH 2.0. Sugar bisphosphates, such as ribulose 1,5-bisphosphate and fructose 1,6-bisphosphate, migrate considerably faster than the corresponding monophosphates because both phosphate groups ionise.

At pH 6.5 (Fig. 3b), each phosphate group carries a stronger negative charge than at pH 2.0 and there is a more reliable correlation between size and mobility (mobility of triose- > tetrose- > pentose- > hexose- > heptose-phosphates). In this case, however, gluconic acid 6-phosphate runs much faster than glucose 6-phosphate because its carboxy group is almost fully ionised at pH 6.5.

Often the isolation of a given *class* of compounds by HVPE at pH 6.5, e.g. the hexose monophosphates, provides the metabolic information required for the project in hand, since Fru-6-P, Glc-6-P, Glc-1-P and Gal-1-P are all readily inter-converted *in vivo*. However, if necessary, a further class separation is easily achieved by graded hydrolysis: the aldose 1-phosphates (Glc-1-P, Gal-1-P, Man-1-P, etc.) are completely hydrolysed to the free monosaccharides under mildly acidic conditions (0.1 M trifluoroacetic acid at 100°C for 25 min), whereas aldose 6-phosphates (e.g. Glc-6-P, Man-6-P), ketose 6-phosphates (e.g. Fru-6-P) and ketose 1-phosphates (e.g. Fru-1-P, although this probably does not occur in plants) are not. Thus, the sugars from the former class are obtained as free monosaccharides after mild acid hydrolysis; thereafter the monosaccharides can be obtained from the remaining unhydrolysed hexose monophosphates belonging to the latter class by digestion with a commercial phosphatase preparation (7).

The major hexose bisphosphate (Fru-1,6-P_2) is not appreciably hydrolysed by mild acid – unlike the UDP-sugars, which release the monosaccharide almost quantitatively. Mild acid removes one phosphate group (the one attached to the anomeric carbon) from Glc-1,6-P_2, Man-1,6-P_2 and Fru-2,6-P_2, leaving a hexose 6-phosphate.

Similar advice applies to phosphorylated sugars other than hexoses but, in the case of pentoses for example, for “6” read “5”.

3.10.4. Nucleotides, Including NDP-Sugars and CoA-Thioesters

As with sugar monophosphates versus bisphosphates at pH 2.0, there is excellent resolution within a given series of nucleotides: in order of decreasing mobility towards the anode, we have ATP, ADP and AMP (Fig. 3a). Sugar-nucleotides tend to migrate fairly close to the corresponding nucleoside diphosphates (e.g. UDP-Glc near UDP, and ADP-Glc near ADP). Some of the nucleoside moieties (adenosine, uridine etc.) differ in charge at pH 2.0 depending on the presence of amino groups. Adenosine has such a significant positive charge at pH 2.0 that AMP (despite its negatively charged phosphate group) has a small net positive charge and therefore moves slightly towards the cathode (relative to the neutral marker). Thus, ADP-hexoses are very well resolved from UDP-hexoses (Fig. 3a). GDP-hexoses migrate only slightly faster than ADP-hexoses at pH 2.0 (data not shown).

At pH 6.5, UDP-glucose resolves well from UDP-glucuronate (8) because the GlcA residue carries a full negative charge. However, at pH 2.0, UDP-glucose runs only slightly slower than UDP-glucuronic acid because the GlcA residue is scarcely ionised at such a low pH. Thus, at pH 2.0, it is possible to obtain very useful class separations of UDP-sugars (including UDP-Glc and UDP-GlcA) in one zone and ADP-sugars + GDP-sugars in a second zone. These two zones can be eluted from the paper for further analysis, e.g. by mild acid hydrolysis (0.1 M trifluoroacetic acid at 100°C for 25 min) followed by paper chromatography or TLC (or HVPE at pH 3.5 for the uronic acids) to resolve the diverse monosaccharides – for example from the UDP-sugar pool, containing UDP-Glc, UDP-D-Gal, UDP-Ara, UDP-Xyl, UDP-Rha, UDP-GlcA and UDP-GalA. Note that the ribose moiety of NDP-sugars is not released by mild acid hydrolysis.

At both pH values, 2.0 and 6.5, NADPH migrates faster towards the anode than $NADP^+$ because the former lacks the extra positive charge (note that both NADPH and so-called "$NADP^+$" both possess a net negative charge; the "$^+$" is only relative) (Fig. 3). At pH 3.5 and 6.5, in contrast to pH 2.0, NDP-sugars consistently migrate slower than the corresponding NDPs.

HVPE at pH 3.5 is useful for class-separating ADP-hexoses ($m_{OG} \approx 0.58$) from GDP-hexoses ($m_{OG} \approx 0.75$). These two classes can subsequently be further analysed, e.g. by acid hydrolysis of the GDP-sugar zone to yield the monosaccharides (typically D-mannose, L-fucose and L-galactose).

Thioesters of coenzyme-A (e.g. acetyl-CoA, feruloyl-CoA etc.) are conveniently analysed by HVPE at pH 2.0 (9), in which buffer they all possess a substantial net negative charge. Commercially available dodecanoyl-CoA is a useful marker for feruloyl-CoA, which has about the same charge:mass ratio. [^{14}C]Cinnamate metabolites with an appreciable net negative charge at pH 2.0 are very likely to be CoA conjugates since nothing else would give them such a charge. They also migrate very rapidly at

pH 3.5 (m_{OG} values: CoA, 1.0; feruloyl-CoA, 0.61). They can be further characterised by mild alkaline hydrolysis, yielding the former acyl residue in free form (ferulate, acetate, etc.).

3.10.5. Amino-Sugars

The amino groups of ManN, GalN and GlcN have pK_a values of about 7.3, 7.7 and 7.8, respectively. These compounds thus carry almost a full positive charge at all pH values commonly used for HVPE and so are not resolved except slightly at pH 6.5. Nevertheless, HVPE at pH 2.0, 3.5 or 6.5 permits the quick and easy class separation of sugar amines from acidic and neutral sugars, including *N*-acetyl amino-sugars e.g. GlcNAc. Similarly, HVPE at pH 2.0 allows excellent class separation of amino-sugar derivatives with crystal violet (CV) as a cationic marker and orange G (OG) as an anionic marker (10):

$m_{CV} = 1.26$: GlcN, GalN
$m_{CV} = 0.20$: GlcN-1-P, GlcN-6-P, GalN-1-P
$m_{CV} = m_{OG} = 0$: GlcNAc, GalNAc
$m_{OG} = 0.57$: GlcNAc-1-P, GlcNAc-6-P, GalNAc-1-P
$m_{OG} = 0.76$: UDP-GlcNAc, UDP-GalNAc

Amino-sugars and their derivatives can be stained with aniline hydrogen-phthalate (unless carrying a phosphate group at position 1) or ninhydrin (unless acetylated on the N).

3.10.6. Amino Acids and Polyamines

α-Amino acids (i.e. compounds with an amino group and a carboxy group attached to the same carbon, the simplest being glycine) have at least one amino group (contributing at least one full positive charge at pH 2.0, 3.5 and 6.5), and an α-carboxy group which bears a full or partial negative charge depending on the pH. If the amino group is free (not involved in a peptide bond), the α-carboxy group has a very low pK_a (in the range 1.8–2.5) and is thus 61–24% fully anionic at pH 2.0, unlike most other carboxy groups which are almost neutral at that pH. The side-chain carboxy groups of Asp and Glu have much higher pK_a values and are only ~1% charged at pH 2.0 but highly charged at pH 3.5 and 6.5. Thus, on HVPE at pH 2.0, all the common α-amino acids have a net positive charge; Arg, Lys and His have a particularly large one owing to the presence of a second positively ionising group.

Cysteic acid (an oxidation product of Cys) is the only commonly encountered α-amino acid with a net negative charge at pH 2.0: this is due to its negatively ionising $-SO_3H$ group (p$K_a = 1.3$). Other than cysteic acid, hydroxyproline stands out on HVPE at pH 2.0 as the slowest-migrating major "amino acid" (strictly an imino acid) because its carboxy group is unusually acidic (p$K_a = 1.8$). Hydroxyproline mono-, di-, tri- and tetra-arabinosides, obtained from some cell-wall glycoproteins such as extensins, migrate progressively slower still (11).

HVPE at pH 2.0 followed by staining with Folin and Ciocalteu's phenol reagent is useful for the detection of tyrosine

and its oxidative coupling products (isodityrosine, pulcherosine, di-isodityrosine), since these are among the very few cationic phenols. Others that do exist include tyramine and *N*-feruloyl-putrescine.

4-Aminobutyrate (GABA) is a significant stress metabolite in plants, sometimes found in the apoplast and thus relevant to wall metabolism. Its carboxy group is not attached to the same C atom as its amino group and thus has a more typical pK_a value (4.0, as opposed to 2.3 for 2-aminobutyrate). Therefore, at pH 2.0, GABA has a net charge of about +1.0 and migrates towards the cathode about 90% as rapidly as lysine, which has two amino groups.

Polyamines possess hydrocarbon chains, usually with two primary amino groups; in addition there may be one or more secondary amino groups. Major examples in plants are putrescine (a diamine), spermidine (a triamine), and spermine and its isomer thermospermine (tetraamines) (12). Their presence in solution in the apoplast and covalently bonded to wall polymers has been reported. Polyamines migrate particularly rapidly towards the cathode during HVPE, not only at pH 2.0 but also at pH 6.5 since the amino groups are essentially fully ionised, there are no negatively ionising groups, and they have low M_r. HVPE thus enables a very convenient class separation, resolving polyamines from all other common phytochemicals. All the common polyamines have $m_{lysine} \approx 1.6$ at pH 2.0, and stain with ninhydrin. Resolution of the various polyamines from each other by HVPE requires a higher pH buffer, closer to the pK_a of the amino groups, e.g. 0.2 M ammonium carbonate (pH 8.7); however, better separation of spermine, spermidine and putrescine is obtained by paper chromatography in butan-1-ol/acetic acid/pyridine/water (4:1:1:2).

It has been suggested that polyamines such as putrescine may be linked via amide (isopeptide) bonds to pectic GalA residues (13). Model compounds with which to search for the natural occurrence of such linkages were synthesised chemically [e.g. *N*-D-galacturonoyl-putrescinamide (GalA–Put) and *N*,*N*′-di-D-galacturonoyl-putrescinamide (GalA–Put–GalA)]. In addition, promising diagnostic "fragments" were isolated by Driselase digestion of artificially putrescine-conjugated homogalacturonan [yielding products such as Put–$GalA_3$ and $GalA_3$–Put–$GalA_3$]. These various novel glycoconjugates were characterised largely by HVPE on the basis of the following rules:

- Carboxy groups: almost fully ionised negatively at pH 6.5, partially at pH 3.5, almost un-ionised at pH 2.0.
- Amino groups: fully ionised positively in all three buffers.
- Amide (–CONH–) groups: un-ionised in all three buffers.

Similar techniques were used in the preparation and characterisation of N^{ε}-D-galacturonoyl-L-lysine and related conjugates,

which are useful model compounds with which to test for the possible occurrence of pectin–extensin amide linkages (14).

Glutathione (GSH, a tripeptide) and its disulphide-bridged oxidation-product (GSSG), both of which have been reported in the apoplast, can also be resolved quickly and cleanly from many co-occurring compounds by HVPE. Pre-labelling with [^{35}S]sulphate is particularly helpful as plants possess few extracellular sulphur compounds. GSH and GSSG have a net positive charge at pH 2.0 and net negative charge at pH 6.5. Selected m_{OG} values at pH 6.5 are: GSH, 0.74; GSSG, 0.88; cysteic acid, 1.29; inorganic sulphate, 2.8; cysteine, 0.00; cystine, 0.00; methionine, 0.00 (15).

3.10.7. Electrophoresis of Neutral Sugars

Neutral sugars and alditols do not migrate on HVPE in ordinary buffers e.g. at pH 2.0, 3.5 and 6.5. However, such sugars can reversibly be given a negative charge by complexation with oxyanions such as borate, molybdate, tungstate, stannate or aluminate (2, 16). Complexation is a very rapid and simple procedure: the sugar sample is loaded in the normal way (Fig. 2), and the paper is wetted with an aqueous solution of the oxyanion, which is used as the electrophoresis buffer (Table 1).

Borate binds to suitably orientated pairs of –OH groups, which occur in most sugars and alditols, conferring a negative charge. Binding is optimal at high pH (e.g. 9.4) and progressively weaker at lower pHs. The borate–sugar dissociation constant (and thus the average number of borate ions bound per unit mass of sugar at equilibrium) determines the electrophoretic mobility. The method is useful for distinguishing oligosaccharides that differ in bond position ((1→2), (1→3), (1→4) etc.) (2, 17, 18). There may also be good separation of pairs of oligosaccharides that differ only in anomeric configuration, e.g. maltose versus cellobiose. Wall-derived oligosaccharides can often be freed of contaminating malto-oligosaccharides on the basis of the slow migration of the latter in borate buffer (19).

Molybdate reversibly binds to alditols and related compounds possessing certain patterns of –OH groups; binding is optimal at pH 2 and is progressively weaker at higher pHs. HVPE in molybdate is particularly effective at resolving reducing oligosaccharides (e.g. the xyloglucan-derived nonasaccharide, XXFG), most of which cannot bind molybdate, from the corresponding reduced oligosaccharides (e.g. XXFGol), which can bind it specifically at the glucitol moiety. Thus, XXFGol is mobile in molybdate buffer, whereas XXFG is not. The m_{OG} value of a reduced oligosaccharide is strongly influenced by the position(s) at which the rest of the oligosaccharide is attached to the alditol moiety, and can therefore give valuable information on sugar–sugar linkages in novel radiolabelled oligosaccharides (2, 20).

4. Notes

1. The applied voltage is typically 4.5 kV.
2. The effective path-length is a little less than 57 cm, the two ends of the paper being submerged in buffer.
3. HVPE can conveniently handle up to twenty samples per sheet if the samples are spot-loaded on No. 1 or 3CHR paper at, respectively, <0.3 or <1.0 μmol of total ions (including any non-volatile salts) per spot. Non-ionic compounds, e.g. glucose or glycerol, can be present in higher amounts as these do not interfere in the ionisation and electrophoresis processes.
4. For preparative work, a single sample containing up to about 25 μmol total ions (equivalent to ~5 mg of galacturonic acid) can be streak-loaded per sheet of 3CHR.
5. If the use of water-immiscible coolant liquids is not feasible, e.g. because hydrophobic compounds are of interest, HVPE can also be performed on a flat-bed system.
6. One potential disadvantage of this method is that non-polar compounds e.g. ferulic acid might partition into the coolant and be lost off the paper. However, the great majority of metabolites of interest in cell wall research are hydrophilic enough to be retained in the aqueous buffer in the paper; even isoleucine (the most "hydrophobic" of the 20 common amino acids) and feruloylated sugars are retained.
7. In this laboratory's experience, this method provides less uniform cooling and therefore greater irregularity in the migration of replicate samples across the width of the paper.
8. The high voltage and short run-time minimise diffusion of the analytes on the wet paper.
9. This entails a considerable heating effect (e.g. at pH 2.0, power = 4,500 V × 0.15 A = 675 W). The thicker 3CHR paper draws an even greater current, and the voltage must be correspondingly reduced (and the run time increased) so that the power remains at <750 W.
10. The charges borne by compounds during electrophoresis depend on the pK_a values of the ionisable groups and the pH of the buffer. Approximate pK_a values are listed in Table 2. Deductions that can be drawn from pH-dependent shifts in electrophoretic mobility, are summarised in Table 3.
11. Borate may interfere with $AgNO_3$ staining; to avoid this on electrophoretograms run in borate buffer, the alkaline solution normally used for $AgNO_3$ staining should be replaced by

80% (v/v) ethanol containing 2% (w/v) NaOH and 4% (w/v) pentaerythritol.

12. Flashing and cooling are not beneficial for autoradiography.

Acknowledgements

I thank numerous past and present colleagues and students for electrophoretic data and experience presented in this chapter, and the UK BBSRC for financial support.

References

1. Offord, R. E. (1966). Electrophoretic mobilities of peptides on paper and their use in the determination of amide groups. *Nature* **211,** 591–593.
2. Fry, S. C. (2000). The Growing Plant Cell Wall: Chemical and Metabolic Analysis, Reprint Edition. The Blackburn Press, Caldwell, NJ, pp. xviii + 333 [ISBN 1-930665-08-3].
3. Green, M. A., and Fry, S. C. (2005) Vitamin C degradation in plant cells via enzymatic hydrolysis of 4-*O*-oxalyl-L-threonate. *Nature* **433,** 83–88.
4. Eshdat, Y., and Mirelman, D. (1972). An improved method for the recovery of compounds from paper chromatograms. *Journal of Chromatography* **65,** 458–459.
5. Wright, K., and Northcote, D. H. (1975) An acidic oligosaccharide from maize slime. *Phytochemistry* **14,** 1793–1798.
6. Popper, Z. A., Sadler, I. H., and Fry, S. C. (2003) α-D-Glucuronosyl-(1→3)-L-galactose, an unusual disaccharide from polysaccharides of the hornwort *Anthoceros caucasicus*. *Phytochemistry* **64,** 325–335.
7. Sharples S. C., and Fry, S. C. (2007) Radioisotope ratios discriminate between competing pathways of cell wall polysaccharide and RNA biosynthesis in living plant cells. *Plant Journal* **52,** 252–262.
8. Kärkönen, A., and Fry, S. C. (2006) Novel characteristics of UDP-glucose dehydrogenase activities in maize: non-involvement of alcohol dehydrogenases in cell wall polysaccharide biosynthesis. *Planta* **223,** 858–870.
9. Fry, S. C., Willis S. C., and Paterson, A. E. J. (2000). Intraprotoplasmic and wall-localised formation of arabinoxylan-bound diferulates and larger ferulate coupling-products in maize cell-suspension cultures. *Planta* **211,** 679–692.
10. Piro, G., Perotto, S., Bonfante-Fasolo, P., and Dalessandro, G. (1988) Metabolism of D-(U-^{14}C)glucosamine in seedlings of *Calluna vulgaris* (L) Hull. *Journal of Plant Physiology* **132,** 695–701.
11. Lamport, D. T. A. (1967) Hydroxyproline-*O*-glycosidic linkage of plant cell plant cell wall glycoprotein extensin. *Nature* **216,** 1322–1324.
12. Takahashi, T., Kakehi, J.-I. (2010) Polyamines: ubiquitous polycations with unique roles in growth and stress responses. *Annals of Botany* **105,** 1–6
13. Lenucci M., Piro, G., Miller, J. G., Dalessandro, G., and Fry, S. C. (2005) Do polyamines contribute to plant cell wall assembly by forming amide bonds with pectins? *Phytochemistry* **66**, 2581–2594.
14. Perrone P., Hewage, C., Sadler, I. H., and Fry, S. C. (1998). N^{α}- and N^{ε}-D-galacturonoyl-L-lysine amides: properties and possible occurrence in plant cell walls. *Phytochemistry* **49,** 1879–90.
15. Kärkönen A., Warinowski, T., Teeri, T. H., Simola, L. K., and Fry, S. C. (2009) On the mechanism of apoplastic H_2O_2 production during lignin formation and elicitation in cultured spruce cells; peroxidases after elicitation. *Planta* **230,** 553–567.
16. Weigel, H. (1963). Paper electrophoresis of carbohydrates. *Advances in Carbohydrate Chemistry* **18,** 61–96.
17. Dumville J.C., and Fry, S. C. (2003) Gentiobiose: a novel oligosaccharin in ripening tomato fruit. *Planta* **216,** 484–495.
18. Narasimham, S., Harpaz, N., Longmore, G., Carver, J. P., Grey, A. A., and Schachter, H. (1980) Control of glycoprotein synthesis: the purification by preparative paper electrophoresis in borate of glycopeptides containing high mannose and complex

oligosaccharide chains linked to asparagine. *Journal of Biological Chemistry* **255,** 4876–4884.

19. O'Looney, N., and Fry, S. C. (2005) Oxaziclomefone, a new herbicide, inhibits wall expansion in maize cell-cultures without affecting polysaccharide biosynthesis, xyloglucan transglycosylation, peroxidase action or apoplastic ascorbate oxidation. *Annals of Botany* **96,** 1097–1107.
20. Wende, G., and Fry, S. C. (1996). 2-*O*-β-D-Xylopyranosyl-(5-*O*-feruloyl)-L-arabinose, a widespread component of grass cell walls. *Phytochemistry* **44,** 1019–1030.
21. Miller J. G., Farkaš, V., Sharples, S. C., and Fry, S. C. (2007) *O*-Oligosaccharidyl-1-amino-1-deoxyalditols as intermediates for fluorescent labelling of oligosaccharides. *Carbohydrate Research* **342,** 44–54.

Chapter 5

Carbohydrate Gel Electrophoresis

Florence Goubet, Paul Dupree, and Katja Salomon Johansen

Abstract

Polysaccharide analysis using carbohydrate gel electrophoresis (PACE) relies on derivatization of the reducing ends of sugars with a fluorophore, followed by electrophoresis under optimized conditions in polyacrylamide gels. PACE is a sensitive and simple tool for studying polysaccharide structure or quantity and also has applications in the investigation of enzyme specificity.

Key words: Oligosaccharide, Monosaccharide, Polysaccharide, Pectin, Hemicellulose, Enzyme

1. Introduction

The PACE method is both simple and robust. It involves two main steps:

1. Conjugation of a fluorophore onto the reducing end of a sugar using different types of fluorophores depending on the sugars under study. In the case of a highly negatively charged sugar, the fluorophore used is uncharged (e.g. *2-aminoacridone*; AMAC) whereas in the case of partially charged or neutral sugars, the fluorophore used is charged (e.g. *8-aminonaphthalene-1,3,6-trisulfonic acid*; ANTS).
2. Electrophoresis at high voltage in thin polyacrylamide gels.

   PACE method can provide information on both polysaccharide structure and substrate specificity of carbohydrate active enzymes.

   The main advantages of the method are:

   - The equipment required is not expensive and is easy to use.

Zoë A. Popper (ed.), *The Plant Cell Wall: Methods and Protocols*, Methods in Molecular Biology, vol. 715,
DOI 10.1007/978-1-61779-008-9_5,

- The sample to be analysed does not need any type of clean-up prior to the derivatization. Each gel will be used once so the purity of the samples is not an issue for preserving the equipment.
- There is a linear relationship between molar amounts of any sugar and the intensity of the signal. This provides data for long oligomers that are superior to the data obtained with the HPLC coupled with amperometric detection.
- PACE can be used as a separation step prior to analysis using mass spectrometry (MS).

2. Materials

2.1. Sample Preparation

1. 0.1 M ANTS in acetic acid/water (3/17, v/v).
2. 0.2 or 1 M $NaCNBH_3$ in DMSO.
3. 50 mM AMAC in acetic acid/DMSO (1.5/18.5, v/v).
4. 0.5 M $NaCNBH_3$ in water.
5. 0.1 M $NaCNBH_3$ in water.
6. 6 M urea in water.
7. Acetic acid/water/DMSO 3/17/20 v/v/v.
8. Monosaccharide or oligosaccharide standards: 1 mM sugars (e.g. of a range of monosaccharides and oligosaccharides) 5 μL is added to a 0.1–2-mL tube (depending on the reaction sample) and dried before derivatization.
9. Polysaccharides: 0.5 mg/mL of a range of polysaccharides in buffer.
10. Enzymes (see Note 1).
11. Incubator.
12. Centrifugal vacuum evaporator.

Buffers: for enzyme reaction

13. 0.1 M ammonium acetate adjusted to pH 4.5–6 with glacial acetic acid.
14. 10 mM Tris–HCl, pH 7–9.
15. 0.1 mM Tris–HCl, 1 mM $CaCl_2$, pH 8.

2.2. Electrophoresis

Buffers:

1. 0.1 M Tris adjusted to pH 8.2 with boric acid.
2. 0.1 M Tris–HCl pH 8.2.
3. 0.15 M Tris adjusted to pH 8.5 with 0.15 M glycine.

Gels:

4. 29:1 (w/v) Polyacrylamide/acrylamide: *N,N*-9-methylenebisacrylamide from Bio-Rad (Hertfordshire, UK).
5. Gel for analysis of neutral oligosaccharides: 20% (w/v) polyacrylamide gel containing 0.5% (w/v) *N,N*-9-methylenebisacrylamide, 0.1 M Tris–borate pH 8.2. Stacking gel for analysis of neutral oligosaccharides: 8% (w/v) polyacrylamide, 0.2% *N,N*-9-methylenebisacrylamide, 0.1 M Tris–borate pH 8.2.
6. Gel for analysis of acidic oligosaccharides: 25% (w/v) polyacrylamide gel containing 0.8% (w/v) *N,N*-9-methylenebisacrylamide, 0.1 M Tris–borate pH 8.2. Stacking gel for analysis of acidic oligosaccharides: 10% (w/v) polyacrylamide, 0.4% *N,N*-9-methylenebisacrylamide, 0.1 M Tris–borate pH 8.2.
7. Hoefer SE 660 vertical slab gel electrophoresis apparatus (Amersham, Buckinghamshire, UK) with 24-cm plates, 0.75-mm spacer, and well of width 0.25 cm (other equipments can also be used).
8. Micro-syringes.
9. Standard glass or low-fluorescent Pyrex plates.

2.3. Gel Imaging (One of the Following Systems Can Be Used)

1. MasterImager CCD camera system (Amersham).
2. G:BOX Chemi HR16 (Syngene, Cambridge, UK).
3. Standard UV transilluminator.

2.4. Gel Analysis

1. GeneTools software (Syngene, Cambridge UK).

2.5. extraction from a gel

1. Nanosep system.
2. MilliQ water.
3. 1% acetic acid.
4. Dialysis tubing.

3. Methods

3.1. Sample Preparation: Hydrolysis of Pure Polysaccharides Using Enzyme Preparations

Polysaccharides (0.5 mg/mL; 100 µL) are suspended with enzymes (see Note 1) in a suitable buffer at a total volume of 250 µL. The suspension is incubated at room temperature (see Note 2) for 1 min to overnight (hydrolysis could be longer but special care must be taken to prevent contamination with fungi or bacteria). Different buffers can be used with a preference of ammonium acetate, which is volatile and thus leaves no salts behind. Buffers containing amino group (e.g. Tris buffer) can increase the background since they can react with the fluorophore.

For pH 4.5–6, the buffer used is 0.1 M ammonium acetate adjusted with glacial acetic acid; for pH 7–9, the buffer is 10 mM Tris–HCl. In order to study lyase activity, 0.1 mM Tris–HCl buffer pH 8 with 1 mM $CaCl_2$ is added in the reaction. Controls without substrates or enzymes are performed under the same conditions to identify any unspecific compounds present in the enzymes preparations, polysaccharides or/and labelling reagents. The reactions are stopped by boiling for 30 min (see Note 3). The samples are dried using a centrifugal vacuum evaporator.

3.2. Sample Preparation: Hydrolysis of Plant Cell Wall Materials

To study the polysaccharide architecture of plant cell walls, highly purified and well-defined enzymes with known activity are used to cleave the polysaccharides into smaller fragments. The resulting oligomers can only arise from polysaccharides containing the particular type of bonds which the enzyme can recognize and cleave. The amount of released products can be quantified or the pattern of bands can be used as an indicator for the presence or absence of a particular saccharide in the cell wall sample.

The plant cell wall contains a mixture of polysaccharides in different ratios (see Note 4). To study them, different protocols could be used. For the study of polygalacturonan, which is very abundant in the cell wall, only a small amount of cell wall material is needed (50 µg; (1)) whereas for the analysis of mannan, which is a minor component of the cell wall, considerably more cell wall material is required (0.5 mg; (2)).

The specific compounds may in some cases be inaccessible to the enzyme. For example, most polygalacturonases are not able to cleave the glycosidic bonds of highly esterified pectin. In this case, the accessibility of the enzyme can be improved by the removal of the methyl groups by pre-treatment either with pectin methyl esterase or by incubation of the cell wall material in an alkaline solution (1). Another example is xylan, which can be esterified and/or closely bound to the cell wall. To eliminate the esterification and partially solubilize it a highly concentrated NaOH solution can be used (3).

The samples are dried using a centrifugal vacuum evaporator.

3.3. Analysis of Neutral Oligosaccharides Derivatized with ANTS

1. Derivatization is carried out in the tubes containing dried polysaccharides, oligosaccharides, or monosaccharides. ANTS are prepared in acetic acid/water (3/17, v/v) at a final concentration of 0.1 M (made freshly or stored at −20°C for at least 6 months). $NaCNBH_3$ (0.1 M, made freshly and used immediately, toxic) is solubilized in DMSO (in a fume hood) for ANTS derivatization.
2. To each dry sample, 5 µL of ANTS solution and 5 µL of the appropriate $NaCNBH_3$ solution are added. The volume can be slightly adjusted if large quantities of cell wall material is used and a very low amount of oligosaccharides produced

(e.g. to detect mannan in *Arabidopsis*, 0.5 mg of cell wall material is needed and the oligosaccharide production is very low (2)). In this case, more solvent can be added with a similar ratio (acetic acid/water/DMSO; 3/17/20 v/v/v) to keep the compounds in suspension.

3. The reagents are briefly mixed (using a vortex), centrifuged and incubated at 60°C overnight. We previously used 1 M of $NaCNBH_3$ and incubated at 37°C; this condition is optimal for the study of most of the oligosaccharides. However, there is a poor recovery of oligosaccharides containing glucosamine using these conditions. To increase their labelling, a decrease of $NaCNBH_3$ concentration, to 0.2 M, and incubation at 60°C is required. Using these conditions, all types of oligosaccharides are derivatized similarly.
4. The solution is dried in a centrifugal vacuum evaporator for 2 h at 40°C (avoid using high temperatures that could increase the background). The derivatized sugars are resuspended in 100 µL of 6 M urea and stored before use at –20°C, and are stable for at least 6 months (the background signal can increase afterwards).
5. Samples (0.5–4 µL depending of the sugar concentration) are loaded to the gel using micro-syringes (see Note 4). In all cases, an Hoefer SE 660 vertical slab gel electrophoresis apparatus (Amersham, Buckinghamshire, UK) is used with 24-cm plates, 0.75-mm spacer, and well of width 0.25 cm. Standard glass or low-fluorescence Pyrex plates is used. Electrophoresis is performed at 10°C in all cases to avoid any heating. The 20% (w/v) polyacrylamide gel contained 0.5% (w/v) *N,N*-9-methylenebisacrylamide with a stacking gel (2 cm) of 8% (w/v) polyacrylamide and 0.2% (w/v) *N,N*-9-methylenebisacrylamide (see Note 5); both gels are made in 0.1 M Tris–borate pH 8.2 (see Note 6). The gels are cast and cooled at least 1 day before they are to be used in order to allow complete polymerization of the acrylamide. The gel is then stored overnight at 4°C so that it will be cold and ready to use. Smaller electrophoresis equipment can also be used but some oligosaccharides may be less well separated (4).
6. The electrophoresis buffer system (cooled at 10°C) is 0.1 M Tris adjusted to pH 8.2 with boric acid (Tris–borate; see Note 6). The samples are electrophoresed first at 200 V for 20 min and then at 1,000 V for 90 min. The buffer can be used several times (see Note 7).

3.4. Analysis of Acidic Oligosaccharides Derivatized with AMAC

1. AMAC is prepared in acetic acid/DMSO (1.5/18.5, v/v) at 50 mM final concentration (made freshly to reduce the background). $NaCNBH_3$ (0.5 M; made freshly and used immediately; toxic) is solubilized in water. To each dry sample, 5 µL

of AMAC solution and 5 µL of the appropriate $NaCNBH_3$ solution were added. The reagents are mixed, centrifuged, and incubated at 37°C overnight. The solution is dried in a centrifugal vacuum evaporator for 2 h at 40°C. The derivatized sugars are resuspended in 100 µL of 6 M urea.

2. To have good derivatization and better gel visualization, when the polysaccharide studied is contained in the cell wall at a low level, more derivatization solvent (to recover the material produced) and a lower concentration of urea are used. The samples can be stored at least 1 month at –20°C. Long-term storage will create background in the samples.
3. Samples (0.5–4 µL depending on the sugar concentration) are loaded to the gel using micro-syringes (see Note 4). In all cases, an Hoefer SE 660 vertical slab gel electrophoresis apparatus (Amersham, Buckinghamshire, UK) is used with 24-cm plates, 0.75-mm spacer, and well of width 0.25 cm. Standard glass or low-fluorescence Pyrex plates is used. The 25% (w/v) polyacrylamide gel contained 0.8% (w/v) *N,N*-9-methylenebisacrylamide with a stacking gel (2 cm) of 10% (w/v) polyacrylamide and 0.4% (w/v) *N,N*-9-methylenebisacrylamide (see Note 5); both gels are made in 0.1 M Tris adjusted to pH 8.2 with HCl (Tris–HCl). The gels are cast and cooled at least 1 day before they are used in order to allow complete polymerization of the acrylamide. The gel is then stored overnight at 4°C ready to be used. The acrylamide percent can be adjusted to study all oligosaccharides as described in Goubet *et al.* (5) (see Note 8).
4. The electrophoresis buffer system (cooled at 10°C) is 0.1 M Tris–HCl pH 8.2 as the anode reservoir buffer and 0.15 M Tris adjusted to pH 8.5 with 0.15 M glycine as the cathode reservoir buffer (see Note 6). The samples are electrophoresed first at 200 V for 20 min and then at 1,000 V for 2 h. The buffer can be used several times (see Note 7).

3.5. Gel Imaging

Different systems can be used to image the gels:

(a) Gels can be scanned using a *MasterImager CCD camera system* (Amersham) with an excitation filter at 400 nm and a detection filter at 530 nm. Exposure time is optimized to increase sensitivity without saturating the intense bands. An image of the gel (resolution 100 µm) can be obtained and exported into a 16-bit file to be quantified.

(b) A *G:BOX Chemi HR16* (Syngene, Cambridge, UK) can also be used. The stacking gel is removed and a small amount of water is added onto each gel prior to imaging to flatten them out and reduce the wrinkling. The gels are then transferred to a G:BOX Chemi HR16 for imaging. Since the emission peak

for ANTS is 356 nm and for AMAC is 420 nm the gels are imaged using short wavelength UV, with UV and short pass emission filters and without neutral fielding (http://www.syngene.com/PACE_Intl_Labmate_Article.pdf).

(c) The gel could also be visualized using a *standard UV transilluminator* (wavelength 360 nm), but this has been found to be less sensitive than the use of the MasterImager, particularly in the case of ANTS derivatization (6, 7).

3.6. Oligosaccharide Separation

All oligosaccharides appear as one clear band (Fig. 1) except for glucosamine and oligo-glucosamines (oligo-chitosans). For these last compounds, each sugar is represented by two bands (data not shown). Compounds that can not be separated are cellobiose and glucose as shown in Fig. 1. However, using different polyacrylamide conditions, those two compounds can be separated (8).

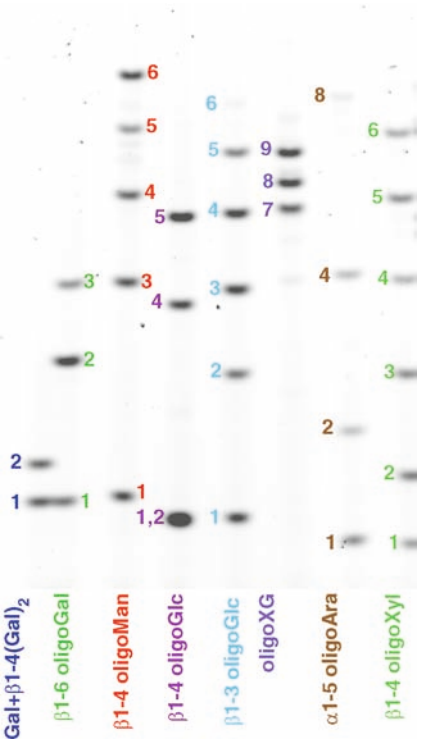

Fig. 1. Different oligosaccharides were derivatized with ANTS and separated in polyacrylamide gel. There is oligosaccharide separation by the composition, size and also by the glycosidic bond. Xyloglucan oligosaccharides (XXXG (DP 7), XXLG/XLXG (DP8) and XLLG (DP 9)), where G is an unsubstituted glucose residue, X is a xylose-substituted glucose residue, and L is a galactosylxylose-substituted glucose residue (14). The number close to each band is the DP for each of the oligosaccharides – colour coded by type of oligosaccharide.

3.7. Gel Analysis

Quantification is performed using GeneTools software (Syngene, Cambridge UK), using rolling ball background detection. Standards (single or multiple) are run in each gel to obtain a standard curve for quantification of sugars in the samples. Derivatized sugars have a linear response between the concentration and signal level. One point to note is that for ANTS derivatization, the signal can go through zero as there is low background; however with AMAC derivatization, the signal can not go through zero due to higher gel background. The consequence is that quantification of ANTS derivatized oligosaccharides can be done using only one standard; however, for AMAC, a minimum of two standards is required to determine the background level. For accuracy in both cases, more standards will be needed. To obtain accurate quantification, pure standards need to be used. The monosaccharides are highly pure whereas not all commercial preparations of oligosaccharides are, as shown in Goubet *et al.* (6). Man and $(Man)_3$ or GalU and $(GalU)_3$ can be used as standards for quantification for either ANTS or AMAC derivatized samples (1). The band intensity is independent of the sugar tested except for oligochitosan. More than one standard gives a greater accuracy of quantification.

3.8. Extraction of Derivatized Oligosaccharides and MS Analysis

1. To determine the identity of oligosaccharides in specific bands, a preparative gel with multiple adjacent lanes loaded with 6 µL of derivatized oligosaccharides is prepared.
2. Bands can be excised while briefly viewing the gel under a UV transilluminator (wavelength 360 nm), and suspended in 1 mL of milliQ water.
3. To extract the oligosaccharides, acrylamide gel slices are partially crushed and subjected to three cycles of freeze/thawing. In the case of purification of esterified oligosaccharides, the pH needs to be slightly acid to reduce any demethylesterification process (9), so acetic acid solution (1%) replaces water to extract the compounds.
4. To eliminate any polyacrylamide fragments, the samples are filtered using the Nanosep system (MWCO of 10,000 Da; Pall, East Hills, NY) and then dialyzed against water using dialysis tubing (MWCO of 500 Da – note that derivatized monosaccharides will be lost).
5. The solution is dried and the pellet is suspended in 10–20 µL of water. Aliquots of the specific derivatized-Me-OGA samples are loaded onto a gel to estimate their quantity.
6. These samples are then analyzed by different MS configurations as described by Goubet *et al.* (9).

4. Results

PACE can resolve many carbohydrates from each other based on their size and composition and function of the glycosidic bond (Fig. 1). Already in monosaccharide form, some isomers can be separated from each other (e.g. glucose (Glc) from galactose (Gal)). The oligosaccharides can also be separated from each other depending on their composition. For example, a dimer of arabinose (Ara) is clearly separated from the dimer of xylose (Xyl); and in this case both monosaccharides are pentose. Another example is that dimer of Gal which is separated from the dimer of mannose (Man) and in this case, the monosaccharide unit for both dimers is a hexose.

The glycosidic bond can also play a role in their separation. In the example given in Fig. 1, a β 1-3 oligoglucan can be separated from a β 1-4 oligoglucan with the same degree of polymerization. Similar observations are made for large oligosaccharides but to achieve better separation, different compositions of polyacrylamide gels need to be used. The same oligosaccharides with substitutions in different places on the backbone can also clearly be separated from each other as shown in Goubet *et al.* (9).

Similar observations were made studying charged oligosaccharides as described in Goubet *et al.* (5) and shown in Fig. 2. Carrageenans are polysaccharides of repeating disaccharide units of 3-linked β-D-galactopyranose and 4-linked α-D-galactopyranose. Three main structural groups are defined based on the presence or absence of α-D-anhydrogalactose in place of α-D-galactopyranose and on the position of sulphate groups as described in Liners *et al.* (10). Oligosaccharides of iota- and kappa-carrageenans (kindly provided by F. Liners and P. Van Cutsem, University of Namur, Belgium) were analysed by PACE. As previously shown, charged oligosaccharides have a size-dependent "turning point" (5). As a consequence of this turning point, some large oligosaccharides could migrate to similar positions as smaller ones. In Fig. 2, two kappa-carrageenans with degree of polymerization (DP) of 4 and 6 respectively co-migrated under the conditions used. To separate them, different polyacrylamide conditions can be used (5). The two types of carrageenan are separated from each other so that PACE can be very useful to study carragenan structure and also some slight changes of structures as already been shown for the methylation of polygalacturonan (9).

Recently, separation of saturated oligosaccharides versus unsaturated ones has also been shown possible using PACE technology (11). This technique could be used for rapid screening of the mode of action of hydrolase and lyase activities.

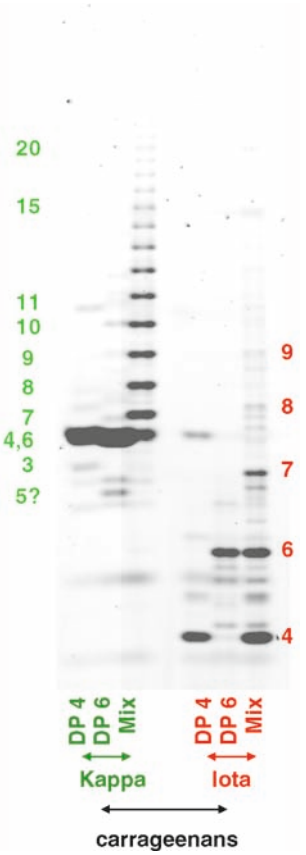

Fig. 2. Analysis of kappa- and iota-oligocarrageenans by PACE – derivatization was carried out using the AMAC fluorophore. The oligosaccharides separated by the size and the composition. The number close to each band is the DP of each oligosaccharide. "Mix" is a partial hydrolysis of the corresponding polysaccharides. Please note that the standards contain additional compounds than the ones indicated. For example, the kappa-carrageenan DP4 contains also two minor compounds that one has been identified as kappa-carrageenan DP3. The other one is unknown and could be a DP2. The number close to each band is the DP for each oligosaccharide – colour coded by type of oligosaccharide. The position of the kappa-penta-carrageenan (DP5) has been indicated as a possible but it has not confirmed.

5. Conclusion

PACE is a versatile method for the separation and detection of any kind of carbohydrate with a reducing end. The power to separate each carbohydrate coupled with its high sensitivity makes PACE an attractive alternative to HPLC, TLC and MS based analysis.

Using this method, polysaccharide structure and quantity and enzyme characteristics can be obtained using simple equipment.

6. Notes

1. If the enzymes are contained in a mixture, pure polysaccharides are required to study the enzyme characteristics as described in Phalip *et al.* (12). Many polysaccharides and oligosaccharides are available from Megazyme (http://www.megazyme.com/) and Sigma Aldrich (http://www.sigmaaldrich.com/sigma-aldrich/home.html) to study the enzyme specificity.
2. Higher temperatures may be appropriate depending on the properties of enzymes used (e.g. their thermostability (13)).
3. To avoid any product modification (e.g. degradation by some enzymes) during derivatization, the reaction is stopped. This will induce protein precipitation which is not an issue for PACE analysis except during loading. To avoid any problems with the micro-syringe, suspend the compounds fully before loading.
4. Cell wall mass is accurately measured by using a cell wall suspension (i.e. 0.5 mg/mL; homogenized using a glass potter) and an aliquot is taken for the analysis. Before taking an aliquot, the suspension is well mixed since the cell wall easily sediments.
5. For acrylamide polymerization, TEMED and APS solutions are used. TEMED solution can be bought ready to use and can be stored at room temperature for at least 1 year. A solution of APS can be stored for couple of months at 4°C, but if polymerization starts to take a longer time, a fresh solution should be made.
6. A 10× stock solution of the following buffers can be made and diluted when needed. The Tris–glycine stock solution can be stored at 4°C for at least 6 months. The Tris–HCl and Tris–borate solutions can be stored at room temperature for at least 6 months. Borate can precipitate if stored for too long or if the storage temperature is too cold.
7. The running solutions can be used several times. Borate salt can precipitate which leads to deteriorating electrophoresis materials. A sign of this is that the electrophoresis takes longer to run, the separation becomes less efficient and the background increases. Prepare a fresh solution if this situation occurs.
8. To study charged oligosaccharides, 1–31% (w/v) polyacrylamide gel contained 0.5–1.1% (w/v) *N,N*-9-methylenebisacrylamide can be used (higher acrylamide percent can also be used) (5).

References

1. Barton, C. J., Tailford, L., Welchman, H., Zhang, Z., Gilbert, H. J., Dupree, P., and Goubet, F. (2006) Enzymatic fingerprinting of *Arabidopsis* pectic polysaccharides using PACE-polysaccharide analysis by carbohydrate gel electrophoresis. *Planta* **224,** 163–174.
2. Handford, M. G., Baldwin, T. C., Goubet, F., Prime, T. A., Miles, J., Yu, X., and Dupree, P. (2003) Localisation and characterisation of mannan cell wall polysaccharides in *Arabidopsis thaliana*. *Planta* **218,** 27–36.
3. Brown, D. M., Goubet, F., Wong, V. W., Goodacre, R., Stephens, E., Dupree, P., and Turner, S. R. (2007) Comparison of five xylan synthesis mutants reveals new insight into the mechanisms of xylan synthesis. *Plant J* **52,** 1154–1168.
4. Karousou, E., Porta, G., De Luca, G., and Passi, A. (2004) Analysis of fluorophore-labelled hyaluronan and chondroitin sulfate disaccharides in biological samples. *J Pharmac Bioch Anal* **34,** 791–795.
5. Goubet, F., Morriswood, B., and Dupree, P. (2003) Analysis of methylated and unmethylated polygalacturonic acid structure by PACE: polysaccharide analysis using carbohydrate gel electrophoresis. *Anal Biochem* **321,** 174–182.
6. Goubet, F., Jackson, P., Deery, M., and Dupree, P. (2002) Polysaccharide analysis using carbohydrate gel electrophoresis (PACE): a method to study plant cell wall polysaccharides and polysaccharide hydrolases. *Anal Biochem* **300,** 53–68.
7. Fliegmann, J., Mithöfer, A., Wanner, G., and Ebel, J. (2004) An ancient enzyme domain hidden in the putative β-glucan elicitor receptor of soybean may play an active part in the perception of pathogen-associated molecular patterns during broad host resistance. *J Biol Chem* **279,** 1132–1140.
8. Jackson, P. (1994) The analysis of fluorophore-labeled glycans by high-resolution polyacrylamide gel electrophoresis. *Anal Biochem* **216,** 243–252.
9. Goubet, F., Ström, A., Quéméner, B., Stephens, E., Williams, M. A. K., and Dupree, P. (2006) Resolution of the structural isomers of partially methylesterified oligogalacturonides by polysaccharide analysis using carbohydrate gel electrophoresis. *Glycobiology* **16,** 29–35.
10. Liners, F., Helbert, W., and Van Cutsem, P. (2005) Production and characterization of a phage-display recombinant antibody against carrageenans: evidence for the recognition of a secondary structure of carrageenan chains present in red algae tissues. *Glycobiology* **15,** 849–860.
11. Phalip, V., Goubet, F., Carapito, R., and Jeltsch, J. -M. (2009) Plant cell wall degradation with a powerful *fusarium graminearum* enzymatic arsenal. *J Microbiol Biotechnol* **19,** 573–581.
12. Phalip, V., Delalande, F., Carapito, C., Goubet, F., Hatsch, D., Leize-Wagner, E., Dupree, P., Dorsselaer, A. V., and Jeltsch, J. M. (2005) Diversity of the exoproteome of *Fusarium graminearum* grown on plant cell wall. *Curr Genet* **48,** 366–379.
13. Palackal, N., Brennan, Y., Callen, N. C., Dupree, P., Frey, G., Goubet, F., Hazlewood, G. P., Healey, S., Kang, Y. E., Kretz, K. A., Lee, E., Tan, X., Tomlinson, G. L., Verruto, J., Wong, V. W. K., Mathur, E. J., Short, J. M., Robertson, D. E., and Steer, B. A. (2004) An evolutionary route to xylanase process fitness. *Protein Sci* **13,** 494–503.
14. Fanutti, C., Gidley, M. J., and Reid, G. J. S. (1996) Substrate subsite recognition of the xyloglucan endo-transglycosylase or xyloglucan-specific endo-(1→4)-β-D-glucanase from the cotyledons of germinated nasturtium (*Tropaeolum majus* L.) seeds. *Planta* **200,** 221–228.

Chapter 6

Capillary Electrophoresis with Detection by Laser-Induced Fluorescence

Andrew Mort and Xiangmei Wu

Abstract

The importance of capillary zone electrophoresis (CZE) has been increasing in use for: structural analysis of plant cell walls, characterization of enzymes that degrade polysaccharides, and profiling of oligosaccharides to characterize cell wall mutants. CZE with laser-induced fluorescence detection provides high separation efficiencies, high speed analysis, with extremely small sample requirements. Here, we describe the instrumentation we use and the methods for attaching fluorescent labels to oligosaccharides so that they can be detected.

Key words: Capillary zone electrophoresis (CZE), Laser-induced fluorescence detection, Oligosaccharide, Separation, Profiling

1. Introduction

Plant cell walls contain polysaccharides with complex structures such as xyloglucans and pectins which vary somewhat from species to species, from cell type to cell type, and even at different locations within the wall around a single cell (1). With the fairly recent availability of pure enzymes (2, 3), one can hydrolyze these polymers into oligomers which can then be separated and characterized.

The oligomers can be labelled at their reducing ends by reacting them with a fluorescent amine at the aldehyde group to form an imine which can be selectively reduced with sodium cyanoborohydride to a stable secondary amine. We use two different aromatic trisulfonated amines; 8-aminonaphthalene-1,3,6-trisulfonate (ANTS), and 8-aminopyrene-1,3,6-trisulfonate (APTS). ANTS is quite inexpensive and in our hands gives few interfering peaks on the CZE trace. However, ANTS absorbs in the UV range and so, requires a UV laser for excitation. APTS is

Zoë A. Popper (ed.), *The Plant Cell Wall: Methods and Protocols*, Methods in Molecular Biology, vol. 715,
DOI 10.1007/978-1-61779-008-9_6,

about 100 times as expensive and gives more interfering signals just from the reagent. It absorbs blue light and fluoresces green, so there is little chance of interfering signals from plant compounds. The sensitivity of detection for APTS-labelled oligomers excited with an Argon-Ion laser at 448 nm is about 50 times greater than that of an ANTS-labelled oligomer excited by a 325 nm Helium Cadmium laser (4). The pyrene ring seems to make the APTS "sticky." Thus, the capillary needs cleaning frequently to avoid traily peaks.

Both ANTS and APTS have three negative charges on them which ensure that all labelled oligomers have a charge of minus three. We use uncoated capillaries for the electrophoresis with a fairly high ionic strength buffer at a pH of 2.5. This low pH ensures that silicic acid groups are protonated so there are no fixed charges on the walls of the capillary and hence no electro-osmotic flow. A pH of 2.5 also causes almost complete protonation of uronic acids, thus both neutral and acidic oligosaccharides should only be charged because of the three sulphonic acid groups on the fluorescent amine label. Since all oligomers will have the same net charge, the driving force of the electric field should be the same for all oligomers. The frictional force on the oligomers will be the product of the velocity of the oligomer times its frictional coefficient. According to Stokes law, the frictional coefficient $f = 6\pi\eta r$, where η is the viscosity of the medium and r is the Stokes radius of the oligomer. Thus, the larger the hydrodynamic radius of the oligomer the slower it will move in the electric field. Electrophoresis of the labelled oligomers therefore allows one to distinguish them according to their size.

So, using these methods one can profile the products of an enzyme digest of cell wall polymers to follow the progress of the digestion, or can compare the profile of products between wild type and potential cell wall mutants.

If one labels a pure oligosaccharide, it can then be used to characterize the mode of action of an enzyme, or to detect the presence of enzymes that act on the oligomer, even in the presence of a very complex medium. For example, we labelled an oligomer from a partial acid hydrolysate of rhamnogalacturonan and used this to detect and characterize the mode of action of rhamnogalacturonan lyase in intact cotton plants (5).

2. Materials

2.1. Preparation of Aminopyrene Trisulfonate- (APTS) Labelled Oligomers

1. 1 mg oligosaccharide in 20 µL dH_2O: purified oligomers such as xylohexaose (Megazyme International Ireland Ltd., Bray Business Park, Bray, Co. Wicklow, Ireland) should be used (see Notes 1 and 2).
2. 0.1 M APTS (Molecular Probes or Sigma) in 25% acetic acid (see Note 3).

3. 1 M sodium cyanoborohydride in dimethylsulfoxide (see Note 4).
4. 50 mM ammonium acetate buffer, pH 5.2: HPLC-grade acetonitrile 3:1 v/v, briefly degassed with a water aspirator.
5. Chromatography materials: HW-40S gel filtration material column (Toyopearl, Supelco) packed in a 100×10 mm stainless steel column.
6. Heating block or other reliable heat source set at 80°C with holes suitable for 500 µL microfuge tubes.
7. Vortex.
8. Microfuge.
9. Speed vac concentrator.
10. Spectrophotometer.

2.2. Labelling with Aminonaphthalene Trisulfonate (ANTS)

1. Polysaccharide solution: 10 mg/mL
2. Internal standard: 1 µg/µL cellobiose or maltose solution.
3. Appropriate buffer.
4. 4 mUnits of the appropriate enzyme.
5. Heating block.
6. Pipette.

Labelling reagents:

7. 23 mM ANTS (Molecular Probes) in 3% w/v acetic acid.
8. 1 M solution of sodium cyanoborohydride in dimethylsulfoxide.
9. 500 µL microfuge tubes.
10. Vortex.
11. Microfuge.

2.3. Determination of Enzyme Activity In Vitro

1. 1:100 dilution of stock APTS-labelled substrate prepared as above.
2. 1 µU of an appropriate hydrolytic enzyme.
3. Spectrophotometer.
4. Heating block.
5. Standard mixture of oligomers prepared either by specific enzyme digestion or TFA hydrolysis of an appropriate polysaccharide e.g. for determination of xylanase activity the oligomers should be generated from xylan.

2.4. In Situ Detection of Enzyme Activity Using APTS

1. 6 pmol/µL APTS-labelled substrate, prepared as above.
2. Gas-tight syringe: 10 µL (1701 RNFS Hamilton Co., Reno, NV, USA) fitted with a needle made of a 15-cm section of 0.17-mm o.d. fused silica capillary (Alltech Associates, Inc., Deerfield, IL, USA).
3. Plant of interest.

4. Temperature-controlled plant growth chamber.
5. 125 mL Erlenmeyer flask.
6. Extracting solvent: 25 mM sodium acetate buffer, pH 5.2, ice-cold.
7. Water aspirator.
8. Paper towels.
9. Tissue.
10. 2-mL Reacti-Vial (Supelco, Inc., Bellefonte, PA, USA).
11. Centrifuge.

2.5. Capillary Electrophoresis Columns and Buffers for APTS and ANTS-Labelled Oligomer Separation

Capillary columns:

1. Column for APTS-labelled oligomer separation: A fused-silica capillary (TSP050375, Polymicro Technologies, http://www.polymicro.com) of internal diameter 50 μm and length 31 cm with a 3–4 mm window burned into the plastic coating 5.7 cm from the anode end. The window is formed by resting the capillary on a glass window etching device (pEZ-Window, J & W Scientific, Folsom, CA, USA) on a heating plate and covering the capillary at that point with a drop of concentrated sulphuric acid. The capillary is carefully inserted into the plastic tube for circulation of the coolant and assembled into the cartridge as instructed by the manufacturer (see Note 5).
2. Column for ANTS-labelled oligomer separation: A fused-silica capillary (TSP050375, Polymicro Technologies, http://www.polymicro.com) of internal diameter 50 μm and length 50 cm with a 3–4 mm window is burned into the plastic coating at 30 cm from the anode end as described above.
3. Running buffer: 0.1 M sodium phosphate, pH 2.5. This buffer is made by slowly adding 0.1 M phosphoric acid to 0.1 M sodium monophosphate until the pH just reaches 2.5 (see Note 6).
4. Rinsing buffer: 1 M NaOH.

2.6. Capillary Electrophoresis System for ANTS-Labelled Oligosaccharides

A custom built CZE system consisting of a high voltage power supply, helium cadmium laser, optical system built on an inexpensive microscope, an intensified CCD camera for light detection, and a computer-controlled variable-light-attenuator. A complete description of the system is available (6) (Fig. 1).

2.7. Capillary Electrophoresis System for APTS-Labelled Oligosaccharides

1. Instrument: Capillary zone electrophoresis (CZE) Biofocus-2000 (Bio-Rad laboratories, http://www.bio-rad.com) CZE apparatus with laser-induced fluorescence detection.
2. Gas pressure: for injection 4.5 lb/in.^{2} of helium pressure for 0.22 s and for rinsing 80 lb/in.^{2}.
3. Excitation: 488 nm light from a 5 mW argon ion laser.

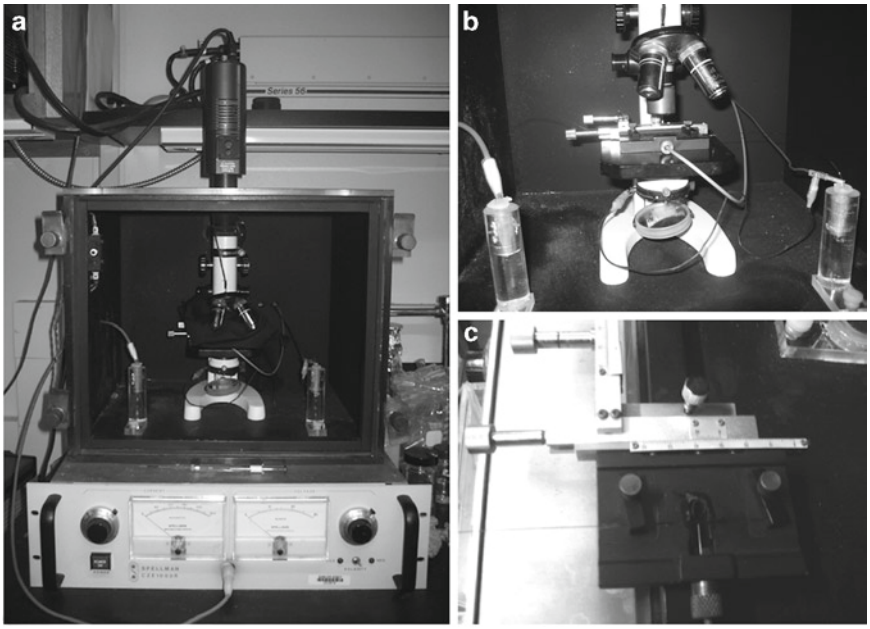

Fig. 1. Pictures showing the major components of the custom built CZE apparatus. (**a**) The complete setup excluding the computer and controller boxes for the attenuator and camera. *Upper right*, Helium Cadmium Laser. *Upper centre*, intensified CCD camera mounted on top of an inexpensive microscope. *Middle left*, micro-switch to ensure that high voltage is disabled if the door to the safety and light excluding enclosure is not in place. *Centre*, microscope. *Lower centre left and right*, plastic holders for the 1.5 mL microfuge vial electrode chambers. *Bottom*, high voltage power supply. (**b**) Close-up view of the holder and X–Y positioner for alignment of the capillary under the microscope objective. (**c**) Close-up of the capillary and the fibre optic held in a stainless steel cannula attached to an eccentric brass nut for movement of the fibre up and down so that it can be aimed directly at the centre of the capillary.

4. Fluorescence emission collection: emission collected through a 520 nm narrow band pass filter.
5. Electrophoresis conditions: 15 kV/70–100 μA with the cathode at the inlet; controlled temperature of 20°C.
6. Data processing: BioFocus 2000 System operating software and BioFocus system integration software.

3. Methods

3.1. Preparation of Aminopyrene Trisulfonate- (APTS) Labelled Substrate

1. Dissolve 1 mg of oligosaccharide in 20 μL of water in a 500-μL microcentrifuge tube.
2. Add 2 μL of 0.1 M APTS in 25% acetic acid and 20 μL of a 1 M solution of sodium cyanoborohydride in dimethylsulfoxide.
3. Vortex-mix well and centrifuge briefly to bring down the liquid, cap the vial tightly.

4. Heat for 60 min at 80°C.
5. After the mixture has cooled to room temperature dilute to about 200 μL with water and pass through a Toyopearl HW-40S (100×10 mm) gel filtration column eluted with 25% acetonitrile and 75% 50 mM ammonium acetate buffer v/v, pH 5.2 at 1 mL/min (see Note 7). The labelled substrate elutes at around 5–6 min and the salts and excess labelling reagents around 10 min. The fractions containing the labelled substrate and free-label can be detected using a fluorescence or visible detector. However, at this scale one can observe with the naked eye where each fraction is.
6. Pool the labelled substrate fractions and evaporate them to dryness in a speed vac concentrator.
7. Re-dissolve the labelled oligomer in 100 μL of water and store frozen.
8. The concentration of APTS-labelled substrate can be determined based on the extinction coefficient of 17,100 M/cm at 456 nm.

3.2. Determination of the Mode of Action of an Enzyme

1. Prepare an appropriate labelled substrate as described above.
2. Estimate the amount of enzyme needed to degrade the substrate over a period of several hours.
3. Incubate an amount of substrate, which will give a total fluorescence intensity of at least 10–50 RFU with the enzyme in an appropriate buffer, taking aliquots after various lengths of time and stopping the reaction by heating at 80°C for 10 min. For xylohexaose, 1 μL of a 1:100 dilution of the stock solution of labelled substrate in a 25-μL incubation with around one micro-unit of enzyme is about right.
4. Generate a standard mixture of labelled oligomers for comparison with the enzyme-produced products e.g. for xylanase take a xylan and digest it for a short time with a xylanase, or hydrolyze it for a short time in trifluoroacetic acid and then label the products as described above (see Note 8).

3.3. Detection of Enzyme Activity in a Complex Medium Such as an Intact Plant Using APTS

Since APTS absorbs blue light and fluoresces green light, the CZE detection system is oblivious to all imaginable plant components. Thus, if one adds an APTS-labelled substrate to a complex system and then analyses the result using CZE with laser-induced fluorescence detection, only the undigested substrate and any degradation products which still contain the label will be visible.

1. Prepare an appropriate labelled substrate and dilute it so that it has a concentration of about 30 pmol/5 μL.

2. Inject 5 μL of the solution into the intercellular spaces of an intact cotton cotyledon using a gas-tight 10 μL-syringe fitted with a needle made of a 15-cm section of 0.17-mm o.d. fused silica capillary.
3. Return the plant to the growth chamber for the desired incubation time.
4. Cut the cotyledon from the plant and place it in an Erlenmeyer flask containing about 30 mL of ice-cold extracting solvent (25 mM sodium acetate buffer, pH 5.2).
5. Apply vacuum for 2 min from a water aspirator.
6. Release the vacuum to cause infiltration of the cotyledon's intercellular spaces by the extracting solvent.
7. Repeat the evacuation and vacuum release 2–3 times.
8. Transfer the cotyledon to paper towels and blot with tissue.
9. Roll the cotyledon in a conical shape and put into a 2-mL Reacti-Vial reaching only half way to the bottom to avoid contact of the cotyledon with the intercellular wash fluid during centrifugation.
10. Centrifuge at 1,500 × *g* for 15 min. About 0.3 mL of intercellular wash fluid per cotyledon will be collected.
11. Analyse the products by CZE and identify them by comparison to standard labelled oligomers.

3.4. Separation of APTS-Labelled Compounds on Capillary Zone Electrophoresis (CZE)

1. Load the samples, running buffer, rinsing buffer, NaOH, and water in the inlet carousel according to the "configuration" stored in the computer memory. Load a vial for waste and running buffer in the outlet carousel according to the "configuration" to be used.
2. Select a "method." For following degradation of xylohexaose we use:
   (a) Inlet buffer: 0.1 M phosphate, pH 2.5.
   (b) Outlet buffer: 0.1 M phosphate, pH 2.5.
   (c) Cartridge temperature 20°C.
   (d) Inverse polarity.
   (e) Voltage 15 kV.
   (f) Current limit 100 μA.
   (g) Run time 8 min.
   (h) Pre-run steps: high pressure rinse with NaOH for 30 s
   High pressure rinse with wash buffer for 60 s.
   Inject 2 psi*s.
   Water dip to prevent carryover between samples.
   Run.

3.5. Profiling and Time Course Analysis of Oligosaccharides Produced by Enzyme Degradation of Polysaccharides

The range of products produced by digestion of a polysaccharide substrate with enzymes can be followed over time by taking small aliquots of the digestion mixture at suitable time points and derivatizing them with ANTS for subsequent analysis by CZE. To make the time course relatively quantitative one can add a constant amount of a commercially available disaccharide such as maltose or cellobiose as an internal standard for comparison of peak heights or areas.

3.5.1. Labelling with Aminonaphthalene Trisulfonate (ANTS)

1. Incubate 25 μL of a 10 mg/mL solution of the polysaccharide in an appropriate buffer with 4 mUnits of enzyme at the temperature optimum for the enzyme.
2. Take duplicate 1 μL aliquots at 0 time, 15, 30 min, 1, 2 and 4 h.
3. Put the aliquots in 500 μL microfuge tubes along with 1 μL internal standard, 1 μL cyanoborohydride solution, and 10 μL ANTS solution. Mix well and then centrifuge briefly to collect the liquid in the tip of the tube.
4. Heat for 1 h at 80°C.

3.5.2. Separation of ANTS-Labelled Compounds by Capillary Zone Electrophoresis (CZE)

1. Turn on power to the laser, the camera, the attenuator controller, and the serial to parallel interface box.
2. Start the CZE control programme on the computer.
3. Set the attenuation to 1 and view the image from the camera.
4. Draw a rectangle around the area that should be used for detection of the fluorescence.
5. Move the rectangle to the top right hand corner of the image and click on the background button.
6. Move the rectangle back over the image of the lumen of the capillary.
7. Designate a file name and path for data storage.
8. Rinse the capillary with running buffer, or with NaOH and then running buffer to remove contaminants from the walls of the capillary. We use a 250 μL gas tight syringe with a replaceable blunt ended needle adapted to press fit onto the capillary with a 1 cm piece of tubing fitting over the needle and a piece of Teflon tubing with ID of 360 nm pushed inside it.
9. Inject the sample by dipping the inlet end of the capillary into the microfuge tube and elevating it 15 cm above the outlet end of the capillary.
10. After 6 s lower the inlet to the same level as the outlet and quickly transfer the inlet end of the capillary to the cathode well (a 1.5 mL microfuge tube with two holes poked in its lid with a push pin, one for the inlet platinum wire electrode and the other for the capillary).

11. Turn on the high voltage to 18 kV with the negative electrode at the inlet. The current should be about 60 μA.
12. Start the run on the computer.
13. After the desired run time, turn off the high voltage and click stop on the computer. The data will automatically be saved.

Figure 2 shows an example of the time course of reaction of endopolygalacturonase with pectic acid.

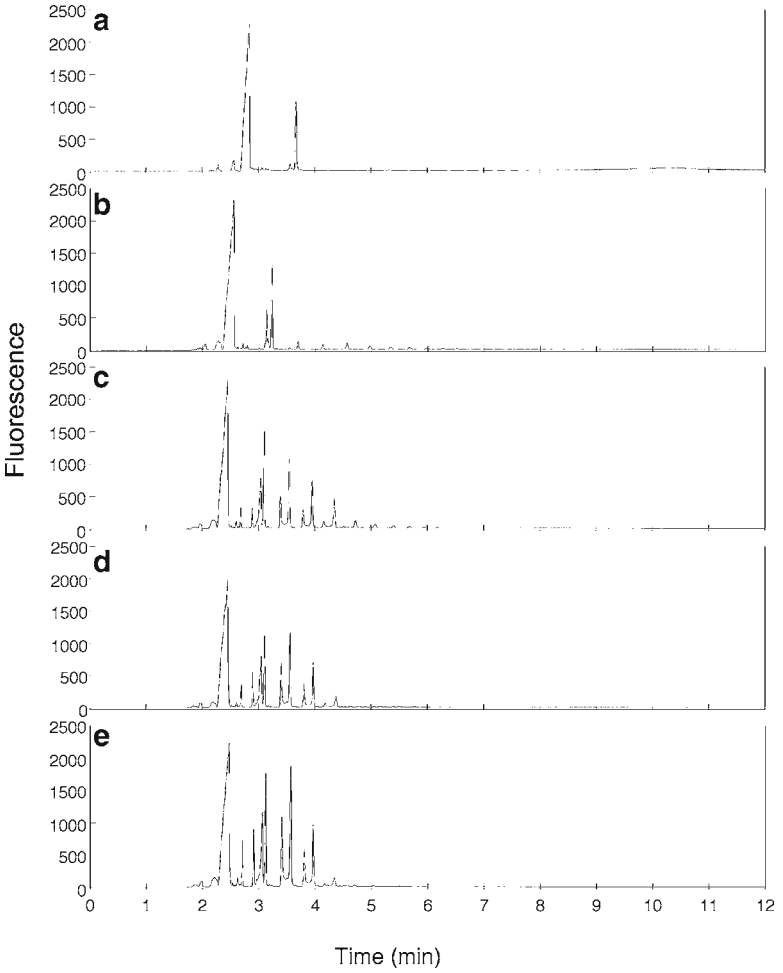

Fig. 2. A time course of degradation of pectic acid with endopolygalacturonase obtained from a *Pichia* clone expressing open reading frame AN 8327. (**a**) No enzyme, just substrate plus cellobiose as an internal standard. The peak at 2.5 min is from the great excess of free ANTS which had not found sugar to attach to. The peak at 3.5 min is from the labelled cellobiose. Note the very low levels of oligomers stretching out until around 11 min where the peaks all fuse together. (**b**) After 3 min of incubation, a series of oligomers is observed with low fluorescent intensity. Remember only the end of the oligomers are labelled so, large oligomers only give a low fluorescence yield per mg. (**c**) After 10 min shorter oligomers predominate. After longer times of incubation (**d**, **e**) only the monomer, dimer, and trimer of GalA remain. Each GalA oligomer gives rise to two peaks because of the tendency of the labelled GalA residue to form a lactone between the carboxyl group and C-3. Thus, part of the oligomer is in the lactone form and part as the free acid. This pattern of degradation reflects a random attack of the polymer by the enzyme.

4. Notes

1. Megazyme has the widest selection of purified oligomers from plant polysaccharides. Many potential substrate oligosaccharides are not commercially available, so must be generated and purified by the individual investigator.
2. An example of purification of rhamnogalacturonan oligomers for investigation of rhamnogalacturonase and rhamnogalacturonan lyase is given in (5).
3. We add 200 µL of 25% acetic acid to the 10 mg vial, we receive the reagent from the manufacturer to avoid the inevitable losses that would occur during transfer of the powder.
4. Use caution when preparing and handling this solution. The cyanoborohydride breaks down slowly to produce HCN and dimethylsulfoxide can carry dissolved substances through skin.
5. We have found the manufacturer's cartridges to be flimsy. They break easily when you tighten the seal at the inlet end to prevent arcing between the inlet electrode and the coolant compartment. A replacement cartridge incorporating the optical bench section of the original cartridge can be made by a competent machine shop and is much sturdier.
6. Too much phosphoric acid makes the current through the capillary at the suggested operating voltage too high.
7. The acetonitrile is necessary to keep the APTS from adsorbing to the gel filtration material.
8. Sub µg amounts of oligosaccharide mixtures can be derivatized in smaller volumes e.g. 5 µL sample in water, 0.5 µL APTS solution and 5 µL cyanoborohydride solution.

References

1. Willats, W. G. T., Knox, J. P., and Mikkelsen, J. D. (2006) Pectin: new insights into an old polymer are starting to gel. *Trends Food Sci Technol* **17,** 97–104.
2. Bauer, S., Vasu, P., Persson, S., Mort, A. J., and Somerville, C. R. (2006) Development and application of a suite of polysaccharide-degrading enzymes for analyzing plant cell walls. *Proc Nat Acad Sci USA* **103,** 11417–11422.
3. De Vries, R. P., and Visser, J. (2001) *Aspergillus* enzymes involved in degradation of plant cell wall polysaccharides. *Microbiol Mol Biol Rev* **65,** 497–522.
4. Evangelista, R. A., Liu, M., and Chen, F. (1995) Characterization of 9-aminopyrene-1,4,6-trisulfonate-derivatized sugars by capillary electrophoresis with laser-induced fluorescence detection. *Anal Chem* **67,** 2239–2245.
5. Naran, R., Pierce, M. L., and Mort, A. J. (2007) Detection and identification of rhamnogalacturonan lyase activity in intercellular spaces of expanding cotton cotyledons. *Plant J* **50,** 95–107.
6. Merz, J. M., and Mort, A. J. (1998) A computer-controlled variable light attenuator for protection and autoranging of a laser-induced fluorescence detector for capillary zone electrophoresis. *Electrophoresis* **19,** 2239–2242.

Chapter 7

Monoclonal Antibodies, Carbohydrate-Binding Modules, and the Detection of Polysaccharides in Plant Cell Walls

Cécile Hervé, Susan E. Marcus, and J. Paul Knox

Abstract

Plant cell walls are diverse composites of complex polysaccharides. Molecular probes such as monoclonal antibodies (MABs) and carbohydrate-binding modules (CBMs) are important tools to detect and dissect cell wall structures in plant materials. We provide an account of methods that can be used to detect cell wall polysaccharide structures (epitopes) in plant materials and also describe treatments that can provide information on the masking of sets of polysaccharides that may prevent detection. These masking phenomena may indicate potential interactions between sets of cell wall polysaccharides, and methods to uncover them are an important aspect of cell wall immunocytochemistry.

Key words: Carbohydrate-binding module, Cell wall immunocytochemistry, Immunofluorescence microscopy, Pectate lyase, Plant cell walls, Monoclonal antibody

1. Introduction

Plant cell walls are diverse composites of structurally complex polysaccharides, phenolic polymers, proteins, ions and water. The macromolecular polysaccharide and phenolic components generate the bulk of cell walls and are major contributors to cell wall properties and functions. Cell wall polysaccharides are highly diverse and vary both in relation to cell wall ultrastructures, cell status and taxonomy (1). The majority of cell wall polysaccharides, including xyloglucan and xylan hemicelluloses and the pectic polysaccharides, contain a range of structural variants that appear to be integral to polymer properties and cell wall functions. To fully understand how the diverse cell wall structures function in cell processes and organ mechanics and respond to environmental impacts, it is important to assess the presence of not only specific

Zoë A. Popper (ed.), *The Plant Cell Wall: Methods and Protocols*, Methods in Molecular Biology, vol. 715,
DOI 10.1007/978-1-61779-008-9_7,

polymers but also specific configurations of polymers in relation to individual cell wall architectures, cell types, and cell status.

One of the best ways to detect and assess the presence of polysaccharides in plant materials is by the use of tagged proteins with specific recognition capacities. Currently, most proteins used for cell wall polysaccharide recognition are rodent monoclonal antibodies (MABs) and carbohydrate-binding modules (CBMs). In the case of complex carbohydrate polymers, purification of immunogens in sufficient amounts for antibody production is often a limiting step. In nature, CBMs of microbial and plant polysaccharide hydrolases are used for carbohydrate recognition. These protein domains encompass a large collection of sequences and a wide range of ligand specificities (2). When produced as separate recombinant his-tagged modules, they can be readily adapted to antibody-style procedures including immunocytochemistry approaches (3). Large sets of these MAB and CBM probes directed to cell wall polysaccharides are now available. This chapter will focus on general factors relating to the use of these probes to detect polysaccharides in conjunction with cell wall imaging using immunocytochemistry with an emphasis on immunofluorescence procedures.

Cell wall immunocytochemistry has entered an exciting and intriguing phase with the recent discovery that polysaccharide epitopes present in cell walls may not be directly detectable due to the presence of other polymers – perhaps indicating intimate associations. To date, this has been demonstrated for pectic homogalacturonan (HG) polysaccharides obscuring or masking xyloglucan and xylan polysaccharides in primary cell walls (4, 5). Combining the use of molecular probes with specific enzymatic treatments provides a more nuanced understanding of the occurrence of polysaccharides in cell walls. Treatments of plant materials to explore these phenomena and to uncover masked epitopes of hemicelluloses are described below.

All MAB and CBM probes can also be used to detect polysaccharides (when isolated from plant cell walls) using microtitre plates, nitrocellulose, and microarray substrates. The general principles of MAB/CBM detection strategies, staged incubations, importance of washing steps, etc. in these cases have been discussed elsewhere (6, 7).

2. Materials

2.1. Molecular Probes

1. A large range of rodent MABs that recognise plant cell wall polysaccharides and proteoglycans is now available as detailed at the online sites of Biosupplies (www.biosupplies.com.au), Carbosource Services (www.carbosource.net) and PlantProbes (www.plantprobes.net). Biosupplies and Carbosource MABs

are derived using mouse hybridoma systems, and thus the probes require anti-mouse secondary reagents whereas those at PlantProbes are mostly rat and require anti-rat secondary reagents (see Note 1).

2. CBMs, derived from cell wall hydrolase enzymes, are generally used as recombinant proteins with polyhistidine tags to allow detection with secondary reagents; however, they can also be used directly as fusion proteins with fluorescent proteins such as GFP, which allows direct imaging using fluorescence microscopy as shown in Fig. 1 (see Note 2). CBMs are not yet as widely available as MABs, but some are available commercially (see online sites above).

2.2. Preparation, Fixation, and Sectioning of Plant Materials

1. Four percent solution of formaldehyde in PEM buffer: 50 mM Pipes, 5 mM EGTA, 5 mM $MgSO_4$; pH adjusted to 7.0 with KOH. Make a 12 or 16% (w/v) stock solution of paraformaldehyde in water by heating up to 70°C and adding 1 M NaOH dropwise until the cloudy solution turns clear. Cool to RT. A good alternative is 16% formaldehyde solution (Agar Scientific, Stansted, UK). Aliquots can be stored at −20°C for up to 6 months (see Note 3).
2. Ethanol to prepare aqueous solutions (30–100%) for dehydration procedures.
3. Wax for embedding. Steedman's wax, an ethanol-soluble low melting point polyester wax (35–37°C), is prepared from a mixture of polyethylene glycol 400 distearate and 1-hexadecanol (cetyl alcohol) (Sigma-Aldrich, Gillingham, UK) (see Note 4).
4. LR White resin (hard grade, containing 0.5% of the catalyst benzoin methyl ether, Agar Scientific) can be used for both light and electron microscopy.

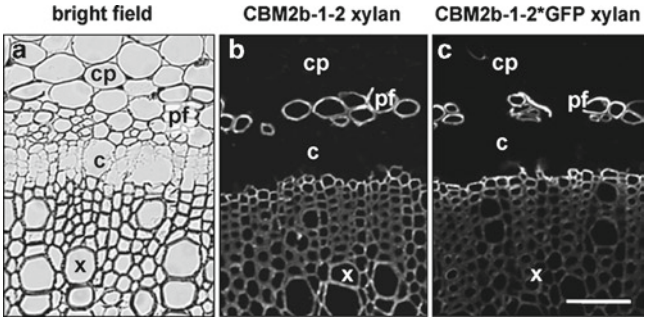

Fig. 1. Micrographs showing comparison of indirect and direct fluorescence labelling procedures for the detection of xylan by the CBM probe CBM2b-1-2. Equivalent transverse sections of tobacco stem showing (**a**) bright field showing all cells, (**b**) section showing indirect labelling of secondary cell walls using his-tagged CBM2b-1-2 and anti-his secondary reagents and (**c**) section showing direct immunolabelling of secondary cell walls with a CBM2b-1-2*GFP construct. Both methods are effective for the detection of xylan in secondary cell walls. *cp* cortical parenchyma; *pf* phloem fibres; *c* cambium; *x* xylem. Bar = 10 μm.

5. Disposable base moulds (15 × 15 × 5 mm, Electron Microscopy Sciences, Hatfield, USA) and embedding cassettes (Simport, Beloeil, Canada) for wax embedding.
6. Gelatine capsules (Agar Scientific) for resin embedding.
7. Polysine-coated microscope slides (VWR, Lutterworth, UK).
8. Vectabond (Vector Laboratories, Peterborough, UK) coated multitest eight-well glass slides (MP Biomedicals, Solon, USA).
9. Nickel grids (Agar Scientific) for electron microscopy.

2.3. Immuno-Microscopies

1. Super PAP hydrophobic pen (Agar Scientific) for marking buffer incubation regions on glass slides.
2. Phosphate-buffered saline (PBS): Prepare 10× stock with 1.37 M NaCl, 27 mM KCl, 100 mM Na_2HPO_4, 18 mM KH_2PO_4 (pH 7.4) and autoclave before storage at room temperature. Prepare working solution by dilution of one part with nine parts water. Alternatively, use prepared 10× PBS (Severn Biotech, Kidderminster, UK).
3. Blocking/antibody dilution buffers. PBS with 3% (w/v) milk protein (e.g. Marvel Milk) (PBS/MP) or 3% (w/v) bovine serum albumin (Sigma-Aldrich) in PBS (PBS/BSA).
4. Secondary antibodies: anti-rat immunoglobulin (whole molecule) reagents coupled to FITC and gold; mouse anti-polyhistidine; anti-mouse immunoglobulin coupled to FITC (Sigma-Aldrich), anti-polyhistidine coupled to Alexafluor 488 (Serotec, Kidlington, UK); anti-rat coupled to AlexaFluor 488 (Invitrogen).
5. Anti-fade reagents. Citifluor glycerol/PBS AF1 (Agar Scientific).
6. Microscope slide cover slips (Scientific Laboratory Supplies, Nottingham, UK)
7. 0.25% (w/v) Calcofluor White (fluorescent brightener, Sigma-Aldrich).

2.4. Enzymatic Pre-Treatments (Pectic HG Removal)

1. High pH solution for pectin de-esterification. 0.1 M sodium carbonate (pH 11.4).
2. Pectate lyase (from *Cellvibrio japonicus*) (Megazyme, Bray, Ireland) (see Note 5).
3. CAPS buffer: 50 mM CAPS, 2 mM $CaCl_2$, pH 10.

3. Methods

Here we focus on immunofluorescence microscopy as this is a sensitive method that can provide an important overview of the occurrence of cell wall epitopes across an organ as well as significant

detail in relation to individual cells. Electron microscopy is useful to locate cell wall polysaccharides in specific cell wall domains and other cell compartments such as the Golgi apparatus.

3.1. Plant Material Preparation, Excision, and Fixation Procedures

1. Small samples such as *Arabidopsis* seeds or seedlings can be plunged directly into formaldehyde fixative. Maintain in fix for at least 2 h and for no more than overnight. Transfer to PEM buffer or PBS and store at 4°C until use.
2. Some relatively stiff materials such as stems are amenable to direct sectioning by hand. Hand-cut sections can be prepared with a razor blade and can be cut from a fresh stem directly into fixative solution or into water if the material is prefixed.
3. For wax- and resin-embedding procedures, pieces of material (generally no thicker than 5 mm) are excised from plant organs and placed in fixative solution. Placing material under vacuum (to expel air) can help with infiltration of the fixative.

3.2. Wax-Embedding Protocol

The wax we use is known as Steedman's wax (8), and is a low melting point polyester wax with good sectioning properties. It is soluble in ethanol and therefore removed prior to immunolabelling resulting in good maintenance of antigenicity.

1. Wash fixed material in PEM buffer or PBS buffer, 2 times 10 min.
2. Dehydrate by incubation in an ascending ethanol series (30, 50, 70, 90, and 100%) with 30 min incubation for each change at 4°C.
3. Move samples to 37°C for next steps.
4. Incubate in molten wax and ethanol (1:1, overnight) and then 100% wax (2 times 1 h).
5. Keep wax molten using a 37°C oven.
6. Fill base mould with molten wax and place sample in the wax. Take care to orientate the sample for optimal sectioning. Fill up with molten wax, and when almost set, apply embedding cassette.
7. Leave at RT overnight to solidify. Can be used 12–24 h after embedding or can be stored in a cool, dry place indefinitely.

3.3. Sectioning Wax-Embedded Material

1. These instructions are for the use of a HM 325 rotary microtome (Microm, Bicester, UK), but they will be readily adapted to other systems.
2. Sections are cut to a thickness of ~10–12 μm to produce ribbons, which are transferred to paper. Sections are selected and placed on polysine slides over a drop of water to promote spreading.
3. Slides are allowed to dry in air overnight.

4. To de-wax and re-hydrate sections, incubate slides with 100% ethanol 3 times 10 min, 90% ethanol/water 10 min, 50% ethanol/water 10 min, water 10 min, water 90 min.
5. Slides are then air-dried and can be stored at RT indefinitely.

3.4. Embedding Protocol for LR White Resin

1. Wash in buffer minus fixative for 3 times 10 min (or overnight at 4°C).
2. Dehydrate using an ascending ethanol series (30, 50, 70, 90, and 100%) with 30 min each change.
3. Infiltrate with resin at 4°C by increasing from 10% resin in ethanol 1 h, 20% 1 h, 30% 1 h, 50% 1 h, 70% 1 h, 90% 1 h, 100% resin overnight, then 8 h, then overnight.
4. Transfer to gelatine capsules and ensure appropriate orientation of plant material. Fill to the top with resin and seal to exclude air.
5. Allow polymerisation of resin either at 37°C for 5 days or by action of UV light at –20°C.

3.5. Sectioning of Resin-Embedded Materials

1. These instructions relate to the use of Reichert-Jung Ultracut Ultramicrotome.
2. Prepare glass knives.
3. For light microscopy, cut sections to a thickness of 1–2 μm onto water.
4. Transfer sections to a drop of water on Vectabond-coated slides and allow them to dry on to the slide in air.
5. For electron microscopy, cut ultrathin sections to a thickness of ~80 nm when they are silvery gold in colour.
6. Collect sections on nickel grids.

3.6. Immunolabelling of Plant Cell Walls Using Monoclonal Antibodies

This procedure is for the indirect immunofluorescence labelling of sections of plant material (see Note 6). Always ensure that there is a no-primary-antibody-control to assess the extent of cell wall autofluorescence present in the material. Here we focus on immunofluorescence procedures, but there are very effective alternatives such as immunogold with silver enhancement for light microscopy (9).

1. Use the hydrophobic pen to isolate regions around sections that will contain incubation solutions.
2. Block non-specific binding sites by incubation with PBS/MP for at least 30 min.
3. Incubate with PBS for 5 min.
4. Incubate with primary monoclonal antibody diluted in PBS/MP for at least 1 h at RT or overnight at 4°C. A five to ten-fold dilution of a hybridoma cell culture supernatant is a good starting point for the primary antibody (see Note 7).

5. Wash with three changes of PBS with at least 5 min for each change.
6. Incubate with a secondary antibody diluted in the region of 100-fold in PBS/MP for at least 1 h at RT. Anti-rat-IgG (whole molecule) linked to FITC is widely used. Another good photostable probe is anti-rat-IgG linked to AlexaFluor 488.
7. Wash with three changes of PBS with at least 5 min for each change.
8. Incubate with a tenfold dilution of the Calcofluor White stock solution for 5 min. (see Note 8).
9. Wash with three changes of PBS.
10. Mount samples using a small drop of anti-fade reagent, cover with coverslip and examine. We use Citifluor AF1 glycerol/PBS-based anti-fade.
11. Examine with a microscope fitted with epifluorescence optics.

3.7. Immunolabelling of Plant Cell Walls Using Recombinant CBMs

1. Isolate sections on slides as appropriate and block non-specific binding sites (as previously explained in Subheading 3.6).
2. Incubate with the CBM diluted in PBS/MP for at least 1 h at RT. The most effective working concentration should be determined by trial studies for each CBM, but most CBMs can be used effectively in the range of 5–20 μg/mL.
3. Ensure that there is a no-CBM-control to assess cell wall autofluorescence in the section.
4. Wash with three changes of PBS.
5. In the case of a CBM fused with a fluorescent protein, proceed directly to step 9. In the case of a CBM with a polyhistidine tag, incubate with anti-polyhistidine antibody diluted in the range 1,000-fold in PBS/MP for at least 1 h at RT.
6. Wash with three changes of PBS.
7. Incubate with the secondary antibody (e.g. anti-mouse coupled with FITC at 100-fold dilution) in MP/PBS for at least 1 h.
8. Wash with three changes of PBS.
9. Incubate with Calcofluor White if required as described in Subheading 3.6.8.
10. Mount slides using anti-fade reagent and examine.

3.8. Immunogold Labelling for the Electron Microscope

1. Block to prevent non-specific binding by floating the EM grid section side down on a droplet (at least 20 μL) of PBS/BSA on Parafilm® for 30 min.
2. Transfer grid to a droplet of primary antibody diluted in PBS/BSA. Monoclonal antibody cell culture supernatants should be diluted between 5- and 200-fold.

3. Wash grids by incubation in a minimum of three changes of PBS.
4. Transfer grids to secondary antibody diluted 1 in 20 with PBS/BSA. We routinely use anti-rat IgG coupled to 10 nm gold.
5. Wash as in step 3 and then extensively in distilled water.
6. Allow the grid to dry and then examine in an electron microscope.

3.9. Section Pre-Treatments Prior to Immunolabelling

To date, the demonstrated cases of cell wall polysaccharide epitope masking are of hemicelluloses by pectic HG. Pectic HG is variously methyl-esterified, and to effect its most efficient removal by pectate lyase or polygalacturonase enzymes, a pre-treatment of the section with a high pH solution is required as shown in Fig. 2. These pre-treatments can be applied to all sectioned materials including wax- and resin-embedded materials (see Note 5).

1. Incubate section with a solution of 0.1 M sodium carbonate (pH 11.4) for 2 h.
2. Wash 2 times 10 min with PBS.
3. Incubate with pectate lyase (10 μg/mL) in CAPS buffer for 2 h.

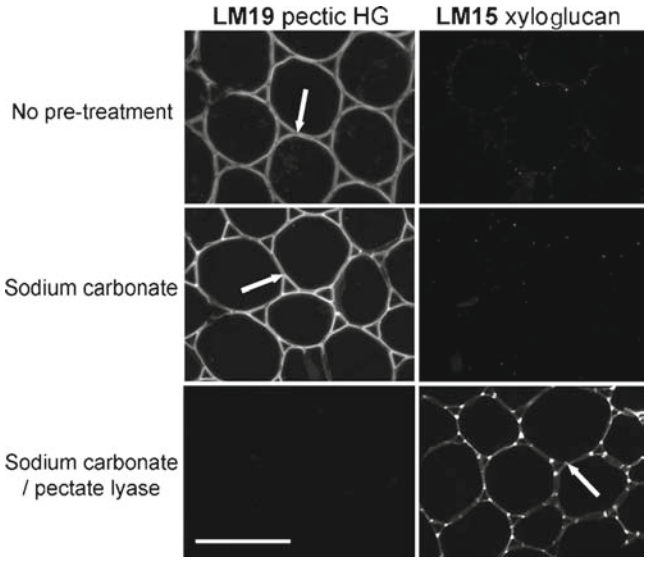

Fig. 2. Micrographs showing impacts of section pre-treatments on the binding of LM19 pectic HG and LM15 xyloglucan MABs to pith parenchyma cell walls in transverse sections of tobacco stem. Immunofluorescence labelling procedures were identical in all cases and representative micrographs are shown with no pre-treatment, with a high pH pre-treatment (sodium carbonate) that would remove methyl esters from HG and with a high pH treatment followed by application of a pectic HG degrading enzyme (sodium carbonate/pectate lyase). The LM15 xyloglucan epitope is abundantly detected at the corners of intercellular spaces after the pectate lyase treatment. *Arrows* indicate the cell walls at the corners of intercellular space. Bar = 100 μm.

4. Wash with three changes PBS.
5. Sections are now ready for immunolabelling as detailed in Subheadings 3.6, 3.7 or 3.8.

4. Conclusion

It is an exciting time for plant cell wall immunochemistry. The combination of extensive sets of molecular probes with methodologies for the enzyme deconstructions and specific removal of cell wall polysaccharides will provide real insights into the range of cell wall structures found in plant cells and organs.

5. Notes

1. The range of available MABs and CBMs is increasing rapidly. Care must, therefore, be taken in probe selection when embarking upon an immunochemical survey of cell walls – especially if an overview is required and there is no focus on a particular subset of cell wall polymers. A good place to start would be with probes directed to pectic HG and also the major hemicellulose that is known for that system/taxon.
2. In the case of a GFP tag, care must be taken to assess the binding ability of the fused CBM. Indeed, depending on the recombinant target, the folding of this bulky tag may impair the recognition ability of the appended CBM by covering its binding site. In this case, the use of another tag is required.
3. Fixatives are needed to stop all cell reactions, and materials are most commonly fixed using aldehyde fixatives. For light microscopy, 4% (w/v) formaldehyde is widely used. For electron microscopy, 2.5% (w/v) glutaraldehyde is used – this is a good fixative but can result in sample autofluorescence and thus is not generally used for light microscopy. However, extensive glutaraldehyde-induced autofluorescence can be effectively quenched by the resin-embedding procedure and so glutaraldehyde-fixed resin-embedded material can be used for both light and electron microscopies. The fixative buffer preferred by some electron microscopists is 0.1 M sodium cacodylate buffer, pH 7.0. Aldehyde fixatives do not directly crosslink polysaccharides and some may remain soluble. This can be assessed by other procedures such as tissue printing (6). Specific fixative procedures to cross-link polysaccharides into materials have not been explored extensively.

4. Melt 900 g of polyethylene glycol 400 distearate and 100 g 1-hexadecanol in a large beaker in an incubator at 65°C. When melted, stir wax very thoroughly using a stirring bar. Pour the wax into a tray lined with aluminium foil (or 50 mL plastic conical tubes) and leave at RT to harden. Prepared wax can be stored at RT indefinitely. For embedding procedures, melt an appropriate amount at 37°C and if using a water bath ensure that container is closed to keep out moisture.
5. The recent discovery that pectic HG can mask or block the detection of hemicellulose polysaccharides requires methods for pectic HG removal from sections by the use of pectic HG-degrading enzymes. Pectate lyase or polygalacturonase can do this effectively. Both of these enzymes act on de-esterified pectic HG and therefore a high pH pre-treatment to remove pectic HG methylesters may optimise subsequent enzyme action and HG removal. Application of pectin-degrading enzymes to material not fixed to a glass slide is likely to result in separation of cells and may cause degradation of samples. Section pre-treatments can also be extended for the enzymatic removal of other cell wall polysaccharides and the enzymes, buffers, and conditions required will need to be determined accordingly.
6. Indirect procedures of immunofluorescence labelling of cell wall are widely used as these are easy and can accommodate the use of several antibodies in the same protocol and also readily allow assessments of non-specific binding and background autofluorescence. The principles of staged incubations in the immunolabelling procedures are the same for intact materials and hand-cut sections, and these materials can be incubated in tubes or plates. Direct immunolabelling procedures, requiring just one step, are rapid and also highly effective as shown in Fig. 1.
7. The recommended dilution of an antibody is the highest dilution that results in a strong specific signal. It is often important to assess a few dilutions to decide on a good working dilution. Manufacturers of secondary reagents provide good guidance. For primary MABs, a five to tenfold dilution of cell culture supernatants is often used; however, in some cases, up to a 200-fold dilution can be highly effective.
8. Calcofluor White is used as a counter stain as it binds widely to β-glycans, including cellulose, and fluoresces under UV excitation and therefore can indicate all cell walls in sections and is useful for orientation and identification of immunolabelling in relation to organ and tissue anatomy. An alternative is to use a bright field image for this purpose.

Acknowledgements

We acknowledge the funding from the UK Biotechnology & Biological Sciences Research Council.

References

1. Knox, J. P. (2008) Revealing the structural and functional diversity of plant cell walls. *Curr Opin Plant Biol* **11**, 308–313.
2. Boraston, A. B., Bolam, D. N., Gilbert, H. J., and Davies, G. J. (2004) Carbohydrate-binding modules: fine-tuning polysaccharide recognition. *Biochem J* **382**, 769–781.
3. McCartney, L., Gilbert, H. J., Bolam, D. N., Boraston, A. B., and Knox, J. P. (2004) Glycoside hydrolase carbohydrate-binding modules as molecular probes for the analysis of plant cell wall polymers. *Anal Biochem* **326**, 49–54.
4. Marcus, S. E., Verhertbruggen, Y., Hervé, C., Ordaz-Ortiz, J. J., Farkas, V., Pedersen, H. L., Willats, W. G. T., and Knox, J. P. (2008) Pectic homogalacturonan masks abundant sets of xyloglucan epitopes in plant cell walls. *BMC Plant Biol* **8**, 60.
5. Hervé, C., Rogowski, A., Gilbert, H. J., and Knox, J. P. (2009) Enzymatic treatments reveal differential capacities for xylan recognition and degradation in primary and secondary plant cell walls. *Plant J* **58**, 413–422.
6. Willats, W. G. T., Steele-King, C. G., Marcus, S. E., and Knox, J. P. (2002) Antibody techniques. In: *Molecular Plant Biology – Volume Two: A Practical Approach* (Gilmartin P. M., Bowler C. (eds)), pp 199–219, Oxford University Press, Oxford, UK.
7. Moller, I., Sørensen, I., Bernal, A. J., Blaukopf, C., Lee, K., Øbro, J., Pettolino, F., Roberts, A., Mikkelsen, J. D., Knox, J. P., Bacic, A., and Willats, W. G. T. (2007) High-throughput mapping of cell wall polymers within and between plants using novel microarrays. *Plant J* **50**, 1118–1128.
8. Steedman, H. F. (1957) A new ribboning embedding medium for histology. *Nature* **179**, 1345.
9. Meloche, C. G., Knox, J. P., and Vaughn, K. C. (2007) A cortical band of gelatinous fibers causes the coiling of redvine tendrils: a model based upon cytochemical and immunocytochemical studies. *Planta* **225**, 485–498.

Chapter 8

Screening and Characterization of Plant Cell Walls Using Carbohydrate Microarrays

Iben Sørensen and William G.T. Willats

Abstract

Plant cells are surrounded by cell walls built largely from complex carbohydrates. The primary walls of growing plant cells consist of interdependent networks of three polysaccharide classes: cellulose, cross-linking glycans (also known as hemicelluloses), and pectins. Cellulose microfibrils are tethered together by cross-linking glycans, and this assembly forms the major load-bearing component of primary walls, which is infiltrated with pectic polymers. In the secondary walls of woody tissues, pectins are much reduced and walls are reinforced with the phenolic polymer lignin. Plant cell walls are essential for plant life and also have numerous industrial applications, ranging from wood to nutraceuticals. Enhancing our knowledge of cell wall biology and the effective use of cell wall materials is dependent to a large extent on being able to analyse their fine structures. We have developed a suite of techniques based on microarrays probed with monoclonal antibodies with specificity for cell wall components, and here we present practical protocols for this type of analysis.

Key words: Carbohydrate microarrays, Plant cell walls, Polysaccharides, Antibodies, CoMPP

1. Introduction

The "comprehensive microarray polymer profiling" or CoMPP technique combines the specificity of monoclonal antibodies (mAbs) with the high-throughput capacity of microarray technology (1). Using CoMPP, profiles of the polysaccharide compositions of large (hundreds) sets of cell wall samples can be rapidly established (within a few days). CoMPP involves the extraction of cell wall components using a series of solvents. The extractions are printed as microarrays and then probed with a series of mAbs or other probes. The signals from the arrays provide semi-quantitative data about the relative abundance of polysaccharides across the sample set (Fig. 1). The technique can be used to analyse a

Zoë A. Popper (ed.), *The Plant Cell Wall: Methods and Protocols*, Methods in Molecular Biology, vol. 715,
DOI 10.1007/978-1-61779-008-9_8,

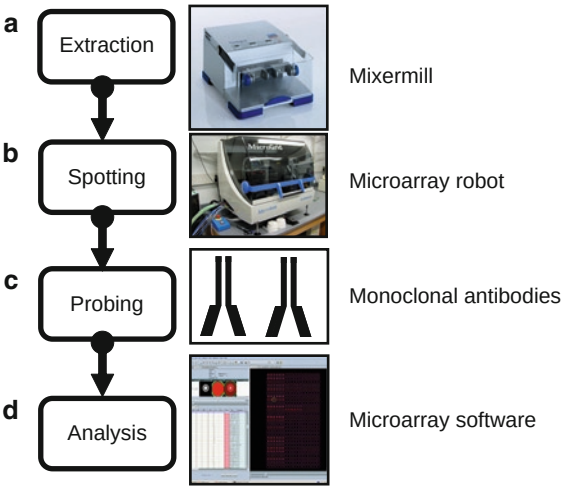

Fig. 1. Cell wall polymer extraction is performed using a 96-well format homogenizer, such as a TissueLyser II (**a**). Using a microarray robot, the samples are printed as microarrays (**b**). The microarrays are probed using monoclonal antibodies (**c**) and the arrays are analysed using microarray analysis software such as ImaGene 6.0 (**d**).

wide range of cell wall materials including different species, developmental stages, mutants or plants exposed to different growth conditions, or processing steps. CoMPP is complementary to established biochemical techniques, such as monosaccharide composition or linkage analysis because antibody binding provides information about the occurrence of larger glycan structures (epitopes) rather than individual sugars that cannot always be assigned with confidence to polysaccharides. CoMPP is highly versatile and can be modified to suit the particular needs of the experiment. Starting materials can be fresh plant tissues, or purified or semi-purified cell walls. The solvents and regimes used to extract polysaccharides can be varied, and so can the set of probes used for analysis. Since only a few milligrammes of starting material is required, CoMPP can be used to fine-map polysaccharide occurrence within single plant organs. CoMPP arrays can be printed onto a variety of surfaces including nitrocellulose membrane or nitrocellulose-covered slides, and the arrays can be printed using either pin-based or piezoelectric robots. The protocols below are a detailed summary of previously published studies (1, 2).

2. Materials

2.1. Extraction Buffers

1. 50 mM diamino-cyclo-hexane-tetra-acetic acid (CDTA), pH 7.5.
2. 4 M sodium hydroxide (NaOH) with 0.1% v/v Sodium borohydride ($NaBH_4$).

3. Cadoxen (31% (v/v) 1,2-diaminoethane with 0.78 M cadmium oxide (CdO)). Prepare cadoxen by stirring 310 mL 1,2-diaminoethane with 720 mL H_2O and 100 g CdO at 20°C for 3 h and 4°C for 18 h. Centrifuge and use supernatant. Store at 4°C (3).

2.2. Other Buffers and Solutions

1. Phosphate buffered saline (PBS): (140 mM NaCl, 2.7 mM KCl, 10 mM Na_2HPO_4, 1.7 mM KH_2PO_4, pH 7.5).
2. Milk powder/PBS (MP/PBS): 5% milk powder (w/v) in PBS. Mix well.
3. Primary mAbs and secondary alkaline phosphatase-conjugated mAbs are diluted in MP/PBS according to supplier's specifications.
4. Alkaline phosphatase (AP) buffer: 100 mM sodium chloride (NaCl), 5 mM magnesium chloride ($MgCl_2$), 100 mM diethanolamine, pH 9.5.
5. 5-Bromo-4-chloro-3′-indolyphosphate (BCIP) stock: 20 mg/mL BCIP in de-ionised water (dH_2O). Store at –20°C.
6. Nitro-blue tetrazolium chloride (NBT) stock: 50 mg/mL NBT in methanol. Store at –20°C.
7. AP developing solution: 10 mL AP-buffer with 66 µL NBT stock and 82.3 µL BCIP stock.

2.3. Materials

1. Nitrocellulose membrane, 0.45 µm pore size (Whatman, Schleicher & Schuell, Dassel, Germany).
2. Eight-strip collection microtubes (Qiagen MM 200, Qiagen Nordic, West Sussex).
3. Metal ball bearings (Qiagen, Qiagen Nordic, West Sussex, UK).

2.4. Equipment

1. TissueLyser II (Qiagen MM 200, Qiagen Nordic, West Sussex, UK).
2. Microarray robot (Microgrid II, Genomic Solutions, Ann Arbor, MI, USA) or (Sprint, ArrayJet, Roslin, Scotland, UK). These are examples that we use and other arraying hardware may perform equally well.
3. Rocking table.

3. Methods

3.1. Plant Cell Wall Material

1. Plant material is collected (e.g. appropriate cell type, tissue, and organs samples), including biological replicates (see Note 1).
2. Samples are homogenised in liquid nitrogen using a mortar and pestle or using a mechanical homogeniser such as the Qiagen TissueLyser II, with appropriate inserts (see Note 2).

3. Alcohol insoluble residue (AIR) is made by adding five volumes of 70% ethanol to the powdered plant material and leaving the sample on a rocking table for 1 h.
4. The samples are spun down at 2,500 × *g* for 10 min and the supernatant discarded.
5. Five volumes of 70% ethanol is added and the samples are shaken for 1 h.
6. Steps 4 and 5 are repeated until the supernatant is clear.
7. A final wash for 5 min in acetone is performed, and the samples are left to air dry, leaving the AIR extract.

3.2. Extraction of Cell Wall Fractions

1. 10 mg of each AIR sample is weighed out and placed in eight-strip collection tubes in 96-tube boxes.
2. A metal ball bearing is placed in each tube and the tubes are capped.
3. Before the extractions, the tubes are submerged in liquid nitrogen and the samples are homogenised once more with the TissueLyser II.
4. 300 µL CDTA is added to each tube, and the samples are shaken on the highest speed (30 Hz) on the TissueLyser II for 2 min before a 2-h extraction at 6–10 Hz (see Note 3).
5. The boxes are placed in a centrifuge and spun down at 2,500 × *g* for 10 min and the supernatants are collected.
6. 300 µL NaOH is added and the procedure is repeated with another 2 h extraction.
7. After the NaOH extraction, the supernatants are collected, 300 µL Cadoxen is added, and the samples are shaken again for 2 h or more.
8. The supernatants are collected.
9. Other solvents or extraction procedures may of course be used, as needed.

3.3. Preparation of Microtiter Plates and Printing of Arrays

1. Samples are transferred to microtiter plates and dilutions are made in PBS, typically a 0, 5 and 25× serial dilution series. Importantly, ink (India ink or other appropriate marker) is used as a marker for the outline of the arrays and is also added to the appropriate wells in the microtiter plate (see Note 4).
2. The microarrayer is loaded with nitrocellulose membrane, pins, and microtiter plates.
3. Parameters such as humidity, collection and dwell time, number replicates, and layout are set.
4. The samples are printed as microarrays (see Note 5).

3.4. Probing of Arrays

The volumes below are optimised for arrays up to 5.7 × 5.7 mm; however, the size of the arrays will vary according to the number of samples printed, and smaller or larger probing containers and volumes of mAb solutions might be used.

1. The membrane is cut into individual arrays.
2. Arrays are blocked individually, for example in weighing boats, in 5 mL MP/PBS solution for 1 h. Remember to include one array as a control (no primary mAb).
3. MP/PBS is discarded.
4. An appropriate dilution of 5 mL mAb in MP/PBS is added, and arrays are left at room temperature for 2 h on a rocking table or overnight at 4°C. The dilutions may have to be tested empirically. The control microarray is incubated in MP/PBS containing no primary antibody.
5. The mAb solution is discarded and arrays are washed 3 times for 5 min in 10 mL PBS on a rocking table.
6. An appropriate dilution of AP-conjugated secondary mAb in MP/PBS (5 mL) is added and arrays are left at room temperature for 2 h on a rocking table, or overnight at 4°C.
7. The mAb solution is discarded, and the arrays are washed 3 times for 5 min in 10 mL PBS and 1 time in 10 mL dH_2O on a rocking table.
8. Arrays are developed using AP developing solution and rinsed in H_2O before placed on filter paper for drying.

3.5. Quantification and Analysis of Arrays

1. The arrays are scanned on a standard commercial desktop flatbed scanner at highest resolution (1,200 dpi) and images saved as 16-bit tiff files, in negative contrast image format (i.e. light-coloured spots on a dark membrane background).
2. The tiff files are uploaded to microarray analysis software (e.g. ImaGene 6.0) and each spot signal quantified, after background corrections are made and the spot areas are appropriately defined, using the parameters of the analytical software.
3. The data is saved as a .txt file and imported into statistical analytical software for further analysis.
4. An appropriate lower limit cut-off value can be introduced in order to avoid false-positive values (see Note 6).

3.6. Online Tools for Analysis

1. A range of tools is available to further extract information from the data and to make more detailed statistical comparisons. For example, heatmaps can be made by uploading the data to the online heatmapper tool (www.bar.utoronto.ca/ntools/cgi-bin/ntools_heatmapper.cgi) in order to present

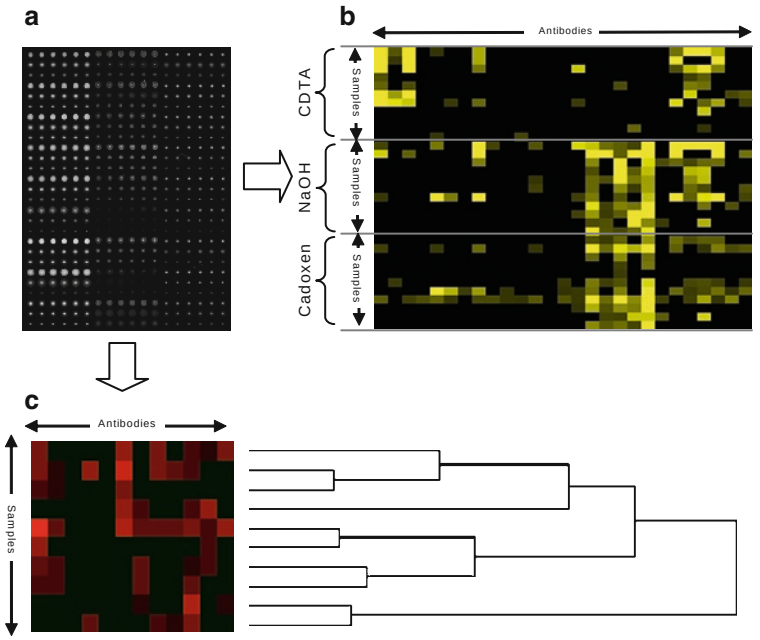

Fig. 2. Example of an array after probing, converted into a negative 16-bit tiff file, is shown in (**a**). The data can be converted into a heatmap format (**b**), or used for a cluster analysis (**c**).

the data in a more visual way. An example is shown in Fig. 2b where the highest value in the data set has been set to 100 and the others adjusted accordingly.

2. Cluster analysis can be performed by uploading the data to the online clustering tool (http://www.bioinf.ebc.ee/EP/EP/EPCLUST/) to reveal the relationship between specific samples. An example is given in Fig. 2c.

4. Notes

1. All plants have different developmentally related cell wall compositions, and when sampling plants outside the lab environment, it is very important to note at least the dates of collection and to preferably collect over a season to ensure the inclusion of as many differentially expressed polymers as possible.
2. Many plants have a very tough cell wall, which can be difficult to homogenise even when frozen in liquid nitrogen and ground with a pestle and mortar. There are several commercially available grinding tools for the mixer mill system, for

example the Retsch stainless steel inserts (Retsch, Haan, Germany), that can be of help.

3. Some plants contain pectic polymers at a level that will make the supernatant in the CDTA extraction very viscous, and depending on the plant material, the AIR to buffer ratio might have to be adjusted.
4. As mentioned, we usually make a 0, 5, and 25× dilution series of our extracts for printing. Depending on the extract, it may, however, sometimes be necessary to start with a 5× dilution to avoid spot saturation.
5. Cadoxen is a very potent cellulose solubiliser and as such will degrade the nitrocellulose over time. Arrays including extracts of this solvent can therefore not be stored as long.
6. The quantification method mentioned above is based on AP-conjugated secondary antibodies but can be adjusted for the use of horseradish peroxide (HRP) or fluorescent quantification systems. The latter is best suited for slide printing, since it requires a slide scanning set-up.

References

1. Moller, I., Sørensen, I., Bernal, A. J., Blaukopf, C., Lee, K., Øbro, J., Roberts, A., Mikkelsen, J. D., Knox, J. P., Bacic, A. and Willats, W. G. T. (2007) High-throughput mapping of cell-wall polymers between and within plants using novel microarrays. *Plant J* **50**, 1118–1128.
2. Sørensen, I., Pettolino, F. A., Wilson, S. M., Doblin, S. M., Johansen, B., Bacic, A. and Willats, W. G. T. (2008) Mixed linkage (1→3),(1→4)-β-D-glucan is not unique to the Poales and is an abundant component of *Equisetum arvense* cell walls. *Plant J* **54**, 510–521.
3. Fry, S. C. (1988) *The Growing Plant Cell Wall: Chemical and Metabolic Analysis.* The Blackburn Press, Caldwell.

Chapter 9

Electron Tomography and Immunogold Labelling as Tools to Analyse De Novo Assembly of Plant Cell Walls

Marisa S. Otegui

Abstract

High-resolution imaging of the membranous intermediates and cytoskeletal arrays involved in the assembly of a new cell wall during plant cytokinesis requires state-of-the-art electron microscopy techniques. The combination of cryofixation/freeze-substitution methods with electron tomography (ET) has revealed amazing structural details of this unique cellular process. This chapter deals with the main steps associated with these imaging techniques: selection of samples suitable for studying plant cytokinesis, sample preparation by high-pressure freezing/freeze substitution, and ET of plastic sections. In addition, immunogold approaches for the identification of proteins and polysaccharides during cell wall assembly are discussed.

Key words: Electron tomography, Cell walls, Cytokinesis, Cryofixation, Immunolabelling

1. Introduction

The formation of a new cell wall during cytokinesis is a highly regulated process that requires coordinated interactions between the cytoskeleton and membrane trafficking pathways. The plant cytokinetic machinery includes three distinct structures: the phragmoplast, the cell plate, and the cell plate assembly matrix (CPAM) (1–3).

The phragmoplast consists of two sets of anti-parallel microtubules (MTs) and actin filaments with their plus/barbed ends facing the division plane. The Golgi apparatus plays a central role during cytokinesis, producing millions of vesicles that provide the building materials for the future cell wall (1). These vesicles are transported along the phragmoplast MTs and fuse with each other at the division plane, giving rise to the cell plate. By the coordinate disassembly and reassembly of phragmoplast MTs,

Zoë A. Popper (ed.), *The Plant Cell Wall: Methods and Protocols*, Methods in Molecular Biology, vol. 715,
DOI 10.1007/978-1-61779-008-9_9,

more vesicles are added to the growing edges of the expanding cell plate. Finally, the cell plate fuses with the parental plasma membrane and a new cell wall forms between the two daughter cells, completing cytokinesis. In addition, a filamentous matrix called CPAM has been found to enclose the cell plate growing edges, fusing vesicles, and most of the MT plus ends at the phragmoplast midline. Although the composition of this matrix is not known, it has been postulated to play an important role in both stabilisation of phragmoplast MT plus ends and membrane fusion (3).

The combination of cryofixation/freeze-substitution methods with electron tomography (ET) has revealed amazing details of this complex process. By combining superb cellular preservation and three-dimensional (3D), high-resolution (4–7 nm) imaging, it has been possible to analyse the architecture of the membranous intermediates that arise during cell plate formation in different plant cell types, the changes in phragmoplast organisation, and even the distribution of individual macromolecules, such as kinesin-like molecules and dynamin rings (1–4). In addition, ET has provided novel information on quantitative changes in cell plate surface area and volume that have been essential to estimate membrane dynamics during cytokinesis (1, 3). No other method has achieved comparable 3D resolution to help us understand plant cytokinesis at the molecular level in the cellular context (5).

To obtain reliable 3D electron tomographic data, it is very important to work with very well-preserved biological sample. Therefore, this chapter will not only deal with the process of calculating and modelling electron tomograms but also with plant sample preparation by the best preservation method available, cryofixation and freeze-substitution. Since it is also very important to be able to correlate structure with composition, protocols for immunodetection of proteins and polysaccharides are also included.

2. Materials

2.1. Plant and Cell Culture Materials

1. Sterile hood.
2. 10% bleach.
3. 70% ethanol.
4. Sterile water.
5. Sterile glass Pasteur pipettes or sterile 1 mL pipette tips.
6. *Arabidopsis* seeds.
7. 0.8% agar plates containing ½ strength, i.e. 2.2 g of powder per litre of Murashige and Skoog (MS) basal medium (Sigma-Aldrich, St. Louis, MO).

8. *Arabidopsis* siliques containing developing seeds (between 5 and 10 days after pollination).
9. Tobacco Bright Yellow-2 (BY-2) cultured cells.
10. BY-2 culture medium: 0.43% (w/v) MS basal medium, 3 μM thiamine-HCl (B1), 0.5 mM myo-inositol, 85 mM sucrose, 1 μM 2,4-dichlorophenoxyacetic acid (2,4-D), 1.3 mM KH_2PO_4, pH 5.5–5.8; autoclave and store at room temperature.
11. Aphidicolin (inhibitor of eukaryotic nuclear DNA replication) (Sigma-Aldrich).
12. Propyzamide (MT assembly inhibitor) (Sigma-Aldrich).

2.2. High-Pressure Freezing

1. High-pressure freezer (Leica EM HPM100 or Bal-tec/ABRA Fluid AG HPM 010).
2. Freezing brass planchettes ("hats") type B (Ted Pella, Redding, CA) if a Bal-tec/ABRA Fluid AG HPM 010 is used.
3. Cryoprotectant: 0.1 M sucrose or 1-hexadecene.
4. 2.0 mL Cryovials (Nalge Nunc, Thermo Fisher Scientific, Rochester, NY).
5. Forceps.
6. Tank of liquid nitrogen.

2.3. Freeze-Substitution and Resin Embedding

1. Cryovials containing 1.5 mL of 2% OsO_4 in anhydrous acetone (Electron Microscope Sciences, Hatfield, PA) (prepare in hood using gloves and store in liquid nitrogen).
2. Cryovials containing 1.5 mL 0.2% glutaraldehyde plus 0.2% uranyl acetate in anhydrous acetone (Electron Microscope Sciences) (prepare in hood using gloves and store in liquid nitrogen).
3. Freeze-substitution/low-temperature resin embedding system (AFS, Leica, Bannockburn, IL).
4. Aluminium block with holes for fitting cryovials.
5. Eponate 12 kit (Ted Pella). Embed 812 kit from Electron Microscope Sciences can also be used.
6. Eponate 12 resin mix without accelerator: 29 g of Eponate 12 resin, 16 g of DDSA, 14.3 g of NMA. It can be kept at 4°C for several days.
7. Eponate 12 resin prepared at the following concentrations: 10% Eponate 12 resin mix, 25% Eponate 12 resin mix, 50% Eponate 12 resin mix, 75% Eponate 12 resin mix.
8. 100% Eponate 12 resin mix with accelerator: 2.5–3% BMPA to freshly prepared Eponate 12 resin mix. It can be kept at 4°C for several days.

9. Lowicryl HM20 resin kit (Polysciences, Warrington, PA, or Electron Microscope Sciences).
10. Flat embedding moulds (Ted Pella).
11. Coverwell Imaging chambers (2.8 mm deep; 20 mm diameter; Electron Microscope Sciences).
12. Dry ice and Styrofoam box.
13. Plastic mounting cylinders (Ted Pella).

2.4. Preparation of Sections for Electron Tomography

1. Copper/rhodium slot grids coated with 0.7–1% (w/v) Formvar in ethylene dichloride (Electron Microscopy Sciences).
2. Ultramicrotome.
3. 2% uranyl acetate on 70% methanol.
4. Reynold's lead citrate: 2.6% lead nitrate and 3.5% sodium citrate, pH 12.
5. 10 or 15 nm colloidal gold particles (Electron Microscopy Sciences) (store at 4°C).
6. Carbon coater.

2.5. Image Acquisition and Calculation of Dual-Axis Electron Tomograms

1. Intermediate voltage (300 kV) electron microscope (for example FEI Tecnai G2 30 TWIN) equipped with high-tilt rod for tomographic image acquisition.
2. Software: SerialEM (6–8) for image acquisition and IMOD (9) package for tomogram reconstruction (can be downloaded from http://bio3d.colorado.edu/docs/software.html) (see Note 1).

2.6. Image Segmentation (Modelling)

1. IMOD package (9) (can be downloaded from http://bio3d.colorado.edu/docs/software.html) (see Note 1).

2.7. Immunolabelling

1. Nickel or gold single slot grids coated with 0.25–0.5% (w/v) Formvar in ethylene dichloride.
2. Phosphate-buffered saline (PBS): Prepare 1 L of 10× stock solution containing 1.76 g of NaH_2PO_4, 11.49 g of Na_2HPO_4, 85 g sodium chloride, pH 6.8 (store at room temperature).
3. PBS-T-0.1%: Dilute 1 mL of 10× PBS with 9 mL of water and add 10 µL of Tween-20.
4. PBS-T-0.5%: Dilute 100 mL of 10× PBS with 900 mL of distilled water and add 0.5 mL of Tween-20.
5. Blocking buffer: 5% (w/v) non-fat milk in PBS-T-0.1%.
6. Primary antibody in blocking buffer.
7. Secondary antibody conjugated to gold particles (5, 10, or 15 nm in diameter) diluted (1:10) in blocking buffer.

8. Cryosubsitution medium: 0.2% glutaraldehyde plus 0.2% uranyl acetate in anhydrous acetone.
9. HM20 resin mix: 2.98 g Crosslinker D, 17.02 g Monomer E, 0.1 g Initiator C. Mix the three ingredients in a brown-coloured glass bottle (HM20 is sensitive to light) and keep it at −20°C.
10. Three HM20 resin: 30, 60, and 100% in anhydrous acetone.

3. Methods

3.1. Plant Material

3.1.1. Arabidopsis Seedlings

On average, the apical root meristem region of an 8-day-old *Arabidopsis* seedling consists of ~52 cells, each of which divides every 18 h (10). Therefore, the chance of finding at least a few cells undergoing cytokinesis in a given root tip is relatively high. To obtain root tips from 8 to 10-day-old seedlings, it is best to germinate seeds on 0.8% agar plates containing ½ strength MS basal medium.

1. Place *Arabidopsis* seeds in plastic tube and add 10% bleach for 5 min, mixing occasionally.
2. Remove bleach using sterile glass Pasteur pipette or sterile 1 mL pipette tips (open the pipette tip box inside the hood) and rinse 3 times with sterile water.
3. Add 70% ethanol, mix, and discard after 5 min.
4. Rinse 3 times with sterile water and place seeds on 0.8% agar plates supplemented with ½ strength MS.

3.1.2. Developing Seeds

Developing seeds are also a very good source of dividing cells. In *Arabidopsis*, the analysis of developing seeds allows for the simultaneous study of somatic cytokinesis in embryo cells and an unconventional cytokinesis that occurs during endosperm cellularisation (1, 11, 12). The endosperm in *Arabidopsis* starts to cellularise at the micropylar region, when the embryo has reached the late globular stage (approximately 5–6 days after pollination). The high rate of cell divisions continues in the embryo until the torpedo/early bent cotyledon stage (approximately 10–12 days after pollination).

3.1.3. Synchronisation of BY2 Cells

The tobacco BY-2 cell line developed by Nagata and co-workers (13, 14) responds well to synchronisation protocols and can provide mitotic indexes of ~39–77%.

1. Grow BY-2 cells in medium containing 3–5 μg/mL aphidicolin for 24 h.
2. Wash out the aphidicolin-containing medium and allow cells to grow in fresh medium for 3 h.

3. Add 6 μM propyzamide to the medium for 6 h (15).
4. After 90–180 min of washing out the propyzamide, most dividing cells undergo cytokinesis (16).

3.2. High-Pressure Freezing

1. 1 mm segments of root tips, whole developing seeds, or excised developing embryos are loaded in a type B freezing planchette containing cryoprotectant (0.1 M sucrose or 1-hexadecene).
2. Another freezing planchette is placed on top to close the chamber. It is important to completely fill the chamber with cryoprotectant, not leaving air bubbles that could collapse during high-pressure freezing.
3. If working with cultured cells grown in a medium with sucrose, a soft pellet of cultured cells can likewise be loaded directly into the freezing planchette.
4. Place freezing planchettes in the sample holder and freeze them under high pressure in a HPM 010 unit.
5. Under liquid nitrogen, split open the two freezing planchettes with the tips of a pair of forceps pre-cooled in liquid nitrogen. The freezing planchettes containing the samples can either be stored in liquid nitrogen (see Note 2) or placed directly in cryosubstitution medium.

3.3. Freeze-Substitution and Resin Embedding

The freeze-substitution medium and resin should be chosen according to the type of analysis one wants to perform. To achieve good preservation and staining of MTs and membranes, freeze-substitution in 2% OsO_4 in acetone followed by Eponate 12 embedding is recommended. However, OsO_4 and epoxy-based resins such as Eponate 12 are not suitable for most immunolabelling approaches. Cryosubstitution in acetone without fixatives or low concentrations of glutaraldehyde (0.2%) and uranyl acetate (0.2%) (17) followed by embedding in methacrylate-based low temperature UV curing resins, such as Lowicryl HM20, are preferred for immunogold labelling applications.

It is important to keep in mind that many antibodies raised against cell wall polysaccharides, such as anti-callose (Biosupplies Australia, Victoria, Australia), anti-xyloglucan (18), and CCRC-M1 (19), and carbohydrate epitopes on arabinogalactan proteins, such as the JIM13 (20) and LM2 (21) antibodies, work well on osmicated samples embedded in Eponate 12.

3.3.1. Structural Analysis Using Dry Ice and Styrofoam Box

1. Place freezing planchettes with frozen samples in cryovials containing 1.5 mL of 2% OsO_4 in acetone. Be sure to keep cryovials in liquid nitrogen during planchette transferring and to pre-cool the tip of the forceps in liquid nitrogen before touching the freezing planchettes.

2. Place the cryovials in an aluminium block pre-cooled in dry ice (at –80°C) inside a Styrofoam box and leave it there for 5 days. Refill the box with dry ice if necessary.
3. Transfer aluminium block with cryovials to a freezer at –20°C for 24 h (see Note 3).
4. Transfer aluminium block with cryovials to fridge at 4°C for at least 3 h (see Note 3).
5. Transfer aluminium block with cryovials to the fume hood and leave it at room temperature for at least 1 h.
6. Discard substitution medium and rinse samples with fresh anhydrous acetone at least 5 times (every 5 min).
7. Remove freezing planchettes (freezing planchettes can be reused if they are cleaned by sonication in methanol or acetone).
8. Rinse samples one more time with fresh acetone.
9. Prepare Eponate 12 resin mix without accelerator.
10. Add increasing concentration of Eponate 12 resin mix (without accelerator) in anhydrous acetone and keep the samples at least 4 h in each of the following resin concentrations: 10% Eponate 12 resin mix, 25% Eponate 12 resin mix, 50% Eponate 12 resin mix, 75% Eponate 12 resin mix.
11. Add 100% Eponate 12 resin mix (without accelerator) for at least 8 h.
12. Prepare 100% Eponate 12 resin mix with accelerator (add 2.5–3% BMPA to freshly prepared Eponate 12 resin mix) (see Note 4). It can be kept at 4°C for several days.
13. Add 100% Eponate 12 resin mix with accelerator for at least 12 h (repeat this step twice).
14. Place samples in flat embedding moulds and polymerise at 60°C for 24 h (see Note 5).
15. Select samples in resin blocks using a dissecting microscope and mount pieces of resin containing the samples on plastic mounting cylinders.

3.3.2. Immunolabelling Using the Leica AFS

Cryosubstitution for immunolabelling can also be performed using "custom" freeze-substitution devices as explained in Subheading 3.3.1. However, if a low temperature UV curing resin is used, it is advisable to use an automatic freeze-substitution device such as the Leica AFS. This device allows for a very precise control of the temperature during freeze-substitution and resin embedding. In addition, it includes a UV lamp that can be directly attached to the sample chamber for resin polymerisation.

1. Under liquid nitrogen, place freezing planchettes containing samples in cryovials containing frozen cryosubstitution medium.

Table 1
Suggested steps/programmes to use during freeze-substitution and resin embedding using a Leica AFS

Step/programme	Temperature 1	Temperature 2 (°C)	Ramp (°C/h)	Duration (h)
0	–90°C	–90	–	120
1	–90°C	–60	5	54
2	–60°C	–50	5	24
3	–50°C/h	18	5	24

2. Set the programme/s in the Leica AFS according to Table 1.
3. Transfer cryovials to the Leica AFS and leave them at –90°C for 5 days.
4. After the AFS chamber has reached –60°C, discard cryosubstitution medium and rinse samples and freezing planchettes with pre-cooled anhydrous acetone at least 3 times.
5. Remove freezing planchettes with pre-cooled forceps. Samples should be free in the acetone by now, completely detached from the freezing planchettes.
6. Prepare HM20 resin mix.
7. Start the infiltration with HM20 by adding increasingly higher concentrations of resin in anhydrous acetone to the cryovials. Three steps can be used: 30, 60, and 100% HM20 resin (at least 3 h for each concentration). All the resin solutions should be pre-cooled to –60°C before being added to the cryovials containing the samples.
8. Add fresh, pre-cooled 100% HM20 resin mix 4–5 times over the next 24 h.
9. With a pre-cooled glass Pasteur pipette, remove samples from cryovials and place them in Coverwell imaging chambers with a glass coverslip on top. Be sure to completely fill the chamber with resin; no air bubbles should be seen after placing the glass coverslip.
10. Attach the UV lamp and adjust the temperature to –50°C.
11. Polymerise at –50°C for 24 h followed by a slow warming up to 18°C over the following 24 h (see Table 1). After 48 h under UV light, the HM20 resin should be completely polymerised.
12. Remove resin blocks with samples from the imaging chambers.
13. Select samples in resin blocks using a dissecting microscope and mount pieces of resin containing the samples on plastic mounting cylinders.

3.3. Preparation of Sections for Electron Tomography

High-pressure frozen/freeze-substituted samples embedded in Eponate 12 can be sectioned in an ultramicrotome (60–70 nm thick section) and analysed in a regular transmission electron microscope to evaluate preservation quality and to identify cells undergoing cytokinesis. Once the right specimens have been selected, semi-thick section for ET can be prepared.

1. Collect 250–300 nm thick sections on single slot specimen grids coated with Formvar.
2. Stain sections with a 2% uranyl acetate in 70% methanol for 10 min (see Note 6) followed by Reynold's lead citrate for 5 min.
3. Apply 10 μL of 10- or 15-nm colloidal gold solution to each side of the sections for 5 min. Remove the excess solution by touching the grid with filter paper. The gold particles are used as fiducials, aiding in the fine alignment of the tilt images during the tomographic reconstruction.
4. Carbon-coat both sides of the grids with the sections to minimise charging and drifting during imaging under the electron beam.

3.4. Image Acquisition and Calculation of Dual-Axis Electron Tomograms

The resolution of a tomographic reconstruction depends on different factors. Given that the quality of the tilt series (image focus and alignment) is optimal, the main factors affecting resolution are (a) the magnification at which the images are collected, (b) the angular interval, (c) the angular range, and (d) section thickness (22, 23). Before collecting the images for calculating tomographic reconstructions, the variables involved in these four factors have to be carefully considered.

(a) Magnification: Very often, large areas of the cells have to be imaged to analyse forming cell walls and associated phragmoplasts. However, imaging at low magnification is not recommended because of the resulting loss in resolution. If a charge-couple device (CCD) camera is used to collect the images, the magnification should be high enough that each pixel in the image is equivalent to ~1 nm in the specimen. If the structure of interest is so large that cannot be imaged in a single frame, montaged images can be used to image large areas without compromising resolution (5).

(b) The angular interval: 1 or 1.5° angular intervals are recommended.

(c) Angular range: Contrary to medical computed tomography in which images of the patient can be collected over a full 360°, the angular range allowed by the conventional tilting specimen holders used for ET is much more restricted, resulting in a wedge of missing information between the maximal tilt angle collected and 90° (6, 24). This results in distorted

tomograms with anisotropic resolution (22). To improve the isotropy in resolution, it is recommended to collect images from two orthogonal axes and combine the two resulting tomograms into a dual-axis tomogram (6).

(d) Section thickness: If an intermediate-voltage (200–300 kV) electron microscope is used, sections thicker than 300 nm will likely result in poor resolution images, particularly at high tilt angles. If larger volumes are required for imaging cell plates and phragmoplasts, serial tomograms can be obtained from serial sections (2, 3). A ribbon of several serial sections can be placed on the same grid and a dividing cell can then be located and imaged on each relevant section in the ribbon. However, it is important to note that this approach suffers from a 15–25 nm gap of missing information between serial tomograms (25). For highly complex cellular structures, this gap in information may cause difficulties in the alignment of serial tomograms.

1. Place specimens in a high-tilt sample holder of an intermediate (300 kV) electron microscope and collect images at 1° angular intervals and over an angular range of ±60–70° using the free software SerialEM (see Note 1) (Fig. 1).
2. After collecting the first stack of images, rotate the grid 90° and collect images at 1° angular intervals along the second axis.
3. Process the resulting images using the *eTomo* programme in the IMOD package (see Note 1) (Fig. 1).

3.5. Modelling and Quantitative Analysis of Tomographic Models

Cellular structures contained in electron tomographic reconstructions can be manually segmented (modelling) using the *3dmod* programme of the IMOD package. Modelling is the creation of graphic objects that accurately represent the 3D positions of features of interest in a tomogram. Image segmentation is the most time consuming part of the process, and it is somehow a subjective task. The *3dmod* programme allows the operator to draw on the image data, placing points, chosen shapes (circles, etc.), or sets of point (lines or curves that match the structure of interest) as "overlays" on the image data. Each such representation is called a contour, and these are generally drawn on a single tomographic slice extracted from the tomogram (Figs. 2 and 3). Contours can be either closed (if they represent something like the membrane that surrounds a vesicle or cisterna) or open (if they represent a fibre, like a MT or actin filament).

Three different types of image displays are generally used during modelling: the Zap window that displays tomographic slices cut parallel to the surface of the physical section that was reconstructed, the Slicer window that allows the operator to display a slice at an arbitrary angle through the volume, and the Model

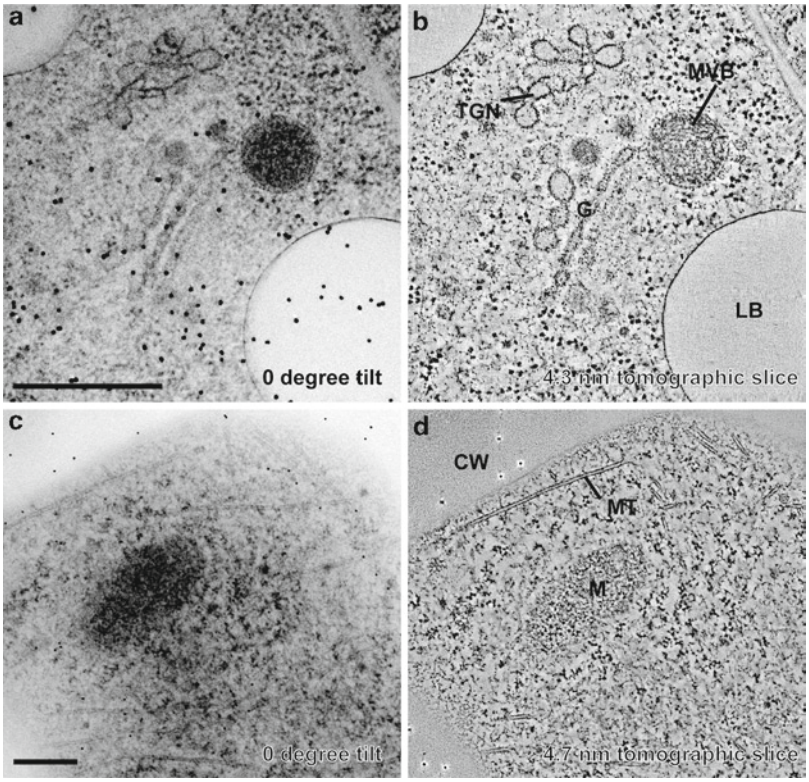

Fig. 1. Image acquisition and ET reconstruction. (**a**, **c**) Semi-thick (300 nm) sections imaged in an FEI Tecnai TF30 at 0° tilt. The small *black dots* are 15 nm gold particles used as fiducials for image alignment. Images were taken every 1° interval, from +60 to −60°, along two orthogonal axes. The two resulting single axis tomograms were combined in a single dual-axis tomogram. (**b**, **d**) Single tomogramic slice show in great detail membrane profiles, microtubules (MTs), ribosomes hardly distinguishable in the original semi-thick sections (**a**) and (**c**), respectively. *CW* cell wall; *G* Golgi; *LB* lipid body; *M* mitochondrion; *MVB* multivesicular body; *TGN trans*-Golgi Network. Scale bars = 500 nm.

View window that shows contours and meshed objects as they are created (Figs. 2 and 3). A general guide that provides a comprehensive description of the *3dmod* modelling programme can be found at http://bio3d.colorado.edu/IMOD.

Quantitative information obtained from tomograms (see below) is based on the tomographic models that have been meshed, a process that generates 3D graphic objects with defined surfaces. However, meshes are derived from contours, so it is extremely important to draw the contours accurately.

3.5.1. Microtubules and Actin Filaments

In the simplest case, MTs and actin filaments can be modelled as hollow tubes of a given diameter.

1. Create a new object under the "Edit" menu of *3dmod* and chose the "open contours" option (Fig. 2a).
2. Move along the stack of tomographic slices using the Zap window, identify one end of the MT and place the first point,

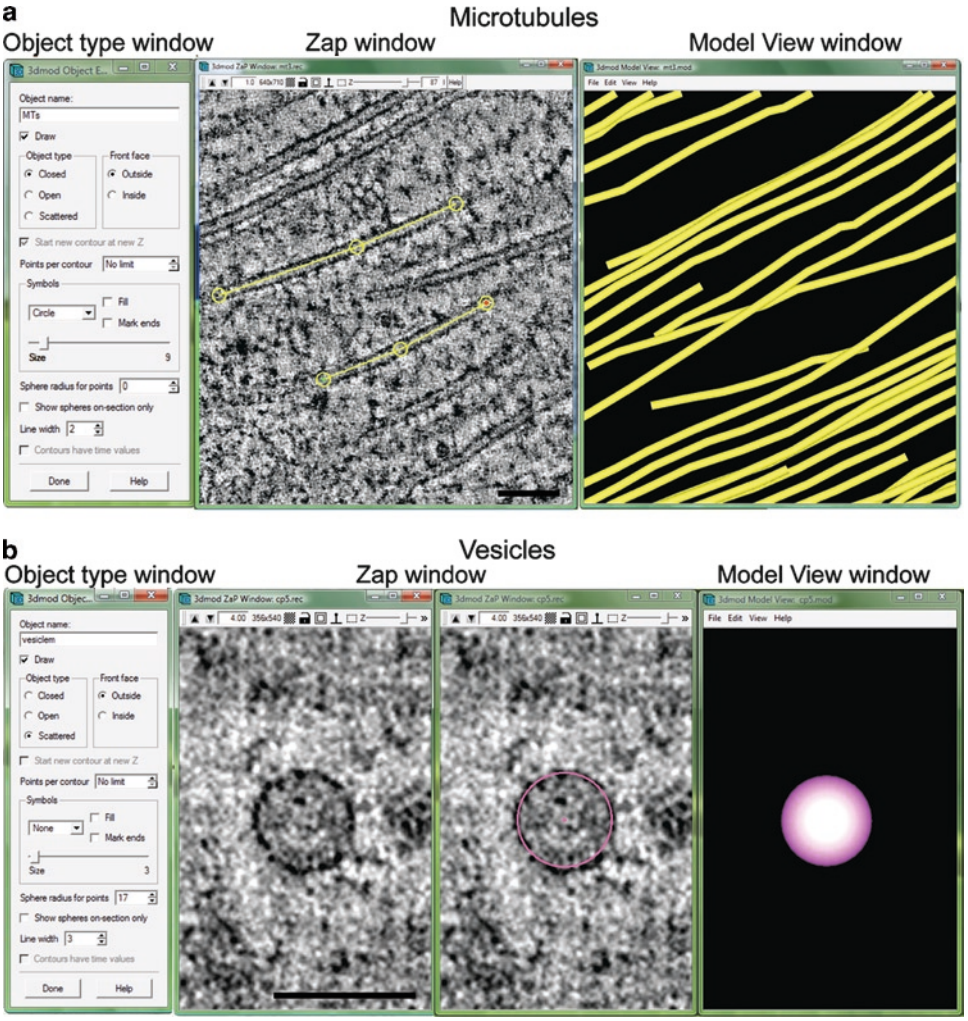

Fig. 2. Segmentation of phragmoplast MTs (**a**) and vesicles (**b**) during cell wall assembly using *3dmod*. MTs are segmented as open contours (*times*) in the Zap window and rendered as hollow cylinders 25 nm in diameter in the Model View window. Vesicles are rendered as spheres of variable radii. Scale bars = 100 nm.

as close to the centre of the MT as possible. Place one or more points at every fifth or sixth tomographic slice along the MT length until reaching the other end of the MT.

3. Alternatively, use the "slicer" window to model MTs (24). Adjust the X, Y, Z sliders to find a tomographic slice that contains as long a segment as possible of the MT axis and place points at the beginning and end of the segment. In either case, each MT/filament should be considered a new contour within one object.
4. To obtain a 3D representation of the MT/filament, use the command *imodmesh* with the options -t, for tube, -d (the pixel diameter of the tube, 25 nm for a MT, 5–9 nm for an actin filament), and -E (this will "cap" the end of the tube).

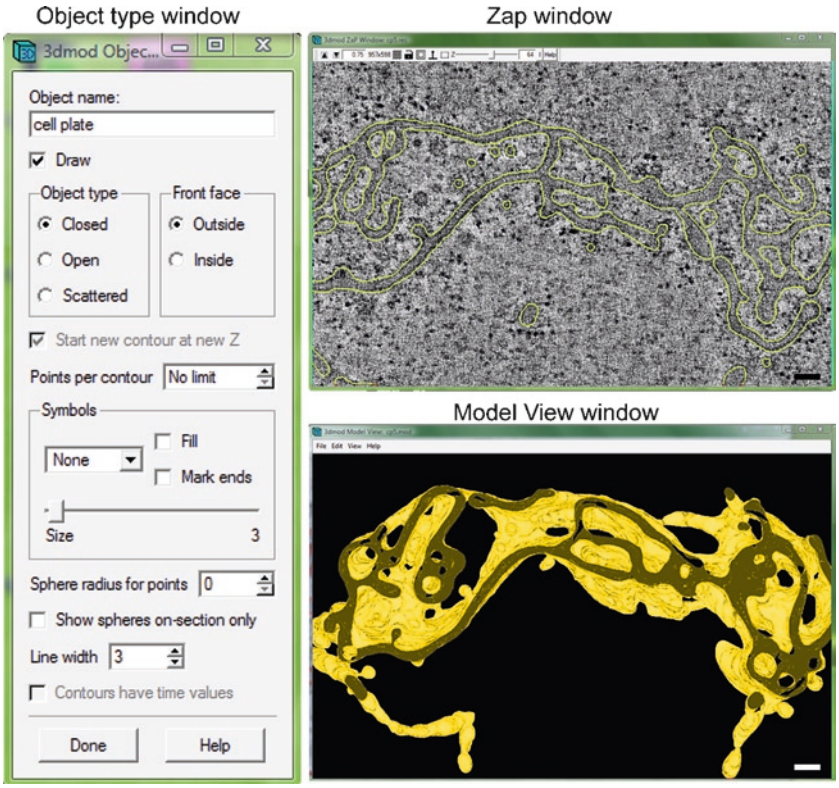

Fig. 3. Segmentation of cell plate domains using the "Closed" object type option in *3dmod*. Cell plate membranes are traced as overlay contours in the Zap window and rendered as a meshed 3D object in the Model View window. Scale bars = 100 nm.

Complete instructions for the use of the *imodmesh* command can be found at http://bio3d.colorado.edu/imod/doc/man/imodmesh.html (see Note 7). Be sure to save the model before running *imodmesh*.

3.5.2. Vesicles

To simplify the modelling of vesicles, it can be assumed that their shape approximately correspond to a sphere. In this case, vesicles can be modelled as "scattered points", where a sphere is computed from a single point placed in the centre of the vesicle, and its size can be adjusted to match the diameter of the vesicle (Fig. 2b). All similar vesicles (for example, all clathrin-coated vesicles) can be contained in a single object.

1. Create a new object under the "Edit" menu and select the "scattered" option.
2. Move along the stack of tomographic slices using the Zap window and identify the centre of the vesicle.
3. Place a point in the centre of the vesicle and define the radius by adjusting the "Sphere radius for points" option.
4. Spheres do not required to be meshed and can be directly displayed as 3D objects in the "Model" window (Fig. 2b).

3.5.3. Cell Plates and Membrane-Bound Organelles

Cell plates, endoplasmic reticulum, and any other membrane-bound organelle under analysis should be modelled as separate closed objects. Non-connected portions of the cell plate or different domains of the endoplasmic reticulum can be modelled as different objects as well. When modelling membranous organelles, it is recommended to place contours in the middle of the lipid bilayer (1, 25).

1. Create a new object under the "Edit" menu and select the "closed" option (Fig. 3).
2. Move along the stack of tomographic slices using the Zap window and draw in each slice the outline of the cellular structure being modelled (Fig. 3).
3. Save model and run the *imodmesh* command. *imodmesh* offers a number of options for capping off objects, connecting contours in non-adjacent tomographic slices, etc. (see Note 7). For a complete reference of *imodmesh* options go to http://bio3d.colorado.edu/imod/doc/man/imodmesh.html.

3.5.4. Quantitative Analysis

One of the powerful advantages of ET is the possibility of obtaining quantitative information from tomographic models. One can analyse spatial relationships between vesicles and MTs, membrane surface area changes during cell plate assembly, frequency and distribution of MT plus ends in the phragmoplast (1, 3, 4). The measurements are generally expressed in terms of the pixel size, which is described in the model header as a number in nanometres. The extent to which the section thinned in the electron beam ("thinning factor") is also described in the model header and is applied to the calculations. Therefore, it is very important to enter accurate values in the model header window (under the "Edit" menu) before performing quantitative calculations.

3.5.5. Quantifying the Volume and Surface Area of Cell Plates

1. Extract randomly located boxes of a defined size along the cell plate.
2. Mesh the portions of cell plates enclosed in these boxes and run the *imodinfo* command to calculate total surface and volume of different modelled structures, using the option –s. A complete description of all options available for the *imodinfo* command can be found at http://bio3d.colorado.edu/imod/doc/man/imodinfo.html (see Note 8).

3.5.6. Quantifying the Density of Ribosomes, Vesicles, or Any Other Structures Modelled as Spheres

1. Ensure that Subheading 3.2.1 all the individual items (for example, individual ribosomes) are points in the same contour of the same object.
2. Extract defined size boxes from the model and run the *imodinfo* command to obtain the number of points contained in the box volume.

3.5.7. Spatial Relationships: MicroTubule Kissing Analysis

To measure the distances between the objects in 3D and to compute an average density of neighbouring items as a function of distance between objects, one can use the microtubule kissing (*MTK*) programme of the IMOD package (9, 26). This programme considers structures of three kinds: open contours, like MTs; scattered point objects, like vesicles; and meshed, closed contour objects like cell plate domains. For MTs, each contour is considered as a separate line. It is possible to calculate the spatial relationship between any object and a whole MT, or to break the MT into multiple segments and measure the closest distances between a chosen object and each of the MT segments. Distances can be measured from the central axis or surface of one object to the central axis or surface of another. A complete explanation of *MTK* and its commands can be found in http://bio3d.colorado.edu/imod/doc/man/mtk.html.

3.6. Immunolabelling

One of the main challenges in this type of imaging analysis is to be able to identify the biochemical identity/composition of the structures reconstructed in electron tomograms. One approach to identify macromolecules in tomographic reconstructions is to perform immunolabelling experiments. This can be done as a correlative approach (the immunolabelling is performed in different sections from the ones that are used for tomographic reconstruction) or a direct approach (when the same sections are used for both immunolocalisation and ET) (27). As an example, correlative immunolabelling experiments with specific antibodies suggested that the electron-dense rings constricting cell plate membranes in endosperm cell plates are dynamin ADL1A/DRP1A polymers (1) (Fig. 4).

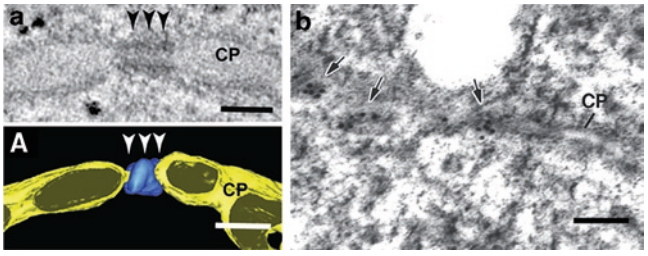

Fig. 4. Identification of protein complexes in electron tomographic reconstructions of *Arabidopsis* endosperm cell plates by correlative immunogold labelling. (**a**, **b**) Membrane-associated rings in endosperm cell plates. (**a**) Tomographic slice and (**a′**) corresponding tomographic model of a cell plate tubule. Note the presence of an electron dense collar (*arrowheads*) associated with a constricted tubule. The identity of the rings as dynamin ADL1A/DRP1A polymers was determined by immunolabelling with specific antibodies (**b**). Scales = 50 nm. Reproduced from Otegui *et al.* (*1*) (Copyright © 2001 American Society of Plant Biologists).

1. Float nickel or gold grids containing section on a drop of 5% milk in PBT-T-0.1% for 20 min.
2. Transfer specimen grid to a drop of primary antibody diluted in 5% milk in PBT-T-0.1% for 1 h.
3. Rinse the grid with a continuous stream of PBS-T-0.5% for 1 min.
4. Remove the excess liquid by touching the grid with filter paper.
5. Place specimen grid in secondary antibody conjugated to gold particles (5, 10, 15 nm in diameter) diluted 1:10 in 5% milk in PBT-T-0.1% for 1 h.
6. Rinse the grid with a continuous stream of PBS-T-0.5% for 1 min, followed by rinsing with distilled water.
7. Post-stained grid with 2% uranyl acetate in 70% methanol and Reynold's lead citrate.

4. Notes

1. SerialEM is a free software package for image acquisition (http://bio3d.colorado.edu/SerialEM) that is compatible with FEI and JEOL electron microscopes. IMOD is a free software package that runs in both PC and Macintosh systems and was developed primarily by David Mastronarde, Rick Gaudette, Sue Held, and Jim Kremer at the Boulder Laboratory for 3D Electron Microscopy of Cells. It contains around 140 programmes for image processing, tomogram calculation, image segmentation, display, and quantitative analysis.
2. High-pressure frozen material can be stored in liquid nitrogen for months or even years without suffering changes in cellular preservation.
3. OsO_4 in acetone is highly volatile. Even when the acetonic OsO_4 solution is kept in closed cryovials, osmication of objects around cryosubstitution vials can easily happen. If a freezer/fridge is used during cryosubstitution with OsO_4, it is advisable to have a freezer/fridge fully dedicated to this use to avoid contamination of other reagents and lab ware.
4. BDMA is recommended as the accelerator for the Eponate 12 resin mix instead of DMP-30 because BDMA has lower viscosity and diffuses more rapidly into tissues.
5. Unpolymerised resin waste, dirty globes, and other resin-contaminated items should be placed in the oven for 24 h for polymerization before discarding them.

6. The use of methanolic solution of uranyl acetate is recommended because it increases the contrast of membrane and cytoskeletal elements more than aqueous solutions do.
7. *imodmesh* generates triangles that connect neighbouring points within a contour and nearby points on adjacent contours. The resulting triangles represent a surface in space that is an excellent approximation to all the contour information, so they are used for all subsequent quantifications of area, volume, and distance. They can also be used to generate a shaded surface that provides a good visual representation of the modelled object.
8. *imodinfo* provides information about IMOD models, such as lists of objects, contours and point data, lengths and centroids of contours, and surface areas and volumes of objects or surfaces.

Acknowledgements

This work was supported by the National Research Initiative of the USDA Cooperative State Research, Education and Extension Service, grant number 2008-35304-18672 to M.S.O.

References

1. Otegui, M. S., Mastronarde, D. N., Kang, B. H., Bednarek, S. Y., and Staehelin, L. A. (2001) Three-dimensional analysis of syncytial-type cell plates during endosperm cellularization visualised by high resolution electron tomography. *Plant Cell* **13,** 2033–2051.
2. Otegui, M. S., and Staehelin, L. A. (2004) Electron tomographic analysis of post-meiotic cytokinesis during pollen development in *Arabidopsis thaliana*. *Planta* **218,** 501–515.
3. Segui-Simarro, J. M., Austin, J. R., II, White, E. A., and Staehelin, L. A. (2004) Electron tomographic analysis of somatic cell plate formation in meristematic cells of *Arabidopsis* preserved by high-pressure freezing. *Plant Cell* **16,** 836–856.
4. Austin, J. R., II, Segui-Simarro, J. M., and Staehelin, L. A. (2005) Quantitative analysis of changes in spatial distribution and plus-end geometry of microtubules involved in plant-cell cytokinesis. *J Cell Sci* **118,** 3895–3903.
5. Otegui, M. S., and Austin, J. R., II (2007) Visualization of membrane-cytoskeletal interactions during plant cytokinesis. *Methods Cell Biol* **79,** 221–240.
6. Mastronarde, D. N. (1997) Dual-axis tomography: an approach with alignment methods that preserve resolution. *J Struct Biol* **120**, 343–352.
7. Mastronarde, D. N. (2005) Automated electron microscope tomography using robust prediction of specimen movements. *J Struct Biol* **152,** 36–51.
8. Mastronarde, D. N. (2008) Correction for non-perpendicularity of beam and tilt axis in tomographic reconstructions with the IMOD package. *J Microsc* **230,** 212–217.
9. Kremer, J. R., Mastronarde, D. N., and McIntosh, J. R. (1996) Computer visualization of three-dimensional image data using IMOD. *J Struct Biol* **116,** 71–76.
10. Beemster, G. T. S., and Baskin, T. I. (1998) Analysis of cell division and elongation underlying the developmental acceleration of root growth in *Arabidopsis thaliana*. *Plant Physiol* **116,** 1515–1526.
11. Otegui, M. S., and Staehelin, L. A. (2000) Cytokinesis in flowering plants: more than one way to divide a cell. *Curr Opin Plant Biol* **3,** 493–502.

12. Otegui, M. S., and Staehelin, L. A. (2000) Syncytial-type cell plates: a novel kind of cell plate involved in endosperm cellularization of *Arabidopsis*. *Plant Cell* **12,** 933–947.
13. Nagata, T., Nemoto, Y., and Hasezawa, S. (1992) Tobacco BY-2 cell line as the "HeLa" cell in the cell biology of higher plants. *Int Rev Cytol* **132,** 1–30.
14. Nagata, T., and Kumagai, F. (1999) Plant cell biology through the window of the highly synchronised tobacco BY-2 cell line. *Methods Cell Sci* **21,** 123–127.
15. Kakimoto, T., and Shibaoka, H. (1988) Cytoskeletal ultrastructure of phragmoplast-nuclei complexes isolated from cultured tobacco cells. *Protoplasma* **S2**, 95–103.
16. Samuels, L. A., Giddings, T. H., and Staehelin, L. A. (1995) Cytokinesis in tobacco BY-2 and root tip cells: a new model of cell plate formation in higher plants. *J Cell Biol* **130,** 1345–1357.
17. Giddings, T. H. (2003) Freeze-substitution protocols for improved visualization of membranes in high-pressure frozen samples. *J Microsc* **212,** 53–61.
18. Moore, P. J., Darvill, A. G., Albersheim, P., and Staehelin, L. A. (1986) Immunogold localization of xyloglucan and rhamnogalacturonan I in the cell walls of suspension-cultured sycamore cells. *Plant Physiol* **82,** 787–794.
19. Puhlmann, J., Bucheli, E., Swain, M. J., Dunning, N., Albersheim, P., Darvill, A. G., and Hahn, M.G. (1994) Generation of monoclonal antibodies against plant cell-wall polysaccharides. I. Characterization of a monoclonal antibody to a terminal alpha-(1→2)-linked fucosyl-containing epitope. *Plant Physiol* **104,** 699–710.
20. Knox, J. P., Linstead, P. J., Peart, J., Cooper, C., and Roberts, K. (1991) Developmentally regulated epitopes of cell surface arabinogalactan proteins and their relation to root tissue pattern formation. *Plant J* **1,** 317–326.
21. Smallwood, M., Yates, E. A., Willats, W. G. T., Martin, H., and Knox, J. P. (1996) Immunochemical comparison of membrane associated and secreted arabinogalactan-proteins in rice and carrot. *Planta* **198,** 452–459.
22. McEwen, B. F., and Frank, J. (2001) Electron tomographic and other approaches for imaging molecular machines. *Curr Op Neurobiol* **11,** 594–600.
23. Marsh, B. J. (2005) Lessons from tomographic studies of the mammalian Golgi. *Biochim Biophys Acta* **1744,** 273–292.
24. O'Toole, E. T., Giddings, J. T. H., Dutcher, S. K., and McIntosh, J. R. (2007) Understanding microtubule organizing centers by comparing mutant and wild type structures with electron tomography. *Methods Cell Biol* **79,** 125–143.
25. Ladinsky, M. S., Mastronarde, D. N., McIntosh, J. R., Howell, K. E., and Staehelin, L. A. (1999) Golgi structure in three dimensions: functional insights from the normal rat kidney cell. *J Cell Biol* **144,** 1135–1149.
26. Marsh, B. J., Mastronarde, D. N., Buttle, K. F., Howell, K. E., and McIntosh, J. R. (2001) Organellar relationship in the Golgi region of the pancreatic beta cell line, HIT-T15, visualised by high-resolution electron tomography. *Proc Natl Acad Sci U S A* **98,** 2399–2406.
27. Donohoe, B. S., Kang, B. -H., and Staehelin, L. A. (2007) Identification and characterization of COPIa- and COPIb-type vesicle classes associated with plant and algal Golgi. *Proc Natl Acad Sci U S A* **104,** 163–168.

Chapter 10

Analysing Cellulose Biosynthesis with Confocal Microscopy

Meera Nair and Seth DeBolt

Abstract

Plant cells are delimited by a rigid cell wall that resists internal turgor pressure, but extends with a remarkable degree of control that allows the cell to grow and acquire specific shapes. Live cell fluorescence microscopy systems have allowed an amazing view into the complex and dynamic lives of individual proteins during cell morphogenesis. The current chapter will focus on methodology for live cell imaging of cellulose synthase (CESA) in *Arabidopsis*, which will also provide a launching pad to explore ones specific protein of interest.

Key words: Cellulose synthesis, Live cell imaging, Confocal microscopy, CESA, AFP, YFP

1. Introduction

1.1. Background

Once a challenging technique with limited accessibility, confocal microscopy has rapidly evolved into a robust technique providing proteome level localization data with quantitative precision (1–5). The capacity to visualise your target protein relies on a fused autofluorescent protein (AFP), which excites when laser is activated. Classic examples are green fluorescent protein (GFP) derived from the jellyfish *Aqueora victoriae* being fused to your plant protein of interest. Since the discovery of GFP 16 years ago (1), numerous forms of AFP have been derived including blue fluorescent protein (BFP), cyan fluorescent protein (CFP), yellow fluorescent protein (YFP), and the mFruits collection (6–8). Monomeric version of photoswitchable or DRfONPA (9) and photoactivatable GFP exist (10). Designing an AFP expression fusion can therefore be a daunting task as there are many considerations including; which AFP, expression vectors, the choice of where to fuse your AFP, what promoter to use, and whether to

Zoë A. Popper (ed.), *The Plant Cell Wall: Methods and Protocols*, Methods in Molecular Biology, vol. 715,
DOI 10.1007/978-1-61779-008-9_10,

use stable or transient expression of your chimeric protein fusion. Furthermore, fluorescence recovery after photobleaching (FRAP; (11)), fluorescence resonance energy transfer (FRET; (12)) and bimolecular fluorescence complementation (BiFC; (13)) could be considered during experimental design depending on your application. This chapter aims to provide researchers with a generalised introduction to the materials and methods needed for performing a live cell imaging analysis of proteins in the plant cell wall.

Live cell imaging has been developed to explore the location of proteins that are fused to AFPs in living tissue by fluorescence microscopy. These tools have been developed alongside sophisticated advances in microscopy, specifically laser assisted confocal microscopy that relies on precise spectral wavelengths produced by different lasers. The morphology and motility of the protein-AFP fusion can then be used to place a protein in a particular part of the cell with the main limitation being the resolution of the focal plane of the confocal microscope. Cell wall biosynthetic proteins have been localised to the plasma membrane, cell wall, the secretory system and the endomembrane system. The central focus of this chapter is on the progression for cloning the gene, sequence checking the gene, the myriad of factors involved in selecting a vector for C or N terminal AFP fusion, selection of a promoter to drive the fusion protein and the binary vector system to introduce the AFP tagged gene into your plant either transiently or stably. Where possible, the numerous pitfalls that must be negotiated during protein localization experiments are highlighted. Once introduced into the transgenic plant, the AFP-fusion protein can be imaged and a brief overview of imaging systems and approaches to quantification has been provided.

1.2. Vector Selection

1.2.1. Promoter

The choice of promoter used to drive the target gene fused to an AFP in the transgenic plant must be made. The two main choices are the use of a native promoter (defined as 1–2 kb of upstream sequence from the target genes start codon), vs. a *Cauliflower mosaic virus* (CaMV) 35S or double 35S constitutive promoter. If one is interested in studying a single protein and there is a requirement for the AFP fusion to function as closely as possible to the native protein with respect to localization, tissue-specificity, timing, and level of expression, then it may be necessary to express the fusion in transgenic plants under control of the native promoter. Moreover, if ones protein of interest can be knocked out in a model organism, for instance in the model plant *Arabidopsis*, one can functionally complement the knockout allele with the AFP-fusion protein as a means to check that mutant phenotypes are restored to that of wild-type plants. This experiment infers functionality of the chimeric protein. At the other extreme, if there is a need to localise thousands of fusions in a relatively short period of time, then transient expression may be the most cost effective as would a high throughput approach with a constitutive promoter

such as 35S using a Gateway® cloning (Invitrogen, Carlsbad, CA) system, using vectors such as pSITE (14) or pMDC (15).

Some consider that expression under the control of native promoters will be always superior to that of employing constitutive promoters. However, simply using the native promoter, or more often 1–2 kb of "upstream" sequence, ignores the fact that promoter/gene duplication may affect expression levels, as will genomic context since the AFP fusion is unlikely to be expressed from the same genetic locus as the native gene (13). It also appears to be a common belief that expression from 35S, or even double 35S, promoters necessarily results in accumulation of fusions proteins of the levels higher than native proteins. However, all such results are highly dependent upon the protein under investigation. Fusion of an AFP to a protein may stabilise it. In systems such as *Arabidopsis*, where it is straightforward to obtain T-DNA insertion alleles for your gene of interest (16), single gene complementation by your AFP-fusion protein provides some confidence of correct functionality of your fusion protein in planta.

1.2.2. Where to Fuse Your AFP: Amino (N), Carboxy (C), or Internal

Where to fuse your AFP? Should one use an amino (N) or a carboxy (C) terminal fusion? While N or C terminal fusions are the most common, and easiest to construct, some proteins may not tolerate AFPs fused to a terminal end and it may be necessary to insert the AFP into an internal site. Moreover, if your target protein contains an N-terminal signal peptide it may result in mislocalisation if expressed as fusions to the C-termini of AFPs (17). To overcome this, computational methods have been developed to predict the effect of an AFP on a particular fusion (17). Most binary expression vector systems, sometimes referred to as destination vectors, have been developed to suite N- or C-terminal fusions (18–20). To head off any potential problems when testing an AFP fusion, both C and N terminal fusions can be made for preliminary studies using a transient expression system prior to stable transformation or detailed quantitative imaging analysis. When considering the vector system you aim to use a question is, whether the researcher will use a Gateway® cloning (Invitrogen, Carlsbad, CA) or non-gateway restriction enzyme based cloning such as pCAMBIA vectors (CAMBIA Corporation, Canberra, Australia). Gateway® cloning technology can be particularly useful for both high throughput studies, as described above, and single protein studies due to its robust and accurate cloning and most of the current vector systems employ this technology. Both of these vector systems have C and N terminal AFP variants or versions with no AFP to allow the user to insert their AFP internally. For Gateway® cloning, the pMDC and pSITE vector systems are good example and for restriction enzyme based, the use of pCAMBIA is ideal for plant-based expression.

1.2.3. Choice of AFP

The demonstration that the GFP (1) isolated from the jellyfish *Aqueora victoriae*, could be linked to proteins of interest in order

to allow *in vivo* examination of protein localization and dynamics in real-time has transformed cell biology in a manner similar to the effect of the polymerase chain reaction on molecular biology. Numerous AFP spectral variants are available in colours such as red fluorescent protein (RFP) (21), YFP (8) and now banana, orange, cherry, tomato, and plum in the mFruits collection (6). Recently, a novel monomeric red fluorescent protein, TagRFP, has been described (22). This protein is brighter and more resistant to photobleaching than mRFP and can be used in combination with GFP in FRET experiments. To this end, despite GFP being a popular AFP tag for creating fusion proteins, currently the most common FRET pair is CFP/YFP. For the case study described herein, YFP was chosen to fuse to cellulose synthase (CESA) because this allowed for CFP to be fused to TUBULIN. Spectral properties of YFP and CFP allow their excitation and thus visualisation in different channels allowing the simultaneous view of two fluorophors in a single plant cell (23).

1.3. Transformation of Your AFP Fusion into a Plant

There is one main question for the choice of transformation for a live cell imaging experiment: are you going to use a stable transformation or a transient one? This decision is not a trivial one. In high throughput circumstances, creating stable transformations is time consuming and can be restrictive depending on laboratory resources. Therefore, for proteome-scale projects transient assays are often preferred. Transient assay systems utilise agroinfiltration of your AFP fusion into *Nicotiana benthamiana* leaves. This simple technique employs injecting an *Agrobacterium* (expressing your AFP fusion) solution directly into the underside of a leaf blade, inoculating for 2–3 days and then imaging the living leaf tissue. Alternatively, stable transformation in *Arabidopsis thaliana* utilises *Agrobacterium* mediated floral dipping methods (24) to introduce your AFP fusion into the genome as a T-DNA insertion. The advantage of stable transformation is the capacity to localise your target protein in numerous tissues and developmental stages. The presence of the AFP fusion protein in the plant can then be checked by western blot using antibodies against your chosen AFP (readily available from common suppliers such as Sigma-Aldrich, St Louis MO).

2. Materials

2.1. Polymerase Chain Reaction (PCR) to Amplify Gene of Interest with Promoter and Subcloning into an Entry Vector

1. Proof reading enzyme for amplification, Platinum® *Pfx*DNA Polymerase, stored at −20°C (Invitrogen, Carlsbad, CA).
2. 5′ and 3′ Primers specific for promoter and gene for CESA. 100 mM stock is diluted to 10 mM sub stock to be used as a working solution. These are stored at −20°C (see Note 1).
3. 10× *Pfx* Buffer 25 mM $MgSO_4$,100 mM dNTPs (Invitrogen Carlsbad, CA), stored at −20°C (see Note 2).

4. Template as genomic DNA (gDNA) (500 ng/μL^{-1}), stored at –20°C (see Note 3).
5. pENTR® dTOPO® vector system (Invitrogen, Carlsbad, CA), stored at –20°C.

2.2. Cloning of Your Gene of Interest into a Compatible Destination Vector to make AFP Fusions and Introducing this Into the Plant by Agrobacterium Mediated Transformation

1. pSITE2NA destination vector (see Note 4), stored at –20°C.
2. Gateway® cloning kits (Invitrogen, Carlsbad, CA) stored at –20°C.
3. *Agrobacterium* competent cells, stored at –80°C (Invitrogen, Carlsbad, CA).

2.3. SDS-Polyacrylamide Gel Electrophoresis (SDS-PAGE)

1. Running buffer (5×): 125 mM Tris, 960 mM glycine, 0.5% (w/v) SDS. Store at room temperature.
2. 2× SDS sample loading buffer: 100 mM Tris–Cl pH 6.8, 4% v/v SDS, 0.2% bromophenol blue, 20% w/v glycerol, stored at room temperature.
3. Pre-stained molecular weight markers: Kaleidoscope markers (Bio-Rad, Hercules, CA).
4. 0.5 M Tris-Cl buffer pH 8.
5. 100 mM Phenylmethanesulfonyl fluoride (PMSF; Sigma Aldrich, St. Louis)) in isopropanol, stored at –20°C.

2.4. Western Blotting for YFP

1. Setup buffer: 25 mM Tris (do not adjust pH), 190 mM glycine, 20% (v/v) methanol, stored at room temperature.
2. Transfer buffer: Setup buffer with the added inclusion of 0.05% (w/v) SDS. Store in the transfer apparatus at room temperature (see Note 5).
3. Supported nitrocellulose membrane from Millipore, Bedford, MA, and 3MM Chromatography paper from Whatman, Maidstone, UK (see Note 6).
4. Tris-buffered saline with Tween (TBS-T): Prepare 10× stock solution containing 1.37 M NaCl; 27 mM KCl; 250 mM Tris–HCl, pH 7.4; 1% Tween-20.
5. Tris-buffered saline with Tween (TBS-T): Prepare 1× stock for use by diluting 100 mL of 10× stock in 900 mL water.
6. Blocking buffer: 5% (w/v) non-fat dry milk in TBS-T.
7. Primary antibody dilution buffer: TBS-T supplemented with 2% (w/v) fraction bovine serum albumen (BSA).
8. Anti-YFP monoclonal antibody (available from Sigma Aldrich, St. Louis) stored at –20°C (see Note 7).

9. Secondary antibody: Anti-mouse IgG conjugated to horse radish peroxidase (available from Sigma Aldrich, St Louis) stored at –20°C (see Note 7).
10. Chemiluminescence detection kit (SuperSignal West Pico Chemiluminescent Substrate (Pierce Biotechnology, Rockford, IL) stored at 4°C.
11. Detection using Bio-Rad ChemiDoc XRS+® (BioRad, Hercules, CA).

2.5. Imaging Analysis

1. Cover slips 48×60, 24×60 (Menzel, Braunschweig Germany).
2. Fine point tweezers #5 Dumont (Electron Microscopy Sciences, Hatfield, PA).
3. Dow Corning High Vacuum Grease (Specialty Fluids Co, Valencia, CA).
4. Sterile water.

3. Methods

Herein, we describe a Gateway® cloning for tagging CESA to YFP and the use of confocal microscopy to visualise it in plants. Gateway-compatible binary vectors have greatly improved the cloning efficiency of AFP tagging projects (15, 19). Briefly, Gateway® cloning uses the lambda phage site-specific recombination system in order to transfer DNA fragments between plasmids containing compatible recombination sites (26). What makes this strategy so attractive is that once DNA clones of interest are captured into an entry vector (pENTR/pDONR), they can be mobilised into a plethora of destination vectors that permit expression in bacteria, insects, yeasts, or plants but also allow for introducing the target gene into an AFP vector with RFP, YFP, CFP, or GFP fluorophors.

Numerous factors influence imaging, for instance, the cell type being imaged, whether your experiments is simply to determine the location of your target protein, or whether you wish to track the dynamic behaviour of the your target protein by time lapse imaging. The best results have been obtained by localising protein dynamics in upper regions of the hypocotyls of etiolated seedlings grown in a vertical position on Murashige-Skoog (MS) agar plates for 2.5–4 days at room temperature (22°C), mounted between cover slips in water and then imaged (23, 27).

3.1. Polymerase Chain Reaction (PCR) to Amplify Gene of Interest and Subcloning into an Entry Vector

1. Independent amplification of the CESA and promoter or your gene of interest achieved using a PCR reaction composed of 1.5 pmol of each primer, 0.3 mM dNTPs, 1× *Pfx* Buffer, 1 mM $MgSO_4$ (see Note 8) and 1.25 units Platinum®*Pfx*DNA Polymerase (Invitrogen, Carlsbad, CA), 1 µL of gDNA, made to 20 µL with deionised H_2O (dH_2O).

The following thermocycler reaction times and temperature can be used, a 3-min heating at 95°C was followed by 32 cycles of 95°C (30 s) denaturation, 55°C (30 s) annealing temp (see Note 9), 1 min per kilobase product size extension times, and a final extension of 7 min.

2. Gateway® cloning of the PCR product into an entry vector is then achieved based on manufacturer's instructions (Invitrogen, Carlsbad, CA).

3.2. Cloning of Your Gene of Interest with Promoter into a Compatible Destination Vector to make AFP Fusions and Introducing this into the Plant by Agrobacterium Mediated Transformation

1. The CESA gene in entry vector can then be cloned in to a destination vector such as pSITE2N using the manufacturer's manual for Gateway® cloning (Invitrogen, Carlsbad, CA). The double CAMV 35S promoter can be excised using compatible restriction enzymes and the amplified promoter region ligated into the vector by directional cloning. This creates an additional step in the cloning and will depend on whether you wish to examine localization of your target gene with a constitutive or native promoter.
2. At this stage a sequence verified version of your target gene (see Note 10), for instance pSITE2NproCESA::CESA (see Note 11), can then be transformed into electro or chemically competent *Agrobacterium tumefaciens* cells according to manufacturer's manual (Invitrogen, Carlsbad, CA).
3. Introducing the transgene into the plant should follow published protocols (24) (see Note 12).
4. Selection of stable transformants in *A. thaliana* will be achieved by growing the T1 progeny on sterile 0.5 strength MS media supplemented with 50 μg/mL^{-1} Kanamycin (Kan^{50}). Plants able to grow on the Kan^{50} media are then transferred to soil and grown.

3.3. SDS Page and Western Blotting for Detection of YFP in Plant Tissue

For simplicity, this method assumes the use of Criterion cell and precast gels from BioRad® (Hercules, CA) as well as the BioRad Trans-Blot® Electrophoretic Transfer Cell®.

1. Total protein from individual transformants is extracted by simply grinding 2–3 leaves using liquid nitrogen in mortar and pestle and 300 μL 0.5 M Tris-Cl buffer with 0.1 mM final concentration PMSF. 1 volume of 2× SDS loading buffer is added to 1 volume of total protein and boiled for 5 min. It is then carefully loaded into the well of the precast gel along with molecular weight markers and the gel is run for 1 h at 80 mA in the Criterion cell system (BioRad® Hercules, CA).
2. After protein separation by SDS-PAGE the samples are transferred to a nitrocellulose membrane according to the manufacturer's instructions (assuming the use of a BioRad Trans-Blot® Electrophoretic Transfer Cell®) (see Note 6).

3. The coloured molecular weight markers should be clearly visible on the membrane. Nitrocellulose membrane is carefully transferred in a solution of blocking buffer for 1 h at room temperature on a shaker.
4. The nitrocellulose membrane is rinsed and then immersed in a solution of 1:10,000 dilution of anti-YFP antibody in TBST/2% BSA for 1 h on a rocking platform (see Note 13).
5. Wash three times for 5 min each with 50 mL TBS-T and then immerse in 1:30,000-fold dilution of the secondary antibody as above. Wash again 3 times for 10 min each with TBS-T. Then incubate in equal volumes of Pico-West (total of 4 mL) (Pierce Biotechnology, Rockford, IL) solution for 1 min, seal in a plastic sleeve and examine chemiluminescent signal in the BioRad® GelDoc. Select transgenic plants that show the presence of YFP for confocal imaging (see Note 14).

3.4. Preparation of Plants for Imaging

1. Once stable transformants expressing YFP::CESA fusion are identified and transferred to soil, the plants are grown to obtain seeds from them.
2. The seeds once ready are harvested in a newspaper piece and dried in a dry corner of the lab for 3–4 days. They are then sterilised using 30% bleach and 5% SDS for surface sterilisation. The seeds are washed thoroughly to remove sterilisation solution using sterile water. It is then resuspended in 0.15% Agar and stored in dark at 4°C for vernalisation for 3 days (see Note 15).
3. *A thaliana* seedlings are grown in dark for 2.5 days on 0.5 strength MS-agar plates at 22°C.

3.5. Imaging Analysis

1. Single seedlings are gently removed from 0.5 strength MS-agar plates and mounted in an aqueous solution between a 48×60 and a 24×60 cover slip.
2. The silicon vacuum grease is carefully applied to the perimeter of the 24×60 cover slips to avoid any water loss or evaporation over the duration of imaging and essentially avoids compression of the epidermal cells of the tissue being imaged (see Note 16).
3. For imaging YFP::CESA, a purpose built spinning disc confocal microscope using Leica X 63 N.A. = 1.4 oil immersion objective and Roper Cascade 512b EMCCD camera can be used (see Note 17).
4. The confocal plane is focused then on the plasma membrane focal plane with an exposure of 600 ms for YFP::CESA (Fig. 1a). A method to improve the signal to background noise ratio is to average multiple frames using the frame averaging feature in the imaging software being used.

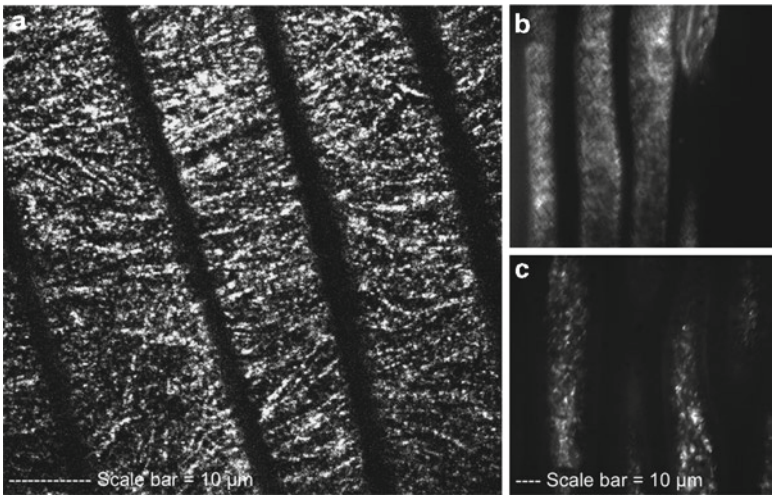

Fig. 1. Live-cell imaging of YFP::CESA (**a**) Plasma membrane focal plane (**b**) *X* and *Y* drift during time lapse image acquisition can reduce image quality and make it difficult to track protein dynamics (**c**) *Z* drift during time lapse image acquisition can reduce image quality and distort protein dynamics analyses.

5. YFP is excited at 488 nm and data is collected through a 525.50 nm band pass filter (Chroma Technologies, Brattleboro, VT) (23). The image can be acquired using image acquisition software and analysed (see Note 18).
6. To obtain multiple frames of a single cell to provide a time-lapse series (i.e. a movie), seek the time-lapse feature in the image acquisition software being used (see Note 18) (select the number of frames to be acquired and the amount of time between each frame) (see Note 19).

4. Notes

1. When the primers arrive dilute them to 100 mM concentration using TE (10 nM Tris-Cl, 1 mM EDTA) buffer and make a 10-mM working solution for yourself.
2. Each of the dNTPs is available as a 100 mM stock which can be combined as a 10-mM sub stock for your use.
3. Here, the cloning strategy calls for the amplification of cellulose synthesising enzyme or CESA with the promoter, thus gDNA needs to be used to include introns as well as exons and regulatory regions. gDNA preparation can be done using the established protocols (25).
4. pMDC and pSITE vectors can be requested from the authors (14, 15).

5. The transfer buffer should be cooled below room temperature before you begin to do the transfer. This can be done by cooling the buffer at 4°C prior to doing western blots.
6. Nitrocellulose membranes should not be touched and should not be handled without using gloves. It would be best to use tweezers to handle the membrane at all times.
7. Primary and secondary antibodies should be aliquoted into 200 µL aliquots and stored at –20°C. When required, a vial should be retrieved and used and the remaining can then be stored at 4°C for multiple uses. This way the main stock will not be contaminated if there is a chance of doing so.
8. $MgSO_4$ levels can be optimised for your specific PCR reaction through a little research.
9. The annealing temperatures have to be optimised for a specific pair of primers; usually a thumb rule of 1° than the melting temperature for the primers is used.
10. It is usually better to sequence your target gene for missense mutations at the DNA level that confer changes in the amino acid sequence of the target protein (Sequencing reactions such as BigDye® (Applied Biosystems, Carlsbad, CA) and nested primer design; for sequencing are not covered in this chapter.
11. Amplification for C-terminal fusions (for purpose of this chapter, this refers to the AFP fusion being fused to the C-terminal end of the target gene) remove the stop codon from the target gene in the 3′ primer. For N-terminal fusions, the AFP is referred to as being fused to the N-terminus of the target gene.
12. You can also do *Agrobacterium* infiltration into *Nicotiana benthamiana* (14) for transient expression.
13. An overnight addition of primary antibody can be done in 4°C cooler with a rocking bottom or shaker.
14. If no signal is obtained for YFP in transgenic plants in stable transformants (*A. thaliana*), check for YFP in all plant samples by PCR in gDNA; if positive, select additional lines for protein analysis by western blotting in the next generation or if negative, retransform and proceed from there.
15. Seed sterilisation should be done under the hood to minimise the chance of contamination. It is always worthwhile to use only less than half of your seed stock so that if a mistake is made in subsequent steps, there are always some transformant seeds available to begin again.
16. For transient expression, a similar strategy is employed, whereby a portion of the infiltrated *N. benthamiana* is physically removed from the leaf and mounted as described above.

17. Numerous confocal microscope systems are available and are equally attractive for live-cell imaging experiments. The leading companies and examples of their confocal systems as of January 2010 are Leica (Leica SP5 AOBS Point Scanning Spectral Confocal Microscope), Olympus (Olympus Fluo View FV1000MPE, a multiphoton laser scanning microscope), Yokagawa (Yokogawa CSU-10 spinning disc confocal microscope) Zeiss 780NLO Laser-Scanning Confocal Microscope.
18. Softwares for imaging analysis: Metamorph – Molecular Devices (Sunnyvale, CA), which can be used for microscope automation and image acquisition. LAS Image Analysis optional software module developed by Leica Microsystems (Bannockburn, IL) provides sequence control assisting acquiring, detecting, and measuring multiple image features. In addition to Leica, all major companies have similar systems (see local representative). ImageJ is a Freeware software programme that has numerous features developed by a worldwide community of cell biologists to streamline quantitative analysis of confocal imaging results. In addition to the numerous image analysis tools built into ImageJ, there are Plugins for tracking position over time by Kymograph, reslicing of stacks, 3D reconstruction, time-stamping, conversion of BioRad stacks to Quicktime format as well as most format conversion, 3D rendering and quantitation (ImageJ, National Institute of Health, Bethedsa, MD).
19. The main pitfall for time-lapse image collection is drift (x, y or z drift). X and Y plane drift can be overcome fairly easily by allowing the drift to occur and then use the Stackreg algorithm ImageJ plugin (http://rsbweb.nih.gov/ij/plugins) after acquisition to correct for the drift (Fig. 1a compared to Fig. 1b). Z drift on the other hand cannot be corrected for and therefore requires manual adjustment during acquisition (Fig. 1c).

References

1. Chalfie, M., Tu, Y., Euskirchen, G., Ward, W. W., and Prasher, D. C. (1994) Green fluorescent protein as a marker for gene expression. *Science* **263**, 802–805.
2. Cutler, S. R., Ehrhardt, D. W., Griffitts, J. S., and Somerville, C. (2000) Random GFP::cDNA fusions enable visualization of subcellular structures in cells of *Arabidopsis* at a high frequency. *Proc Natl Acad Sci* USA **97**, 3718–3723.
3. Tian, G. W., Mohanty, A., Chary, S. N., Li, S., Paap, B., Drakakaki, G., Kopec, C. D., Li, J., Ehrhardt, D., Jackson, D., et al (2004) High-throughput fluorescent tagging of full-length *Arabidopsis* gene products *in planta*. *Plant Physiol* **135**, 25–38.
4. Heazlewood, J. L., Verboom, R. E., Tonti-Filippini, J., Small, I., and Millar, A. H. (2007) SUBA: The *Arabidopsis* subcellular database. *Nucleic Acids Res* **35**, D213–D218.
5. Moore, I. and Murphy, A. (2009) Validating the location of fluorescent protein fusions in the endomembrane system. *Plant Cell* **21**, 1632–1636.
6. Shaner, N. C., Campbell, R. E., Steinbach, P. A., Giepmans, B. N., Palmer, A. E., and Tsien, R. Y.

(2004) Improved monomeric red, orange and yellow fluorescent proteins derived from *Discosoma* sp. red fluorescent protein. *Nat Biotechnol* **22**, 1567–1572.

7. Shaner, N. C., Steinbach, P. A., and Tsien, R. Y. (2005) A guide to choosing fluorescent proteins. *Nat Methods* **2**, 905–909.
8. Zhang, J., Campbell, R. E., Ting, A. Y., and Tsien, R. Y. (2002) Creating new fluorescent probes for cell biology. Nat Rev *Mol Cell Biol* **3**, 906–918.
9. Habuchi, S., Ando, R., Dedecker, P., Verheijen, W., Mizuno, H., Miyawaki, A., and Hofkens, J. (2005) Reversible single-molecule photoswitching in the GFP-like fluorescent protein Dronpa. *Proc Natl Acad Sci* USA **102**, 9511–9516.
10. Patterson, G. H., and Lippincott-Schwartz, J. (2004) Selective photolabeling of proteins using photoactivatable GFP. *Methods* **32**, 445–450.
11. Bates, I. R., Wiseman, P. W., and Hanrahan, J. W. (2006) Investigating membrane protein dynamics in living cells. *Biochem Cell Biol* **84**, 825–831.
12. Hink, M. A., Bisselin, T., and Visser, A. J. (2002) Imaging protein-protein interactions in living cells. *Plant Mol Biol* **50**, 871–883.
13. Bhat, R. A., Lahaye, T., and Panstruga, R. (2006) The visible touch: in planta visualization of protein-protein interactions by fluorophore-based methods. *Plant Methods* **2**, 12.
14. Goodin, M. M., Chakrabarty, R., Banerjee, R., Yelton, S., and DeBolt, S. (2007) New gateways to discovery. *Plant Physiol* **145**, 1100–1109.
15. Curtis, M. D. and Grossniklaus, U. (2003) A gateway cloning vector set for high-throughput functional analysis of genes *in planta*. *Plant Physiol* **133**, 462–469.
16. Alonso, J. M., Stepanova, A. N., Leisse, T .J., Kim, C. J., Chen, H., Shinn, P., Stevenson, D. K., Zimmerman, J., Barajas, P., Cheuk, R., et al. (2003) Genome-wide insertional mutagenesis of *Arabidopsis thaliana*. *Science* **301**, 653–657.
17. Simpson, J. C., Neubrand, V. E., Wiemann, S., and Pepperkok, R. (2001) Illuminating the human genome. *Histochem Cell Biol* **115**, 23–29.
18. Chakrabarty, R., Banerjee, R., Chung, S. M., Farman, M., Citovsky, V., Hogenhout, S. A., Tzfira, T., and Goodin, M. (2007) pSITE vectors for stable integration or transient expression of autofluorescent protein fusions in plants: probing *Nicotiana benthamiana*-virus interactions. *Mol Plant Microbe Interact* **20**, 740–750.
19. Earley, K. W., Haag, J. R., Pontes, O., Opper, K., Juehne, T., Song, K., and Pikaard, C. S. (2006) Gateway-compatible vectors for plant functional genomics and proteomics. *Plant J* **45**, 616–629.
20. Tzfira, T., Tian, G. W., Lacroix, B., Vyas, S., Li, J., Leitner-Dagan, Y., Krichevsky, A., Taylor, T., Vainstein, A., and Citovsky, V. (2005) pSAT vectors: a modular series of plasmids for autofluorescent protein tagging and expression of multiple genes in plants. *Plant Mol Biol* **57**, 503–516.
21. Matz, M. V., Fradkov, A. F., Labas, Y.A., Savitsky, A. P., Zaraisky, A. G., Markelov, M.L., and Lukyanov, S.A. (1999) Fluorescent proteins from nonbioluminescent Anthozoa species. *Nat Biotechnol* **17**, 969–973.
22. Merzlyak, E. M., Goedhart, J., Shcherbo, D., Bulina, M. E., Shcheglov, A. S., Fradkov, A. F., Gaintzeva, A., Lukyanov, K. A., Lukyanov, S., Gadella, T. W., et al (2007) Bright monomeric red fluorescent protein with an extended fluorescence lifetime. *Nat Methods* **4**, 555–557.
23. Paredez, A. R., Somerville, C. R., and Ehrhardt, D. W. (2006) Visualization of cellulose synthase demonstrates functional association with microtubules *Science* **312**, 1491–1495.
24. Clough, S. J. and Bent, A. (1998) Floral dip: a simplified method for Agrobacterium-mediated transformation of *Arabidopsis thaliana*. *Plant J.* **16**, 735–743.
25. Lukowitz, W., Gillmor, C. S., and Scheible, W. R. (2000) Positional cloning in Arabidopsis Why it feels good to have a genome initiative working for you. *Plant Physiol* **123**, 795–805.
26. Walhout, A. J., Temple, G. F., Brasch, M. A., Hartley, J. L., Lorson, M. A., van den Heuvel, S., and Vidal, M. (2000) GATEWAY recombinational cloning: application to the cloning of large numbers of open reading frames or ORFeomes. *Methods Enzymol* **328**, 575–592.
27. Gutierrez, R., Lindeboom, J. J., Paredez, A. R., Emons, A. M. C., and Ehrhardt, D. W. (2009) *Arabidopsis* cortical microtubules position cellulose synthase delivery to the plasma membrane and interact with cellulose synthase trafficking compartments. *Nat Cell Biol* **11**, 797–806.

Chapter 11

Visual Mapping of Cell Wall Biosynthesis

Yumiko Sakuragi, Morten H.H. Nørholm, and Henrik V. Scheller

Abstract

Biosynthesis of pectin and hemicelluloses occurs in the Golgi apparatus and is thought to involve spatial regulations and complex formation of biosynthetic enzymes and proteins. We have demonstrated that a combination of heterologous expression of recombinant proteins tagged with fluorescent proteins and live cell imaging with confocal laser scanning microscopy (CLSM) allows efficient visualization of biosynthetic enzymes and proteins in subcellular compartments. We have also successfully utilized bimolecular fluorescence complementation (BiFC) for *in situ* visualization of protein–protein interactions of pectin biosynthetic enzymes and for the determination of their membrane topology in the Golgi apparatus.

Key words: Bioimaging, Cell wall biosynthesis, Uracil-excision cloning, Bimolecular fluorescence complementation, Protein–protein interaction, Subcellular localization, Glycosyltransferase, Pectin

1. Introduction

1.1. Background

Plant cells are surrounded by a strong wall composed primarily of polysaccharides. The wall is essential for giving strength and shape to plant cells, thereby allowing plants to stand upright, and in addition serves as a barrier against invading pathogens. Cell wall polysaccharides are traditionally grouped into cellulose, hemicelluloses, and pectin. Although these polysaccharides can have a very complex structure, the basic structural features have been reasonably well described. In contrast, the biosynthetic apparatus responsible for synthesising the wall is poorly understood and its identification and characterization is one of the major challenges in plant biochemistry.

Pectin and hemicellulose biosynthesis has been shown to occur in the lumen of the Golgi apparatus, although it cannot be excluded that some early steps in the biosynthesis take place in the endoplasmic reticulum (ER). Hence, most, if not all of the proteins,

Zoë A. Popper (ed.), *The Plant Cell Wall: Methods and Protocols*, Methods in Molecular Biology, vol. 715,
DOI 10.1007/978-1-61779-008-9_11, © Springer Science+Business Media, LLC 2011

involved in these biosynthetic processes must be localized in the Golgi lumen either as soluble proteins or as embedded in the surrounding membranes. Proteins involved include glycosyltransferases that catalyze transfer of activated sugar molecules to acceptor molecules, nucleotide sugar inter-converting enzymes that supply the substrates to these glycosyltransferases, and nucleotide sugar transporters and modifying enzymes (e.g. acetyltransferases and methyltransferases). Glycosyl hydrolases may also take part in the biosynthetic process, and they may function in the Golgi or after secretion of precursor polysaccharides to the apoplast. The majority of glycosyltransferases are predicted Type II membrane proteins with the catalytic domains in the Golgi lumen. Important exceptions to this are the glycosyltransferases belonging to the Cellulose Synthase Like group of proteins. These are multi-spanning membrane proteins, and it is not yet clear on which side of the Golgi membrane the catalytic domain is found. For recent reviews on biosynthesis of hemicelluloses and pectin see refs. (1–4).

In the protein glycosylation pathways in animals, and in cellulose and callose synthesis in plants, protein–protein interactions act as an important organising principle with regard to biosynthetic coordination, subcellular localisation, and direct regulation of enzymatic activity (5–7). A school of thought exists that proteins involved in biosynthesis of a particular pectin or hemicellulose polymer form protein complexes or loose metabolons inside the Golgi for optimal and coordinated actions of the enzymes. However, until recently, direct evidence for such complexes had been lacking in pectin and hemicellulose biosyntheses, largely due to our limited knowledge of polysaccharide biosynthesis in general. For example, overexpression of ARAD1, a putative arabinosyltransferase, and XGD1, a putative xylosyltransferase, in *Arabidopsis* did not lead to more arabinan or xylogalacturonan, respectively (8, 9). This could suggest that these proteins function in biosynthetic complexes and that another component was limiting in the over-expression studies. However, several other explanations are possible, e.g. substrate limitation or feedback regulation. Another study showed that mutation of one isoform of UDP-glucose-4-epimerase resulted in a lack of galactose in arabinogalactan proteins and in a specific xyloglucan fraction, whereas pectic galactan was unaffected (10). This result suggests that specific epimerase isoforms are associated with a subset of glycosyltransferases. UDP-arabinopyranose mutase, also known as reversibly glycosylated protein, has been shown to form heterodimeric complexes (11, 12), although it is not yet clear how these proteins are linked to polysaccharide biosynthesis. The most compelling evidence for the role of protein complexes in biosynthesis of pectin has been provided by Mohnen and colleagues. GAUT1, a galacturonosyltransferase that is responsible for homogalacturonan biosynthesis, has been shown to interact with

GAUT7, a homolog of GAUT1 with no demonstrated enzymatic activity (3, 13). This interaction was found to be essential for the accumulation of GAUT1 in the Golgi apparatus (Atmodjo, Sakuragi, Scheller, Mohnen, unpublished).

Rapid progress in determining genome sequences of plants has led to the discovery of a large repertoire (ca. 1,500) of putative proteins involved in cell wall biosynthesis on the basis of their sequence similarity to known proteins and their predicted subcellular localizations. Experimental validation of the predicted subcellular localisations, membrane topology, and protein complex formation of these proteins remain to be carried out. Rapid methods for expression and visualisation of cell wall biosynthetic proteins *in planta* are described here.

1.2. General Principles of the Methods

The protein of interest is recombinantly fused to fluorescent proteins (green fluorescent protein (GFP) and its variants) and transiently expressed in the tobacco plant *Nicotiana benthamiana*. Highly efficient recombinant gene technologies used in our laboratories are Gateway® and uracil-excision cloning methods. A detailed protocol of Gateway® cloning is made available by the manufacturer (Invitrogen) and therefore is not discussed here. The uracil-excision cloning method is a method for simple, yet versatile ligase-independent cloning (14, 15). It requires only few reagents and enzymes, and these can be purchased from commercial vendors. Briefly, our compatible vectors contain cloning sites consisting of PacI and Nt. BbvCI restriction endonuclease recognition sequences and are digested by these enzymes to generate unique 3′-octanucleotide overhangs allowing directional insertion of the genes of interests. A gene to be inserted is amplified by the polymerase chain reaction (PCR) with synthetic oligonucleotides, which, in addition to the sequence specific to the target DNA, contain uracil-containing tails. Upon treatment with USER™ enzymes (New England Biolab), which is a mixture of uracil DNA glycosylase and DNA glycosylase-lyase Endo VIII, the uracils are excised, which results in 3′-overhangs complementary to those in the digested vector. Annealing between the insert and the digested vector is stable during chemical transformation of *Escherichia coli* and becomes covalently linked *in vivo*. There are various approaches by which constructions of fluorescently tagged proteins of interests can be performed. The simplest way is to insert the gene coding for the protein of interest into an existing vector that is uracil-excision-cloning compatible and contains a gene encoding a fluorescent protein tag. A variety of such vectors have been reported (14) and we have expanded this repertoire with, e.g., C-terminal eGFP fusion vectors (Table 1, see Note 1). When suitable vectors are not available, a three-fragment cloning approach can be employed between the expression vector, the tag and the gene-of-interest to generate a seamless translational fusion

Table 1
Plasmid vectors and strains of *Agrobacterium tumefaciens* PGV3850 C58C1

Strain[a]	Plasmid	Vector backbone	GOI[b]	Fluorescent tag	Reference
N.A.[c]	pCAMBI-A330035Su	pCAMBIA3300			(14)
N.A.[c]	USER-eGFP	pCAMBIA330035Su		eGFP	This work
YS28[d]	pGFP-HDEL	pTXS.P3C2		eGFP	(18)
YS60	pSTtmd-YFP	pCAMBIA330035Su	STtmd	Venus:1–238	Unpublished
YS63	pSTtmd-Yn	pCAMBIA330035Su	STtmd	Venus:1–155	Unpublished
YS64	pSTtmd-Yc	pCAMBIA330035Su	STtmd	Venus:156–238	Unpublished
YS66	pUXS2-YFP	pCAMBIA330035Su	UXS2	Venus:1–238	Unpublished
YS70	pUXS2-Yn	pCAMBIA330035Su	UXS2	Venus:1–155	Unpublished
YS71	pUXS2-Yc	pCAMBIA330035Su	UXS2	Venus:156–238	Unpublished
YS14	pARAD1-YFP	pCAMBIA330035Su	ARAD1	Venus:1–238	Unpublished
YS18	pARAD1-Yn	pCAMBIA330035Su	ARAD1	Venus:1–155	Unpublished
YS19	pARAD1-Yc	pCAMBIA330035Su	ARAD1	Venus:156–238	Unpublished
P19[d]	P19	pBin61	P19		(18)

[a]Agrobacterial strain catalogue numbers in our laboratory
[b]Gene of interest
[c]Not available, only available as purified plasmids
[d]Available but not distributable, the readers are advised to contact the original authors in respective references

protein construct in one step (15). For generating a series of fusion constructs for a given protein, we have found that a sequential two-step, two-fragment cloning approach is somewhat more practical than those described above. A detailed procedure is found in ref. (14). Briefly, the gene-of-interest is first inserted into the uracil-excision cloning site of an expression vector while regenerating the uracil-excision cloning site at the appropriate end. In the second cloning step, genes coding for fluorescent proteins (YFP, GFP, CFP, Yn, Yc, see below) are inserted into the regenerated cloning site. This approach minimizes the number of DNA sequence reactions to be carried out for verification of the correct insert.

The translational fusion constructs generated above are introduced into *Agrobacterium tumefaciens* for transient expression in tobacco plants. Most of the fluorescent fusion proteins we have tested so far resulted in detectable signals upon live cell imaging as described below.

Live cell imaging directly on leaf tissues is carried out by confocal laser scanning microscopy (CLSM). CLSM allows optical sectioning of complex biological specimen in a non-invasive manner,

thus making it possible to determine subcellular localization and dynamics of fluorescently tagged proteins in living cells. In combination with an acousto-optical beam splitter that allows flexible tuning of the detection wavelengths, simultaneous detection of GFP- and YFP-tagged proteins is rendered straightforward (see Note 2). *In situ* detection of protein complex formation is carried out by using bimolecular fluorescent complementation (BiFC) (16, 17). YFP is split in two non-fluorescent parts, and the N-terminal (e.g. YFP amino acid residues 1–155, denoted as Yn) and C-terminal (e.g. residues 156–238, denoted as Yc) halves are fused to the proteins of interest and are brought together to reconstitute the fluorescent properties of YFP, should the selected proteins interact. We found that expression levels of the proteins need to be carefully adjusted and appropriate negative controls must be included in the analysis in order to minimize false positive unspecific interactions. We have also found that STtmd (N-terminal 52 amino acid residues of rat sialyltransferase containing the transmembrane domain) is a promiscuous interacter that complements fluorescence in the BiFC assay with all Golgi proteins we have tested so far. By exploiting this promiscuity, we have established a BiFC-based system for determining the membrane topology of Golgi localising proteins.

2. Materials

2.1. Growth of Nicotiana benthamiana

1. Cylindrical plastic pots (ca. 4 cm diameter, ca. 4 cm height) and a tray.
2. Potting soil available in gardening shops. (Optional) Vermiculite can be added to potting soil in 1:2 ratio.
3. Greenhouse or growth facility with the following day and night setting: daytime temperature 24°C and 12 h light; night temperature 18°C and 12 h dark. These settings can be modified, for example, we have used plants grown at 28°C day temperature successfully.
4. Bactimos (Garta, Odense, Denmark), a larvicide based on *Bacillus thuringiensis israelensis* for minimising fungus gnat infestation. In the US, a similar product named "Gnatrol WDG" is manufactured by Valent (Walnut Creek, CA) and available from various suppliers.
5. Plant nutrients available in gardening shops.

2.2. Plasmids, Bacterial Strains, Media, and Incubators

1. For plasmids used in this study, see Table 1.
2. GenElute™ Plasmid Miniprep Kit (Sigma-Aldrich) or most of commercial miniprep kits.
3. Chemical competent cells of *E. coli* DH10B or DH5α.

4. Electrocompetent cells of *Agrobacterium tumefaciens* PGV3850 C58C1.
5. Lurie-Bertani (LB) medium (1 L): 10 g Bacto Tryptone, 5 g Yeast Extract, 5 g NaCl, and 15 g Bacto Agar for solid media. Autoclaved.
6. 80% (v/v) Glycerol, autoclaved.
7. Double distilled water (ddH_2O).

2.3. Uracil-Excision Cloning, E. coli, and A. tumefaciens Transformation

1. Enzymes and buffers: PfuTurbo® C_x polymerase and 10× reaction buffer (Stratagene) (see Note 3); USER™ enzyme mix, PacI, Nt. BbvCI, 10× NEB buffer 1, 10 mg/mL bovine serum albumin (BSA) (New England Biolabs); TAE buffer (40 mM Tris base, 40 mM acetic acid, 1 mM EDTA at pH 8.0); a standard loading buffer.
2. 10 mM dNTP containing 2.5 mM each of dATP, dTTP, dGTP, dCTP.
3. Synthetic oligonucleotides engineered with uracil-containing tails at 5′ends and template DNAs (e.g. cDNA clones or genomic DNA) containing genes of interest.
4. Antibiotics: in *E. coli*, kanamycin 50 μg/mL, ampicillin 100 μg/mL; in *A. tumefaciens*, kanamycin 50 μg/mL, ampicillin 100 μg/mL, rifampicin 100 μg/mL.
5. A heat block or water bath set at 42°C and a shaker incubator set at 37°C.
6. An electroporator, electroporation cuvettes (0.1 or 0.2 cm).

2.4. Transfection of N. benthamiana

1. Infiltration buffer: 10 mM 2-(*N*-morpholino)ethanesulfonic acid (MES), pH. 5.6, 10 mM $MgCl_2$, 100 μM acetosyringone.
2. 1-mL syringes.

2.5. Confocal Laser Scanning Microscope

1. Glass slides and double-sided adhesive tape.
2. Leica TCS SP2 confocal scanning laser microscope equipped with acousto-optical beam splitter, Argon laser (excitation wavelengths at 458, 477, 488, and 514 nm) and He-Ne laser (excitation wavelengths at 543 and 633 nm) and a 40× water immersion objective (Leica Microsystems).

3. Methods

3.1. Growth of N. benthamiana

1. Plastic pots placed in a tray are filled with potting soil and are showered with Bactimos until the soil is visibly soaked.
2. Two seeds of *N. benthamiana* are planted per pot by using a toothpick.

3. The tray is placed in the greenhouse. (Optional) The tray is covered for a few days with a clear cover or a plastic wrap with perforations for maintaining moisture. After germination, the cover/wrap is removed.
4. The plants are watered two or three times per week. At least once a week plant nutrient is included in the water. Plants that are 4–5-week-old were used for transfection.

3.2. Construction of Recombinant Proteins fused to YFP, GFP, Yn, or Yc by Uracil-Excision Cloning Strategy

1. Preparation of uracil-excision compatible vectors: up to 2 μg of column purified uracil-excision compatible vectors are digested overnight at 37°C with 20 units of PacI in the presence of 1× NEB buffer 1 and 100 μg/mL BSA in a final volume of 20 μL. Five units each of PacI and the nicking enzyme Nt. BbvCI are added to the mixture, and the mixture is incubated for 5–6 h at 37°C. Forty microlitres of ddH_2O is added to the mixture, and the mixture is incubated at 80°C for 20 min. The digested vectors can be stored at –20°C until used (see Note 4).
2. Preparation of PCR products: reactions containing 1.25 units PfuTurbo® C_x DNA polymerase, 1× reaction buffer, 0.5 μM each of forward and reverse primers, 0.2 mM dNTPs, and 50 ng template DNAs are prepared. The following PCR condition is routinely used: initial denaturing at 94°C for 2 min; followed by 30 cycles of denaturing at 94°C for 0.5 min, annealing at 50°C for 0.5 min, and extension at 72°C for 1 min/kb; final extension at 72°C for 10 min. Three microlitres of the product is subjected to agarose-gel electrophoresis in the TAE buffer followed by visualization under UV transilluminator light. The product that consists primarily of the amplicon of the target and very little primer dimers or satellite bands can be directly used without further purification for annealing below. Otherwise, gel purification of the target amplicon is highly recommended.
3. USER reaction and annealing: a typical reaction consists of 5 μL PCR product, 2 μL digested vector, and 1 μL USER™ enzyme mix. The reaction mix is incubated for 30 min at 37°C for uracil-excision, which is followed by 30 min incubation at 25°C for annealing the cohesive ends. The volume of the PCR product and the digested vector can be varied (see Note 5). The following negative controls should be included: a reaction in which PCR product is replaced by ddH_2O and a reaction in which the digested vector is replaced with ddH_2O.
4. Chemical transformation: 40 μL *E. coli* competent cells are thawed in ice and mixed with 4 μL of the uracil-excision reaction. The mix is kept on ice for 30 min, thereafter transferred to 42°C for 2 min and then placed on ice for 1 min.

One hundred microlitres of LB medium is added, and the mixture is shaken at 37°C for 45 min. The entire mixture is plated over an LB plate containing appropriate antibiotics. Colonies should be visible after 12–14 h at 37°C (see Note 6).

5. Typically, three colonies per transformation are individually transferred to 3 mL of LB medium containing appropriate antibiotics and grown overnight at 37°C. The plasmids are isolated from the culture and the insert verified by sequencing. The plasmids can be stored at –20°C. The plasmids are introduced into *Agrobacteria* as described below.

3.3. Transformation of A. tumefaciens

1. Ca. 200 ng of the isolated plasmid in no more than 1 μL water is added to 40 μL of *A. tumefaciens* electrocompetent cells. The mixture is transferred to a 0.1-cm-cuvette, which is subjected to electroporation with the following setup: resistance, 400 Ω; voltage, 2.5 kV; capacitance, 25 μF.
2. Five hundred microlitres of LB medium is added to the cuvette, and the mixture is incubated at 28°C for 1–2 h. Ten and hundred microlitres of the mixture are spread on LB plates containing rifampicin 100 μg/mL, ampicillin 50 μg/mL, and appropriate antibiotics for selection of the plasmids. The plates are incubated at 28°C for 2 days.
3. Colonies are transferred to LB medium containing the appropriate antibiotics and grown overnight at 28°C. Freezer stocks are prepared by mixing with 80% glycerol to achieve a final glycerol concentration of 20% (v/v).

3.4. Transfection of N. benthamiana

1. Three microlitres of overnight cultures of Agrobacterial strains is centrifuged and the cell pellets are resuspended in 3 mL of the infiltration buffer.
2. For co-expression of recombinant proteins, the Agrobacterial strains carrying the respective constructs are combined such that the cell densities of individual strains adjusted to desired values between 0.02 and 0.6 at optical density at 600 nm (OD_{600nm}). The combined resuspensions are allowed to stand at room temperature for 1 h before infiltration.
3. By using a 1-mL syringe, the resuspension is infiltrated into the leaf tissue. With the syringe tip gently pressed against the underside (abaxial side) of the leaf, the resuspension is injected into the leaf tissue by slowly pressing down the piston. An area of at least 2 cm diameter should be infiltrated. The area of successful infiltration is apparent by its water-soaked appearance. For each construct, at least one leaf from three independent plants is infiltrated. Up to four independent infiltrations are made routinely in each leaf without overlapping.

4. The infiltrated plants are placed in greenhouse for subsequent microscopical observation between 2 days post infiltration (dpi) and 6 dpi.

3.5. Standard Procedure for CLSM

1. For each expressed protein, the three independently infiltrated areas of the leaves are excised (ca. 1.5 cm × 1.5 cm) with scissors and are fixed with upper side down on the microscope glass slide by using double adhesive tape.
2. A drop of water is placed between each specimen and the 40× water immersion objective.
3. The typical set up used for imaging fluorescent signals by using Leica TCS SP2 CLSM is summarized is Table 2. Gain of each photomultiplier (PMT) is typically between 700 and 850.
4. Images of at least three randomly selected positions per leaf specimen are recorded, and three leaf specimens are analysed for each expressed protein. The signal morphology and intensity across different cells should be largely identical. If the signal intensity is too weak or no signal was detected, the expression may be optimized either by increasing the Agrobacterial inoculum in the infiltration mixture and/or by co-infiltrating with Agrobacterial strain harbouring P19 for suppressing post-transcriptional gene silencing mechanism (18). If the signal is saturating and is observed in non-specific subcellular localizations, the expression may be optimized by reducing the cell density of the Agrobacterial inoculum or by making

Table 2
Parameters used for confocal scanning laser microscopy (Leica TCS SP2)

Fluorophores	Excitation (nm)	Emission (nm)	Sequential scanning	Scanning speed (Hz)	Line average
Single expression					
PMT1 (GFP)	488	495–535		800, 1,000	8, 16
PMT1 (YFP)	514	535–560		800, 1,000	8, 16
Co-expression					
PMT1 (Yn/Yc)	514	535–560		800, 1,000	8, 16
PMT1(GFP), PMT2 (YFP)	495, 514	495–510, 545–560	Between lines	800, 1,000	8, 16
Chloroplast detection					
PMT3	488 or 514	650–707		800, 1,000	8, 16

PMT photomultiplier

observations at later time point (e.g. 4 dpi and onwards). For obtaining optimal expression conditions for a fusion protein, we routinely start with OD_{600nm} of 0.05, and optimize the conditions by shifting the OD_{600nm} values to 0.02, 0.05, 0.1, 0.2, 0.4, 0.6 with and without P19, which is routinely included at the OD_{600nm} of 0.1, and making observations at 2, 4, and 6pi.

3.6. Co-Expression and Visualization of GFP- and YFP-Tagged Proteins: ARAD1-YFP, STtmd-GFP, and HDEL-GFP

1. Optimization of expression conditions should be carried out for individual proteins as described above. For ARAD1-YFP, STtmd-GFP, and GFP-HDEL, OD_{600nm} of 0.05 without P19, at 4–6 dpi is optimal. STtmd is the N-terminal 52 amino acid residues of the rat sialyltransferase that contains a transmembrane domain and is widely used as a Golgi marker (19). GFP-HDEL is a widely used maker for ER, where the GFP is retained in the ER by the tetrapepide ER retention signal (HDEL) instead of being secreted to the apoplast (20).
2. Because of the overlap of the spectral properties of GFP and YFP, it is critical that gain setup in each detection channel is adjusted in order to minimize signal crosstalk. To this end, negative controls that are transfected with individual construct are prepared. The negative controls are scanned in the sequential line scanning mode with two parameter sets: (1) 488 nm excitation with 495–513 nm emission; (2) 514 nm excitation with 545–560 nm emission (see Table 2). The gain of the photomultiplier detecting GFP (GFP channel) is first adjusted by using the YFP-expressing negative control (i.e. ARAD1-YFP) such that either no or minimal signal crosstalk of YFP signal occurs in the GFP channel. The gain of the YFP channel is then adjusted by using the GFP-expressing negative control (i.e. STmd-GFP, GFP-HDEL) such that either no or minimal signal crosstalk of GFP signal occurs in the YFP channel.
3. With the gain setup chosen above, leaf specimen co-expressing both GFP- and YFP-tagged proteins are scanned (Fig. 1). Examples of simultaneous imagines of GFP- and YFP-tagged proteins are found in refs. (9) and (21).

3.7. In Situ Protein–Protein Interaction Detection by BiFC: ARAD1 and UXS2

1. Optimization of parameters of transfection and expression should be carried out for individual proteins by using the full-length YFP fusion as described above. For ARAD1-YFP and UXS2-YFP (see below), OD_{600nm} of 0.05 without P19 at 4–6 dpi observation is optimal.
2. The detection of BiFC signals is carried out in the same way as that of YFP (Table 2).
3. *Negative controls.* It has been reported that the split halves of YFP can drive the interaction of proteins themselves and

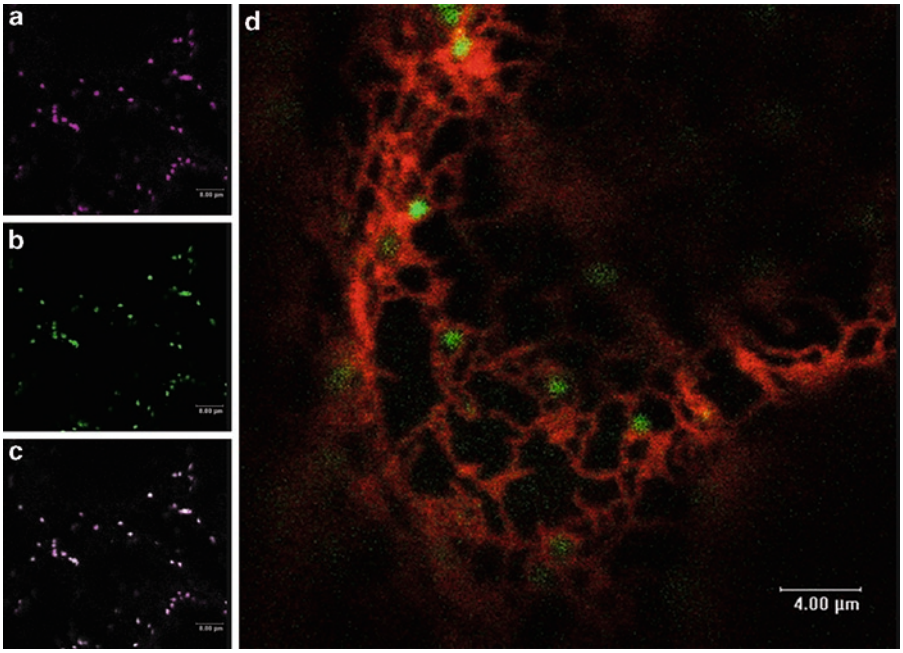

Fig. 1. Subcellular localization of ARAD1-YFP, STtmd-GFP, and GFP-HDEL imaged by confocal laser scanning microscopy. (**a**–**c**) Co-expression of ARAD1-YFP and STtmd-GFP. (**a**) ARAD1-YFP detected in the YFP channel (*magenta*). (**b**) STtmd-GFP detected in the GFP channel (*green*). (**c**) Merge of (**a**) and (**b**). The perfect overlap of the YFP and GFP signals is evident, which indicates that ARAD1-YFP localizes in Golgi. (**d**) Co-expression of ARAD1-YFP and GFP-HDEL. The images acquired in the YFP and GFP channels are shown in *green* and *red*, respectively. Distinct patterns of the GFP and YFP signals due to distinct subcelluar localizations of the two proteins are evident. Little signal cross-talk between the GFP and YFP detection channels is observed.

thereby giving rise to false positive results (22). Therefore, a set of negative controls that target the same cellular compartment and has an expression level similar to the test protein must be included in order to ascertain the relevance of the observed interaction. Here we test the homodimerization of ARAD1 and UXS2, an UDP-glucuronic acid decarboxylase (23). It has been reported that these Golgi proteins form homodimers ((23), Søgaard, Scheller, Sakuragi, unpublished). They are not functionally related, thus they serve as a negative control. We transfected *N. benthamiana* with (1) ARAD1-Yn, (2) ARAD1-Yc, (3) UXS2-Yn, (4) UXS2-Yc, (5) ARAD1-Yn and UXS-Yc, (6) ARAD1-Yc and UXS-Yn, (7) ARAD1-Yn and ARAD1-Yc, (8) UXS2-Yn and UXS2-Yc. Experiments (1) to (4) show no signal, thus serving as technical controls (data not shown). Experiments (5) and (6) show no signal, thus serving as negative interaction controls (Fig. 2c). Only the experiments (7) and (8) give rise to fluorescent signals with typical Golgi morphology (Fig. 2b, d).

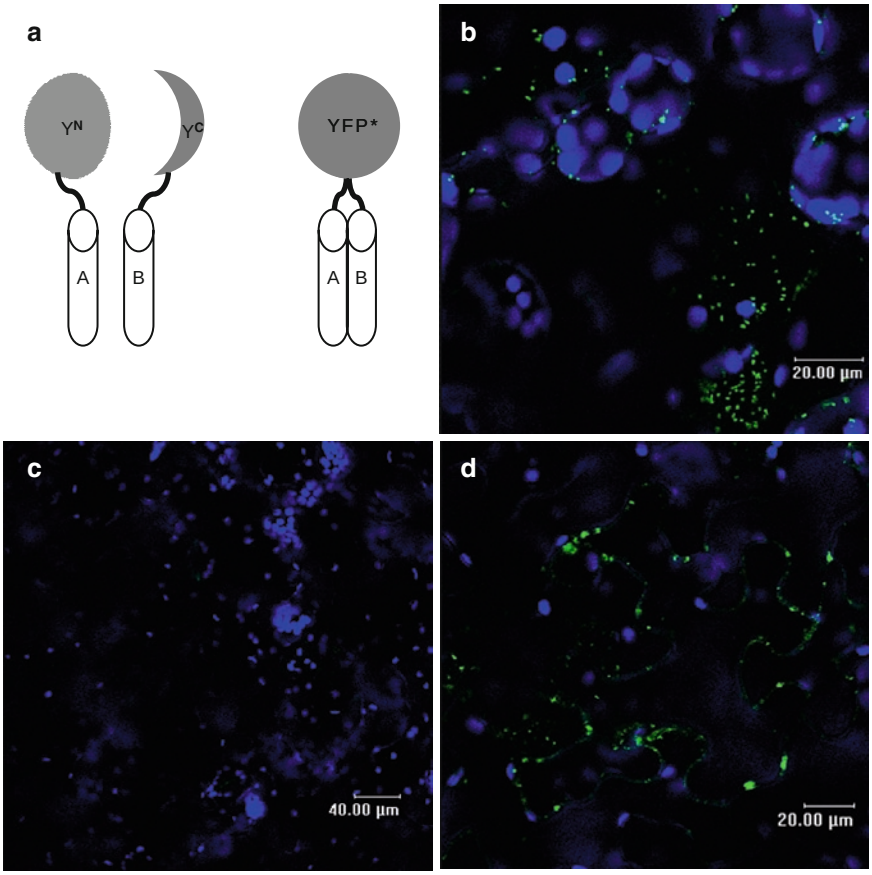

Fig. 2. BiFC analysis of ARAD1 and UXS2 homodimerization. (**a**) An illustration of the principle of BiFC, where the protein A and B are fused to Yn and Yc and are brought together to complement fluorescence upon interaction between the proteins. (**b**) Co-expression of ARAD1-Yn and ARAD1-Yc. (**c**) Co-expression of ARAD1-Yn and UXS2-Yc. (**d**) Co-expression of UXS2-Yn and UXS-Yc. YFP fluorescence is shown in *green*. The *red* autofluorescence from chloroplasts is shown in blue to make it distinguishable from the YFP fluorescence even for persons with impaired colour vision.

Combined results thus demonstrate that fluorescence complementation between ARAD1-Yn and ARAD1-Yc is mediated by homodimerization of ARAD1 protein *in situ*.

4. *Positive controls.* The following positive controls may be included. The purpose of the positive controls is to ascertain that the Yn and Yc fusion proteins are expressed and correctly folded to be compatible for BiFC. In split-ubiquitin system, the wild-type Nub spontaneously assembles with Cub due to a high affinity and is used for such control (24). However, there has been no report of an equivalent positive control for BiFC in Golgi. We observed that STtmd is a promiscuous interacter and, fused to Yn and Yc, complements fluorescence with all the Golgi-localising proteins tested so far (Sakuragi, Scheller, unpublished). As a result, STtmd can

serve as a positive control to show that Golgi-localized BiFC constructs are functional. The basis for the observed promiscuity of STtmd-Yn/Yc is not clear. It is predicted that this truncated protein consists of a short cytosolic N-terminus of 9 amino acid residues, a transmembrane domain of 17 amino acid residues, and a Golgi-lumen-exposed C-terminus. The C-terminal portion is predicted to be disordered by the three web-based programmes, DisEMBL, DISOPRED, and GlobPlots. It is known that intrinsically disordered proteins are often involved in protein–protein interactions and that disordered regions are thought to be structurally extended and flexible, which enhances an initial, relatively non-specific, association between the proteins (25). Therefore, it is plausible that the non-specific interaction observed for STtmd-Yn and Yc with the other BiFC proteins is mediated by the disorder in the C-terminus.

3.8. In Situ Protein Membrane Topology Analysis (PROMTO) of Cell Wall Biosynthetic Enzymes in Golgi

Membrane topology of cell wall biosynthetic enzymes localized in the Golgi can be analysed by BiFC using STtmd-Yn/Yc. We have verified by protease K susceptibility assay that the C-terminus of STtmd is indeed localized in the lumen while the N-terminus is in the cytosol and that successful BiFC occurs between proteins that expose the Yn and Yc domain to the same side of the membrane (i.e. STtmd-Yn and STtmd-Yc, and Yn-STtmd and Yc-STtmd) (Søgaard, Scheller, Sakuragi, unpublished). We have carried out PROMTO analysis of ARAD1-Yn/Yc, UXS-Yn/Yc, GAUT7-Yn/Yc, GUT1-Yn/Yc and observed fluorescence complementation with STtmd-Yc/Yn. These results indicate that C-termini of these CW biosynthetic proteins are oriented to the lumen side of the Golgi membrane, which is in agreement with the bioinformatic prediction of their type II membrane topology.

4. Notes

1. We constructed a vector for expression in plants with a C-terminal eGFP-tag by amplifying the eGFP coding sequence with the two oligonucleotides used for generating the plasmid pPS48uYFP (13). The resulting eGFP PCR fragment was cloned by uracil-excision into pCAMBIA 2300u (13), regenerating the uracil-excision compatible cloning site.
2. A series of fluorescent proteins with distinct spectral properties has been reported. In our laboratories, we have so far not been able to detect fluorescent signals from tdTomato, mOrange, and mCherry expressed transiently in tobacco.
3. PfuTurbo® C_x DNA polymerase is the only commercially available proofreading DNA polymerase that can read through

uracils in DNA templates (Stratagene). Recently, a new highly efficient DNA polymerase was developed specifically for use in uracil-excision cloning (26).

4. The complete digestion of the vector is crucial for efficient cloning. It is recommended that a small aliquot (ca. 1 μL) of the digest is analysed by gel electrophoresis before heat inactivation of the enzymes. The digested vectors can be purified by PCR purification kit (Qiagen), although we have not noticed significant improvements in cloning efficiency with purification as compared to heat inactivation.
5. Successful uracil-excision cloning appears to be dependent, to some extent, on the sufficient amount of vector. If a spectrophotometer for the assessment of DNA concentration is not available, DNA concentration can be roughly estimated on TAE agarose gel electrophoresis. In this case, 1 μL of digested DNA should result in a band with an appropriate size with intensity readily visible under UV light.
6. The efficiency of chemically competent cells need not be high, and home-made chemically competent cells with an efficiency of 10^7 CFU/μg DNA (supercoiled pUC19) should result in sufficient numbers of colonies ranging up to 100–200 transformants. Typically, we obtain between 10 and 200 transformants per reaction. For negative controls, the number of transformants, or background, is kept less than 10. In case this number is higher than 10, we carry out another round of digestion in order to reduce background.

Acknowledgements

This work was supported by the U.S. Department of Energy, Office of Science, Office of Biological and Environmental Research, through contract DE-AC02-05CH11231 between Lawrence Berkeley National Laboratory and the U.S. Department of Energy; by the Danish Villum Kann Rasmussen Foundation through the VKR centre Pro-active Plants; and by the Danish Agency for Science, Technology and Innovation.

References

1. Lerouxel, O., Cavalier D. M., Liepman, A. H., and Keegstra K. (2006) Biosynthesis of plant cell wall polysaccharides – a complex process. *Curr Op Plant Biol* **9**, 621–630
2. Scheller, H. V., Jensen, J. K., Sorensen, S. O., Harholt, J., and Geshi, N. (2007) Biosynthesis of pectin. *Physiologia Plantarum* **129**, 283–295
3. Mohnen, D. (2008) Pectin structure and biosynthesis. *Curr Opin Plant Biol* **11**, 266–277
4. Scheller, H. V. and Ulvskov, P. (2010) Hemicelluloses. *Ann Rev Plant Biol*, **61**, 263–289
5. Doblin, M. S., Kurek, I., Jacob-Wilk, D., and Delmer, D. P. (2002) Cellulose biosynthesis

in plants: from genes to rosettes. *Plant Cell Physiol* **43**, 1407–1420

6. Hong, Z. L., Zhang, Z. M., Olson, J. M., Verma, D. P. S. (2001) A novel UDP-glucose transferase is part of the callose synthase complex and interacts with phragmoplastin at the forming cell plate. *Plant Cell* **13**, 769–779
7. Young, W. W. (2004) Organization of Golgi glycosyltransferases in membranes: complexity via complexes. *J Membr Biol* **198**, 1–13
8. Harholt, J., Jensen, J. K., Sørensen, S. O., Orfila, C., Pauly, M., and Scheller, H. V. (2006) ARABINAN DEFICIENT 1 is a novel glycosyltransferase involved in biosynthesis of pectic arabinan in *Arabidopsis*. *Plant Physiol* **140**, 49–58
9. Jensen, J. K., Sørensen, S. O., Harholt, J., Geshi, N., Sakuragi, Y., Møller, I., Zandleven, J., Bernal, A. J., Jensen, N. B., Sørensen, C., Pauly, M., Beldman, G., Willats, W. G. T., and Scheller, H. V. (2008) Identification of a xylogalacturonan xylosyltransferase involved in pectin biosynthesis in *Arabidopsis*. *Plant Cell* **20**, 1289–1302
10. Nguema-Ona, E., Andeme-Onzighi, C., Aboughe-Angone, S., Bardor, M., Ishii, T., Lerouge, P., and Driouich, A. (2006) The reb1-1 mutation of Arabidopsis. Effect on the structure and localization of galactose-containing cell wall polysaccharides. *Plant Physiol* **140**, 1406–1417
11. Langeveld, S. M. J., Vennik, M., Kottenhagen, M., van Wijk, R., Buijk, A., Kijne, J. W., and de Pater, S. (2002) Glucosylation activity and complex formation of two classes of reversibly glycosylated polypeptides. *Plant Physiol* **129**, 278–289
12. de Pino, V., Borán, M., Norambuena, L., González, M., Reyes, F., Orellana, A., and Moreno, S. (2007) Complex formation regulates the glycosylation of the reversibly glycosylated polypeptide. *Planta* **226**, 335–345
13. Sterling, J. D., Atmodjo, M. A., Inwood, S. E., Kumar Kolli, V. S., Quigley, H. F., Hahn, M. G., and Mohnen, D. (2006) Functional identification of an Arabidopsis pectin biosynthetic homogalacturonan galacturonosyltransferase. *Proc Natl Acad Sci U S A* **103**, 5236–5241
14. Nour-Eldin, H. H., Hansen, B. G., Nørholm, M. H., Jensen, J. K., and Halkier, B. A. (2006) Advancing uracil-excision based cloning towards an ideal technique for cloning PCR fragments. *Nucleic Acids Res* **34**, e122
15. Geu-Flores, F., Nour-Eldin, H. H., Nielsen, M. T., and Halkier, B. A. (2007) USER fusion: a rapid and efficient method for simultaneous fusion and cloning of multiple PCR products. *Nucleic Acids Res* **35**, e55
16. Hu, C. D., Chinenov, Y., and Kerppola, T. K. (2002) Visualization of interactions among bZIP and Rel family proteins in living cells using biomoleuclar fluorescence complementation. *Mol Cell* **9**, 789–798
17. Kerppola, T. K. (2006) Visualization of molecular interactions by fluorescence complementation. *Nat Rev Mol Cell Biol* **7**, 449–456
18. Voinnet, O., Rivas, S., Mestre, P., and Baulcombe, D. (2003). An enhanced transient expression system in plans based on suppression of gene silencing by the p19 protein of tomato bushy stunt virus. *Plant J* **33**, 949–956
19. Boevink, P., Oparka, K., Santa Cruz, S., Martin, B., Betteridge, A., and Hawes, C. (1998) Stacks on tracks: the plant Golgi apparatus traffics on an actin/ER network. *Plant J* **15**, 441–447
20. Boevink, P., Santa Cruz, S., Hawes, C., Harris, N., and Oparka, K. J. (1996) Virus-mediated delivery of the green fluorescent protein to the endoplasmic reticulum of plant cells. *Plant J* **10**, 935–941
21. Voinonen, J. P., Sakuragi, Y., Stael, S., Tikkanen, M., Allahverdiyeva, Y., Paakkarinen, V., Aro, E., Suorsa, M., Scheller, H. V., Vener, A. V., and Aro, E. M. (2008) Light regulation of CaS, a novel phosphoprotein in the thylakoid membrane of *Arabidopsis thaliana*. *FEBS J* **275**, 1767–1777
22. Lalonde, S., Ehrhardt, D. W., Loque, D., Chen, J., Rhee, and S. Y., Frommer, W. B. (2008) Molecular an cellular approaches for the detection of protein-protein interactions: latest techniques and current limitations. *Plant J* **53**, 610–635
23. Gu, X., and Bar-Peled, M. (2004) The biosynthesis of UDP-galacturonic acid in plants. Functional cloning and characterization of *Arabidopsis* UDP-D-glucuronic acid 4-epimerase. *Plant Physiol* **136**, 4256–4264
24. Stagliar, I., Korostensky, C., Johnsson, N., and te Heesen, S. (1998) A genetic system based on split-ubiquitin for the analysis of interactions between membrane proteins *in vivo*. *Proc Natl Acad Sci U S A* **95**, 5187–5192
25. Tompa, P. (2005) The interplay between structure and function in intrinsically unstructured proteins. *FEBS Lett* **579**, 3346–3356
26. Norholm, M. H. H. (2010) A mutant Pfu DNA polymerase designed for advanced uracil-excision DNA engineering. *BMC Biotechnol* **10**, 21

Chapter 12

Atomic Force Microscopy of Plant Cell Walls

Andrew R. Kirby

Abstract

Atomic force microscopy (AFM) can be used to obtain high-resolution images on a wide variety of materials. Unfortunately, plant cell wall material is typically too rough to be imaged as native tissue by AFM. Small tissue fragments can be produced through careful ball milling. These fragments can subsequently be imaged at high resolution in near native conditions showing the overall architecture and the arrangement of the individual cellulose fibrils. An overview of items that can cause practical difficulties is given, as is a description of common image artifacts.

Key words: Atomic force microscopy, Tissue, Artifact

1. Introduction

Since its inception in the 1980s, atomic force microscopy (AFM) has matured into an immensely powerful technique for studying surfaces at high resolution. It is particularly suited to tackle problems in biology since the sample preparation is usually kept to an absolute minimum, without the need for fixation, dehydration or metal coating. The technique employs a sharp microfabricated stylus that "feels" the sample surface in a way that is analogous to a blind person reading Braille. In order to minimize the forces applied to the sample, and therefore reduce any potential damage, the stylus (more usually called the tip) is mounted on the end of an extremely flexible cantilever (Fig. 1).

The AFM tip can "feel" the sample so delicately that it is routinely possible to image individual molecules on flat surfaces without displacing or shearing them. The tiny vertical movements of the tip are detected using an optical lever; a laser beam is reflected off the end of the cantilever and onto a photodiode

Zoë A. Popper (ed.), *The Plant Cell Wall: Methods and Protocols*, Methods in Molecular Biology, vol. 715,
DOI 10.1007/978-1-61779-008-9_12,

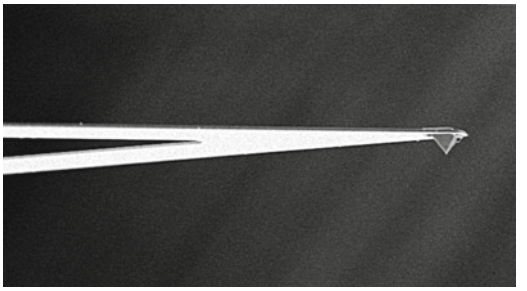

Fig. 1. A typical AFM cantilever with a pyramidal stylus on the end. This particular cantilever has a "V" shape, but rectangular beam varieties are also available. Typical cantilever lengths span 40–200 μm. SEM micrograph courtesy of Paul Gunning.

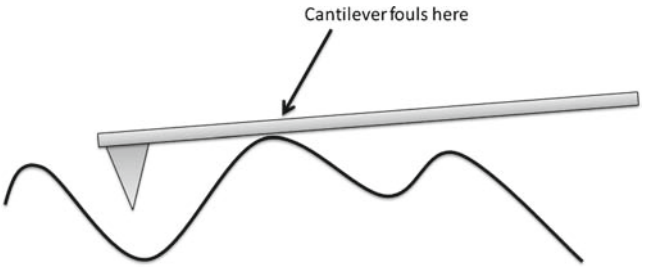

Fig. 2. On rough materials, there is a real danger that the underside of the cantilever can foul on the sample, particularly when scanning over larger areas. This can lead to a variety of artifacts in the image.

detector. Unfortunately, when the sample is relatively rough, i.e., its vertical topography varies in the order of a few microns (which is in the same size range as the dimensions of the tip), then the tip will track the sample surface poorly and the legs of the cantilever may foul on the sample (Fig. 2).

This results in an inaccurate image of the sample being recorded, with many of the features being artifacts. In this case, more consideration of the sample preparation procedure and the adjustment of the instrument parameters are essential. For a more rigorous introduction to the technique see Morris *et al.* (1).

2. Materials

2.1. Microscopy Instrumentation

1. The principal requirement is an AFM with a reasonably large range scanner. This is the piezoelectric device that raster scans the tip relative to the sample. In order to cope with the large variations in sample topography of the plant cell wall material,

a scanner with ~10 μm in vertical displacement is desirable. An AFM mounted on an optical microscope provides a quick and convenient way of finding regions of interest before scanning at high resolution with the AFM. This is important because even large AFM scanners typically have only 100 μm range in X and Y. Suitable Instruments that the author has experience with include MFP-3D (Asylum Research, Santa Barbara, CA), Bioscope Catalyst (Veeco Instruments, Santa Barbara, CA), and the Nanowizard III (JPK Instruments AG, Berlin, Germany), although no doubt others are available.

2. AFM cantilevers. NP general purpose 100–200 μm in length (Veeco Instruments, Santa Barbara, CA).
3. The sample itself needs to be supported by a rigid substrate; this can be a cleaved mica (Agar Scientific Ltd., Stansted, UK) or simply a conventional clean glass microscope slide.

Chemicals:

4. 1.5% SDS and $Na_2S_2O_5$ containing 5 mL octanol/L.
5. 0.5% SDS and $Na_2S_2O_5$ containing 2.5 mL octanol/L.
6. I_2KI solution: 3 g/L iodine crystals, 15 g/L potassium iodide dissolved in water.

2.2. Sample Preparation

1. Ball mill for reducing the size of the plant tissue fragments (Capco Test Equipments Ltd., Wickham Market, Suffolk, UK).
2. Waring Blender (Christison Particle Technologies Ltd., Gateshead, UK).
3. Ystral Homogeniser (Ystral GmbH, Dottingen, Germany).
4. Nylon mesh (BioDesign Inc., NY).

3. Methods

3.1. Preparation of Cell Wall Material from Potatoes

Although this method is particular to potatoes, with minor modifications it can be successfully used to extract cell wall material from many plants.

1. Slice potatoes transversely (approximately 5 mm thick).
2. Cut out parts within the vascular ring from the slices and from the central third of the potato.
3. For interim storage freeze the tissue in liquid nitrogen.
4. Using a Waring blender blend 500 g batches of the potato tissue for 3 min in 1 L of 1.5% SDS and $Na_2S_2O_5$ solution + 5 mL octanol.

5. Filter out any unblended tissue with a 2 mm mesh.
6. Using an Ystral Homogeniser break down the filtrate at 16,000 rpm for 1 min.
7. Filter on a 200-μm nylon mesh.
8. Wash the retained material with water and then resuspend in 0.5% SDS and $Na_2S_2O_5$ solution + 2.5 mL octanol.
9. Add the solution to a 2.5-L ball mill pot until only the very tops of the balls are showing. A few drops of octanol can reduce excessive foaming. Ball mill for 1–2 h at 60 rpm.
10. Pour out the liquor and wash each ball with water.
11. Remove the starch by filtering on a 100 μm nylon mesh and wash the material with 10 L of water.
12. Resuspend in water, homogenize again at 1,600 rpm for 1 min.
13. Filter and wash with 10 L of water on 100 μm nylon mesh.
14. Check for the absence of starch by staining a small amount of tissue on a microscope slide with I_2KI solution. Any remaining granules should appear blue/black in color. If there are still a significant amount of granules remaining, repeat steps 12 and 13.
15. Resuspend the cell wall material in water then freeze until needed.

3.2. Microscopy

1. Prepare the AFM for use by inserting a new undamaged tip, then align the laser and photodiode in the normal manner.
2. The instrument will be operated in contact mode, and should be set up as for imaging in air.
3. If mica is selected as the preferred substrate, it will first need to be cleaved by inserting a sharp object, such as a pointed set of forceps, at one edge and peeling the layers apart to expose a clean flat surface. Alternatively, a glass slide that has been cleaned with water and ethanol can be used.
4. Apply a drop (~100 μL) of a dilute solution of tissue fragments onto the chosen substrate with a pipette. In order to prevent the pipette tip from blocking, it may be necessary to enlarge the aperture by cutting the end back obliquely.
5. Using a low power optical microscope as a visual aid, distribute the tissue fragments across the substrate using a toothpick or similar. This is to prevent the sheets of cell wall material aggregating and stacking up, which would form a very rough surface.

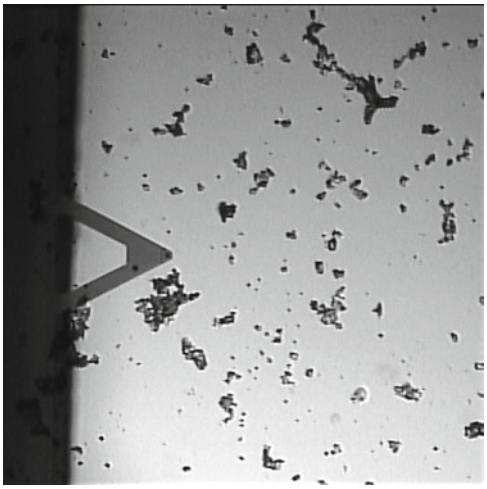

Fig. 3. An instrument that is combined with an optical microscope is a great aid to locating appropriately sized tissue fragments and positioning the tip. On the left is the cantilever as seen from above. This cantilever is 200 μm in length. Notice that the actual tip is not visible at this magnification.

6. Blot away any excess water using filter paper, but leave the sample still moist (see Notes 1 and 2).
7. Select an area of interest using the optical microscope. This will be a fragment of tissue ~100 μm in diameter (Fig. 3), and set the AFM tip to approach this region (see Note 3).
8. When the tip is in contact with the surface of the sample, imaging can begin. This should be at a slow rate, for example 0.5 Hz or less, i.e., one raster scan line every 2 s or less. The scan size should initially be modest, for example ≤3 μm. Check that the sample is not being pushed around by the tip (see Notes 4–6). Typical detailed images of a variety of plant tissues are shown (Fig. 4). Additionally, the reader is directed to other examples in the literature (2–6).
9. In addition to recording the topography image, it is a good idea to also record the error signal image as this can provide more fine details on rougher materials. It is worth stressing that the topography image appears to degrade as the error signal image improves and vice versa.
10. During the experiment, try increasing the instrument gain to improve the tracking of the tip over tall features on the sample (see Note 7).
11. If it is still difficult to obtain undistorted images, try experimenting with longer cantilevers (see Note 8).

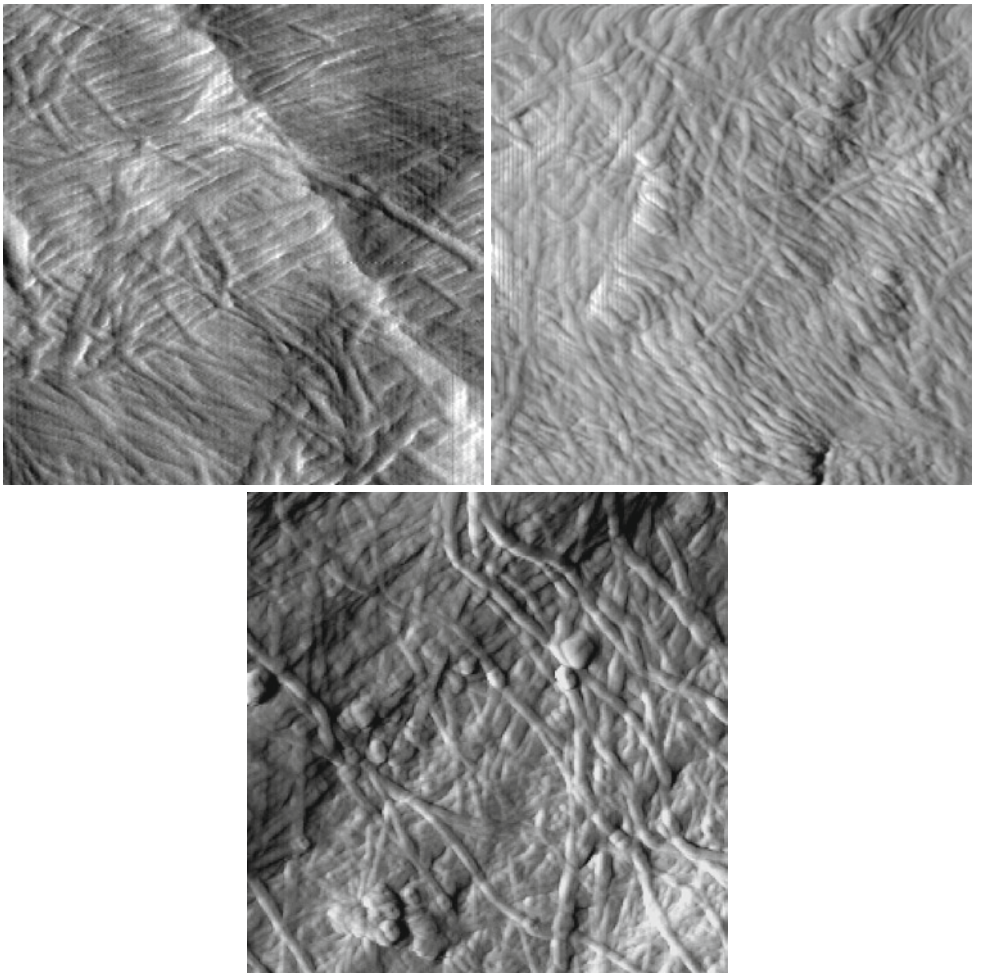

Fig. 4. Three examples of what you should see when things go correctly! *Top*: AFM error signal image of apple cell wall, size 1×1 μm. *Middle*: AFM error signal image of potato cell wall. Size 2×2 μm. *Below*: AFM error signal image of nettle cell wall. Size 2.5×2.5 μm. Nettle image courtesy of Patrick Gunning.

4. Notes

1. Over time, the sample will dry out and become more difficult to image. The principle reason for keeping the cell wall tissue moist is that the cellulose microfibrils stick upward like little "hairs" when completely dry. The AFM cannot properly track this kind of surface as the microfibrils are simply pushed aside by the tip during the scanning process. The surface tension of the thin liquid layer helps pull the microfibrils down so that they lay flat and immobile on the substrate (5). Additional water may be required after an hour or so, depending on the ambient conditions.
2. Do not forget to blot away any excess water (see Subheading 3.2, part 6), otherwise the liquid layer will spill over onto the back of

the cantilever and it will be impossible to find the laser spot due to refraction of the laser beam. Worse still, the tissue fragments may detach from the substrate and float above it.

3. If it is not possible to find any tissue fragments that are flat enough to image, then the ball milling time could be empirically increased to reduce the fragment size. However, if the tissue is ball milled for too long, then there is a risk of excessive disruption and resulting images that are not truly representative of the bulk sample.
4. Start by scanning small areas (see Subheading 3.2, part 8). Larger scan areas contain greater extremes in topography and are therefore more difficult, or impossible, for the AFM to track properly, unless the instrument parameters are perfect.
5. You will most likely find that there is a practical limit to the maximum scan size you can perform before the images appear distorted or the tip mistracks (known as a "tip jump") due to excessive sample roughness (Figs. 5 and 6). Attempting to perform even larger scan sizes will only result in tip damage or contamination.

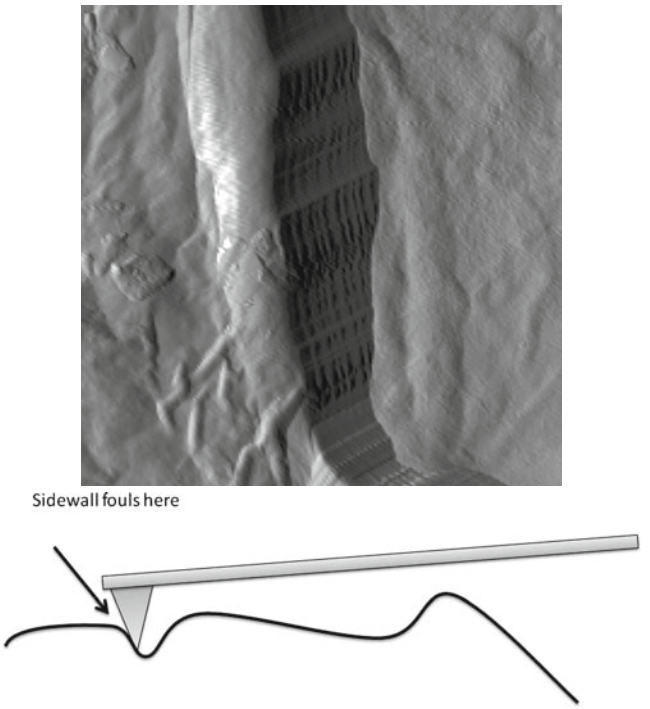

Fig. 5. Image artifacts can and will occur, particularly with rough samples. *Top*: an AFM image where the sample has interacted with the sidewall of the tip causing the image to appear "blurred." Note the tell-tale "cliff-edge" feature in the center of the image. If this type of artifact appears, it would be sensible to try reducing the scan speed. *Below*: schematic illustrating this type of tip-sample interaction.

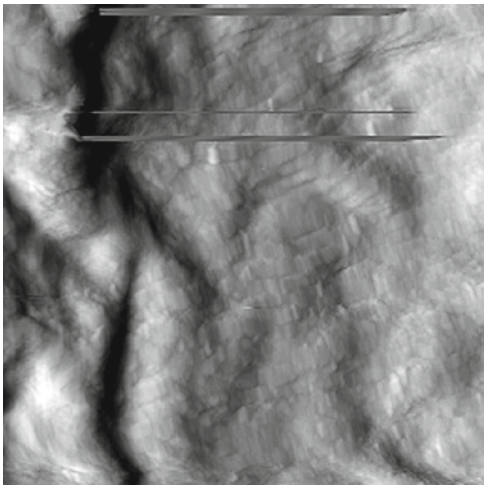

Fig. 6. Streaks or tip jumps in the image. This is caused by the tip momentarily sticking to the sample surface or sudden mistracking due to movement of the sample.

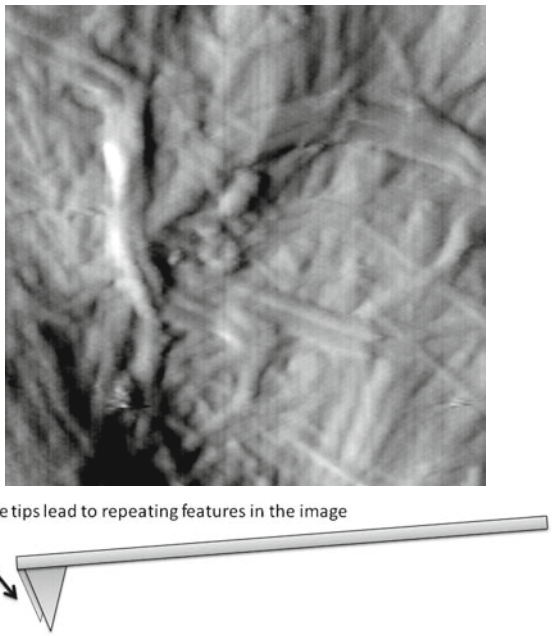

Fig. 7. The same features appear multiple times in the image (*top*). This is most commonly called a "multiple tip" artifact. This arises due to tip damage or contamination and is most frequently observed at small scan sizes. *Below*: schematic illustrating this type of tip-sample interaction.

6. Additionally, there is another artifact that can occur because of tip wear, damage, or contamination. The apex of the tip is no longer just a single sharp point but multiple points. This manifests itself as repeating structures or side-by-side features in the image (Fig. 7). When this occurs the only option is to replace the tip.

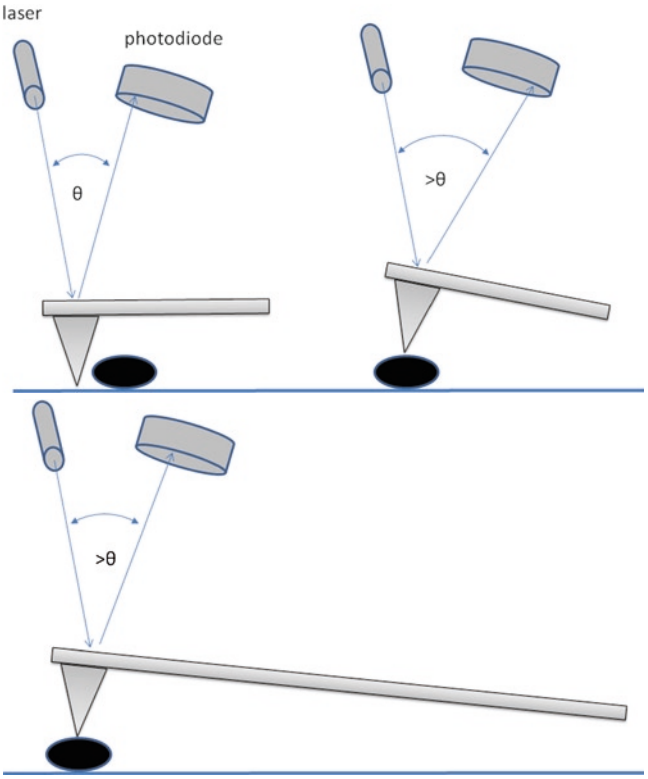

Fig. 8. Schematic diagram showing that shorter cantilevers move through large angles (*top*). This can pose a problem with rough samples because the laser beam could miss the photodiode altogether. In this case, longer cantilevers are preferred as the angular sensitivity is reduced (*bottom*).

7. The speed of response of the AFM to large features can be improved by increasing the instrument gain (see Subheading 3.2, part 10). However, if the gain value is set too high, it can lead to the appearance of vertical lines in the image due to uncontrolled tip oscillations.
8. The cantilever length plays an important role in the vertical sensitivity of the instrument. Shorter cantilevers can detect smaller variations in the height of the sample because they deflect the laser beam through wider angles than their longer counterparts (Fig. 8). However, for rough samples, longer cantilevers are preferred since it is vital that the reflected laser beam actually remains on the face of the photodiode without spilling over the side.

Acknowledgements

The research described in this article was funded through the BBSRC core support grant to the Institute of Food Research.

References

1. Morris, V. J., Kirby, A. R., and Gunning, A. P. (2010) Atomic Force Microscopy for Biologists. Imperial College Press, London.
2. Marga, F., Grandbois, M., Cosgrove, D. J., and Baskin, T. I. (2005) Cell wall extension results in the coordinate separation of parallel microfibrils: evidence from scanning electron microscopy and atomic force microscopy. *Plant Journal* **43**, 181–190.
3. Ding, S. -Y., and Himmel, M. E. (2006) The maize primary cell wall microfibril: a new model derived from direct visualization. *Journal of Agricultural and Food Chemistry* **54**, 597–606.
4. Kirby, A. R., Ng, A., Waldron, K. W., and Morris, V. J. (2006) AFM investigations of cellulose fibers in bintje potato (*Solanum tuberosum* L.) cell wall fragments. *Food Biophysics* **1**, 163–167.
5. Kirby, A. R., Gunning, A. P., Waldron, K. W., Morris, V. J., and Ng, A. (1996) Visualization of plant cell walls by atomic force microscopy. *Biophysical Journal* **70**, 1138–1143.
6. Thimm, J. C., Burritt, D. J., Ducker, W. A., and Melton, L. D. (2000) Celery (*Apium graveolens* L.) parenchyma cell walls examined by atomic force microscopy: effect of dehydration on cellulose microfibrils. *Planta* **212**, 25–32.

Chapter 13

Using Solid-State ^{13}C NMR Spectroscopy to Study the Molecular Organisation of Primary Plant Cell Walls

Tracey J. Bootten, Philip J. Harris, Laurence D. Melton, and Roger H. Newman

Abstract

Studies of the mobilities of polysaccharides or parts of polysaccharides in a cell-wall preparation may give clues about the molecular interactions among the polysaccharides in the cell wall and the relative locations of polysaccharides within the cell wall. A number of solid-state ^{13}C NMR techniques have been developed that can be used to investigate different types of polysaccharide mobilities: rigid, semi-rigid, mobile, and highly mobile. In this chapter, techniques are described for obtaining spectra from primary cell-wall preparations using CP/MAS, proton-rotating frame, proton spin-spin, spin-echo relaxation spectra, and single-pulse excitation. We also describe how proton spin relaxation editing can be used to obtain subspectra for cell-wall polysaccharides of different mobilities.

Key words: Primary cell walls, Polysaccharide mobility, Solid-state ^{13}C NMR, Proton-spin relaxation editing, Single-pulse excitation NMR, TEM, X-ray diffraction

1. Introduction

Primary walls surround growing plant cells and are composed of rigid cellulose microfibrils embedded in a gel-like matrix of non-cellulosic polysaccharides with a range of different structures (1, 2). The major non-cellulosic, matrix polysaccharides of the primary cell walls of eudicotyledons and non-commelinid monocotyledons are xyloglucans (XG), and pectic polysaccharides (2). The pectic polysaccharides consist mainly of homogalacturonan (HG) and rhamnogalacturonan I (RG-I), with smaller proportions of the substituted galacturonans rhamnogalacturonan II (RG-II) and xylogalacturonan (XGA). Arabinans, galactans, and arabinogalactans are attached as side chains to RG-I (3). The major

Zoë A. Popper (ed.), *The Plant Cell Wall: Methods and Protocols*, Methods in Molecular Biology, vol. 715,
DOI 10.1007/978-1-61779-008-9_13,

polysaccharides of the primary cell walls of many commelinid monocotyledons are glucuronoarabinoxylans (GAXs) with smaller proportions of pectic polysaccharides and XGs (2, 4). Variable proportions of (1→3),(1→4)-β-glucans also occur in the primary walls of grasses and cereals (Poaceae) and related families (5).

Solid-state ^{13}C nuclear magnetic resonance (NMR) spectroscopy is one of several techniques used to study the molecular organisation of such walls. In contrast to TEM, this technique can be used on cell walls that have never been dried, thereby minimising possible chemical and physical modifications. Moreover, in contrast to X-ray diffraction, this technique does not require multiple planes of ordered molecules. Solid-state ^{13}C NMR is sensitive to ordering over relatively short dimensions, and measurements of chemical shifts can indicate differences in the conformations of backbone chains or side-chains (6). Measurements of spin relaxation time constants can indicate differences in the short-range environment, specifically the nature and dynamics of neighbouring molecules. In studies of the cellulose in walls, solid-state ^{13}C NMR can be used to distinguish between molecules on the surfaces of crystallites and those in the interior, since their molecular conformations differ (7–9). This information can be used to estimate the lateral dimensions of cellulose crystallites. In this application, solid-state ^{13}C NMR is particularly informative when the crystallites are of such a small cross-section that there are as many chains exposed on surfaces as contained in the interior, as occurs in primary-wall cellulose (6, 10). TEM and X-ray diffraction are more informative if the cellulose crystallites are of a relatively large cross-section (8).

Solid-state ^{13}C NMR spectroscopy can also be used to distinguish cell-wall polymers that have different mobilities because of their locations and interactions with other molecules within the cell wall (11). A summary of how this type of mobility-resolved NMR may help to identify polysaccharide domains and interactions within the cell wall is shown in Fig. 1. For example, the (1→4)-β-D-glucan backbones of XG molecules, or parts of molecules, adsorbed on to the surface of cellulose microfibrils *in muro* are predicted to adopt a rigid, flattened conformation, rather than the twisted backbone conformation of free XG (12). These two different conformations can be detected by solid-state ^{13}C NMR spectroscopy (13, 14) (Fig. 1). Therefore, not only is solid-state ^{13}C NMR spectroscopy useful for determining the mobilities of different components in plant cell walls, but it also effectively makes *in situ* investigations (15).

Two main types of mobility-resolved solid-state ^{13}C NMR experiments are commonly used to investigate primary cell walls, cross-polarisation (CP) NMR and single-pulse excitation (SPE) NMR. Both are generally used in combination with MAS, hence they are referred to as CP/MAS NMR and SPE/MAS NMR (16).

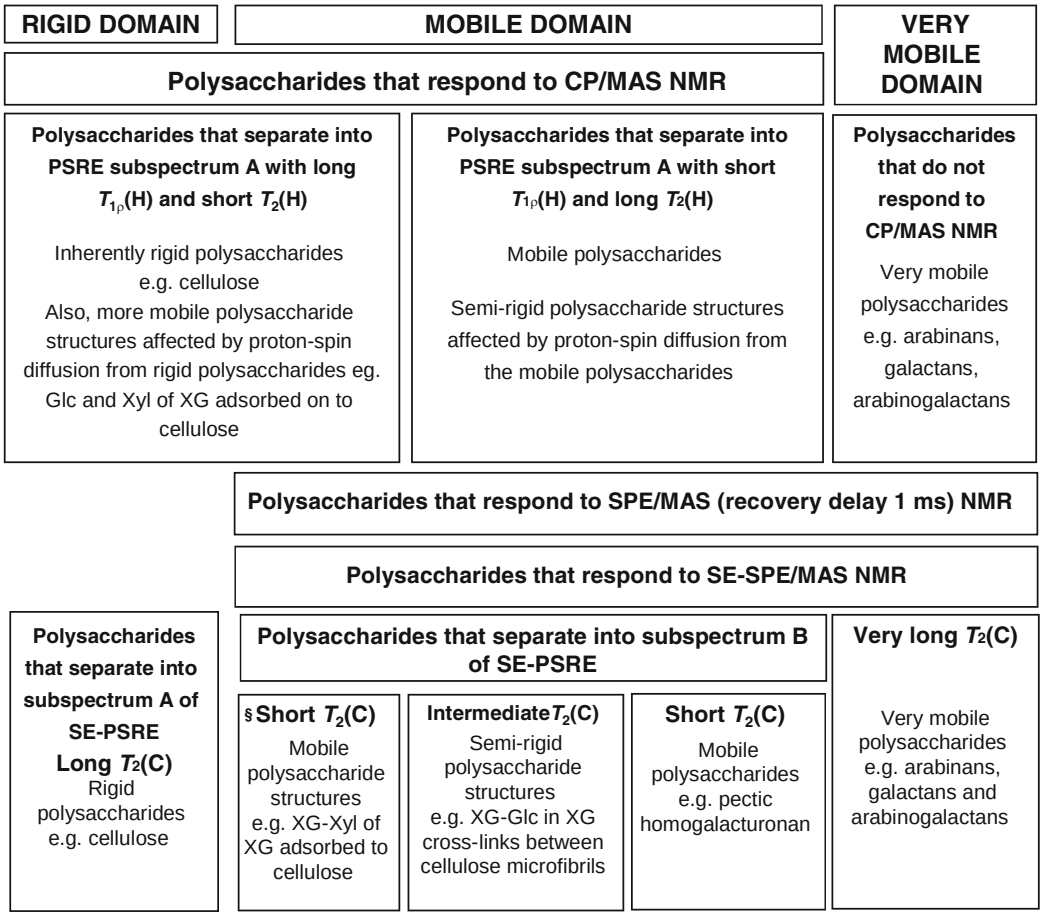

Fig. 1. Solid-state ^{13}C NMR, proton- and ^{13}C- spin relaxation techniques described in this chapter and used to identify polysaccharides of different mobilities in cell-wall preparations. §These mobile polysaccharides separate into the same $T_{1\rho}$(H) and T_2(H) subspectra as cellulose due to proton spin diffusion from adjacent cellulose but separate into the mobile T_2(C) subspectra as these structures are inherently mobile.

CP/MAS NMR suppresses signals from relatively mobile molecules, and SPE/MAS NMR suppresses signals from relatively rigid molecules (17).

Cross-polarisation NMR combines both the magnetic spins of protons and ^{13}C nuclei. By transferring the magnetisation from protons to ^{13}C, the range of dispersion of the chemical shifts is increased compared to the range of chemical shift values for proton NMR, thus increasing the resolution of the signals from solid-state samples (18). CP/MAS NMR also allows the indirect measurement of proton NMR relaxation by variations in the strengths of selected ^{13}C signals (19). The proton relaxation process is complicated by spin diffusion where neighbouring nuclei exchange spin information (20). Proton spin diffusion may occur over distances of nanometers and over time scales of milliseconds (21). Therefore, proton spin relaxation time constants

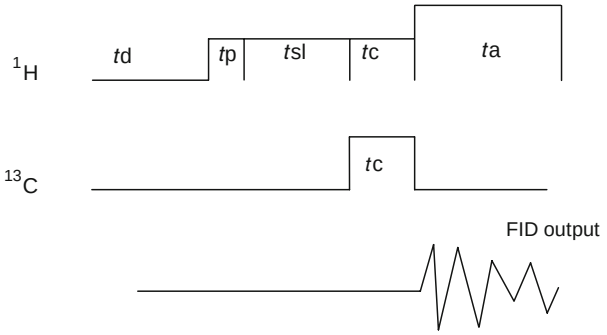

Fig. 2. Schematic representation of a proton rotating-frame spin relaxation pulse sequence. *t*p: preparation pulse; *t*sl: spin-locking pulse; *t*c: cross-polarisation contact time; *t*a: data acquisition time; *t*d: recovery delay. In each case, *t*=time. Adapted from Newman and Hemmingson (28), de Gruyter.

are mean values for all protons within a finite volume, irrespective of the ^{13}C-signal used to monitor the proton relaxation.

Two main approaches using CP/MAS NMR are used to investigate polysaccharide mobility in primary cell walls. Both approaches exploit the fact that the relaxation of spins of magnetic nuclei for polysaccharides in cell walls can be sensitive to the molecular conformations of those polysaccharides. First, proton-spin relaxation editing (PSRE) can be used to separate NMR subspectra containing signals from polysaccharides in rigid and mobile domains of the cell wall (7). To do this, a proton spin relaxation event is introduced prior to the CP contact time. A typical PSRE pulse sequence is illustrated in Fig. 2. Linear combinations, generated from spectra obtained under the normal CP/MAS and the PSRE conditions, can then be used to edit the CP/MAS spectra (17). Second, a number of PSRE experiments may be carried out each with different recovery delays (22). From these spectra, full relaxation curves for component signals may be constructed. The shape of the relaxation curve and the time constants associated with the proton relaxations can be used to distinguish between polysaccharides in rigid and mobile domains in the cell wall, remembering that the proton spin relaxation time constants of a particular polysaccharide will be similar to those of the polysaccharides in its immediate vicinity.

Segmental motion within a polysaccharide can be investigated by measuring relaxation of the ^{13}C-nuclei by using a spin-echo (SE) NMR pulse sequence. The rarity of the ^{13}C-isotope (1.1% of carbon) means the diffusion of ^{13}C spin information is relatively slow (23). Therefore, unlike proton spin relaxation, ^{13}C relaxation is sensitive to segmental motion of the polysaccharide at the site of the ^{13}C nucleus and is much less sensitive to the motion of more distant segments of the same polysaccharide chain or other polysaccharide chains.

There are three main spin-relaxation processes that have been used to investigate primary cell walls: spin-lattice relaxation with time constants $T_1(H)$ and $T_1(C)$, rotating-frame relaxation with time constants $T_{1\rho}(H)$ and $T_{1\rho}(C)$, and spin-spin relaxation with time constants $T_2(H)$ and $T_2(C)$ (6, 18). Newman *et al.* (6) found that the most useful relaxation processes for investigating proton relaxations of polysaccharides in primary cell walls were the rotating-frame and spin-spin experiments.

SPE/MAS NMR is an excellent complementary technique to CP/MAS NMR (22) for investigating mobile polysaccharides in cell-wall preparations. The CP/MAS NMR spectra of the cell-wall preparations are generally dominated by signals assigned to cellulose, and the broader underlying signals are assigned to non-cellulosic polysaccharides, along with, in primary cell-wall preparations containing predominantly pectic polysaccharides, signals at 173, 54, and 22 ppm assigned to carboxylic acid, methoxyl, and acetyl carbons, respectively. As cellulose generally accounts for less than half of the primary cell wall, a portion of the non-cellulosic material must be too mobile to respond to the cross-polarisation pulse sequence. Although SPE/MAS can potentially detect all components in the cell-wall preparations (16), the highly mobile cell-wall components, which are less responsive to CP/MAS NMR (24, 25), are particularly responsive to SPE/MAS. By using a short recovery delay in the SPE/MAS pulse sequence (1 s), signals that have long $T_1(C)$ relaxations, such as the rigid cellulose molecules, are suppressed (16, 25) (Fig. 1).

Studies of polysaccharide mobility in an isolated cell-wall preparation should use not only the relaxation properties of the proton or ^{13}C of that moiety, as indicated in Table 1, but also take into account alterations in the chemical shift for that polysaccharide or monosaccharide or part of the polysaccharide. Generally, polysaccharides investigated using solution NMR will have lower chemical shifts than in solid-state NMR (Table 1). These different chemical shifts may indicate differences in molecular conformations, e.g. extended chains rather than coiled chains (14). Chemical shifts can therefore provide insights into the reasons for reduced mobility within the cell wall, particularly when combined with the relaxation studies described above.

2. Materials

1. Plant material of interest.
2. Cell wall isolation buffer: 20 mM HEPES-KOH buffer, pH 6.7 containing 10 mM dithiothreitol (DTT) (see Note 1).
3. DTT-free buffer: 20 mM HEPES-KOH, pH 6.7.

Table 1
Cited solid-state ^{13}C NMR assignments for the main primary cell-wall polysaccharides of eudicotyledons and non-commelinid monocotyledons

	Assignment	Chemical shift ppm	Reference
C-1 Glc	Cellulose I_α (interior)	105.6	(35)
	Cellulose I_β (interior)	106.5, 104.4	(35)
	Cellulose II	107.6	(36)
C-4 Glc	Cellulose I_α (interior)	90.3 and 89.4	(37, 38)
	Cellulose I_β (interior)	89.4 and 88.5	(37, 38)
	Cellulose I (surface)	84.8 and 83.9	(39)
	Cellulose II	89.4 and 88.2	(40)
C-6 Glc	Cellulose I_α (interior)	65.2	(36)
	Cellulose I_β (interior)	66.3 and 65.2	(36)
	Cellulose I (surface)	63.1 and 62.1	(36)
	Cellulose II	63.5 and 62.5	(38)
C-1 XG-Xyl	Cyclamen seed XG	99.8	(41)
	Tamarind XG	99.8	(42)
	Arabidopsis cell walls (chemically extracted to remove pectic polysaccharides)	100.0	(43)
	Tamarind/BC composite	100.3	(44)
	Rubus suspension cells	100.4[a]	(45)
	Tamarind XG	99.1–100[a]	(46)
	Cyclamen seed XG	100.2[a]	(41)
C-4 XG-Xyl	Tamarind XG	70.1–70.4[a]	(46)
	Cyclamen seed XG	70.8[a]	(41)
C-1 XG-Glc	Tamarind XG	103.6	(42)
	Rubus suspension cells	103.9[a]	(45)
	Tamarind XG	103.1–103.7[a]	(46)
	Cyclamen seed XG	103.5[a]	(41)
C-4 Glc	Cyclamen seed XG	82–85	(41)
	Tamarind XG	70.3–80.5[a]	(46)
	Cyclamen seed XG	79.5–80.8[a]	(41)
C-1	5-Ara Arabinans	108.4[a]	(47)
	5-Ara Arabinans	108.5[a]	(48)
	4-Gal Galactans	105.2[a]	(47)
	4-GalA HG	101.1	(29)
	4-GalA HG	99.8[a]	(48)

(continued)

Table 1 (continued)

	Assignment	Chemical shift ppm	Reference
C-4	4-Ara Arabinans	83.2[a]	(47)
	4-GalA HG	79–80	(29)
	4-Gal Galactans	78.5[a]	(47)
	4-Ara Arabinans	77.7[a]	(47)
	t-Gal Galactans	61.8[a]	(47)
-$COOCH_3$	HG	52.8–53.7	(29)

BC bacterial cellulose
[a]Solution NMR spectroscopy; all other values were obtained with CP/MAS of solid material

4. Ponceau 2R solution: Make up an aqueous solution of 0.2% w/v Ponceau 2 R (CI 16150) and add 2 drops/100 mL of 18 M H_2SO_4. Store solution at 4°C.
5. Polydimethylsilane was from Hüls America Incorporated, Cincinnati, OH, USA (see Note 2).
6. Polytrichlorofluoroethylene grease was from Halocarbon Products Corporation, River Edge, NJ, USA (see Note 3).
7. Polytron blender (Model PT10-35, Kinematica, Luzern, Switzerland).
8. 15 mL Tenbroeck ground glass homogenizer (Kontes Glass Company, Vineland, NJ, USA).
9. Centrifuge.
10. Nylon mesh with pore size 11 µm.
11. 80% v/v ethanol.
12. Glass-fibre filter (GF/C, Whatman Scientific, Maidstone, Kent, UK).
13. Freeze-drier.
14. 7 mm-diameter cylindrical silicon nitride rotor with Vespel end caps.
15. Inova-200 NMR spectrometer (Varian, Palo Alto, CA, USA).

3. Methods

3.1. Preparation of Cell Walls

A cell-wall preparation should be free of cytoplasmic contents as NMR signals from proteins and lipid can interfere with the NMR signals from polysaccharides. To achieve this, cell walls are

isolated by mechanically breaking the cells open and washing out the cells contents with cold aqueous buffer (26, 27). All procedures are carried out at 4°C.

1. Plant tissue (approximately 20 g wet weight) is homogenised in 100 mL of cell wall isolation buffer, using a Polytron blender on full power (3 times for 20 s).
2. The tissue can be further homogenised using a 15-mL-Tenbroeck ground-glass homogeniser. Breakage of the cells is monitored using bright-field microscopy after staining with Ponceau 2R solution, which stains protein red (26).
3. The homogenate is centrifuged (250×*g*, 10 min), and the pellet washed 3 times by centrifugation with buffer (with DTT omitted), followed by 6 times with water.
4. The pellet is resuspended in water, washed onto nylon mesh (pore size 11 μm), and the residue on the mesh washed with water (500 mL).
5. The water content of the cell-wall preparation should be reduced but not completely eliminated for solid-state NMR (see Note 4). Two methods can be used to do this:
   (a) The preparation is washed 3 times by centrifugation with 80% (v/v) ethanol and the final suspension kept at 4°C in 80% (v/v) ethanol until NMR spectroscopy can be done (see Note 5). Preparations in 80% (v/v) aqueous ethanol are prepared for NMR by filtering portions of the suspensions onto a glass-fibre filter (GF/C, Whatman Scientific, Maidstone, Kent, UK) and part-drying in air to a water-content of approximately 40% (w/w). This weight is estimated from the dry weight of an aliquot of preparation that is removed and freeze-dried.
   (b) An aliquot of the preparation is removed and freeze-dried to estimate the water. The remaining preparation is frozen and dried, carefully, under vacuum to a water-content of approximately 40% (w/w) based on the dry weight of the sub-sample. If this method is used, NMR spectroscopy must be done immediately to avoid possible sample degradation. The exact moisture content of the preparation can be determined by oven drying to constant weight (105°C) following the completion of the NMR experiments.

3.2. Solid-State ^{13}C-NMR Spectroscopy

1. The never-dried cell-wall preparation is packed in a 7-mm-diameter cylindrical silicon nitride rotor, and retained with Vespel end caps. An internal standard of polydimethylsilane can be added to the centre of the sample during the packing of the rotor. Polydimethylsilane contributes a ^{13}C signal at

–1.96 ppm (see Note 2). As the cell-wall preparations are partly hydrated, polytrichlorofluoroethylene grease (see Note 3) is used to ensure a water-tight seal between the cylinder and the end caps. The grease should be spread on the internal surface of the rotor, not on the cap, to avoid expelling grease when the cap is inserted. It is important that there should be no grease on the external surfaces of the rotor or caps, otherwise the NMR stator will become contaminated and sample spinning will be impeded.

2. The rotor is spun at 4 kHz in a magic-angle spinning probe for ^{13}C NMR spectroscopy at 50.3 MHz. In the worked example, the probe was supplied by Doty Scientific (Columbia, SC, USA) and the Inova-200 spectrometer was supplied by Varian (Palo Alto, CA, USA). Slower spinning can cause interference from spinning-sideband signals, while faster spinning can cause physical degradation of the cell-walls because of the centrifugal forces generated.

3.3. CP/MAS Spectroscopy

In cross-polarisation (CP) NMR experiments, each 90° proton preparation pulse is followed by a 1-ms CP contact time, 51 ms of data acquisition, and a recovery delay of 1.0 s before the sequence was repeated (see Note 6). The correct duration of the 90° proton preparation pulse can be measured by using trial values and selecting the value that provides the best signal strength. A typical value is 6 μs, as used to illustrate this chapter. Both proton and ^{13}C transmitters are left on for the duration of the contact time. It is also important that the power levels are adjusted for a Hartman-Hahn match, that is, the measurement of a 90° pulse should give the same value for both nuclei. Measurement of a 90° pulse for ^{13}C is discussed below, under the Subheading 3.5.2. The proton transmitter output is increased during data acquisition, to provide adequate power for spin decoupling, i.e., a target power level corresponding to a precession frequency >40 kHz and typically between 53 and 59 kHz as in the experiments used to illustrate this chapter. Lower power levels will cause noticeable broadening of the NMR signals.

3.4. Proton Spin Relaxation Experiments

Proton rotating-frame spin relaxation with time constant $T_{1\rho}(H)$ and proton spin-spin relaxation with time constant $T_2(H)$ are characterised by inserting relaxation intervals of duration t_1 or t_2, respectively, between the proton preparation pulse and the CP contact time (Fig. 2). The values for t_1 and t_2 are chosen to be within the ranges of values for $T_{1\rho}(H)$ and $T_2(H)$, respectively, to optimise the signal-to-noise ratios in separate subspectra (28). Protons are spin-locked during t_1, but the proton transmitter is switched off during t_2.

PSRE NMR subspectra are generated by combining spectra labelled S, S′ and S″, where S is obtained by the normal cross-polarisation pulse sequence, S′ with $t_1 = 4$ ms and S″ with $t_2 = 15$ μs. The experimental spectra are obtained in the order CP/MAS (S), proton-rotating frame experiment (S′) and proton spin-spin experiment (S″).

The number of transients of the pulse sequences required to obtain adequate signal to noise ratios from averaged spectra needed for PSRE editing varies, but 40,000 up to 100,000 transients is usual. This corresponds to 30–80 h of data accumulation time for a full PSRE experiment.

3.5. Separating the Proton-Spin Relaxation Edited (PSRE) Subspectra

The principles behind PSRE NMR have been described in Newman (17) and are summarised in the Introduction. In the simplest case, a spectrum S is the sum of subspectra A and B from two distinct types of domains.

A partly-relaxed spectrum S′ is then:

$$S' = f_a A + f_b B, \tag{1}$$

where f_a and f_b are signal suppression factors.

The subspectra can then be separated by computing:

$$A = kS + k'S', \tag{2a}$$

$$B = (1 - k)S - k'S', \tag{2b}$$

where

$$k = f_b / (f_b - f_a), \tag{3a}$$

$$k' = -1 / (f_b - f_a). \tag{3b}$$

In the context of a cell-wall preparation, subspectra A and B usually contain signals from the cellulose and non-cellulosic polysaccharides, respectively.

Two NMR signals, characteristic of the two mobility domains, are selected for proton rotating-frame relaxation experiments. The signal at 89 ppm (assigned to C-4 of cellulose crystallite-interior) is selected as representative of cellulose crystallites, appearing at a chemical shift for which there is little overlap with signals from other polysaccharides. A signal at 69 ppm (assigned to C-2, C-3, and C-5 of GalA residues in pectic homogalacturonans) (29, 30) is selected as representative of mobile polysaccharides for those primary walls containing high proportions of pectic polysaccharides (1, 2). (NB. See ref. (25) for appropriate editing signals for GAX-rich primary walls).

1. Because the $T_1\rho(H)$ relaxation time constants for the 69 ppm signal were not greatly different, it was not possible to achieve

Table 2
Suppression factors, linear combinations and the corresponding relaxation time constants used to generate PSRE subspectra A and B for mung bean cell walls

Suppression factors		
$T_{1\rho}$(H) ms	f_a	0.69
	f_b	0.27
T_2(H) µs	f_a	0.30
	f_b	0.60
Linear combinations		
$T_{1\rho}$(H) ms	Subspectrum A	–0.64S + 2.38S′
	Subspectrum B	1.64S + 2.38S′
T_2(H) µs	Subspectrum A	2.00S–3.33S″
	Subspectrum B	–1.00S + 3.33S″
Relaxation time constants		
$T_{1\rho}$(H) ms	Subspectrum A	10.8
	Subspectrum B	3.1
T_2(H) µs	Subspectrum A	9.7
	Subspectrum B	14.8

total elimination of signals from non-cellulosic polysaccharides without also suppressing signals from cellulose, so linear combinations of S and S′ are generated to enhance signal suppression (Table 2).

2. Initial estimates of f_a and f_b are calculated from signal heights (Fig. 3).
3. The values for f_a and f_b are used to determine the linear combinations used to separate the subspectra from the CP/MAS data, using (3a) and (3b) then (2a) and (2b).
4. Values for f_a and f_b are then adjusted until the signal at 89 ppm is eliminated from subspectrum B and signal at 69 ppm, assigned to pectic polysaccharides, are suppressed in subspectrum A without allowing any signals to become inverted. For example, for the spectra from mung bean (*Vigna radiata*) cell walls shown in Fig. 3, the final suppression factors from the proton rotating frame experiment were:

   $f_a = 0.69$ and $f_b = 0.27$; therefore, $k = -0.64$ and $k' = -2.38$

   In the worked example, the linear combinations used to separate subspectra A and B from the CP/MAS NMR data were:

   Subspectrum A = –0.64S + 2.38S′ and Subspectrum B = 1.64S + 2.38S′

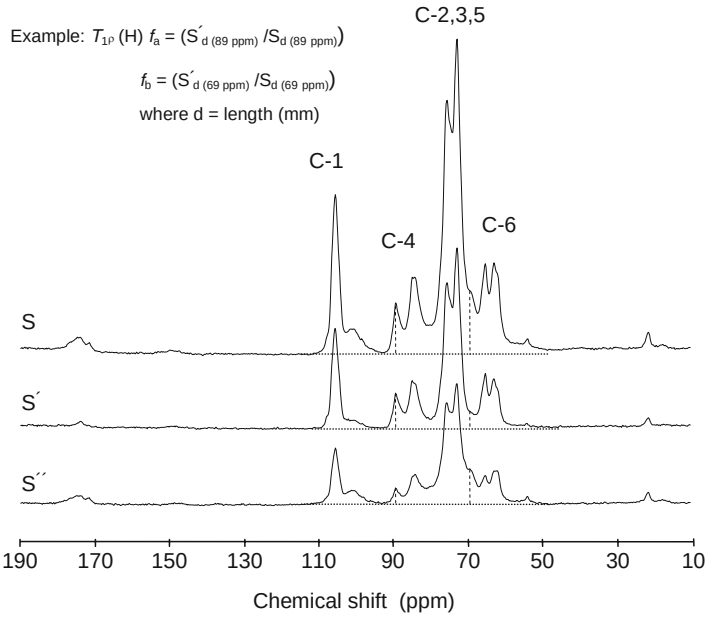

Fig. 3. Calculating suppression factors from the CP/MAS and PSRE spectra obtained of a mung bean cell-wall preparation. *S* obtained by the normal CP/MAS pulse sequence; *S′* with 4 ms of proton rotating-frame spin relaxation; *S″* with 15 μs of proton spin-spin relaxation. Carbon numbers refer to the Glc residues of cellulose.

The separation is successful when signals assigned to cellulose and mobile non-cellulosic polysaccharides appeared in subspectra A and B, respectively. The resulting separated subspectra are shown in Fig. 4.

5. The final values of f_a and f_b can then be used to calculate improved values of the proton spin relaxation time constants. For example, if the spin relaxation process is exponential then:

$$f_a = \exp[-t_1(\text{ms}) / T_{1\rho}(\text{H})]$$

Taking natural logarithms of both sides:

$$ln\ f_a = -t_1(\text{ms}) / T_{1\rho}(\text{H})$$

This can be rearranged to:

$$T_{1\rho}(\text{H}) = -t_1(\text{ms}) / ln\ f_a$$

If f_a is 0.69 and the t_1 value for the $T_{1\rho}(\text{H})$ experiment is 4 ms, then the estimated $T_{1\rho}(\text{H})$ value for subspectrum A in the proton rotating-frame experiments is 10.8 ms. The relaxation

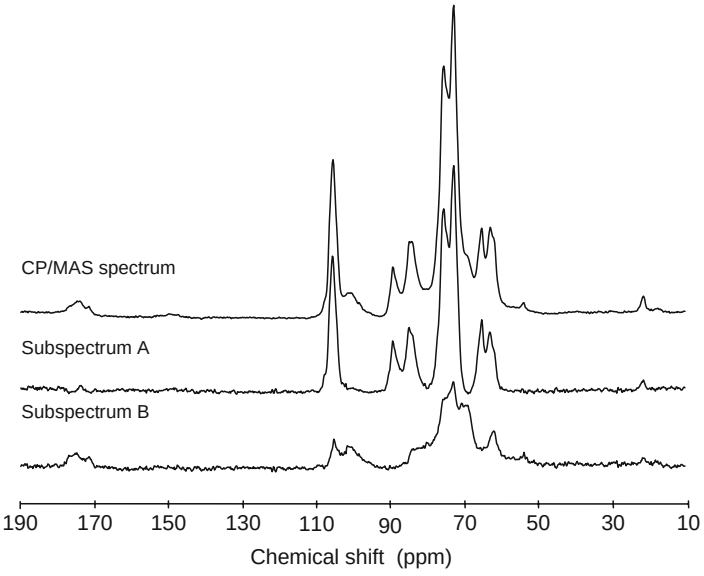

Fig. 4. Normal CP/MAS spectrum and separated PSRE subspectra of a cell-wall preparation of the hypocotyls from mung bean seedlings. Subspectra are obtained by exploiting the differences in proton rotating-frame spin relaxation. Subspectra A and B display signals assigned primarily to cellulose and the non-cellulosic matrix, respectively.

time constant for subspectrum B using f_b can be calculated using the same equations.

6. The editing process is repeated to separate the T_2(H) subspectra. This spin relaxation process suppresses cellulose signals more than the other signals, but does not eliminate them entirely. Linear combinations can again be generated to enhance the amount of suppression. Like the $T_{1\rho}$(H) relaxation, the separation is successful in that signals assigned to cellulose and non-cellulosic polysaccharides appear in A and B, respectively.
7. As for $T_{1\rho}$(H) relaxation, the final values of f_a and f_b can be used to calculate improved values of the spin-spin relaxation time constants for the two subspectra. However, the relaxation curves for rigid solids, such as crystalline cellulose and more mobile polysaccharides, such as pectic homogalacturonans, are described by different functions (6):

$$f_a = \exp[-\{t_2(\text{ms}) / T_2(\text{H})\}^2 / 2],$$

$$f_b = \exp[-t_2(\text{ms}) / T_2(\text{H})]$$

Table 2 shows the adjusted suppression factors, linear combinations and relaxation time constants from the PSRE experiments obtained for a preparation of mung bean cell walls.

3.5.1. Spin Echo NMR with PSRE (SE-PSRE)

As discussed above, unlike $T_{1\rho}(H)$ and $T_2(H)$, $T_2(C)$ is sensitive to segmental motion of the polysaccharide at the site of the ^{13}C nucleus and is insensitive to the motion of more distant polysaccharides. Therefore, in SE-PSRE NMR experiments, the $T_2(C)$ values for a polysaccharide will indicate the mobility of that particular polysaccharide, whereas the $T_{1\rho}(H)$ and $T_2(H)$ relaxation values will reflect the averaged molecular motion of the surrounding polysaccharides. For example, if a relatively rigid XG chain extends through a domain containing relatively flexible pectic polysaccharides, values of $T_{1\rho}(H)$ and $T_2(H)$ measured from XG signals will reflect molecular motion in the pectic polysaccharide environment. In this example, the values of $T_2(C)$ measured from xyloglucan signals will reflect the rigidity of the XG chain and not the mobility of the pectic polysaccharide environment (11).

1. $T_2(C)$ relaxation is characterised by a spin-echo sequence in which a delay of duration t_2 is inserted between the CP contact time and commencement of data acquisition (6). A 180° refocusing pulse is applied halfway through t_2.
2. Multiple values of t_2 can be chosen so that $0.5t_2$ is always a multiple of the rotor rotation period, and protons are decoupled with an attenuated power output corresponding to a precession frequency of 43 kHz throughout t_2.
3. Proton spin relaxation edited (PSRE) NMR subspectra are generated for each of the $T_2(C)$ spectra using the same S and S′ values used for editing the proton spin-relaxation spectra.
4. Relaxation time constants for $T_2(C)$ can be calculated as described in Subheading 3.5. As indicated above, these relaxation values will reflect the mobility of that particular polysaccharide in the cell-wall preparation.

3.5.2. Single Pulse Excitation/Magic Angle Spinning (SPE/MAS) NMR

As discussed in the Introduction, SPE/MAS is a useful technique for investigating the mobility of the very mobile polysaccharides in the cell wall, such as the pectic polysaccharide side chains on RG-I.

1. Single pulse excitation/magic angle spinning (SPE/MAS) spectra are obtained with a pulse sequence in which each 90° ^{13}C excitation pulse is followed by 51 ms of data acquisition time and a 1 s recovery delay (25). The correct duration of the 90° ^{13}C pulse can be measured by using trial values and selecting the value that provides the best signal strength. A typical value is 6 μs, as used to illustrate this chapter. The 1.0 s delay is used to maximise the response from mobile components and minimise the response from rigid components of the cell walls (25). The proton decoupler

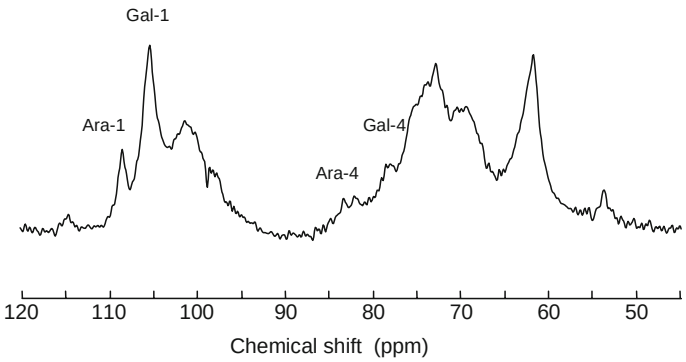

Fig. 5. SPE/MAS NMR spectrum of cell-wall preparation from hypocotyls of mung bean seedlings. Assignments refer to the carbon numbers of Ara or Gal in arabinans or galactans (see Table 1).

transmitter power is increased during data acquisition and should correspond to a precession frequency >40 kHz and preferably between 53 and 59 kHz.

2. As with all NMR experiments, the signal to noise ratio will improve with increased number of experimental transients. However, care must be taken to avoid sample degradation during long experiments (see Note 7). The SPE/MAS spectrum for a cell-wall preparation of mung bean hypocotyls, shown in Fig. 5, was acquired by the averaging of 23,931 experiment transients. This equated to approximately 6.7 h of data accumulation time.

3.5.3. Spin Echo with SPE/MAS NMR (SE-SPE/MAS)

The SE-SPE/MAS pulse sequence is similar to the SE-PSRE sequence except it is run with SPE/MAS and not PSRE, and spectra are not separated into mobility domains. The SE-SPE/MAS experiments will provide mobility information about a particular monosaccharide component within the polysaccharide, provided the signal is relatively free from other overlapping signals.

Each 90° ^{13}C excitation pulse is followed by a t_2 delay then 51 ms of data acquisition time and a 1 s recovery delay. A 180° refocusing pulse is applied halfway through t_2, and values of t_2 are chosen so that $0.5t_2$ is always a multiple of the rotor rotation period, and protons are decoupled with an attenuated power output corresponding to a precession frequency >40 kHz throughout t_2. The durations of the 90° and 180° ^{13}C pulses are typically 6 and 12 μs respectively.

4. Notes

1. The reducing agent DTT is added to the isolation buffer to prevent the oxidation of phenols to quinones (26, 31). Quinones can polymerise to form red/brown products and may also form covalent bonds with proteins resulting in insoluble precipitates (26). Alternatively, buffer containing 10 mM 2-mercaptoethanol may replace DTT.
2. The negative chemical shift (−1.96 ppm) of polydimethylsilane is outside the range normally seen for cell-wall polysaccharides, and therefore does not interfere with signals from cell-wall material. An alternative standard could be polydimethylsiloxane, showing a ^{13}C signal at 1.50 ppm, which is closer to the range associated with cell wall material (32). Polydimethylsiloxane is readily available from Sigma-Aldrich, whereas no supplier of small amounts of polydimethylsilane could currently be found by the authors.
3. The polytrichlorofluoroethylene grease from Halocarbon is thickened with silica and provides a water tight seal for the Vespel end caps. Neither the grease nor the thickener contributes signal strength to the cross-polarisation ^{13}C NMR spectra.
4. Moisture is essential for distinguishing polysaccharides in different molecular environments in a cell-wall preparation, for example, cellulose molecules at the surface of the crystallite (7). However, over-drying or drying and re-hydrating of the preparation can result in irreversible changes in the molecular order of the polysaccharides (33, 34). Excessively high moisture contents dilute down the amount of carbon that can be packed into the rotor and therefore diminish the NMR signal. The ideal water content is between 30 and 50% w/w in many cases.
5. Exposure of cell-wall preparations to ethanol may, in principle physically alter polysaccharides (33), as well as denature and precipitate proteins. Although we have not seen evidence in the NMR spectra of such changes, we recommend caution.
6. Preliminary $T_1(H)$ experiments indicated that a 1.0 s delay was adequate for the recovery of proton magnetisation in relatively mobile segments of polysaccharides, as was also shown in experiments on other cell walls (6, 7).
7. It is desirable to check for sample degradation using SPE experiments. This can be achieved by breaking the experiment into several periods of data accumulation and comparing the spectra to test for changes. If the spectra are all similar, they may be added together to improve the signal-to-noise ratio.

References

1. Harris, P. J. (2005) Diversity in plant cell walls. In: *Plant diversity and evolution: genotypic and phenotypic variation in higher plants.* Henry, R. J., ed. CAB International: Wallingford, pp 201–227.
2. Harris, P. J., and Stone, B. A. (2008) Chemistry and molecular organization of plant cell walls. In: *Biomass recalcitrance: deconstructing the plant cell wall for bioenergy.* Himmel, M. E., ed. Blackwell Publishing, Oxford. pp 61–93.
3. Mohnen, D. (2008) Pectin structure and biosynthesis. *Curr Opinion Plant Biol* **11**, 266–277.
4. Hsieh, Y. S. Y., and Harris, P. J. (2009) Xyloglucans of monocotyledons have diverse structures. *Mol Plant* **2**, 943–965.
5. Trethewey, J. A. K., Campbell, L. M., and Harris, P. J. (2005) (1→3),(1→4)-β-D-glucans in the cell walls of the Poales (*sensu lato*): an immunogold labelling study using a monoclonal antibody. *Am J Bot* **92**, 1660–1674.
6. Newman, R. H., Davies, L. M., and Harris, P. J. (1996) Solid-state ^{13}C nuclear magnetic resonance characterisation of cellulose in the cell walls of *Arabidopsis thaliana* leaves. *Plant Physiol* **111**, 475–485.
7. Newman, R. H., Ha, M.-A., and Melton, L. D. (1994) Solid-state ^{13}C NMR investigation of molecular ordering in the cellulose of apple cell walls. *J Agric Food Chem* **42**, 1402–1406.
8. Newman, R. H. (1999) Estimation of the lateral dimensions of cellulose crystallites using ^{13}C NMR signal strengths. *Solid State Nucl Magnet Reson* **15**, 21–29.
9. Newman, R. H., and Davidson, T. C. (2004) Molecular conformations at the cellulose-water interface. *Cellulose* **11**, 23–32.
10. Bootten, T. J., Harris, P. J., Melton, L. D., and Newman, R. H. (2008) WAXS and ^{13}C-NMR study of *Gluconoacetobacter xylinus* cellulose in composites with tamarind xyloglucan. *Carbohyr Res* **343**, 221–229.
11. Bootten, T. J., Harris, P. J., Melton, L. D., and Newman, R. H. (2004) Solid-state ^{13}C-NMR spectroscopy shows that the xyloglucans in the primary cell walls of mung bean (*Vigna radiata* L.) occur in different domains: a new model for xyloglucan-cellulose interactions in the cell wall. *J Exp Bot* **55**, 571–583.
12. Levy, S., Maclachlan, G., and Staehelin, L. A. (1997) Xyloglucan sidechains modulate binding to cellulose during *in vitro* binding assays as predicted by conformational dynamics simulations. *Plant J* **11**, 373–386.
13. Horii, F., Hirai, A., and Kitamaru, R. (1984) Cross-polarization/magic angle spinning ^{13}C-NMR study. Molecular chain conformations of native and regenerated cellulose. In: *Polymers for fibers and elastomers.* Arthur, J.C. Jr, Diefendorf, R.J., Yen, T.F., Needles, H.L., Schaefgen, J.R., Jaffe, M., and Logothetis, A.L. eds. American Chemical Society, **260**, pp 27–42.
14. Jarvis, M. C. (1994) Relationship of chemical shift to glycosidic conformation in the solid state ^{13}C NMR spectra of (1→4)-linked glucose polymers and oligomers: anomeric and related effects. *Carbohydr Res* **259**, 311–318.
15. Jarvis, M. C., and Apperley, D. C. (1990) Direct observation of cell wall structure in living plant tissues by solid-state ^{13}C NMR spectroscopy. *Plant Physiol* **92**, 61–65.
16. Tang, H., Belton, P. S., Ng, A., and Ryden, P. (1999) ^{13}C MAS NMR studies of the effects of hydration on the cell walls of potatoes and Chinese water chestnuts. *J Agric Food Chem* **47**, 510–517.
17. Newman, R. H. (1999) Editing the information in solid-state carbon-13 NMR spectra of food. In: *Advances in magnetic resonance in food science.* Belton, P. S, Hills, B. P, and Webb, G. A., eds. The Royal Society of Chemistry: Cambridge, pp 144–157.
18. Newman, R. H. (1992) Solid-state carbon-13 NMR spectroscopy of multiphase biomaterials. In: *Viscoelasticity of biomaterials.* Glasser, W. G., and Hatakeyama, H., eds. American Chemical Society: Washington, pp 311–319.
19. Tekely, P., and Vignon, M. R. (1987) Proton T_1 and T_2 relaxation times of wood components using ^{13}C CP/MAS NMR. *J Polym Sci Part C Polym Lett* **25**, 257–261.
20. Hediger, S., Emsley, L., and Fischer, M. (1999) Solid-state NMR characterization of hydration on polymer mobility in onion cell-wall material. *Carbohydr Res* **322**, 102–112.
21. Zumbulyadis, N. (1983) Selective carbon excitation and the detection of spatial heterogeneity in cross-polarization magic-angle-spinning NMR. *J Magn Reson* **53**, 486–494.
22. Tang, H., and Hills, B. P. (2003) Use of ^{13}C MAS NMR to study domain structure and dynamics of polysaccharides in the native starch granules. *Biomacromolecules* **4**, 1269–1276.
23. VanderHart, D. L. (1987) Natural-abundance ^{13}C-^{13}C spin exchange in rigid crystalline solids. *J Magn Reson* **72**, 13–47.
24. Foster, T. J, Ablett, S., McCann, M. C., and Gidley, M. J. (1996) Mobility-resolved

^{13}C-NMR spectroscopy of primary plant cell walls. *Biopolymers* **39**, 51–66.

25. Smith, B. G., Harris, P. J., Melton, L. D, and Newman, R. H. (1998) The range of mobility of the non-cellulosic polysaccharides is similar in primary cell walls with different polysaccharide compositions. *Physiol Plant* **103**, 233–246.
26. Harris, P. J. (1983) Cell walls. In: *Isolation of membranes and organelles from plant cell walls.* Hall, J. L. and Moore, A. L., eds. Academic: London, pp 25–53.
27. Melton, L. D., and Smith, B. G. (2005). Isolation of plant cell walls and fractionation of cell wall polysaccharides**.** In: *Handbook of food analytical chemistry: water, proteins, enzymes, lipids and carbohydrates.* Wrolstad, R. E., ed. Wiley: Hoboken, pp 697–719.
28. Newman, R. H., and Hemmingson, J. A. (1990) Determination of the degree of cellulose crystalinity in wood by carbon-13 nuclear magnetic resonance spectroscopy. *Holzforschung* **44**, 351–355.
29. Sinitsya, A., Čopíková, J., and Pavlíková, H. (1998) ^{13}C CP/MAS NMR spectroscopy in the analysis of pectins. *J Carbohydr Chem* **17**, 279–292.
30. Jarvis, M. C., and Apperley, D. C. (1995) Chain conformation in concentrated pectic gels: evidence from ^{13}C NMR. *Carbohydr Res* **275**, 131–145.
31. Bootten, T. J., Harris, P. J., Melton, L. D., and Newman, R. H. (2009) A Solid-state ^{13}C-NMR study of a composite of tobacco xyloglucan and *Gluconacetobacter xylinus* cellulose: molecular interactions between the component polysaccharides. *Biomacromolecules* **10**, 2961–2967.
32. Jelinski, L. W., and Melchior, M. T. (1996) High-resolution NMR of solids. In: *NMR spectroscopy techniques. Practical Spectroscopy Series,* 2. Bruch, M. D., ed. Marcel Dekker: New York, pp 417–486.
33. Thimm, J. C., Burritt D. J., Ducker, W. A., and Melton, L. D. (2000). Celery (*Apium graveolens* L.) parenchyma cell walls examined by atomic force microscopy. *Planta* **212**, 25–32.
34. Newman, R. H. (2004) Carbon-13 NMR evidence for cocrystallization of cellulose as a mechanism for hornification of bleached kraft pulp. *Cellulose* **11**, 45–52.
35. Newman, R. H. (1997) Crystalline forms of cellulose in the silver tree fern. *Cyathea Dealbata Cellulose* **4**, 269–278.
36. Newman, R. H., and Redgwell, R. J. (2002) Cell wall changes in ripening kiwifruit: ^{13}C solid state NMR characterisation of relatively rigid cell wall polymers. *Carbohydr Polym* **49**, 121–129.
37. Atalla, R. H., and Vanderhart, D. L. (1984) Native cellulose: a composite of two distinct crystalline forms. *Science* **223**, 283–285.
38. Newman, R. H., and Hemmingson, J. A. (1995) Carbon-13 NMR distinction between categories of molecular order and disorder in cellulose. *Cellulose* **2**, 95–110.
39. Newman, R. H. (1998) Evidence for assignment of ^{13}C NMR signals to cellulose crystallite surfaces in wood, pulp and isolated celluloses. *Holzforschung* **52**, 157–159.
40. Hirai, A., Horii, F., and Kitamaru, R. (1990) Carbon-13 spin-lattice relaxation behaviour of the crystalline and non-crystalline components of native and regenerated celluloses. *Cellulose Chem Technol* **24**, 703–711.
41. Braccini, I., Hervé du Penhoat, C., Michon, V., Goldberg. R., Clochard, M., Jarvis, M. C., Huang, Z.-H., and Gage, D.A. (1995) Structural analysis of cyclamen seed xyloglucan oligosaccharides using cellulase digestion and spectroscopic methods. *Carbohydr Res* **276**, 167–181.
42. Gidley, M. J., Lillford, P. J., Rowlands, D. W., Lang, P., Dentini, M., Crescenzi, V., Edwards, M., Fanutti, C., and Reid, J. S. G. (1991) Structure and solution properties of tamarind-seed polysaccharide. *Carbohydr Res* **214**, 299–314.
43. Davies, L. M., Harris, P. J., and Newman, R. H. (2002) Molecular ordering of cellulose after extraction of polysaccharides from primary cell walls of *Arabidopsis thaliana*: a solid-state CP/MAS ^{13}C NMR study. *Carbohydr Res* **337**, 587–593.
44. Whitney, S. E. C., Brigham, J. E., Darke, A. H., Reid, J. S. G., and Gidley, M. J. (1995) *In vitro* assembly of cellulose/xyloglucan networks: ultrastructural and molecular aspects. *Plant J* **8**, 491–504.
45. Joseleau, J. P., Cartier, N., Chambat, G., Faik, A., and Ruel, K. (1992) Structural features and biological activity of xyloglucans from suspension-cultured plant cells. *Biochemie* **74**, 81–88.
46. York, W. S., Harvey, L. K., Guillen, R., Albersheim, P., and Darvill, A. G. (1993) Structural analysis of tamarind seed xyloglucan oligosacharides using β-galactosidase digestion and spectroscopic methods. *Carbohydr Res* **248**, 285–301.
47. Ryden, P., Colquhoun, I. J., and Selvendran, R. R. (1989) Investigation of structural features of the pectic polysaccharides of onion by ^{13}C-N.M.R. spectroscopy. *Carbohydr Res* **185**, 233–237.
48. Saulnier, L., Brillouet, J. -M., and Joseleau, J. -P. (1988) Structural studies of pectic substances from the pulp of grape berries. *Carbohydr Res* **182**, 63–78.

Chapter 14

Formation of Cellulose-Based Composites with Hemicelluloses and Pectins Using *Gluconacetobacter* Fermentation

Deirdre Mikkelsen and Michael J. Gidley

Abstract

Gluconacetobacter xylinus synthesises cellulose in an analogous fashion to plants. Through fermentation of *Ga. xylinus* in media containing cell wall polysaccharides from the hemicellulose and/or pectin families, composites with cellulose can be produced. These serve as general models for the assembly, structure, and properties of plant cell walls. By studying structure/property relationships of cellulose composites, the effects of defined hemicellulose and/or pectin polysaccharide structures can be investigated. The macroscopic nature of the composites also allows composite mechanical properties to be characterised.

The method for producing cellulose-based composites involves reviving and then culturing *Ga. xylinus* in the presence of desired hemicelluloses and/or pectins. Different conditions are required for construction of hemicellulose- and pectin-containing composites. Fermentation results in a floating mat or pellicle of cellulose-based composite that can be recovered, washed, and then studied under hydrated conditions without any need for intermediate drying.

Key words: Plant cell wall, Cellulose, Composites, *Gluconacetobacter xylinus*, Pectin, Hemicellulose, Arabinoxylan, β-Glucan, Xyloglucan

1. Introduction

The cell walls of plants are typically complex in terms of their measured average composition, with variation being exhibited not only between different plant types, but also between local tissue types and even within a single cell wall. While some information on the relationships between composition and properties of cell walls can be deduced through studies of e.g. plant mutants lacking defined compositional features, the isolation of plant cell wall material for the study of structure/property relationships has

Zoë A. Popper (ed.), *The Plant Cell Wall: Methods and Protocols*, Methods in Molecular Biology, vol. 715,
DOI 10.1007/978-1-61779-008-9_14,

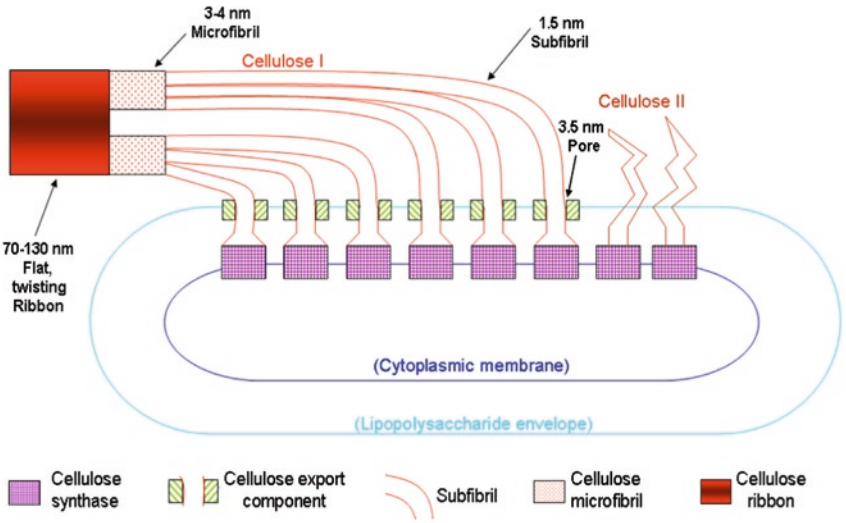

Fig. 1. Schematic illustration of cellulose biosynthesis by *Gluconacetobacter xylinus* (adapted from Brown (1)).

major limitations due to microheterogeneity within the plant and the need for harsh extraction conditions.

Gluconacetobacter xylinus (previously known as *Acetobacter xylinus* or *A. xylinum*) has been used as a model for cellulose biosynthesis because it has the same general features of cellulose deposition as plants (Fig. 1). A transmembrane assembly of catalytic (cellulose synthase) and structural proteins produces strands of (1→4)-β-D-glucan that associate, first into small sub-fibrils, then into microfibrils which subsequently aggregate into a characteristic flat, twisting ribbon (Fig. 1). Although plant cellulose is usually more cylindrical in its final aggregated state, all other stages of cellulose synthesis are shared with *Ga. xylinus*. Cellulose secreted by bacteria into an aqueous fermentation medium is used as a model for plant cellulose secreted extracellularly into a nascent cell wall. In plants, cellulose is deposited into an environment containing a complex mixture of other cell wall polymers. In the bacterial model system, the extracellular environment is controlled and can be used to investigate the potential of each type of cell wall polymer to form composite structures with cellulose and to investigate the molecular, microscopic, and macroscopic properties of the resulting materials. Validation of the system as a model comes from (a) microscopic observation of similar architectures in cellulose/xyloglucan composites (2) as in de-pectinated cell walls of e.g. onion (3), (b) responsiveness of hemicellulose/cellulose composites to application of expansin proteins (4) and xyloglucan endo-transglycosylase (5) similar to that found or

expected in plant tissues, and (c) conversion of highly crystalline *Ga. xylinus* cellulose into a less crystalline form (characteristic of plant cell walls) in the presence of hemicelluloses (2, 6). While there are limitations to this model system, it is experimentally straightforward and provides insights into the effects of polymer components of defined chemistry that are not possible from cell walls isolated from plants. Furthermore, as cellulosic materials can be produced in multi-centimetre pieces, mechanical measurements can be made that are highly informative in defining the principles of cell wall materials properties (7–9).

In the absence of polymers in the fermentation medium, a cellulose "mat" or pellicle is produced that is highly hydrated but mechanically tough. In outline, the formation of cellulose composites with hemicellulose or pectin is accomplished by fermenting *Ga. xylinus* in liquid fermentation containing the hemicellulose and/or pectin of interest. The cellulose produced by bacteria (Fig. 1) thus comes into contact with the added polymer(s) as soon as it is secreted from the bacteria. For hemicelluloses that can associate (bind) molecularly to cellulose, the fact that the crystallinity of cellulose is affected greatly (2, 6) is interpreted to mean that added polymers can access cellulose microfibrils prior to their aggregation into the final ribbon assembly (Fig. 1). The negative charge on pectins means that there is no direct binding between the two backbones (although arabinan side chains may bind (10)), and composite formation requires the presence of a pre-formed pectin network (11). Thus, the fermentation medium contains a weak gel which can be varied by choice of pectin type (particularly degree of methyl esterification) and calcium level.

Following fermentation, composites are recovered from the medium, and washed to remove bacteria and any polymers that are held non-specifically. The isolated solid composite material can then be analysed by chemical, spectroscopic, microscopic, or mechanical methods.

2. Materials

1. Laminar flow cabinet and appropriate facilities for observing good microbiological practice (e.g. autoclave).
2. Bacterial strain: *Ga. xylinus* (formerly *A. xylinus* and *A. xylinum*) strain ATCC 53524 frozen (−80°C) stock (see Note 1).

   Growth media:
3. Hestrin and Schramm (HS) medium (12) containing (per litre) 5 g peptone, 5 g yeast extract, 3.38 g $Na_2HPO_4 \cdot H_2O$, 1.15 g citric acid, and 20 g glucose (see Note 2). HS agar medium (containing 15 g/L agar) is used for maintenance

and long-term storage of the bacterial strain. HS liquid medium is used for composite preparation. Preferably, the medium is made fresh as required. Alternatively, sterile medium stored at 4°C is stable for up to 1 week.

4. Modified HS broth medium containing hemicelluloses: The medium is prepared as a concentrated (2×) solution by adding 5 g peptone, 5 g yeast extract, 3.38 g $Na_2HPO_4 \cdot H_2O$, and 1.15 g citric acid to 400 mL deionised water. The pH is adjusted to 5.0 with 10 M HCl, and the volume of the solution is adjusted to 460 mL with sterile deionised water. The medium is sterilised by autoclaving at 121°C for 15 min. After cooling the sterile medium to 55°C, 40 mL of 0.22 μm filtered sterilised glucose solution (50% w/v), and 500 mL of the 1% (w/v) polysaccharide solution are added aseptically.
5. Modified HS broth medium containing pectins: The medium is prepared as a concentrated (2×) solution by adding 5 g peptone, 5 g yeast extract, 3.38 g $Na_2HPO_4 \cdot H_2O$, and 1.15 g citric acid to 400 mL deionised water. The pH is adjusted to 5.0 with 10 M HCl, and the volume of the solution is adjusted to 460 mL with sterile deionised water. The medium is sterilised by autoclaving at 121°C for 15 min. After cooling the sterile medium to 55°C, 40 mL of 0.22 μm filtered sterilised glucose solution (50% w/v), and 500 mL of the 1% (w/v) pectin solution is added aseptically.
6. Long-term storage of *Ga. xylinus*: Microbank™ preservation cryovials (Pro-Lab Diagnostics, ON, Canada).
7. Hemicellulose solutions (see Note 3): Prepare a 1% (w/v) solution by accurately weighing out 5 g of powdered substrate with a sterilised spatula into a sterile 1 L dry Pyrex beaker in a laminar flow cabinet. Add a sterile magnetic stirrer bar, followed by 400 mL of hot (90°C) sterile deionised water (see Note 4). Immediately place the beaker containing the mixture on a magnetic hotplate-stirrer and heat at a setting of 100°C with vigorous stirring. Loosely cover the beaker with aluminium foil, stirring and boiling the contents until the hemicellulose dissolves completely (see Note 5). Adjust the volume of the solution to 500 mL with sterile deionised water. Make solution fresh as required (see Note 6).
8. Pectin solutions (see Note 7): Prepare a 1% (w/v) solution by accurately weighing out in a laminar flow cabinet 7 g of powdered pectin with a sterilised spatula into a sterile 1 L Schott bottle containing 489.5 mL of sterile deionised water. Add a sterile magnetic stirrer bar, place the sealed bottle containing the mixture on a magnetic stirrer and stir vigorously overnight (see Note 8). Once the pectin is completely in solution, the volume of the solution can be adjusted to 500 mL with sterile deionised water. Make solution fresh as required.

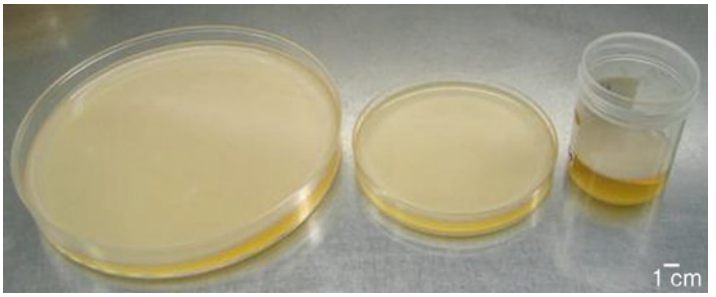

Fig. 2. Examples of sterile containers used for composite preparation. These include (from *left* to *right*) sterile 150 × 20 mm and 92 × 16 mm Petri dishes, as well as sterile screw lid containers with 70 mL capacity and 40 mm diameter.

9. 0.125 M calcium chloride ($CaCl_2$) solution, sterilised by autoclaving at 121°C for 15 min.
10. 12.5 mM $CaCl_2$ solution, sterilised by autoclaving at 121°C for 15 min.
11. Sterile culture containers (see Note 9; Fig. 2).
12. 0.02% (w/v) sodium azide solution made with deionised water (see Note 10).
13. 0.02% (w/v) sodium azide solution made with sterile 12.5 mM $CaCl_2$ solution (see Note 10).
14. Deionised water, sterilised by autoclaving at 121°C for 15 min.
15. Temperature-controlled growth facilities.
16. Desiccator.

3. Methods

3.1. Revival and Maintenance of Ga. xylinus

1. Frozen stocks: Under aseptic conditions, open the cryovial and using a sterile needle, remove one bead to inoculate each HS agar plate (inoculate two plates). Use the bead to directly streak onto the solid medium to get isolated pure colonies (13). Incubate at 30°C for 3–4 days.
2. Maintenance of culture: Two plates of the culture are inoculated as one plate is reserved for starting a new working culture when required (see Note 11), and the other plate is used for routine transfers as required. The plates are wrapped with Parafilm® and stored at 4°C. The cultures remain viable for 1 month.

3.2. Long-Term Storage of Ga. xylinus (see Note 12)

1. Under aseptic conditions open the screw cap of the Microbank™ cryovial.
2. Inoculate the cryopreservative fluid with a loopful of young colony growth (72 h) picked from a pure culture.

3. Close vial tightly and invert four to five times to emulsify organism. A vortex mixer must not be used.
4. The excess cryopreservative must be well aspirated leaving the inoculated beads free of liquid as much as possible.
5. Inoculated cryovials are closed finger tight and stored at –80°C (shelf-life 3–4 years).

3.3. Composite Preparation with Hemicelluloses

Bacterial cellulose–hemicellulose (0.5% w/v) composites are constructed as follows:

1. For primary inoculum preparation: Inoculate 20 mL modified HS broth medium containing hemicelluloses with a few colonies of bacteria from the HS agar plate used to maintain the strain. Incubate under static conditions at 30°C for 72 h (see Note 13).
2. For scale-up preparation: Inoculate 18 mL modified HS broth medium with 2 mL primary inoculum and incubate without agitation at 30°C for 48 h (arabinoxylan or β-glucan composite) or 72 h (for xyloglucan composite).
3. Harvesting of hemicellulose composites: After incubation, the composite pellicle is removed with forceps and washed at room temperature by gentle agitation (50 rpm), in a sterile 3 L glass beaker containing excess ice-cold sterile deionised water (Fig. 3) (see Note 14).
4. Short-term preservation: Composites are stored in the hydrated state in 0.02% (w/v) sodium azide solution at 4°C (see Note 15).

3.4. Composite Preparation with Pectins

The level of pectin incorporation within the cellulose network is dependent on the interaction between pectin and Ca^{2+} ions present in the medium. A preformed gel of the desired strength,

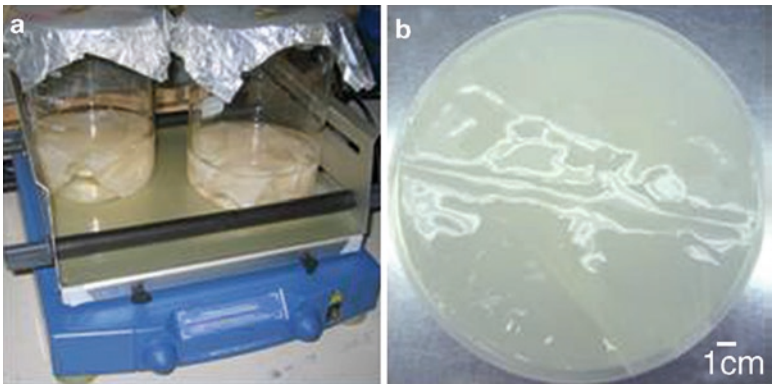

Fig. 3. Purification of hemicellulose composites by washing with gentle agitation (50 rpm) at room temperature, with excess ice-cold sterile deionised water (**a**). Having removed the excess medium and bacterial cells, the purified pellicle is *white* (**b**).

which will allow for sufficient gelling as well as cellulose microfibril penetration, must be achieved in order to form a composite. The following detailed method describes the preparation of bacterial cellulose–pectin composites using pectin of degree of methyl esterification (DM) of 30%. Previous research (11) has determined that the highest pectin incorporation in cellulose composites occurs when using pectin of ~DM 30. When attempting to construct bacterial cellulose–pectin (0.5%) composites with other DM values, different $CaCl_2$ concentrations may be added to the modified HS medium as appropriate.

1. For primary inoculum preparation: Inoculate 18 mL modified HS broth medium containing pectins with two to three colonies of bacteria from the HS agar plate used to maintain the strain. Place the inoculated container on a platform shaker and under vigorous shaking (~250 rpm), add 2 mL of 0.125 M $CaCl_2$ solution. Shake the inoculated container for a further 5 min (see Note 16; Fig. 4). Incubate under static conditions at 30°C for 72 h.
2. For scale-up preparation: Inoculate 16 mL modified HS broth medium with 2 mL primary inoculum. As above, place the inoculated container on a platform shaker and under vigorous shaking (~250 rpm), add 2 mL of 0.125 M $CaCl_2$ solution. Shake the inoculated container for a further 5 min and incubate under static conditions at 30°C for 72 h.
3. Harvesting of pectin composites: After incubation, remove the composite pellicle by carefully pouring out the pellicle

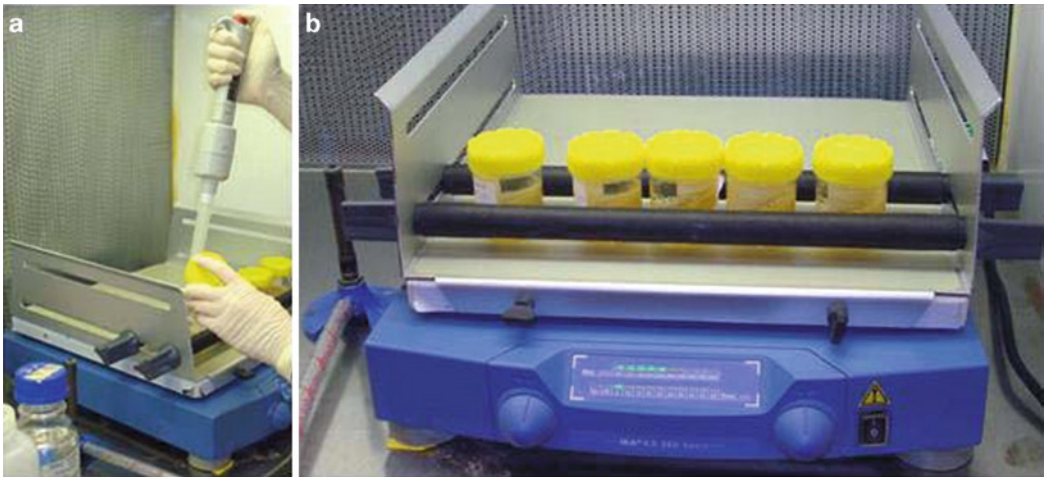

Fig. 4. Preparation of bacterial cellulose–pectin composites. The inoculated container is placed on a platform shaker and $CaCl_2$ solution (to give a final concentration of typically 12.5 mM) is added under vigorous shaking (**a**), followed by a further 5 min of shaking (**b**), to allow the HS-pectin medium to gel in a uniform manner. A uniform pre-formed gel results in a relatively homogeneous composite.

into a gloved hand, while letting the excess medium drain through the fingers (like separating the yolk from the white of an egg) (see Note 17). Place the pectin composite in a sterile glass beaker containing excess ice-cold sterile $CaCl_2$ solution of the same concentration as the incubation medium (e.g. 12.5 mM), and wash at room temperature by gentle agitation (50 rpm) (see Note 18).

4. Short-term preservation: Pectin composites are stored in the hydrated state in 0.02% (w/v) sodium azide solution containing the appropriate concentration of $CaCl_2$, at 4°C (see Note 19).

4. Notes

1. *Ga. xylinus* ATCC 53524 is the strain of choice in our laboratory, as it produces cellulose that is chemically pure and highly crystalline (14). In particular, this strain does not produce the water-soluble polysaccharide acetan, a heteropolymer containing glucose, mannose, glucuronic acid and rhamnose in a molar ratio of 4:1:1:1 that is characteristic of other *Gluconacetobacter* strains (15, 16).
2. The medium detailed in this chapter is typically used in our laboratory. Alternatively, glucose can be substituted with other carbon sources such as mannitol or glycerol (14), as well as deuterated carbon sources including D-glucose and D-glycerol (unpublished work).
3. The hemicelluloses routinely used in our laboratory include arabinoxylan (wheat, medium viscosity ~25 cSt), β-glucan (barley, medium viscosity ~28 cSt), and xyloglucan (tamarind seed; high viscosity ~6.5 dL/g) (Megazyme International Ireland Ltd., County Wicklow, Ireland). They are stored at room temperature in a desiccator.
4. The hemicellulose solution cannot be sterilised by autoclaving or micro-filtration as this may depolymerise or remove some of the polymer respectively. Thus, in order to prevent contamination, it is imperative to use sterilised equipment and diluent when making up the solution. Although it is common practice to add the polymer slowly to solvent, when working in a laminar flow cabinet, the air flow makes it difficult to handle fine powders.
5. Wetting the plant cell wall polysaccharide with 40 mL of 95% (v/v) ethanol is recommended by the manufacturer. However, this is not appropriate as *Ga. xylinus* is able to utilise ethanol as a carbon source (19). Subsequently, this results in a significant (P <0.05) increase in bacterial cell

Table 1
The effect of ethanol on the growth of *Ga. xylinus* ATCC 53524

HS medium	Increase in cell growth (log_{10}CFU mL^{-1})[a]	Final pH[b]	Cellulose yield at 48 h (g)
With EtOH	4.58	3.23	0.0353
Without EtOH	2.85	5.01	0.0356

[a]Values are the difference between cell growth at $t = 0$ h and $t = 48$ h. All values are presented as mean colony counts
[b]Initial pH = 5.0. Results are presented as means of triplicates

numbers, but not in the rate of cellulose production (Table 1). By omitting substrate wetting with alcohol, the approximate solubilisation times for arabinoxylan, β-glucan, and xyloglucan are 30–60 min.

6. Arabinoxylan solutions typically have a slight off-white opalescent appearance, while xyloglucan and β-glucan solutions are sometimes very slightly turbid. This may be due to the presence of trace amounts of protein (Megazyme product datasheet).
7. The pectins routinely used in our laboratory include commercially produced citrus extracted pectins of degree of methyl esterification (DM) 30–35 and 60–65. All pectins are stored at −20°C as the DM is stable for up to a year. However, whether the pectin is stored at room temperature or at −20°C, it is recommended that when preparing the pectin solution, the DM is routinely determined; this involves using titrimetry (17, 18). Briefly, aliquots (1–5 mL) of a 1% pectin solution are titrated to between pH 7 and 8 with 0.02 M NaOH and the titre is recorded. Thereafter, 1 mL 0.5 M HCl solution is added and the solution is titrated again to pH 7–8. Blank values, obtained by substituting pectin with water, are subtracted from the titre of pectin. The DM can be calculated directly from the titres using the following equation:

$$\mathrm{DM} - 100 \times V_s / V_t$$

where V_s is the hydrolysed (or saponification) titre in millilitres, and V_t is the total titre (sum of initial titre plus hydrolysed titre) in millilitres (17, 18).

8. We choose to stir the pectin solution overnight as this ensures complete dissolution. Due to this overnight process, and the fact that the pectin solution cannot be sterilised by autoclaving or means of filtration, contamination is minimised/prevented by using sterilised equipment and diluent when making up the solution. Pectins are heat labile, so no heating is used during the dissolution process.

9. The size of culture container depends on the desired size of the composite pellicle. Sterile yellow lid specimen containers (70 mL capacity; 40 mm diameter), standard size (92 × 16 mm) sterile Petri dishes, and large size (150 × 20 mm) sterile Petri dishes are commonly used in our laboratory. If yellow lid specimen containers are used, care must be taken to ensure that the lid is screwed on only very loosely. As this organism is an obligate aerobe (16), this allows for adequate aeration of the culture medium and subsequently pellicle formation is not negatively impacted.
10. Great care must be taken when preparing 0.02% (w/v) sodium azide solution. Appropriate personal protective equipment (specified in the Material Safety Data Sheet) must be worn when weighing out the powder. Sterilised deionised water may be used for the preparation of the solution to be used for the hemicellulose composites. For pectin composites, sterile $CaCl_2$ solution of the appropriate concentration (e.g. 12.5 mM for DM 30 pectin composites) should be used when preparing the 0.02% (w/v) sodium azide solution. Once sodium azide is added, under no circumstances should these solutions be sterilised by autoclaving.
11. The culture from the revival plate is only sub-cultured once, and cultures over 1 month old are discarded. This approach is adopted to not only avoid spontaneous mutation of the bacterium, but also to consistently use healthy, viable cultures.
12. Microbank™ is a cryopreservation system commercially available from Pro-Lab Diagnostics (Ontario, Canada). Each vial contains a cryopreservative solution and approximately 25 porous beads which serve as carriers to support microorganisms. Using this long-term storage solution, we have successfully stored our stock cultures for over 4 years and still have 100% success with revival as well as no contamination.
13. Primary inoculum volumes depend on the desired scale-up volume. Always prepare sufficient primary inoculum to ensure that exactly 10% (v/v) primary inoculum is used during scale-up.
14. Washing of composite pellicle after harvesting is carried out to remove excess medium, polysaccharides non-specifically trapped within the cellulose mat, and bacterial cells. This process is carried out until the pellicle changes from off-white to white colour. This is typically achieved by carrying out at least six washes (three times 30 min, followed by three times 10 min washes).
15. It is our experience that hemicellulose/cellulose composites are stable for up to approximately 2 months when stored at 4°C. After this period, degradation is observed with the edges of the otherwise opaque pellicle becoming translucent – this

observation is prominent in pellicles that have been stored at 4°C for 6 months.

16. The inoculated container is placed on a platform shaker and $CaCl_2$ solution is added under vigorous shaking, followed by a further 5 min of shaking, as this allows the HS-pectin medium to subsequently gel under quiescent conditions in a uniform manner. Uniformity of the preformed gel is important for the formation of a relatively homogeneous composite.
17. Avoid using forceps when harvesting the bacterial cellulose–pectin composites, as the pellicles can be fragile and tear easily. Moreover, due to their highly extensible or "stretchy" nature, the use of forceps can impact on their shape. This is important to note when handing the samples for tensile stress/strain measurements, and also applies to other "weak" composites such as those produced after limited incubation times (e.g. 24 h).
18. Note that the purification of pectin composites by washing with $CaCl_2$ solution causes the pellicle to shrink slightly (see Fig. 5).
19. In order to ensure good storage conditions for pectin composites, it is critical to use 0.02% (w/v) sodium azide solution containing the appropriate concentration of $CaCl_2$. If sodium azide solution made up with deionised water is used, composites are stable for up to approximately 2 months when stored at 4°C. After this period, pellicle degradation is observed, with the sodium azide solution becoming viscous and the pellicle loosing some of its characteristic "lumpy" texture (due to precipitation of pectin from the composite) – this observation is prominent in pellicles that have been stored at 4°C for 6 months.

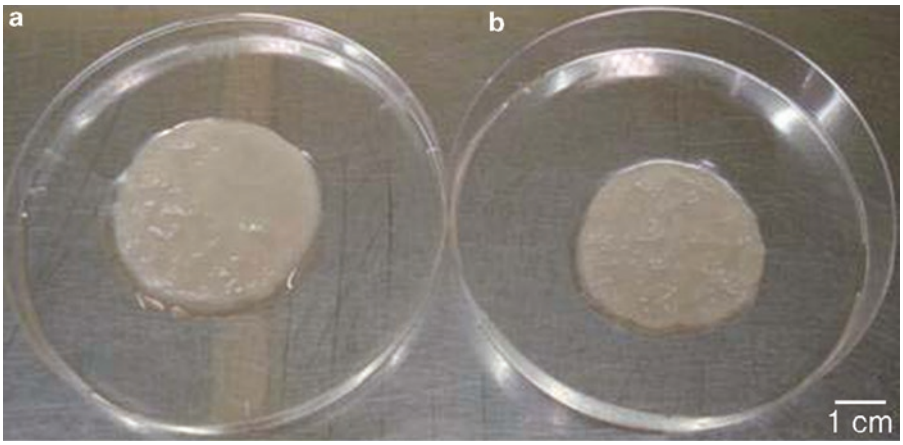

Fig. 5. Bacterial cellulose–pectin composites before (**a**) and after (**b**) washing with $CaCl_2$ solution (typically 12.5 mM), demonstrating typical shrinkage from 4.2 cm in width to 3.8 cm after washing the pellicle.

References

1. Brown, R. M. (1989) Bacterial cellulose. In: *Cellulose: structural and functional aspects*, (Phillips, G. O., Kennedy, J. F., and Williams, P. A., eds.), Ellis Horwood Ltd, New York, pp. 145–151.
2. Whitney, S. E. C., Brigham, J. E., Darke, A., Reid, J. S. G., and Gidley, M. J. (1995) *In vitro* assembly of cellulose/xyloglucan networks: ultrastructural and molecular aspects. *Plant J* **8,** 491–504.
3. McCann, M. C., Wells, B., and Roberts, K. (1990) Direct visualization of cross-links in the primary plant-cell wall. *J Cell Sci* **96,** 323–334.
4. Whitney, S. E. C., Gidley, M. J., and McQueen-Mason, S. J. (2000) Probing expansin action using cellulose/hemicellulose composites. *Plant J* **22,** 327–334.
5. Chanliaud, E., DeSilva, J., Strongitharm, B., Jeronimidis, G., and Gidley, M. J. (2004) Mechanical effects of plant cell wall enzymes on cellulose/xyloglucan composites. *Plant J* **38,** 27–37.
6. Whitney, S. E. C., Brigham, J. E., Darke, A., Reid, J. S. G., and Gidley, M. J. (1998) Structural aspects of the interaction of mannan-based polysaccharides with bacterial cellulose. *Carbohydr Res* **307,** 299–309.
7. Chanliaud, E., Burrows, K. M., Jeronimidis, G., and Gidley, M. J. (2002) Mechanical properties of primary plant cell wall analogues. *Planta* **215,** 989–996.
8. McKenna, B. A., Mikkelsen, D., Wehr, J. B., Gidley, M. J., and Menzies, N. W. (2009) Mechanical and structural properties of native and alkali-treated bacterial cellulose produced by *Gluconacetobacter xylinus* strain ATCC 53524. *Cellulose* **16,** 1047–1055.
9. Whitney, S. E. C., Gothard, M. G. E., Mitchell, J. T., and Gidley, M. J. (1999) Roles of cellulose and xyloglucan in determining the mechanical properties of plant cell walls. *Plant Physiol* **121,** 657–663.
10. Zykwinska, A. W., Ralet, M. C. J., Garnier, C. D., and Thibault, J. F. J. (2005) Evidence for *in vitro* binding of pectin side chains to cellulose. *Plant Physiol* **139,** 397–407.
11. Chanliaud, E., and Gidley, M. J. (1999) *In vitro* synthesis and properties of pectin/*Acetobacter xylinus* cellulose composites. *Plant J* **20,** 25–35.
12. Hestrin, S., and Schramm, M. (1954) Synthesis of cellulose by *Acetobacter xylinum*. 2. Preparation of freeze-dried cells capable of polymerizing glucose to cellulose. *Biochem J* **58,** 345–352.
13. Willey, J. M., Sherwood, L. M., and Woolverton, C. J. (2008) *Prescott, Harley, and Klein's microbiology*, McGraw-Hill, New York, p. 115.
14. Mikkelsen, D., Flanagan, B. M., Dykes, G. A., and Gidley, M. J. (2009) Influence of different carbon sources on bacterial cellulose production by *Gluconacetobacter xylinus* strain ATCC 53524. *J Appl Microbiol* **107,** 576–583.
15. Couso, R. O., Ielpi, L., and Dankert, M. A. (1987) A xanthan-gum-like polysaccharide from *Acetobacter xylinum*. *J Gen Microbiol* **133,** 2123–2135.
16. Kersters, K., Lisdiyanti, P., Komagata, K., and Swings, J. (2006) The family Acetobaceraceae: the genera *Acetobacter, Acidomonas*, *Asaia*, *Gluconacetobacter*, *Gluconobacter* and *Kozakia*. In: *The prokaryotes: an evolving electronic resource for the microbiological community*, (Dwokin, M., ed.), Springer, New York, pp. 163–200.
17. Marga, F., Morvan, C., and Morvan, H. (1995) Pectins in normal and vitreous apple microplants cultured in liquid-medium. *Plant Physiol Biochem* **33,** 81–86.
18. Wehr, J. B., Menzies, N. W., and Blamey, F. P. C. (2004) Alkali hydroxide-induced gelation of pectin. *Food Hydrocolloid* **18,** 375–378.
19. Ross, P., Mayer, R., and Benziman, M. (1991) Cellulose biosynthesis and function in bacteria. *Microbiol Rev* **55,** 35–58.

Chapter 15

Structural Proteins of the Primary Cell Wall: Extraction, Purification, and Analysis

Derek T.A. Lamport, Li Tan, and Marcia J. Kieliszewski

Abstract

Structural proteins of the primary cell wall present unusual but interesting problems for structural biologists in particular and plant biologists in general. As structure is the key to function; then the biochemical isolation of these glycoproteins for further study is paramount. Here, we detail the "classical" method for isolating soluble extensin monomers by elution of monomeric precursors to network extensin from tissue cultures. We also outline an additional approach involving genetic engineering that can potentially yield the complete genomic range of extensins and other hydroxyproline-rich glycoprotein (HRGPs) currently underutilized for biotechnology.

Key words: Extensin, Primary cell wall, HRGPs, AGPs, Cultured cells

1. Introduction

The year 2010 marks the fiftieth birthday of the cell wall protein extensin (1), a hydroxyproline-rich glycoprotein (HRGP), arguably the planet's most abundant. Belatedly recognized as the third network of the primary cell wall (2) after cellulose (Anselme Payen in 1838) and pectin (Henri Bracconot in 1825), extensins play an essential role in cytokinesis as self-assembling amphiphiles that template new cross wall deposition presumably as extensin pectate. The discovery of cell wall protein by a graduate student working with D.H. Northcote in the Department of Biochemistry at Cambridge, was fortuitously in a lab adjacent to Fred Sanger, 1958 Nobel laureate and architect-in-chief of modern sequence analysis. The inspirational Sanger school, *the* world centre of protein chemistry at that time, generated methods and advice that "topped up" a pre-eminent undergraduate course of practical biochemistry with classical methods still relevant – a judicious mix of enzymic

Zoë A. Popper (ed.), *The Plant Cell Wall: Methods and Protocols*, Methods in Molecular Biology, vol. 715,
DOI 10.1007/978-1-61779-008-9_15,

degradation and chemical methodology ranging from the Sanger reagent to partial and complete acid/base hydrolysis – precursor to HF-solvolysis for the deglycosylation of glycoproteins (3).

There was just one problem – the Hyp-rich wall-bound (crosslinked) protein resisted solubilization as an intact protein (4); this stymied initial attempts to deploy classical methods of protein characterization. For example, heat denaturation melts the triple helix of Hyp-rich collagen to yield gelatin but did not solubilize the cell wall protein. Miniscule amounts of soluble protein precursors ionically bound to the wall of sycamore or carrot cells were insufficient for thorough analysis until an improved experimental system – tomato cell suspension cultures – yielded sufficient material. Subsequent chromatographic purification, peptide mapping, and sequence analysis of extensin monomers demonstrated the exceptional peptide periodicity of extensins (5) and their diagnostic motifs, Ser-Hyp_4 (6) and intramolecular isodityrosine (Idt) (7) amply confirmed by later genomic analysis.

Some members of the extensin superfamily, typically arabinogalactan proteins (AGPs) although transiently GPI-anchored are not covalently crosslinked and therefore are readily solubilized by mechanical cell disruption (8). However, AGPs resist purification because extensive glycosylation by acidic arabinogalactan polysaccharides swamps properties of the protein. HF-solvolysis at 4°C surmounts this problem by selective glycosidic bond cleavage with peptide bonds remaining intact; deglycosylation of an AGP enables purification of its polypeptide backbone. Thus, salt-elution of extensin from intact cells and HF-deglycosylation of both extensins and AGPs are effective methods for isolating the polypeptides when present in appreciable amounts.

A more recent general method involves genetic engineering and yields the intact glycoproteins: overexpressing the gene of choice attached to a green fluorescent protein tag enables visual selection of transformed cells with generally high yields of the native glycoprotein. Crucially, the hydrophobic GFP adduct facilitates clean chromatographic separation of hydrophilic AGPs compared with other methods that can yield ambiguous or misleading results (9, 10).

2. Materials

2.1. Elution of Extensin Monomers from Intact Cells

1. Cell culture of plant of interest (see Notes 1 and 2).
2. Ice.
3. Vacuum (see Note 3).
4. Coarse-sintered funnel.
5. 50 mM $CaCl_2$.

6. Freeze-drier.
7. 5% Trichloroacetic acid (TCA).
8. Ice.
9. Bench centrifuge.
10. Centrifuge tubes.
11. Distilled water.
12. 30 mM Sodium phosphate buffer, pH 7.6.
13. Biorex 70 cation exchange column: 90× 1.5 cm.
14. Monitor suitable for detecting wavelength of column eluent.
15. Column reservoir buffer: 30 mM Sodium phosphate buffer pH 6.1, 1 M NaCl.
16. Dialysis tubing.
17. Dialysis clips.

2.2. Isolation of Periplasmic and Extracellular AGPs

1. Cell cultures (see Notes 1 and 2).
2. Ice.
3. Coarse-sintered funnel.
4. Vaccum apparatus.
5. 1% NaCl.
6. Sonicator.
7. TCA.
8. Bench centrifuge.
9. Dialysis tubing.
10. Dialysis clips.
11. 2% NaCl.
12. β-D-Glucosyl Yariv reagent.
13. Sodium dithionite.
14. Screw-cap vial.
15. Centrifuge tubes.
16. Block heater or oven at 45°C.

2.3. Transformation of Tobacco BY-2 Cells

1. *Agrobacterium* competent tobacco BY-2 cells.
2. pBI plasmid containing constructed gene cassettes.
3. Eppendorf tubes.
4. Liquid nitrogen.
5. 37°C incubator.
6. LB medium: 10 g tryptone, 5 g yeast extract, 5 g NaCl, 1 mL/L 1 N NaOH.
7. Incubated shaker at 28°C.

8. LB plates containing 30 μg/mL kanamycin.
9. Petri dishes.
10. Centrifuge.
11. LB culture medium containing 100 mg/L kanamycin, 400 mg/L timentin and solidified with 0.8–1.5% w/v agar.
12. LB culture medium containing 100 mg/mL kanamycin.

2.4. Isolation of Fusion Proteins

1. Transgenic cultures prepared as described in Subheading 3.5: 12–18 day-old.
2. Rotoevaporator.
3. Dialysis tubing.
4. Filter paper.
5. Funnel.
6. Solid NaCl.
7. Centrifuge.
8. Pre-treated phenyl sepharose hydrophobic interaction chromatography column: Pretreat the column by washing with distilled water and equilibrate with 2 M NaCl.
9. 2 M NaCl.
10. Fluorescence detector (excitation 488 nm, emission 520 nm).
11. Hamilton PrP-1 reverse-phase chromatography system.
12. 80% v/v Acetonitrile in 0.1% v/v TFA.
13. Double distilled water.

3. Methods

3.1. Elution of Extensin Monomers from Intact Cells (11)

The primary cell wall is largely pectin that is highly methyl-esterified and therefore weak acidic macromolecule binds to weak basic extensin monomers as extensin pectate. Thus, extensins can be eluted from acidic pectin because it behaves as a cation exchange resin. Like other highly glycosylated glycoproteins extensin is soluble in TCA. Low yields may result from crosslinkage by extensin peroxidase in the presence of trace amounts of hydrogen peroxide derived from reactive oxygen species (ROS) like superoxide e.g. ROS → hydrogen peroxide → crosslinked extensin.

1. Grow appropriate species in shake culture (12) (see Notes 1 and 2).
2. Harvest after 4–8 days in rapid growth phase.
3. Cool cells on ice.

4. Suction filter 50–500 g fresh weight cells gently on a coarse-sinter funnel.
5. Wash briefly with cold water.
6. Elute cells with 2× volume of cold 50 mM $CaCl_2$.
7. Freeze-dry eluate.
8. Redissolve eluate in ice-cold 5% TCA and stand for 1 h (see Note 4).
9. Centrifuge at 9,000 rpm for 60 min and discard precipitate.
10. Dialyze supernate against distilled water at 4°C.
11. Freeze-dry.
12. Re-dissolve in 30 mM sodium phosphate buffer, pH 7.6.
13. Load onto a 90× 1.5 cm BioRex 70 cation exchange column.
14. Elute from the column at a flow rate of 60 mL/h with a gradient produced by having 300 mL of 30 mM sodium phosphate buffer, pH 7.6 in the mixing chamber and 300 mL of 30 mM sodium phosphate buffer, pH 6.1 containing 1 M NaCl in the reservoir.
15. Monitor the eluent at 200 nm and collect appropriate fractions.
16. Dialyze, freeze-dry and store at –20°C.

Although network extensin per se cannot be isolated, peptide fragments can be obtained, analyzed, and identified by chymotryptic/tryptic degradation of isolated cell walls after partial removal of polysaccharides by enzymic (4) or chemical degradation (13) or removal of all polysaccharides by HF-solvolysis (14).

3.2. Isolation of Periplasmic and Extracellular AGPs from Cultured Cells (8)

In growing cells, phospholipase C continuously releases GPI-anchored AGPs that cover the outer surface of the plasma membrane. Following addition to the wall by apposition, these soluble AGPs trapped by the limiting porosity of the pectic matrix do not diffuse freely but migrate through the expanding wall by "plug flow" extrusion into the culture medium as soluble AGPs. Intact cells typically contain a total of ~600 μg AGP/g fw of which roughly half is soluble periplasmic AGP that is released by cell disruption. AGPs *in muro* are trapped in the pectic matrix and released by appropriate disruption of this matrix e.g. by boiling or pectinase treatment. The method for isolation of periplasmic AGPs is given below. AGPs from the culture medium filtrate can be prepared in the same way except that the amount of extracellular AGP in the medium of a friable culture is generally similar to the soluble periplasmic AGP content of its intact cells.

1. Grow appropriate species in shake culture.
2. Harvest after 4–8 days in rapid growth phase.

3. Cool cells on ice.
4. Suction filter 1–100 g fresh weight cells on a coarse-sinter funnel.
5. Wash briefly with 1% NaCl.
6. Disrupt cells by sonication in an ice bath.
7. Add TCA to final concentration of 5%.
8. Centrifuge at 10,000 rpm.
9. Discard the TCA precipitate.
10. Dialyze supernate exhaustively.
11. Freeze-dry.
12. Dissolve in a small volume of 2% aqueous NaCl.
13. Add excess (see Note 5) β-D-glycosyl Yariv reagent.
14. After 1 h at RT collect AGP-Yariv precipitate by low speed centrifugation.
15. Add excess sodium dithionite in a small screw cap vial.
16. Fill tube to minimize oxidation of dithionite to yield elemental sulphur.
17. Heat at 45°C till colour fades to disrupt the AGP-Yariv complex.
18. Dialyze and freeze-dry the purified AGPs.

3.3. Design of Genes for Expression and Detection of HRGP-GFP Chimeras

The repetitive peptide periodicity of extensins allows the use of a head-to-tail method (15, 16) or a modified polymerization method (17), to polymerize single repeats of oligonucleotides encoding an extensin repeat into large repetitive genes. The head-to-tail method involves polymerization of three pairs of partially overlapping oligonucleotides. However, it is difficult to control the degree of polymerization (Fig. 1). The longest gene synthesized was 600 bp encoding $(ThrPro)_{100}$ (16). The modified polymerization method (17) can be used to synthesize genes of specific sizes; e.g. the synthetic *rsh* gene encoding 13 repeats of a 28-amino-acid peptide (Tan and Kieliszewski, unpublished data) (Fig. 2).

Four great advantages of making chimeras of extensin (or AGPs) with the enhanced green fluorescent protein (GFP) are; (1) GFP fluorescence enables facile identification of transformed BY-2 cells, (2) GFP fluorescence indicates the highest yielding cell lines, (3) GFP hydrophobicity facilitates chromatographic separation of hydrophilic HRGPs, and (4) GFP fluorescence simplifies the monitoring of column eluates.

1. Design gene using appropriate software, such as Primer Premier (Premier Biosoft International).
2. Choose codons favoured by plants (18). Clone the synthetic gene into the plasmid *pUC18-SS^{tob}-EGFP* vector (15) (Fig. 3)

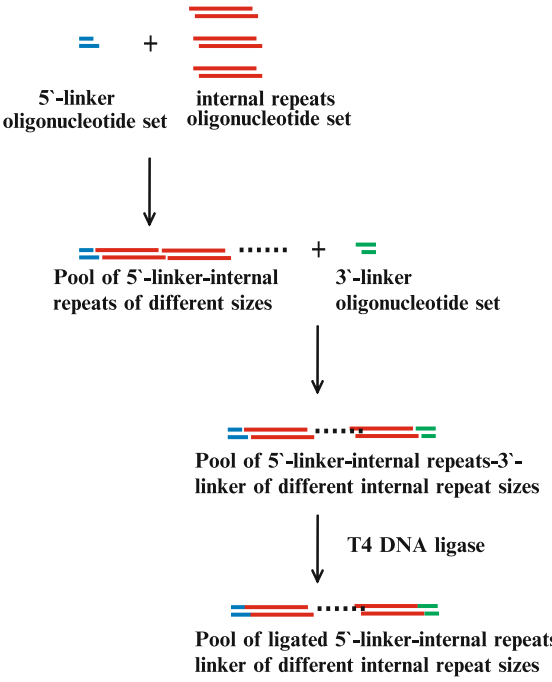

Fig. 1. Flow chart of the head-to-tail polymerization method. In brief, the annealed 5′-linker oligonucleotide set is mixed with an excess of the annealed internal repeats oligonucleotide set which encode part of the target gene (e.g. 5 to 1 molar ratio of internal repeats to 5′-linker oligonucleotide sets). The pool formed of 5′-linker-internal repeats of different internal repeats is then capped with 3′-linker. The different sized gene pool is then ligated by T4-DNA ligase. The restriction sites on both 5′- and 3′-end linkers allow further cloning of the synthetic genes into *pUC18-SS^{tob}-EGFP* vector.

which contains the following restriction sites: BamHI–(*SS^{tob}*)–XmaI–NcoI–(GFP)–BsrGI–SacI.

SS^{tob} represents an extensin signal sequence gene, while *GFP* is a gene encoding the enhanced green fluorescent protein.

3. Ligate the synthetic gene:
   a. Into the *pUC18-SS^{tob}-EGFP* vector as a XmaI-NcoI fragment to form *pUC18-SS^{tob}-target gene* plasmid (15, 17) or
   b. Behind the *EGFP* gene as a BsrGI-SacI fragment to form *pUC18-SS^{tob}-EGFP-target gene* plasmid (19).
4. Subclone the resulting gene cassette, *SS^{tob}-target gene-EGFP* or *SS^{tob}-EGF target gene* into the *plant transformation vector, pBI121*, as a BamHI-SacI fragment replacing the β-glucuronidase reporter gene. The gene cassette is then under regulation of a CaMV S35 promoter for overexpression and contains the neomycin phosphotransferase (NPT) II gene that confers resistance to kanamycin.

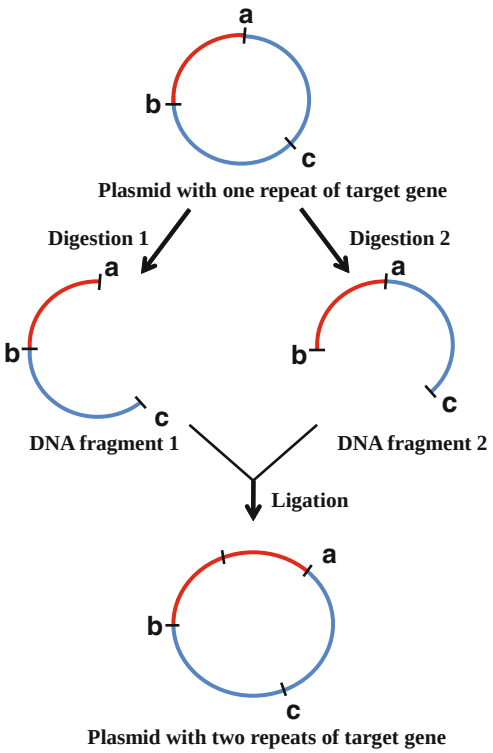

Fig. 2. Flow chart of a controlled polymerization method. A plasmid is digested with two sets of restriction enzymes, e.g. a/c and b/c as showed. This method requires that restriction enzymes a and b should yield the same sticky ends. After digestion, the two fragments each with a single repeat of the target gene are purified via agarose gel electrophoresis, and ligated with T4-DNA ligase to yield two repeats of the target gene with reconstituted restriction sites between them. These procedures can be repeated to build desired target genes of defined sizes.

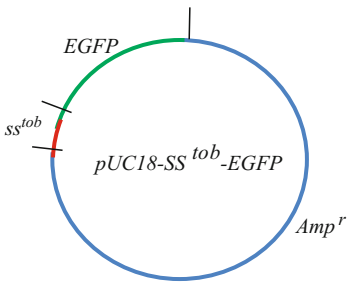

Fig. 3. A plasmid map of *pUC18-SS^{tob}-EGFP*. *SS^{tob}* represents an extensin signal sequence gene, while *GFP* encodes the enhanced green fluorescent protein. The *SS^{tob}* gene is flanked by a BamHI restriction site and a XmaI restriction site, with XmaI site located at its 3′-end. Downstream of the XmaI site, an NcoI restriction site (at the 5′-end) and a BsrGI restriction site (at the 3′-end) sandwich the *GFP* gene. A SacI restriction site behind the BsrGI site, together with a BamHI site, allow further cloning of the gene cassette into the *pBI121* vector.

3.4. Transformation of Tobacco BY-2 Cells and Selection of Cell Lines

Transform *Agrobacterium tumefaciens* with the pBI plasmid constructs via the freeze-thaw method (20) as follows:

1. Add ~1 μg of pBI plasmid containing the constructed gene cassettes to 100 μL *Agrobacterium* competent cells, prepared by a method similar to *E. coli* (20).
2. Freeze *Agrobacterium* cells in a sterile Eppendorf tube in liquid nitrogen.
3. Transfer tube of frozen *Agrobacterium* cells to 37°C for 5 min.
4. Add 1 mL LB medium.
5. Incubate on shaker at 28°C for 3–4 h.
6. Spread *Agrobacterium* on LB plates containing 30 μg/mL kanamycin.
7. Incubate plates at 28°C for 2–3 days.
8. The colonies contain transformed *Agrobacterium* which can be used to transform tobacco BY-2 cells.
9. Transfer 5 mL tobacco BY-2 cells (4-days old) to 10 cm Petri dish.
10. Add 200 μL from transformed *Agrobacterium* cultured overnight on LB.
11. Co-culture for 2–3 days at 28°C in the dark.
12. Wash the infected cells with liquid culture medium three times by low speed centrifugation (~500 × *g*).
13. Spread washed cells on solid culture medium containing kanamycin and timentin.
14. Incubate for 4–5 weeks.
15. Identify transformed cells.
16. Subculture BY-2 cells into liquid culture medium containing 100 μg/mL kanamycin.
17. Shake cultures at 92 rpm at room temperature for protein expression.

3.5. Isolation of Fusion Proteins from the Culture Medium

1. Filter culture medium from 12- to 18-day transgenic cultures.
2. Concentrate filtrate via rotoevaporation at 28°C to 10% of initial volume.
3. Dialyze against ddH_2O for 2 days.
4. Add solid NaCl to a final concentration of 2 M.
5. Spin at 10,000 × *g* for 30 min.
6. Remove and discard any pellet.
7. Load clarified supernatant onto a phenyl sepharose hydrophobic interaction chromatography column, previously washed with dH_2O and equilibrated with 2 M NaCl.

8. Elute the column with a linear NaCl gradient decreasing from 2 to 0 M.
9. Monitor column via fluorometry (Excitation 488 nm; emission 520 nm).
10. Fluorescent fractions contain EGFP fusion proteins of ~85% homogeneity.
11. Further purify by reversed phase chromatography on Hamilton PRP-1 with a gradient of 0–70% of 80% acetonitrile in 0.1% TFA in 100 min. The EGFP fusion glycoproteins elute at ~35% acetonitrile in 0.1% TFA (21).

4. Notes

1. Expect a wide variation in yields between cultures. Yield is typically in the range of 5–500 μg/g fresh weight of cells.
2. Ideally cultures should be friable. Friability maximizes release of AGPs from an expanding wall. Cultures that grow as tight micro-calli release much less as they expose a much smaller proportion of the cell surface to the growth medium.
3. Vacuum can be provided either by using a vacuum pump at a low setting or by suction provided using a system attached to a tap with running water. The latter is easier to control.
4. Minimal time in TCA avoids degradation of acid-labile arabinofuranosides.
5. Greater than 1 mg β-D-glycosyl Yariv reagent per mg of AGP.

References

1. Lamport, D. T. A., and Northcote, D. H. (1960) Hydroxyproline in primary cell walls of higher plants. *Nature* **188,** 665–666.
2. Kerr, T., and Bailey, I. W. (1934) The cambium and its derivative tissues. X Structure, optical properties and chemical composition of the so-called middle lamella. *J Arnold Arbor* **15,** 327–349.
3. Mort, A. J., and Lamport, D. T. A. (1977) Anhydrous hydrogen fluoride deglycosylates glycoproteins. *Anal Biochem* **82,** 289–309.
4. Lamport, D. T. A. (1965) The protein component of primary cell walls. *Adv Bot Res* **2,** 151–218.
5. Smith, J. J., Muldoon, E. P., Willard, J. J., and Lamport, D. T. A. (1986) Tomato extensin precursors P1 and P2 are highly periodic structures. *Phytochemistry* **25,** 1021–1030.
6. Lamport, D. T. A., Katona, L., and Roerig, S. (1973) Galactosyl serine in extensin. *Biochem J* **133,** 125–131.
7. Epstein, L., and Lamport, D. T. A. (1984) An intracellular linkage involving isodityrosine in extensin. *Phytochemistry* **23,** 1241–1246.
8. Lamport, D. T. A., Kieliszewski, M. J., and Showalter, A. M. (2006) Salt-stress upregulates periplasmic arabinogalactans-proteins: using salt-stress to analyse AGP function. *New Phytol* **169,** 479–492.
9. Baldwin, T. C., McCann, M. C., and Roberts, K. (1993) A novel hydroxyproline-deficient arabinogalactan protein secreted by suspension-cultured cells of *Daucus carota*. *Plant Physiol* **103,** 115–123.
10. Baldwin, T. C., Domingo, C., Schindler, T., Seetharaman, G., Stacey, N., and Roberts, K. (2001) DcAGP1, a secreted arabinogalactans

protein, is related to a family of basic proline-rich proteins. *Plant Mol Biol* **45,** 421–435.

11. Smith, J. J., Muldoon, E. P., and Lamport, D. T. A. (1984) Isolation of extensin precursors by direct elution of intact tomato cell suspension cultures. *Phytochemistry* **23,** 1233–1239.
12. Lamport, D. T. A. (1964) Cell suspension cultures of higher plants, isolation and growth energetics. *Exp Cell Res* **33,** 195–206.
13. Lamport, D. T. A. (1969) The isolation and partial characterization of hydroxyproline-rich glycopeptides obtained by enzymic degradation of primary cell walls. *Biochemistry* **8,** 1155–1163.
14. Frueauf, J. B., Dolata, M., Leykam, J. F., Lloyd, E. A., Gonzales, M., VandenBosch, K., and Kieliszewski, M. J. (2000) Peptides isolated from cell walls of *Medicago trunculata* nodules and uninfected root. *Phytochemistry* **55,** 429–438.
15. Shpak, E., Leykam, J. F., and Kieliszewski, M. J. (1999) Synthetic genes for glycoprotein design and the elucidation of hydroxyproline-*O*-glycosylation codes. *Proc Natl Acad Sci U S A* **96,** 14736–14741.
16. Tan, L., Leykam, J. F., and Kieliszewski, M. J. (2003) Glycosylation motifs that direct arabinogalactans addition to arabinogalactan-proteins. *Plant Physiol* **132,** 1362–1369.
17. Held, M. A., Tan, L., Kamyab, A., Hare, M., Shpak, E., and Kieliszewski, M. J. (2004) Di-isodityrosine is the intermolecular cross-link of isodityrosine-rich extensin analogs cross-linked *in vitro*. *J Biol Chem* **279,** 55474–55482.
18. Li, S., and Showalter, A. M. (1996) Cloning and developmental/stress regulated expression of a gene encoding a tomato arabinogalactan protein. *Plant Mol Biol* **32,** 641–652.
19. Zhao, Z. D., Tan, L., Showalter, A. M., Lamport, D. T. A., and Kieliszewski, M. J. (2002) Tomato LeAGP-1 arabinogalactan-protein purified from transgenic tobacco corroborates the Hyp contiguity hypothesis. *Plant J* **31,** 431–444.
20. An, G., Ebert, P. R., Mitra, A., and Ha, S. B. (1988) Binary vectors. Plant Molecular Biology Manual. Gelvin, S.B. and Schilperoort, R.A. (eds). Dordrecht, Netherlands: Martinus Nijhoff, p. 1–19.
21. Xu, J., Tan, L., Goodrum, K. J., and Kieliszewski, M. J. (2007) High-yields and extended serum half-life of human interferon alpha 2b expressed in tobacco cells as arabinogalactan-protein fusions. *Biotechnol Bioeng* **97,** 997–1008.

Chapter 16

New Insights into the Control of Cell Growth

Claudia Blaukopf, Matthäus Z. Krol, and Georg J. Seifert

Abstract

Undoubtedly, the function of the plant cell wall in the control of cell growth far exceeds its mechanical role. The plant's monitoring of cell wall function and integrity comprises a central checkpoint to integrate cues for survival and division, expansion and differentiation, as well as fluctuations in the biotic and abiotic environment (Somerville *et al.,* Science 306:2206–2211, 2004). With their biochemical nature yet unknown, the identification of molecular constituents of cell wall performance, and integrity control initially depends on a combination of genetic and physiological approaches.

Key words: Cell wall integrity control, Forward genetics, Map based cloning, Programmed cell death, Yariv, Arabinogalactan proteins

1. Introduction

In the recent past, there have been significant advances in the analysis of structural components of the plant cell wall and likewise, the cell wall biosynthetic machinery is being elucidated at an ever increasing pace, largely by using methods presented in this volume. However, conceptually, the molecular components of the hypothetical cell wall performance and integrity control system are not even laid out yet. Some serendipitous insights into potential ingredients have been derived from genetic screens for constitutive activation of stress response or sugar signaling. The finding that elevated expression of several stress-induced genes is triggered by defects in cellulose biosynthesis, identified jasmonate (JA) and ethylene signaling as potential pathways involved in cell wall integrity control. Intriguingly, the combination of JA and ethylene insensitivity partially suppressed the reduction of hypocotyl elongation seen in the *cesA3/cev1* cellulose synthase mutants (2).

Zoë A. Popper (ed.), *The Plant Cell Wall: Methods and Protocols*, Methods in Molecular Biology, vol. 715,
DOI 10.1007/978-1-61779-008-9_16,

Another example for the fortuitous identification of a component of cell wall integrity control was the demonstration that the cell wall matrix compositional mutants *mur4, mur1 and mur3* (3) all display *PRL1* dependent glucose hypersensitivity (4). As the pathways that signal cell wall stress, sugar response and growth regulator stimuli are thought to interact with many other regulatory pathways; such pioneering findings encourage a more systematic search for components of cell wall performance and integrity control. As it can be assumed that there exist receptor-like sensors of cell wall integrity, a systematic reverse genetic search for receptor mutants seems an attractive possibility. One recent example was the identification of the pair of the *FEI1* and *FEI2* loci that in combination are required for normal growth at elevated levels of salt and sugar (5). Further genetic analysis indicated that *FEI1* and *FEI2* might act in the same pathway that is responsible for salt oversensitivity in the *sos5* mutant that expresses a defective variant of the fasciclin-like arabinogalactan protein (AGP) 4 (FLA4) in *Arabidopsis* (6). Although a valuable contribution to our knowledge of cell wall signaling, this study also highlights an important limitation of reverse genetics, namely that genetic redundancy has to be overcome by cumbersome creation of multiple mutant combinations. A central strategy to identify players in cell wall performance and integrity control is forward genetics. On the one hand, there will be new screens for genetic modifiers of cell wall mutants. On the other hand, several chemicals induce cell wall defects, and mutants displaying altered sensitivity towards such drugs can lead to the identification of positive and negative regulators of cell wall integrity sensing. A rationale behind sensitized screens is the hypothesis that the physiological and morphological responses to a mutation in cell wall structure such as inhibited growth, disease resistance, or cell death are the consequence of a hyperactivated cascade of sensory and signal transduction processes that normally probe the function of the wild type cell wall during growth and stress. So far, there are only few examples for systematic cell wall mutant modifier screens, the most notable being the identification of the *THESEUS1* (*THE1*) locus encoding an active receptor-like kinase that is responsible for the dwarfed phenotype of cellulose biosynthetic mutants (7) and was originally identified in a screen for genetic suppressors of the CesA6 mutant *procuste*. Although its biochemical mode of action and potential ligands are unknown, the THE1 receptor-like kinase comprises the first obvious candidate of a molecular component of cell wall integrity sensing. Chemically sensitized screens have previously been performed to isolate mutants insensitive to cellulose synthase inhibitors (8–10) and cytoskeletal drugs (11, 12). Although the identified genes were either directly related to cell wall biosynthesis and cytoskeletal assembly or were postulated to be involved in drug transport, there is a strong

requirement for more extensive screens to identify components of cell wall performance and integrity control. The fact that a mutation in the *FLA4* locus is responsible for salt oversensitive root growth (6) highlights the potential role of AGPs in cell wall integrity sensing. Because AGPs are often tethered to glycosylphosphoinositol lipid anchors at the plasma membrane and can bind glycans, AGPs might act as coreceptors presenting cell wall structure to transmembrane receptor like kinases or membrane channel type receptors (13). Despite the genetic role of AGPs in cell survival, cell division, and cell elongation, a direct implication of plasma membrane AGPs in cell wall integrity control is still speculative. Genetic approaches are needed to establish a link between the phenotypes of AGP mutants and a cellular sensing and signal transduction machinery. As a long-term goal, hypothetical receptor complexes have to be reconstituted in recombinant systems that allow for all the required posttranslational modifications that are expected to be crucial in the function of AGPs.

In summary, very little is known about the molecular players in cell wall performance and integrity control, and novel insights in the control of cell growth can be obtained from well designed modifier screens as well as chemically sensitized screens. As examples for screens involving defective AGPs, we describe how we generated chemically mutagenized populations of the conditional AGP glycosylation and protein structural mutants *uge4-3* (14, 15) and *sos5* (6), respectively, how we screened for enhancer and suppressor mutants including additional selection filters, and how we are proceeding towards map-based cloning of the mutant loci. We also describe how to cheaply synthesize gram quantities of the AGP binding drug β-glucosyl Yariv that interferes with cell growth (16) and survival (17, 18) and apply it in a genetically amenable assay.

2. Materials

2.1. EMS Mutagenesis

1. Bulked mutant seeds (*uge4-3*, *sos5*).
2. 0.1% KCl.
3. Prepare in chemical hood on day of use: Ethyl methanesulfonate (EMS) buffer: 100 mM (290 µL per 20 mL) EMS, 0.1 M Na-phosphate buffer (pH 5), 5% dimethylsulfoxide (DMSO).
4. Quenching buffer: 0.1 M Na-thiosulfate (0.791 g/50 mL).
5. Solid Na-thiosulfate.
6. Cryosanitized soil (peat:humus:sand 5:5:1; frozen at −80° for 48 h; this treatment in combination with keeping Perspex lids

on plant trays during early growth helps to control insect and mite infestations). Soil is thawed over night and distributed into 6×6 cm pots before use.

7. Germination trays with Perspex hoods. "Seed propagator" bought at local house ware supply store.

2.2. Primary and Secondary Screens of uge4-3 Enhancers and sos5 Suppressors

1. Sterilization solution: Typically a 1:9 solution of hypochlorite containing household bleach. Alternative 3% sodium hypochlorite and 0.2% sodium dodecyl sulfate (SDS) in water.
2. Standard germination medium (SGM): Murashige and Skoog salts including vitamins and MES-buffer (Duchefa, M0255.0001), 1% sucrose, 0.8% Phytagel (Sigma-Aldrich, P8169). Dissolve Murashige and Skoog salts and sucrose and adjust the pH to 5.8, add Phytagel and autoclave, then bring to 55°C before pouring into 90 mm Petri dishes.
3. Galactose-selection medium: SGM including 5 mM D-galactose (prepare 1 M stock solution, sterile filtered, add to autoclaved SGM prior to plating).
4. SGM including 4% sucrose.
5. High salt medium: SGM including 100 mM NaCl.
6. Seed dispensing pipette. Ultipette Variable Volume 1–10 µL (Barky Instr. Intl., UK) and plastic tips, Ultipette capillary tips, 0.5–10 µL (Barky Instr. Intl., UK).
7. Stereomicroscope (e.g., Olympus SZX7 magnification 0.8–5.6×10). When plates are directly placed on the diffuse bright field illumination screen, contrast of roots is too low for efficient observation and should be increased by lifting dishes 3–5 cm above the diffuse light source on an workshop made glass table. In other microscopes (Zeiss Stemi 2000-C or Leitz LM10) the built-in illumination produces sufficient contrast.

2.3. Establishing a Genetic Model and a Mapping Population

1. Suitable parental plants (acceptor and donor plants).
2. Sharp forceps.
3. Labeling tape.
4. Nail scissors (optional).
5. Magnifying goggles or Macromicroscope (optional).
6. High salt medium: SGM (see Subheading 2.2) including 100 mM NaCl.

2.4. Genomic DNA Extraction

2.4.1. Protocol 1: Modified from (19)

1. Mortar.
2. 1.5 mL Eppendorf tubes.
3. 100–1,000 µL pipettes and tips.

4. DNA extraction buffer: 200 mM Tris–HCl (pH 7.5) (Duchefa Biochemie, NL-Haarlem), 250 mM NaCl, 25 mM EDTA, 0.5% SDS.
5. Isopropanol.
6. Double distilled water.

2.4.2. Protocol 2: Rapid DNA Extraction from Leaves

1. 200 µL PCR tubes.
2. 20–200 µL pipettes and tips.
3. QuickExtract™ Plant DNA extraction solution (EPICENTRE biotechnologies, Madison, WI, USA).
4. Thermocycler.

2.5. Genotyping: Confirmation of the Mutant Status by CAPS Markers

1. Mastermix for a 10 µL reaction using Biotherm DNA polymerase: 6.25 µL Double distilled water, 1 µL 2 mM Di-nucleotide-tri-phosphates (dNTP) (Fermentas GmbH, Leon-Rot, Germany), 1 µL 10× Reaction buffer Biotherm containing 15 mM $MgCl_2$ (Fermenta GmbH, Leon-Rot, Germany), 0.5 µL 5 µM Forward primer, 0.5 µL 5 µM Reverse primer, 0.05 µL DNA polymerase (5 units/µL; Biotherm, Gene Craft, Cologne, Germany).

   Add 0.7 µL plant DNA per reaction.
2. Mastermix for a 10 µL reaction using KAPA 2G Robust: 6.36 µL Double distilled water, 0.2 µL 10 mM dNTPs (Kapa Biosystems), 2 µL 5× Buffer B (Kapa Biosystems, USA) ,0.3 µL 5 µM Forward primer, 0.3 µL 5 µM Reverse primer, 0.02 µL Kapa 2G Robust polymerase (5 units/µL; Kapa Biosystems, USA).

   Add 0.7 µL Plant DNA per reaction.
3. *Ava*II mastermix for *uge4-3* genotyping: 0.25 µL *Ava*II restriction endonuclease (5 units/µL; Fermentas GmbH, Leon-Rot, Germany), 2 µL 10× Buffer Red (Fermentas GmbH, Leon-Rot, Germany), 7.75 µL Double distilled water.
4. *Bfu*I mastermix for *sos5* genotyping: 0.25 µµL *Bfu*I restriction endonuclease (5 units/µL; Fermentas GmbH, Leon-Rot, Germany), 2 µL 10× Buffer *Bfu*I (Fermentas GmbH, Leon-Rot, Germany), 7.75 µL Double distilled water.
5. PCR strips or plates.
6. Loading dye/buffer: (60% glycerol, 50 mM Tris–HCl (pH 8.0), 25 µg/mL bromophenol blue).
7. Agarose gel (1.4% for CAPS markers): 1× TAE: 40 mM Tris-acetate, 1 mM EDTA, LE Agarose 1 g/100 mL 1× TAE (Biozym Scientific GmbH, Oldenburg, Germany).

2.6. Rough Mapping

1. Materials (see Subheading 2.5).
2. Molecular markers to distinguish ecotypes Columbia and Landsberg at various locations on each chromosome. We generally start with three different molecular markers per chromosome. Additional markers might be required depending on initial data. Sequences of all nga markers are published (20). Other markers are described in http://www.arabidopsis.org.

   Chromosome 1: nga63, F19G10 (forward: AGTTGGTC CTCGAGCTCTCC, reverse: AAGAACTTAATTTCT CTCACCCG), nga111.

   Chromosome 2: RGA (*RsaI* for restriction digestion (see Subheading 2.5) forward: TTCGATTCAGTTCGGTT TAG, reverse: GTTTAAGCAAGCGAGTATGC), ciw3 (forward: GAAACTCAATGAAATCCACTT, reverse: TGAACTTGTTGTGAGCTTTGA), nga168.

   Chromosome 3: nga172, nga162, nga6.

   Chromosome 4: nga8, ciw6 (forward: CTCGTAGTGCACT TTCATCA, reverse: CACATGGTTAGGGAAACAATA), nga1107.

   Chromosome 5: nga106, nga76, ciw10 (forward: CCACA TTTTCCTTCTTTCATA, reverse: CAACATTTAGCAA ATCAACTT).

2.7. Fine Mapping

1. Materials (see Subheading 2.6).
2. Additional molecular markers in the region determined by rough mapping. Markers can be found either on the *Arabidopsis* homepage (http://www.arabidopsis.org; marker search tool), or can be designed using the Monsanto polymorphism collection (also available at http://www.arabidopsis.org; registration required to access the data).

2.8. Sequencing

1. DNA of the plants of interest.
2. Primers flanking the region of interest (5 μM for PCR, 1.5 μM for sequencing). Use a primer length of 20–25 base pairs (bp) to ensure binding specificity, the GC content should be ≥40% and the first 1–2 bp at the 3′ end should be a G or a C.
3. PCR and Gel electrophoreses (see Subheading 2.5).
4. PCR purification or Gel extraction kit (Qiagen, Hilden, Germany).
5. Sequence viewer software such as Chromas (Freeware, Technelysium Pty Ltd, Tewantin QLD, Australia).

2.9. Initial Characterization of uge4-3 Enhancers by Immunohistochemistry

2.9.1. Fixation and Embedding

1. 100 mM phosphate buffer, pH 7.
2. Paraformaldehyde-glutaraldehyde-fixative, final concentrations:

   100 mM Phosphate buffer pH 7, 2% paraformaldehyde, 2.5% glutaraldehyde. Preparation of 10% paraformaldehyde stock solution from powder: add 2 g of PFA powder to 20 mL dH_2O and heat up to 60–65°C. Add a few drops of 1 N NaOH until the solution turns clear and leave to cool at room temperature.
3. Ethanol in the following concentrations: 30, 50, 70, 80, 90, and 96%.
4. LR White Embedding Kit for heat polymerization or accelerated polymerization at room temperature.
5. Molding trays with lid (Plano, IL, USA) or gelatine capsules with holder (Plano). Alternatively, 0.5 or 0.2 mL Eppendorf tubes (depending on the specimen size) can be used (Eppendorf, Hamburg, Germany).
6. 60°C cabinet for polymerization.
7. Razor blades for trimming (Plano).
8. Low melting point agarose (Sigma).
9. Two-component glue (e.g., UHU plus endfest 300).

2.9.2. Sectioning

1. (Ultra) Microtome (e.g., Leica Ultracut R, Leica, Wetzlar Germany).
2. Diamond knife (Diatome, Biel, Switzerland, Diatome histo).
3. Multiwell (5–6 mm well-diameter) microscope slides, adhesive (Tekdon inc., Myakka City, FL, Slide-ID: 12-54). Alternatively, adhesive slides without wells can be used, and wells can be produced with a grease pencil (e.g., Pap Pen, Plano, IL, USA).
4. Distilled Water and Pasteur pipette for wetting microscope slides.
5. Eyelash glued to matchstick to transfer sections to microscope slide.
6. Heating block for drying slides.

2.9.3. Antibody Labeling

1. 1× PBS: 137 mM NaCl, 2.7 mM KCl, 10 mM Na_2HPO_4, 2 mM KH_2PO_4.
2. 3% Bovine serum albumin (BSA) in 1× PBS.
3. Staining jar (Plano, Plano, IL, USA).
4. Primary antibodies. Frequently used monoclonal antibodies reacting with cell wall carbohydrate e.g., LM2 (21), LM5 (22), CCRC-M1, CCRC-M7 (23), were the generous gift of

Paul Knox and Michael Hahn and can be obtained at http://www.plantprobes.net/ and http://www.ccrc.uga.edu/~carbosource/CSS_home.html.

5. Secondary antibody (goat antimouse IgG + IgM Immunogold conjugated, British Bio Cell Int. Cardiff, UK). This secondary antimouse antibody can be used for both mouse and rat primary antibodies.
6. Silver enhancement kit (BBI international, Cardiff, UK).
7. Glycerol (Roth, Karlsruhe, Germany).
8. Cover glass.

2.9.4. Microscopic Examination

1. Fluorescence microscope (e.g., Zeiss Axiovert 200M) equipped with mercury lamp (OSRAM, Augsburg, Germany, product no. HBO 103W/2), suitable filter set and camera (e.g., AxioCam MRc5). Lenses: Zeiss Plan-Apochromat 63× oil; Zeiss Plan-Neofluar 40× oil; Zeiss LC Achroplan 20×.
2. Confocal microscope.

   Argon Laser (488 nm) for reflection contrast of immunogold labeling, UV laser (405 nm) for Calcofluor. Reflection: $\lambda_{em} = 470–500$; Calcofluor: $\lambda_{em} = 400–450$ nm; Image size 2,048 × 2,048 pixel. Lens: 63× oil.

2.10. Synthesis of β-Glucosyl Yariv Reagent (24)

1. *p*-Nitrophenyl-β-D-glucopyranoside (Sigma, Saint Louis, MO, USA).
2. Round bottom flask with septum and hollow needle.
3. Anhydrous methanol.
4. Charcoal with 10% Pd (Aldrich, Saint Louis, MO, USA).
5. Ammonium formate.
6. Celite packed column (250 mL capacity).
7. Vacuum pump with suction filter.
8. 5% H_2SO_4.
9. 5% NaOH.
10. Double distilled H_2O.
11. Magnetic stirrer.
12. Temperature-controlled water bath.
13. Rotary Evaporator.
14. Sodium nitrite (Aldrich, Saint Louis, MO, USA) solution (1.0288 g in 56 mL HQ H_2O).
15. Phloroglucinol (Sigma, Saint Louis, MO, USA) solution (0.5952 g in 192 mL HQ H_2O).
16. Ethanol abs.
17. HPLC (and NMR) to test product purity.

2.11. Assay for β-Glucosyl Yariv Sensitivity

1. 6-well-plates (Greiner, Frickenhausen, Germany).
2. SGM (0.4% Phytagel) (see Subheading 2.3).
3. Liquid SGM (SGM without Phytagel).
4. β-glucosyl Yariv (see Subheading 2.10).
5. Propidium iodide (PI) (Molecular Probes, Eugene, OR, USA). CAUTION: Toxic! Use gloves!
6. Additional compounds to be tested in the assay (in dH_2O or DMSO).
7. Microscope (e.g., Zeiss Axiovert 200M with Axio Vision 4.6 software) equipped with a mercury lamp and a suitable fluorescent filter set (Zeiss filter set 15 Ex 546/12 for propidium iodide $\lambda_{ex} = 536$ nm, $\lambda_{em} = 617$ nm).
8. Software for data analysis (ImageJ/NIH image, public domain software; http://rsb.info.nih.gov/nih-image/).

3. Methods

3.1. EMS Mutagenesis

1. Imbibe 100–200 mg of homozygous *uge4-3* and *sos5* seeds overnight in 20 mL 0.1% KCl at room temperature.
2. *In chemical hood*: After discarding the supernatant, incubate seeds in 20 mL EMS solution for 3 h at room temperature on a rotary shaker (200 rpm).
3. *In chemical hood*: Dispose EMS solution supernatant by pouring into beaker containing 10 g solid Na-thiosulfate. Rinse seeds twice in quenching buffer. After 30 min quenching, EMS waste can be disposed off.
4. Rinse seeds four times in dH_2O (nonsterile).
5. Suspend seeds in 30–50 mL dH_2O and distribute 1 mL aliquots to 6×6 cm pots filled with cryosanitized soil. Intermittent stirring of seed suspension ensures that numbers of M0 individuals are similar in each pool.
6. Germinate seedlings under Perspex hood in greenhouse using mixed natural and 16 h artificial light.
7. When plants start flowering, remove hoods and separate plant pots sufficiently to avoid cross-contamination.
8. Upon senescence, wrap plant clusters in glassine paper bags and keep watering until fully senescent.
9. Collect M1 seed pools for screening.

3.2. Primary Screen of uge4-3 Enhancers and sos5 Suppressors

1. Approximately 300–400 seeds from each M1 seeds pool are suspended in sterilization solution in 1.5 mL plastic tubes, mixed initially by vortexing and intermittently by inversion

for 10–20 min. In separate tubes wild type (Col-0), mutant background (*uge4-3*, *sos5*) and full loss of function *uge4* mutants (*uge4-4*) are prepared as controls. Depending on the experience of the worker 10–20 M1 populations can be processed on 1 day (2–6,000 individual seeds).

2. Sterilization solution is decanted and seeds are rinsed three times with sterile dH_2O.
3. Seeds are placed individually onto SGM plates (for *uge4-3*) or SGM 4% sucrose (for *sos5*) in 2–3 mm distance in lines 20 mm apart.
4. To facilitate simultaneous germination, plates are cold-treated at 4°C in the dark for 48 h.
5. For germination plates are incubated at 25°C in continuous light in an almost vertical slightly inclined position in a way that lines of seeds are horizontal.
6. Morphological appearance of root tips is visually screened in a dissecting microscope at approximately five to tenfold magnification and putative *uge4-3* enhancers and *sos5* suppressors are marked on the bottom of the Petri dish. While *uge4-3* looks like wild type under the screening conditions, putative enhancer mutants of *uge4-3* appear similar to full loss of function *uge4-4*, displaying root epidermal bulging, collapsed epidermal cells, and wrinkled roots (14). Under the described conditions, *sos5* mutants can be distinguished from wild type by their fatter root. Putative suppressors of *sos5* display a more wild-type-like root morphology. The typical *sos5* phenotype is only seen upon transfer to high salt medium (6). Germination on high salt medium is not recommended as it reduces germination efficiency of both mutant and wild-type seedlings.
7. To perform an additional confirmation of the nature of the putative modifier mutations, putative *uge4-3* enhancer seedlings are transferred to plates containing Gal-selection medium and putative *sos5* suppressor seedlings are transferred to high salt medium. Because the effect of the *uge4* mutation on cell walls is suppressed by 5 mM galactose (15), a *uge4-3* enhancer *uge4-3* double mutant appears more like wild type on Gal-selection medium. The phenotype of *sos5* is clearly distinct from wild type upon transfer to high salt medium. A *sos5 suppressor*, *sos5* double mutant looks more like wild type under these conditions.
8. After the appearance of the putative modifier mutants is confirmed for 48 h on second selection plates, seedlings are transferred to soil to harvest M2 seeds.

3.3. Secondary Screen

1. To confirm heritability of the modifier trait, M2 families of putative double mutants are plated and germinated on SGM (see Subheading 3.2).

2. Five days after germination, equal numbers of putative *uge4-3* enhancers are transferred to Gal-selection medium and SGM. Phenotype of a genuine enhancer should be clearly distinct on the two media. Putative *sos5* suppressors are transferred to high salt medium and SGM. Phenotypes of genuine suppressors should be similar on either medium.

3.4. Establishing a Genetic Model and a Mapping Population

A crucial part of mutant gene localization and mapping approaches and following the initial mutagenesis of *Arabidopsis thaliana* plants is the crossing of mutant lines. The back-crosses are performed between modifier mutants and their genetic background i.e., *uge4-3* and *sos5* single mutants, respectively. Because neither very weak *uge4* nor *sos5* mutant alleles exist in a non-Columbia background, we generate outcrosses for mapping with *Landsberg erecta* (*Ler*) plants. To generate mapping populations, the mutant status of individual F2 plants at the background loci is to be determined by genotyping as described above.

3.4.1. Pollination

1. Choose a suitable acceptor plant (see Note 1) and remove all interfering parts, like pollinated siliques, open flowers, or very young buds (see Fig. 1) with sharp forceps or with scissors.

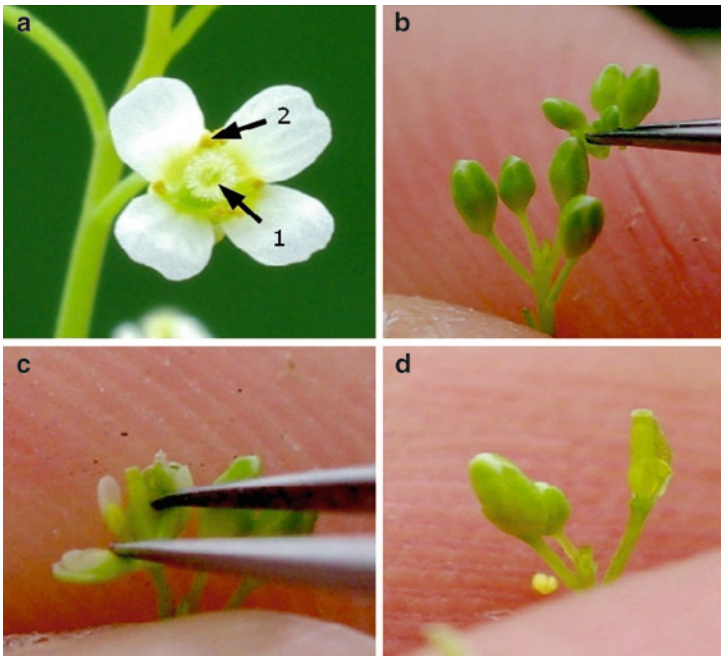

Fig. 1. Preparation for crossing. (**a**) Open donor flower with carpel (*arrow 1*) and stamens containing mature pollen (*arrow 2*). (**b**–**d**) Preparation of the acceptor. (**b**) Removal of very young buds. (**c**) Loosening of a not yet opened acceptor bud to reveal the carpel. (**d**) Carpel after removal of petals and stamens ready for fertilization by a donor flower.

Do not damage the stem while removing the siliques, flowers, or buds.

2. Normally three to five closed big buds are used for the crossing.
3. Puncture the sepal of the closed buds with sharp forceps and carefully open the bud to make the anthers accessible (see Note 2).
4. Remove all anthers to prevent self-fertilization (see Note 2).
5. Excise donor flowers shortly after opening of petals. Squeeze the flower near the base with the forceps and brush it across the exposed acceptor carpels. Pollen should be visible on the stigma.
6. Label the acceptor inflorescence with the donor genotype using adhesive tape. Check the plants after 4–5 days. If the cross was successful, the siliques should be elongated.
7. Before opening of siliques, wrap the pollinated inflorescence into a glassine paper bag (6 × 3 cm) to collect the seeds (see Note 3).

3.4.2. Genetic Analysis of F1 and F2 Offspring

1. Sterilize and plate the seeds on SGM and observe seedlings.
2. In case *uge4-3* is genetically enhanced by a recessive second site mutation, F1 appear like wild type. In case of a dominant enhancer locus, depending on its zygosity in the maternal genome, 50 or 100% of F1 offspring show the enhanced phenotype.

3.4.2.1. F1 Backcrosses

3. Suppressed *sos5* mutant F1 seedlings are transferred to high salt medium. In case of a recessive suppressor mutation in the maternal genome, all seedlings display *sos5* phenotype (6) (see Note 1). In case the maternal genome contained a dominant suppressor mutation, F1 offspring displays salt sensitivity similar to wild type.
4. Allow F1 to self-pollinate to generate a large number of F2 offspring.

3.4.2.2. F2 Backcrosses

1. Sterilize, plate, and observe several hundred F2 seeds.
2. Count the phenotypic and wild type-looking plants.
3. Because the background is homozygous for *uge4-3*, recessive and dominant *uge4-3* enhancer mutations lead to 25 and 75% phenotypic plants, respectively. Recessive and dominant *sos5* suppressors segregate 75 and 25% phenotypic seedlings, respectively after high salt selection. Deviations from these values indicate the presence of more than one modifier mutation in the population.

4. When the segregation ratio indicates simple interactions, additional backcrosses are essential before the mutants are further characterized.

3.4.2.3. F2 Outcrosses

1. Sterilize, plate, and observe several hundred F2 seeds.
2. In the presence of an unlinked, recessive, or dominant *uge4-3* enhancer, 6.25 or 18.75% respectively, of the offspring are expected to be phenotypic. In the outcross of the *sos5* suppressor mutants, 18.75 or 6.25% of F1 show the normal *sos5* phenotype (on high salt medium) in the presence of an unlinked, recessive, or dominant suppressor, respectively.
3. Confirm the expected mutant status via genotyping of phenotypic *uge4-3* plants. Genotype the phenotypically wild type plants at the *SOS5* locus to identify suppressed homozygous *sos5* plants. These plants are expected to contain the *sos5* suppressor mutation and are subsequently used for rough mapping.

3.5. Genomic DNA Extraction

The extraction of genomic DNA from a large number of individual plants is essential for map-based cloning approaches and is inherently time consuming. The presented two alternative extraction protocols are both "quick and dirty" but individually offer advantages in higher DNA yield and lower cost or increased speed, respectively. We recommend protocol 3.5.1 (see Subheading 3.5.1) for rough mapping and protocol 3.5.2 (see Subheading 3.5.2) for collection of recombinant chromosomes during fine mapping.

3.5.1. Genomic DNA Extraction for Rough Mapping (Modified from (19))

1. Leaves or inflorescences are excised and macerated in Eppendorf tubes containing 400 µL of DNA extraction buffer.
2. Debris is pelleted by centrifugation.
3. 300 µL of the extract is transferred into a fresh Eppendorf tube and 300 µL of isopropanol is added to precipitate the DNA.
4. Centrifuge at 16,110 × *g* for 5 min and discard the solution to dry the DNA pellet (see Note 4).
5. After all isopropanol is vaporized, the DNA pellet is resuspended with 50 µL sterile deionised water (see Note 5).

3.5.2. QuickExtract™ Plant DNA Extraction for Fine Mapping

1. Pipette 35 µL of the QuickExtract™ buffer into 200 µL PCR tubes.
2. Transfer excised leaf fragments (ca. 2 × 3 mm) into the buffer.
3. Incubate the leaves at 37°C for 12 min in a thermocycler.
4. Inactivate the enzymes in the buffer at 65°C for 15 min.

3.6. Genotyping: Confirmation of the Mutant Status by (CAPS) Markers

3.6.1. uge4-3 Genotyping

1. Primers: UGE4Seq2F, AGATCATGGACAAAATCTCACC GTCCACCAG; EPIM5R, ATTACTTCCAAAAGTGTAAT AGTCGCAATC.
2. In 200 µL PCR tubes, add 0.7 µL DNA to 9.3 µL of the mastermix for each reaction. Include wild type and mutant controls.
3. Amplify using the following PCR protocol.

94°C	2 min	1 cycle
94°C	10 s	
56°C	10 s	
72°C	35 s	to step 2, 35 cycles
15°C	for ever	for ever

4. Add 10 µL of *Ava*II mastermix and incubate at 37°C for 12 h and at 65°C for 20 min.
5. Add 3 µL of loading buffer to each reaction.
6. Load 10 µL of each reaction to 2% agarose gel and run electrophoresis in 1× TAE buffer (80 V for a 100 mL gel or 100 V for a 250 mL gel).
7. Image the gel in a UV transilluminator after 35 min. Compare the DNA samples with your wild type control and your mutant control to see if they have a *uge4-3* mutation, are heterozygote, or wild type plants.
8. The PCR reaction produces a 708 bp product, which in the wild type, is cut by *Ava*II at one position to yield 425 bp and 283 bp fragments. The *uge4-3* allele is not cut.

3.6.2. sos5 Genotyping

1. Primers: FLASeq3F, ATCACAGTCTTCGTCCCCACCG ACTC; FLASeq3R, TAAAAATAAATAAAGCCCTAATC GAAGG.
2. In 200 µL PCR tubes, add 0.7 µL DNA to 9.3 µL of the mastermix for each reaction. Include wild type and mutant controls. Amplify using the following PCR protocol.

92°C	2 min	1 cycle
92°C	10 s	
68°C	10 s	
72°C	45 s	to step 2, 27 cycles–0.5°C per cycle
92°C	10 s	
54°C	10 s	
72°C	50 s	to step 5, 30 cycles
15°C	for ever	

3. Add 10 µL of *Bfu*I mastermix and incubate at 37°C for 12 h and 65°C for 20 min.
4. Analyze products on a 2% agarose gel.
5. The PCR reaction generates a 603 bp product, which in the wild type, is cut by *Ava*II at one position to yield 324 bp and 279 bp fragments. The *sos5-1* allele is not cut.

3.7. Rough Mapping

Rough mapping positions a mutant locus to an approximate genetic locus on a chromosomal arm. Here, we provide a protocol for a simple mapping procedure as applied to recessive modifiers of *uge4-3* and *sos5*. For general literature on gene mapping in *Arabidopsis* see (20, 25).

1. F2 plants are selected as described in Subheading 3.4.2 (see Note 1).
2. Identify homozygous double mutants for DNA isolation. (In case of *uge4-3* enhancers, confirm homozygous *uge4-3* mutant status and galactose rescuable *uge4* phenotype. In case of *sos5* suppressors, confirm homozygous *sos5* mutant status and absence of high salt induced root swelling.)
3. Make PCR mastermix and use the different primers of the molecular markers to cover all five chromosomal arms (see Subheadings 2.5 and 2.6).
4. Pipette 0.7 µL of DNA into 9.3 µL of the mastermix for each molecular marker.
5. Modify the PCR protocol (see Subheading 3.5.1) by decreasing the annealing temperature to 50°C for nga63, F19G10, nga111, RGA, ciw3, nga172, nga162, nga6, nga8, ciw6, nga1107, nga106, and ciw10 and to 53° for nga168 and nga76.
6. The CAPS marker RGA needs an additional restriction endonuclease digestion step (see Subheading 2.5) using *Rsa*I as the restriction enzyme.
7. Analyze PCR products on 4% agarose gel.
8. Determine the frequency of chromosomes from Columbia vs. Landsberg: A single band counts for two chromosomes for the respective genotype, a doublette counts one for each genotype. Note that the frequency of Landsberg chromosomes will be much less than 50% at two genetic loci. One locus is the original mutation and the other locus is the modifier mutation.
9. To confirm the recessive nature of the mutation, approximately 100 F3 seeds are germinated and inspected at selective conditions to confirm homozygosity of the modifier allele.

3.8. Fine Mapping

After the approximate location has been roughly mapped, the exact location can be determined by searching for wild type DNA on either side of the rough location. Fine mapping usually requires the generation of new markers at high density close to the mutant locus. Markers can be self-designed by using the Monsanto polymorphism collection (also available at http://www.arabidopsis.org; registration required to access the data), which comprises of polymorphisms, either single nucleotide (SNP), or single sequence length polymorphisms (SSLP) between the two ecotypes Columbia (col-0) and Landsberg (ler).

1. Sterilize and plate seeds of the mapping population (see Subheading 3.2).
2. Select phenotypic plants.
3. Extract DNA of phenotypic plants (see Subheading 3.5).
4. In case of a secondary mutation (enhancer or suppressor of a primary mutant), genotype the primary mutant locus to make sure the plants used for mapping are homozygous for the mutation at this locus or heterozygous. This information is crucial, as ratio of phenotypic to nonphenotypic plants in the F3 generation determines the status of the modifier locus.
5. Identify recombinant plants by testing each DNA with two markers, one on each site of the rough location of the mutation. Plants in which the genotypes at these two markers differ from each other are considered recombinants and can be used to further delimit the locus.
6. Transfer recombinant plants to soil and collect F3 seeds.
7. Plate approximately 100 F3 seeds of each population and assess phenotype to determine mutant status and zygosity at the modifier locus.
8. The presence of Columbia (mutant) and Landsberg (wild type) chromosomes has to be equivalent to the genotype of modifier locus as determined in the F3 population. If the genotype at a particular marker is different from the genotype of the modifier background, then the corresponding genomic position can be ruled out as candidate region. Gradually, identifying more genetic markers and recombinant chromosomes closer to the mutant locus allows delimitation of the position of the modifier locus until sequencing of candidate genes becomes economically feasible.

3.9. Sequencing

1. Using mutant DNA as template, amplify overlapping fragments of open reading frame under investigation, and purify DNA using PCR purification kit or gel extraction kit depending on the specificity of the reaction, according to manufacturer's instructions.

2. Supply isolated DNA and primers to commercial sequencing service.
3. Compare resulting sequences with published wild type sequence.

3.10. Initial Characterization of uge4-3 Enhancers by Immunohistochemistry

3.10.1. Fixation and Embedding

1. Up to eight samples (depending on the material) are arranged side by side and embedded in a block of 2.5% low melting agarose (LMA) prior to fixation. Place a Petri dish on a heating table set to 30°C and add LMA (~1 mL per block). Place the samples parallel to each other into a drop of 2.5% LMA using forceps, until they are covered with LMA. Place them closely to each other but avoid contact between them. Let the LMA drop harden at room temperature and cut out a block containing the sample with a razor blade (see Note 6).
2. Transfer the agarose embedded samples into freshly prepared paraformaldehyde-glutaraldehyde-fixative (1 mL in 1.5 mL tubes).
3. Apply vacuum for 15 min to enhance fixation efficiency, followed by incubation at 4°C for 3 h.
4. Rinse three times 20 min in 0.1 M phosphate buffer, pH 7.
5. Dehydrate the samples in a graded ethanol series in the following concentrations: 30, 50, 70, 80, 90, and 96%, each step for 20 min at 4°C.
6. Remove all ethanol and incubate samples two times with 1 mL LR-White at 4°C, each time for 3 h.
7. Each sample is transferred to individual gelatine capsules or molding trays containing LR-white (two-thirds of final volume). In case of using a molding tray, it is crucial that it can be closed with a lid because oxygen inhibits LR polymerization. Arrange the samples with forceps in a way that the desired orientation is orthogonal to the length axis of the gelatine capsule, fill container with LR White and close the lid (see Note 7).
8. Polymerize at 60°C for 24 h or at room temperature using the accelerator comprised in the embedding kit. Allow blocks to remain at room temperature for at least 12 h after polymerization and before sectioning (see Note 8).

3.10.2. Sectioning

1. Remove the (gelatine) capsule and trim the area containing the samples with a razor blade by cutting away the resin that surrounds sample material. The resulting block containing the sample should be as small as possible. Also make sure to trim the cut surface in the desired angle (in case of transverse sections, orientate the cut surface perpendicular to the length axis of the sample).

2. For immunohistochemistry, sections of 0.5–2 μm are cut either with a glass knife or with a diamond knife on an ultramicrotome.
3. Transfer sections to multiwell microscope slide (add drop of water onto wells to allow sections to spread). If a diamond knife with water bath is used, the sections float on the surface and can be easily transferred with an eyelash. Depending on the size of the section, 3–6 sections can be put on the same well. Evaporate water using a 60°C hot heating block plate (see Note 9).

3.10.3. Antibody Labeling

1. Block slides with 3% BSA in PBS for 1.5 h at room temperature by adding 40 μL aliquots onto slide wells.
2. Remove blocking solution carefully using a micropipette and add 40 μL primary antibody (diluted in blocking solution) to each well and incubate for 2 h at room temperature (see Note 10). In case of the negative control, use blocking solution instead.
3. Wash three times with PBS in the same way as described for other buffers for 1–5 min per washing step.
4. Incubate with secondary antibody (diluted in blocking solution) for 2 h at room temperature (see Note 10) (in case of CBMs: antipoly Histidine, in case of JIMs and LMs gold-conjugated antimouse).
5. Wash three times with PBS.
6. In case of CBMs: Incubate with gold-conjugated antimouse diluted in blocking solution for 2 h at room temperature.
7. Washing (in staining jar): Three times with PBS, one time with PBS containing 0.5% glutaraldehyde, three times with PBS, and one time with dH_2O.
8. Silver enhancement: Mix the required amount (1 drop = 38 μL) of the enhancer and the initiator solution 1:1 and apply 20 μL of the mixture to each well. Incubate for 2 min.
9. Rinse with tap water for at least 10 min.
10. Incubate 5 min with Calcofluor White (0.1% w/v).
11. Briefly wash two times with dH_2O in staining jar.
12. Air dry slides, mount coverslip with glycerol (see Note 11).

3.11. Synthesis of β-Glucosyl Yariv Reagent (24)

1. Place 4 g *p*-nitrophenyl-β-D-glucoside in a flame dried round bottom flask, add 400 mL anhydrous methanol and stir until the compound is completely dissolved (sonication can be used to facilitate dissolving). It is important to maintain anhydrous conditions because water deactivates the catalyst.
2. Add 0.8 g charcoal with 10% Pd as catalyst and stir until evenly suspended.

3. Add 3.84 g ammonium formate as H-donor for the reduction of NO_2 to NH_2 and stir at room temperature until dissolved. Close the flask with a septum and pierce it with a hollow needle to allow H_2 to effuse.

   CAUTION: Use fumehood to prevent the formation of oxyhydrogen!

4. Stir 20 min at 50°C to allow the conversion of NO_2 to NH_2. Let the solution cool down completely.
5. Filter solution, under vacuum, through a methanol prewashed Celite packed column (to remove 10% Pd/C) and wash Celite column with ~300 mL methanol to enhance the yield.
6. Evaporate methanol at 40°C, 100 mbar (The substance starts foaming when methanol is removed) and dissolve in 80 mL HQ H_2O.
7. Removal of ammonium formate: Add ~6 mL 5% H_2SO_4 until pH 3 is reached (use pH test strips) to displace formic acid by the stronger acid H_2SO_4, and distil off ~40 mL at 29°C, 11 mbar. Fill up to 80 mL with HQ water. In order to displace ammonium by the stronger base NaOH, add ~12 mL 5% NaOH until pH 9.2 is reached (use pH test strips) and distil off ~40 mL at 29°C, 11 mbar. Fill up to 80 mL with HQ H_2O.
8. Cool the flask to 0–5°C in an ice-bath and monitor the temperature of the contents. It is crucial that the temperature stays between 0 and 5°C, to enable the subsequent reaction.
9. Prepare sodium nitrite (1.029 g in 56 ml H_2O) and phloroglucinol solution (0.5952 g in 192 mL H_2O).
10. Add sodium nitrite solution drop-wise, keeping the temperature between 0 and 5°C.
11. Add phloroglucinol drop-wise, keeping the temperature between 0 and 5°C.
12. Keep flask on ice (0–5°C) for 30 min.
13. Place flask onto bench allowing the contents to regain room temperature.
14. Adjust to pH 9 adding 5% NaOH.
15. Leave reaction at room temperature for 1.5 h and adjust pH to 9 using 10% NaOH in case it drops below 9 (pH stabilizes after approximately 1.5 h).
16. Slowly add an equal volume (500 mL) absolute ethanol and keep at 4°C over night.
17. Recover the precipitate (=β-glucosyl Yariv) by filtration through a Buechner funnel (pore size 4) and wash two times with absolute ethanol (centrifuge each time before ethanol is decanted).
18. Recover the precipitate by filtration and dry over night using high-vacuum.

19. Test purity of the product using HPLC (and NMR).

    Expected results:

    HPLC: Retention time for *p*-nitrophenyl-β-D-glucopyranoside is 13.5 min, retention time for β-D-glucosyl-Yariv is 12.0 min.

    NMR: *p*-Nitrophenyl-β-D-glucoside (DMSO) δ8.1 (d, 2H, J = 12.0 Hz), δ7.1 (d, 2H, J = 9.0 Hz); β-D-glucosyl-Yariv (DMSO) δ7.5 (d, 6H, J = 12.0 Hz), δ7.1 (d, 6H, J = 12.0 Hz).

3.12. A Semiquantitative Assay for β-Glucosyl Yariv Sensitivity of Arabidopsis Roots

This assay can be used to semiquantitatively determine the sensitivity of seedlings to β-Yariv, a chemical that specifically binds AGPs and hence interferes with their function. This treatment induces programmed cell death (PCD) in roots. Cell death is measured using propidium iodide, a nuclear dye that accumulates in damaged cells. Subsequently the effect of small molecular compounds, or the sensitivity of mutants can be investigated.

1. Sterilize seeds and plate them on 6-well plates, each well containing 1.5 mL SGM (0.4% Phytagel) in a horizontal row in the upper third of each well, and keep plates at 4°C in the dark for 2 days. Use three replicas (1 well = 1 replica) per treatment (see Note 12).
2. Transfer the plates to light and place them horizontally, to allow germination and root grow into the medium, along the bottom of the plate, for 3–4 days. Place the plates vertically for another 1–2 days to allow the roots to grow in parallel and unidirectionally.
3. Apply 1.5 mL of liquid SGM containing β-glucosyl Yariv (to 50 μM of DMSO stock solution) and, for visualization of cell death, PI (3 μL of 1 mg/mL) to each well in the sterile bench and seal the plate with Parafilm® (see Note 13).

   CAUTION: PI is toxic and Yariv dyes are irritant. Always wear gloves!
4. After addition of liquid SGM, incubate plates horizontally.
5. Monitor the increase of PI staining directly on the plates without removing the lid using an inverse fluorescence microscope (e.g., Zeiss Axiovert 200 M with Axio Vision 4.6 software) equipped with a mercury lamp and a suitable fluorescent filter set (Zeiss filter set 15 Ex 546/12 for propidium iodide λ_{ex} = 536 nm, λ_{em} = 617 nm) and record images (e.g., Axio Cam MRc5) of each root tip every 60 min (starting ~3 h after the beginning of Yariv exposure ;which is the duration for the first signs of cell death and hence propidium iodide staining to become visible under the described conditions) for a period of 24 h using a 5× lens (Zeiss A-Plan 5×/0.12). For each time point record around ten root tips. To keep exposure within

the limits of measurement, use PI stained positive control roots (e.g., *uge4-4*) that exhibit a strong cell death phenotype. To set black level, adjust an empty area to zero.

6. In case of partial or complete suppression of cell death, contrast of PI images is low. Therefore, we also record bright field images of each root of the same position and magnification as used for PI images to facilitate the selection of the area used for PI measurement.
7. Image analysis using ImageJ

   This analysis is based on the determination of gray level histograms in a defined area throughout a time course, resulting in an approximate quantification of the increase of cell death.

   Perform image adjustments to maximize contrast across the entire data set (black level subtraction, contrast spread).

   In ImageJ, select the root elongation area using the rectangular selection tool (see white box in Fig. 2a) starting at the region just above the lateral root cap extending to the root hair differentiation zone. Measure the distance from the root tip to the onset of the selection rectangle in the first root and

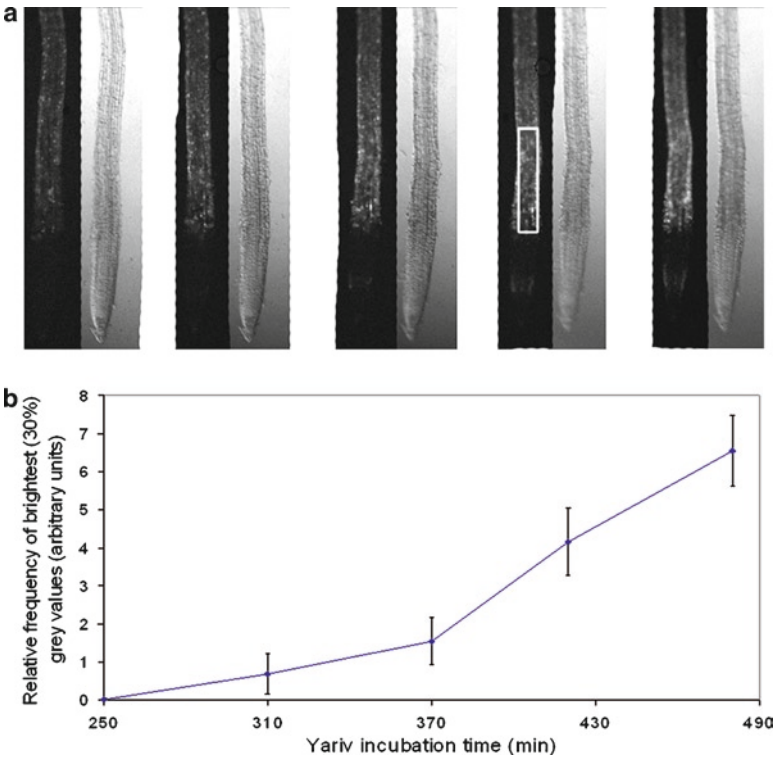

Fig. 2. Analysis of Yariv assay. (**a**) Aligned (representative) PI and bright field images of wild type root tips of each time point of Yariv exposure with selected area for histogram analysis. (**b**) Curve of Histogram analysis representing the increase of PI staining over time.

use this distance as guide for positioning the selection rectangle in all other roots. Use the corresponding bright field images for orientation (Fig. 2a). Perform a histogram analysis and save the values in tabular form. Given correct image adjustments, the top 30% of the recorded gray values represent very bright dead cells and cells undergoing cell death (Fig. 2b).

4. Notes

1. Under our growth conditions in the green house (14 h artificial light mixed with day light and shading of direct sunlight), 40–50 day old plants are at an optimal stage for crosses. Pollination efficiency of greenhouse grown plants shows seasonal and diurnal variation. Sunny morning periods from September to May have been found to yield the most consistent results. Pests such as thrips and aphids greatly reduce success rate hence high phytosanitary standards are essential.
2. Even though the anthers are visible to the naked eye, the use of a magnifying device, such as a dissecting microscope or magnifying goggles, is recommended. We prefer to use goggles in the greenhouse, because plants are continuously exposed to greenhouse conditions and are not heat and light-stressed by microscope illumination.
3. Due to seed dormancy, F1 seeds germinate most efficiently at least 4 weeks after pollination.
4. Optionally, wash pellet with 70% ethanol for better removal of isopropanol.
5. With plant DNA extracted with the QuickExtract™, amplification using KAPA 2G Robust from Kapa Biosystems, we consistently achieved good results.
6. The diameter of the gelatine capsule/tube used for polymerization limits the block size. In case of a gelatine capsule size 0, the block should not be broader than 7 mm.
7. If orienting the sample in the desired way is not possible, the solid resin fragment containing the sample can be cut off and trimmed and glued to the polymerized LR White block in the desired orientation using a two-component glue.
8. In case of heat polymerization, stable temperature conditions are crucial for proper polymerization (±2°C). In case of polymerization at room temperature using the accelerator, polymerization takes place within 10–20 min. Use 1 drop of accelerator per 10 mL LR-White. Addition of the accelerator causes an exothermic reaction, therefore cooling of the molding tray or gelatine capsules on ice is recommended.

9. The negative control is crucial for antibody labeling, therefore an additional well with sections should be prepared.
10. All incubation steps at room temperature can alternatively be done at 4°C over night.
11. In order to prevent the coverslip from slipping off the slide, it is useful to fix it with a piece of sticky tape on both ends.
12. Use Phytagel as gelling agent! Agar is not suitable at such a low concentration.
13. As negative control add the according amount of DMSO. Alternatively, inactive Yariv reagent (e.g., β-Gal Yariv) can be used.

Acknowledgements

We gratefully acknowledge the provision of immunoprobes from Paul Knox and Michael Hahn and *sos5* seeds from Jian-Zhang Zhu. We thank Markus Blaukopf for assisting with the preparation of β-Yariv reagent. This work was supported by the Austrian Science foundation FWF grant P19788.

References

1. Somerville, C., Bauer, S., Brininstool, G., Facette, M., Hamann, T., Milne, J., Osborne, E., Paredez, A., Persson, S., Raab, T., Vorwerk, S., and Youngs, H. (2004) Toward a systems approach to understanding plant cell walls. *Science* **306,** 2206–2211.
2. Ellis, C., Karafyllidis, I., Wasternack, C., and Turner, J. G. (2002) The *Arabidopsis* mutant *cev1* links cell wall signaling to jasmonate and ethylene responses. *Plant Cell* **14,** 1557–1566.
3. Reiter, W. D., Chapple, C., and Somerville, C. R. (1997) Mutants of *Arabidopsis thaliana* with altered cell wall polysaccharide composition. *Plant J* **12,** 335–345.
4. Li, Y., Smith, C., Corke, F., Zheng, L., Merali, Z., Ryden, P., Derbyshire, P., Waldron, K., and Bevan, M. W. (2007) Signaling from an altered cell wall to the nucleus mediates sugar-responsive growth and development in *Arabidopsis thaliana*. *Plant Cell* **19,** 2500–2515.
5. Xu, S. L., Rahman, A., Baskin, T. I., and Kieber, J. J. (2008) Two leucine-rich repeat receptor kinases mediate signaling, linking cell wall biosynthesis and ACC synthase in *Arabidopsis*. *Plant Cell* **20,** 3065–3079.
6. Shi, H., Kim, Y., Guo, Y., Stevenson, B., and Zhu, J. K. (2003) The *Arabidopsis SOS5* locus encodes a putative cell surface adhesion protein and is required for normal cell expansion. *Plant Cell* **15,** 19–32.
7. Hématy, K., Sado, P. E., Van Tuinen, A., Rochange, S., Desnos, T., Balzergue, S., Pelletier, S., Renou, J. P., and Höfte, H. (2007) A receptor-like kinase mediates the response of *Arabidopsis* cells to the inhibition of cellulose synthesis. *Curr Biol* **17,** 922–931.
8. Desprez, T., Vernhettes, S., Fagard, M., Refregier, G., Desnos, T., Aletti, E., Py, N., Pelletier, S., and Höfte, H. (2002) Resistance against herbicide isoxaben and cellulose deficiency caused by distinct mutations in same cellulose synthase isoform CESA6. *Plant Physiol* **128,** 482–490.
9. Scheible, W. R., Eshed, R., Richmond, T., Delmer, D., and Somerville, C. (2001) Modifications of cellulose synthase confer resistance to isoxaben and thiazolidinone herbicides in *Arabidopsis* Ixr1 mutants. *Proc Natl Acad Sci U S A* **98,** 10079–10084.
10. Scheible, W. R., Fry, B., Kochevenko, A., Schindelasch, D., Zimmerli, L., Somerville, S., Loria, R., and Somerville, C. R. (2003) An *Arabidopsis* mutant resistant to thaxtomin A, a cellulose synthesis inhibitor from *Streptomyces* species. *Plant Cell* **15,** 1781–1794.

11. Gu, Y., Deng, Z., Paredez, A. R., DeBolt, S., Wang, Z. Y., and Somerville, C. (2008) Prefoldin 6 is required for normal microtubule dynamics and organization in *Arabidopsis*. *Proc Natl Acad Sci USA* **105,** 18064–18069.
12. Paredez, A. R., Persson, S., Ehrhardt, D. W., and Somerville, C. R. (2008) Genetic evidence that cellulose synthase activity influences microtubule cortical array organization. *Plant Physiol* **147,** 1723–1734.
13. Seifert, G. J., and Roberts, K. (2007) The biology of arabinogalactan-proteins. *Annu Rev Plant Biol* **58,** 137–161.
14. Baskin, T. I., Betzner, A. S., Hoggart, R., Cork, A., and Williamson, R. E. (1992) Root morphology mutants in *Arabidopsis thaliana*. *Aust J Plant Physiol* **19,** 427–437.
15. Seifert, G. J., Barber, C., Wells, B., Dolan, L., and Roberts, K. (2002) Galactose biosynthesis in *Arabidopsis*: genetic evidence for substrate channeling from UDP-D-galactose into cell wall polymers. *Curr Biol* **12**, 1840–1845.
16. Willats, W. G., and Knox, J. P. (1996) A role for arabinogalactan-proteins in plant cell expansion: evidence from studies on the interaction of β-glucosyl Yariv reagent with seedlings of *Arabidopsis thaliana*. *Plant J* **9,** 919–925.
17. Guan, Y., and Nothnagel, E. A. (2004) Binding of arabinogalactan proteins by Yariv phenylglycoside triggers wound-like responses in *Arabidopsis* cell cultures. *Plant Physiol* **135,** 1346–1366.
18. Gao, M., and Showalter, A. M. (1999) Yariv reagent treatment induces programmed cell death in *Arabidopsis* cell cultures and implicates arabinogalactan protein involvement. *Plant J* **19,** 321–331.
19. Edwards, K., Johnstone, C., and Thompson, C. (1991) A simple and rapid method for the preparation of plant genomic DNA for PCR analysis. *Nucleic Acids Res* **19,** 1349.
20. Bell, C. J., and Ecker, J. R. (1994) Assignment of 30 microsatellite loci to the linkage map of *Arabidopsis*. *Genomics* **19,** 137–144.
21. Smallwood, M., Yates, E. A., Willats, W. G., Martin, H., and Knox, J. P. (1996) Immunochemical comparison of membrane associated and secreted arabinogalactan-proteins in rice and carrot. *Planta* **198,** 452–459.
22. McCartney, L., Steele-King, C. G., Jordan, E., and Knox, J. P. (2003) Cell wall pectic (1→4)-β-D-galactan marks the acceleration of cell elongation in the *Arabidopsis* seedling root meristem. *Plant J* **33**, 447–454.
23. Freshour, G., Clay, R. P., Fuller, M. S., Albersheim, P., Darvill, A. G., and Hahn, M. G. (1996) Developmental and tissue-specific structural alterations of the cell-wall polysaccharides of *Arabidopsis thaliana* roots. *Plant Physiol* **110,** 1413–1429.
24. Basile, D. V., and Ganjian, I. (2004) Beta-D-glucosyl and alpha-D-galactosyl Yariv reagents: syntheses from p-nitrophenyl-D-glycosides by transfer reduction using ammonium formate. *J Agric Food Chem* **52,** 7453–7456.
25. Lister, C., and Dean, C. (1993) Recombinant inbred lines for mapping Rflp and phenotypic markers in *Arabidopsis thaliana*. *Plant J* **4,** 745–750.

Chapter 17

Extraction and Detection of Arabinogalactan Proteins

Zoë A. Popper

Abstract

Arabinogalactan proteins are a diverse group of plant cell wall-associated proteoglycans. While structural and molecular genetic analyses have contributed to the emerging improved understanding of the wide-range of biological processes in which AGPs are implicated; the ability to detect, localise, and quantify them is fundamentally important. This chapter describes two commonly used methods, histological staining and radial gel diffusion, both of which utilise the ability of Yariv reagent to bind to AGPs.

Key words: Yariv reagent, Arabinogalactan proteins, Radial gel diffusion, Semi-quantitative detection, Arabinogalactan protein detection

1. Introduction

One of the defining features of plants is that their cells are surrounded by a cell wall consisting of structural polysaccharides and associated proteins. One class of proteins, the arabinogalactan proteins (AGPs), has been strongly implicated in terrestrial plant developmental processes, but their roles are as yet poorly defined (1–7). A further complexity in understanding AGP function is that microarray analysis suggests that it is likely that different AGPs have different functions (8–11).

AGPs consist of two distinct moieties, the carbohydrate and the protein domain. The carbohydrate component typically accounts for 90–98% of an AGP by weight and is rich in arabinose and galactose residues. The protein moiety, accounting for ~10% of an AGP by weight is hydroxyproline-rich (7). However, there is a wide range of variability in the structure and composition of AGPs such that they are frequently classified as being classical or non-classical AGPs (9–15). Classical AGPs contain a hydrophobic transmembrane domain, which in mature AGPs is replaced by a

Zoë A. Popper (ed.), *The Plant Cell Wall: Methods and Protocols*, Methods in Molecular Biology, vol. 715,
DOI 10.1007/978-1-61779-008-9_17,

glycosylphosphatidylinositol (GPI) lipid anchor (10, 14, 16–18); this domain appears to be lacking from the non-classical AGPs (10). Non-classical AGPs also tend to be less heavily glycosylated (19). Differences in AGP composition have also been discovered, which can be related to terrestrial plant taxonomy, for example, bryophyte AGPs contain the sugar residue 3-*O*-methyl-L-rhamnose, which appears to be absent from flowering plant AGPs (20).

AGPs are widespread in land plants (21) and more recently have been found in the cell walls of fresh-water green algae, *Micrasterias* (22) and *Chara corallina* (23), and green seaweeds including *Codium fragile* (24). It is not yet possible to determine whether and which types of AGPs are present in specific plants based on the analysis of genetic sequence data (5). There are several methods, both *in situ* and *ex situ*, which can be used to detect, quantify, and localise AGPs; each method has been essential to our understanding of AGP structure, function, and localisation. However, all of the methods have some advantages and disadvantages, caused by the structural and compositional diversity present within both the protein and carbohydrate components of AGPs. These are discussed in the introduction to this chapter and because several of the methods are detailed within other chapters of this volume, the protocols for radial-gel diffusion and *in situ* staining with Yariv reagents only are included in this chapter.

Immunocytochemistry (described by Hervé *et al.*, Chapter 7) is one of the most informative methods currently available for the detection and localisation of AGPs within plant tissues. Furthermore, there are several monoclonal antibodies including CCRC-M7 (25), JIM4 (26–28), JIM13–16 (1, 28), LM2 (28, 29), LM14 (30), and MAC207 (21, 28) which are known to recognise specific epitopes present in AGPs and which are commercially available (Biosupplies, Australia; CarboSource, http://www.ccrc.uga.edu/~carbosource/CSS_mabs7-07.html; PlantProbes, http://www.plantprobes.net/). This epitope specificity means that it is likely that a specific monoclonal antibody may recognise a specific AGP or a group of AGPs containing the same epitope. However, it is this specificity which currently poses some limitations because while there are several monoclonal antibodies which are known to detect and bind to epitopes present in AGPs (25–32), it is likely that at present not all AGPs can currently be detected in this way. This problem will eventually be circumvented by the generation and characterisation of a greater array of AGP-specific monoclonal antibodies making monoclonal antibody-based methods even more powerful for the investigation of AGP function.

However, it can also be useful to apply more broad-spectrum methods of detection and several such methods for detecting the presence of AGPs have been developed. These methods nearly all

employ a group of red-brown synthetic phenylglycoside dyes known as Yariv reagents (33). Although the exact mechanism of interaction between Yariv reagents and AGPs has not yet been fully explained (5), they are widely used in detecting and purifying AGPs (34). β-D-Glucosyl and β-D-galactosyl Yariv reagents bind to and precipitate AGPs whereas α-D-galactosyl and α-D-mannosyl Yariv regents do not and are often used as controls (5, 33). Yariv reagents can be used in both *in situ* and *ex situ* methods of AGP detection and quantification. They have also been a key factor enabling determination of the function of AGPs (2, 33). A method for *in situ* Yariv staining of plant tissues is detailed in Subheading 2 and is widely used (34–38). However, it has the disadvantage that staining may be obscured if the plant tissues are deeply pigmented or similarly coloured (red–brown) to Yariv reagent. Colorimetric methods have been used to determine the concentration of AGPs present in plant tissues (39). This method has the advantage that it is quantitative. However, it is not known whether some AGPs are capable of binding greater (or lesser) concentrations of AGPs than others, and it is suggested that non-classical AGPs may display variable binding to β-D-glucosyl Yariv reagent (40). A further problem associated with *in situ* staining and the *in situ* colorimetric method is that Yariv reagents also bind to cellulose (41) giving a slightly coloured background making very low concentrations of AGPs less easy to determine and localise. Therefore, while it has the disadvantage that information regarding tissue-specific localisation is lost, it can be informative in some cases to extract, concentrate, and detect AGPs by Yariv staining *ex situ*. The radial gel diffusion assay developed by Van Holst and Clarke (42) and described below enables detection of low concentrations of AGPs in a cellulose-free environment. The method is semi-quantitative in comparison with a dilution series of gum arabic, and tissue specificity can be partially accommodated by carefully selecting the tissues prior to extraction and has been used to determine which fractions of plant extracts contain AGPs (43, 44).

2. Materials

1. 10 g plant tissue of interest.
2. Extraction buffer: 50 mM Tris–HCl, pH 8, 10 mM EDTA, 0.1% v/v β-mercaptoethanol, 1% w/v Triton X-100 (see Note 1).
3. Ethanol.
4. 50 mM Tris–HCl, pH 8.
5. Bench centrifuge.
6. 1% w/v NaCl.

7. 0.15 M NaCl.
8. Freeze drier.
9. Agarose gel containing β-D-glucosyl Yariv reagent: 1% w/v agar, 0.02% w/v β-glucosyl Yariv reagent (commercially available from Biosupplies Australia, Victoria, Australia or they can be synthesised (33, 45–47) as described by Blaukopf *et al.*, Chapter 16), 0.15 M NaCl, 0.02% w/v sodium azide (see Notes 2 and 3).
10. Agarose gel containing α-D-galactosyl Yariv reagent: 1% w/v agar, 0.02% w/v α-galactosyl Yariv reagent (Biosupplies Australia, Victoria, Australia) (see Note 4), 0.15 M NaCl, 0.02% w/v sodium azide.
11. 2 mg/mL β-D-glucosyl Yariv reagent in 0.15 M NaCl.
12. 2 mg/mL α-D-galactosyl Yariv reagent in 0.15 M NaCl.
13. Autoclave.
14. Petri dishes.
15. 4 mg/mL gum arabic.
16. Parafilm®.
17. Aluminium foil.
18. Scanner or digital camera.
19. Automatic pipettes.
20. 50 and 50 mL screw-capped centrifuge tubes.
21. Magnetic stirrer bar and stirring plate.
22. Glass Pasteur pipette or core borer.
23. Mortar and pestle.
24. Liquid nitrogen.
25. Freezer: –20°C.
26. Microscope slides.
27. Cover slips.
28. Microscope with digital camera attachment.
29. White ceramic tile.
30. Backed razor blade.
31. Rocking platform.
32. 1.5 mL Eppendorf tubes.

3. Methods

3.1. In Situ Staining of AGPs Using Yariv Reagents

1. Cut sections of the plant tissue of interest. We find that careful hand-sectioning with a backed razor-blade on a white ceramic tile works well (see Note 5).

2. Incubate the plant materials in an Eppendorf tube containing 1 mL of 2 mg/mL β-D-glucosyl Yariv reagent in 0.15 M NaCl for 1 h, at room temperature, on a rocking platform.
3. As a control, incubate a duplicate set of plant materials e.g., sections from the same plant tissues in 1 mL of 2 mg/mL α-D-galactosyl Yariv reagent in 0.15 M NaCl under the same conditions.
4. After 1 h, carefully remove the Yariv reagent taking care not to damage the plant materials (see Note 6).
5. Add 1 mL of 0.15 M NaCl to each of the Eppendorf tubes and incubate at room temperature for 5 min.
6. Steps 4 and 5 should be repeated several times until the 0.15 M NaCl is no longer appreciably red.
7. Transfer the sections to microscope slides, examine and record using a light microscope with a digital camera attached to it (35–38).

3.2. Extraction of Arabinogalactan Proteins

1. Grind 10 g of plant material to a fine power in liquid nitrogen in a mortar and pestle (see Note 7).
2. Add 10 mL of extraction buffer (50 mM Tris–HCl, pH 8, 10 mM EDTA, 0.1% v/v β-mercaptoethanol, 1% w/v Triton X-100) to the plant material and incubate at 4°C for at least 3 h.
3. Centrifuge for 10 min at 4,000 × *g*.
4. Carefully remove the supernatant using a Pasteur pipette and precipitate polysaccharides and glycoproteins with 5 volumes of ethanol at 4°C for at least 16 h.
5. Centrifuge for 2 min at 2,000 × *g*.
6. Carefully remove the supernatant taking care not to disturb the pellet (see Note 8).
7. Resuspend the pellet in 5 mL of 50 mM Tris–HCl, pH 8.
8. Centrifuge for 10 min at 4,000 × *g*.
9. Collect the supernatant into a polypropylene tube.
10. Resuspend the remaining pellet in 5 mL 50 mM Tris–HCl, pH 8.
11. Centrifuge for 10 min at 4,000 × *g*.
12. Carefully remove the supernatant and pool it with that collected in step 9.
13. Freeze and freeze dry the supernatant.
14. Dissolve the dried supernatant in 500 µL 1% w/v NaCl (see Notes 9–11) (48).

3.3. Detection of Arabinogalactan Proteins by Radial Gel-Diffusion

Extracts using methods including the one described above may be used to detect the presence of AGPs in plant materials. It is semi-quantitative if a serial dilution of a known source of AGPs e.g., gum arabic is included in the assay for comparison. A degree of tissue specificity is enabled by carefully selecting the plant materials from which the extracts are made. Additional samples that can be investigated for the presence and concentration of AGPs include the culture medium of plant tissue cultures. Some AGPs are secreted into the culture medium (15, 49), which can be filtered to remove any cell debris, and then freeze-dried prior to use in the assay (42).

1. Use the end of a glass Pasteur pipette or a core borer to cut out wells in the agarose gel containing β-D-glucosyl Yariv reagent.
2. Into one well load 20–50 μL of 1% w/v NaCl (see Note 12).
3. Into another well load a known amount of gum arabic. If you are investigating whether AGPs are present or not, then 20–40 μL of a 4 mg/mL solution of gum arabic is suitable. However, if you are trying to quantify the concentration of AGPs in the extract or for a given quantity of plant tissue, then it is advisable to include several wells on the plate, which are loaded with a dilution series of gum arabic starting with 2–4 mg/mL. The minimum concentration of gum arabic that will give a positive result using this method is 0.25 mg/mL.
4. Load your extract prepared as described in Subheading 3.1 into remaining wells. It can be useful to load your extracts into two different wells at two different loadings i.e., in one well load twice the volume that you load in another well (see Note 13).
5. Seal plates with Parafilm® to prevent them drying out.
6. Store the plates at room temperature, in darkness, for at least 48 h (see Notes 14 and 15).
7. After 48 h, the results can be recorded either by scanning the plate or by taking a photograph using a digital camera (see Note 16). An example is shown in Fig. 1.

4. Notes

1. The extraction buffer generally requires at least 2 h stirring to sufficiently dissolve the Triton X-100.
2. Caution, sodium azide is highly toxic. Gloves should be worn.
3. Inclusion of sodium azide means that sterile conditions are not required. The AGP extracts contain high sugar content

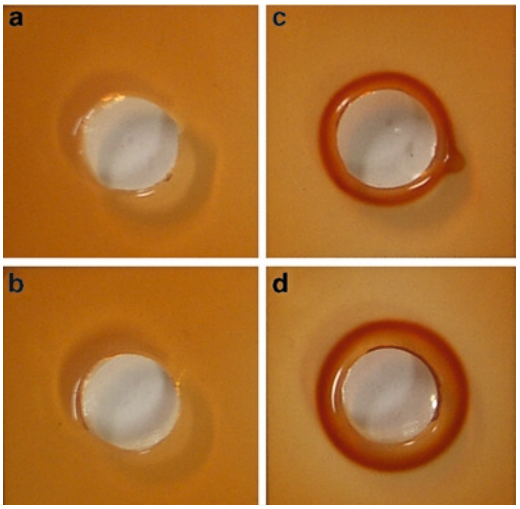

Fig. 1. Radial gel diffusion assay. (**a**, **b**) 20- and 40-μL loadings of 0.15 M NaCl. (**c**, **d**) 20- and 40-μL loadings of a solution of 4 mg/mL gum arabic in 0.15 M NaCl.

and could quickly become contaminated with microbes. However, heat sterilisation could be damaging to the AGPs, and filter sterilisation is not practical owing to the viscosity of many of the extracts.

4. α-D-Mannosyl Yariv reagent (Biosupplies, Australia Pty Ltd.) can be used in place of α-D-galactosyl Yariv reagent.
5. Microalgae and other plant materials can also be surface-labelled using the same procedure but in this case are not sectioned prior to incubation.
6. We often find that some very thin hand sections can be damaged if bathing solutions are removed too rapidly. One way to minimise this is by using a glass Pasteur pipette which has been heated and stretched so that the opening is narrower than normal. This also helps prevent uptake into the glass Pasteur pipette which may occur if the sections or plant materials that are being stained are either very thin and/or very small.
7. In order to protect the mortar and pestle from possible damage due to sudden temperature changes, it is best to cover the mortar and pestle in cling film/Saran wrap® and place it in a –20°C freezer for at least 2 h prior to use.
8. One of the easiest ways to do this is by using a Pasteur pipette which has been stretched over a flame to reduce the width of the tip.
9. It is useful to weigh the freeze-dried sample so that the mg/mL of dissolve extract used in radial gel diffusion can be calculated.
10. Some of the extracts may have a high sugar content and fail to freeze at –20°C, or once frozen they thaw rapidly. In this

case, the extracts may be frozen at –80°C or alternatively can be dialysed against distilled water, at 4°C, to remove any sugars with a low degree of polymerisation (DP). To prevent microbial growth in the extract, it is recommended that dialysis is against 0.05% w/v chlorbutol (1,1,1-trichloro-2-methyl-2-propanol), which is volatile so will be removed on freeze drying (49).

11. If at this concentration the solution is extremely viscous or if there is a large amount (greater than 0.2 g) of freeze-dried extract, it is advisable to dissolve the sample in a larger volume of 1% w/v NaCl.
12. If your samples are not dissolved in 1% w/v NaCl, then load the buffer that they were dissolved in the control wells instead of the 1% w/v NaCl.
13. It is essential that each well on the plate is clearly labelled. We find this easiest to do by printing a grid of 1.2×1.2 cm squares onto an acetate sheet, which can be stuck to the back of the Petri dish. Each well is then punched into the centre of a square.
14. Darkness can be achieved by wrapping the plates in aluminium foil.
15. The plates can be stored for several weeks, even in the light, at room temperature provided that they are sealed with Parafilm® and do not dry out.
16. It takes ~48 h for the AGPs to diffuse into the gel and the Yariv reagent to bind to and precipitate them.

Acknowledgements

Quentin Coster, a visiting MSc student from the Université Catholique de Louvain, Belgium, and Tanya Slattery, an undergraduate project student in Botany and Plant Science at NUI Galway, are thanked for their technical assistance.

References

1. Knox, J. P., Linstead, P. J., Peart, J., Cooper, C., and Roberts, K. (1991) Developmentally-regulated epitopes of cell surface arabinogalactans-proteins and their relation to root tissue pattern formation. *Plant J* **1**, 317–326.
2. Lee, K. J. D., Sakata, Y., Mau, S.-L., Pettolino, F., Bacic, A., Quatrano, R.S., Knight, C. D., and Knox, J. P. (2005) Arabinogalactan proteins are required for apical cell extension in the moss *Physcomitrella patens*. *Plant Cell* **17**, 3051–3065.
3. Basile, D. V., Kushner, B. K., and Basile, M. R. (1989) A new method for separating and comparing arabinogalactan proteins in the Hepatica. *Bryologist* **90**, 401–404.
4. Basile, D. V. (1980) A possible mode of action for morphoregulatory hydroxyproline-proteins. *Bull Torrey Bot Club* **107**, 325–338.
5. Seifert, G. J., and Roberts, K. (2007) The biology of arabinogalactan proteins. *Annu Rev Plant Biol* **58**, 137–161.

6. Seifert, G. J., Barber, C., Wells, B., and Roberts, K. (2004) Growth regulators and the control of nucleotide sugar flux. *Plant Cell* **16**, 723–730.
7. Fincher, G. G., Stone, B. A., and Clarke, A. E. (1983) Arabinogalactan-proteins: structure, biosynthesis and function. *Annu Rev Plant Physiol* **34**, 47–70.
8. Schultz, C. J., Rumsewicz, M. P., Johnson, K. L., Jones, B. J., Gaspar, Y. M., and Bacic, A. (2002) Using genomic resources to guide research directions. The arabinogalactan protein gene family as a test case. *Plant Physiol* **129**, 1448–1463
9. Gaspar, Y., Johnson, K. L., McKenna, J. A., Bacic, A., Schultz, C. J. (2001) The complex structures of arabinogalactan-proteins and the journey towards understanding function. *Plant Mol Biol* **47**, 161–176.
10. Majewska-Sawka, A., and Nothnagel E. A. (2000) The multiple roles of arabinogalactan proteins in plant development. *Plant Physiol* **122**, 3–9.
11. Kieliszewski, M. J., and Lamport, D. T. A. (1994) Extensin: repetitive motifs, functional sites, post-translational codes, and phylogeny. *Plant J* **5**, 157–172.
12. Nothnagel, E. A., Bacic, A., and Clarke, A. E. (2000) Cell and Developmental Biology of Arabinogalactan-proteins. *New York: Kluwer.*
13. Nothnagel, E. A. (1997) Proteoglycans and related components in plant cells. *Int Rev Cytol* **174**, 195–291.
14. Du, H., Simpson, R. J., Clarke, A. E., and Bacic, A. (1996) Molecular characterization if a stigma-specific gene encoding an arabinogalactan protein (AGP) from *Nicotiana alata*. *Plant J* **9**, 313–323.
15. Mau, S. L., Chen, C. G., Pu, Z, Y, Moritz, R. L., Simpson, R. J. and Bacic, A. (1995) Molecular cloning of cDNAs encoding the protein backbones for arabinogalactan proteins from the filtrate of suspension-cultured cells of *Pyrus communis* and *Nicotiana alata*. *Plant J* **8**, 269–281.
16. Oxley, D., and Bacic, A. (1999) Structure of the glycosylphosphatidylinositol membrane anchor of an arabinogalactan protein from *Pyrus communis* suspension-cultured cells. *Proc Natl Acad Sci USA* **6**, 14246–14251.
17. Svetek, J., Yadav, M. P., and Nothnagel, E. A. (1999) Presence of a glycosylphosphatidylinositol lipid anchor on rose arabinogalactan proteins. *J Biol Chem* **274**, 14724–14733.
18. Youl, J. J., Bacic, A., and Oxley, D. (1998) Arabinogalactan-proteins from *Nicotiana alata* and *Pyrus communis* containglycosylphosphatidylinositol membrane anchors. *Proc Natl Acad Sci USA* **95**, 7921–7926.
19. Showalter, A. M. (2001) Arabinogalactan proteins: Structure, expression and function. *Cell Mol Life Sci* **58**, 1399–1417.
20. Fu, H., Yadav, M. P., and Nothnagel, E. A. (2007) *Physcomitrella patens* arabinogalactan proteins contain abundant terminal 3-*O*-methyl-L-rhamnosyl residues not found in Angiosperms. *Planta* **226**, 1511–1524.
21. Pennell, R. I., Knox, J. P., Scofield, G. N., Selvendran, R. R., and Roberts, K. (1989) A family of abundant plasma membrane-associated glycoproteins related to the arabinogalactan proteins is unique to flowering plants. *J Cell Biol* **108**, 1967–1977.
22. Eder, M., Tenhaken, R., Driouich, A., and Lütz-Mendel, U. (2008) Occurrence and characterization of arabinogalactan-like proteins and hemicelluloses in *Micrasterias* (Streptophyta). *J Phycol* **44**, 1221–1234.
23. Domozych, D. S., Sørensen, I., and Willats, W. G. T. (2009) The distribution of cell wall polymers during antheridium development and spermatogenesis in the Charophycean green alga, *Chara corallina*. *Ann Bot* **104**, 1045–1056.
24. Estevez, J. M., Fernández, P. V., Kasulin, L., Dupree, P., and Ciancia, M. (2009) Chemical and *in situ* characterization of macromolecular components of the cell walls from the green seaweed *Codium fragile*. *Glycobiology* **19**, 212–228.
25. Steffan, W., Kovác, P., Albersheim, P., Darvill, A. G., and Hahn, M. G. (1995) Characterization of a monoclonal antibody that recognizes an arabinosylated (1→6)-β-D-galactan epitope in plant complex carbohydrates. *Carbohydr Res* **275**, 295–307.
26. Knox, J. P., Day, S., and Roberts, K. (1989) A set of cell wall surface glycoproteins forms a marker of cell position, but not cell type, in the root apical meristem of *Daucus carota* L. *Development* **106**, 47–56.
27. Stacey, N. J., Roberts, K., and Knox, J. P. (1990) Patterns of expression of JIM4 arabinogalactan protein epitope in cell cultures and during somatic embryogenesis in *Daucus carota* L. *Planta* **180**, 285–292.
28. Yates, E. A., Valdor, J. F., Haslam, S. M., Morris, H. R., Dell, A., Mackie, W., and Knox, J. P. (1996) Characterization of carbohydrate structural features recognised by anti-arabinogalactan-protein monoclonal antibodies. *Glycobiology* **6**, 131–139.

29. Smallwood, M., Yates, E. A., Willats, W. G. T., Martin, H., and Knox, J. P. (1996) Immunochemical comparison of membrane-associated and secreted arabinogalactan-proteins in rice and carrot. *Planta* **198**, 452–459.
30. Moller, I., Marcus, S. E., Haeger, A., Verhertbruggen, Y., Verhoef, R., Schols, H., Mikkelsen., J. D., Knox, J. P., and Willats, W. G. T. (2008) High-throughput screening of monoclonal antibodies against plant cell wall glycans by hierarchical clustering of their carbohydrate microarray binding profiles. *Glycoconj J* **25**, 37–48.
31. Norman, P. M., Wingate, V. P. M., Fitter, M. S., and Lamb, C. J. (1986) Monoclonal antibodies to plant plasma-membrane antigens. *Planta* **167**, 452–459.
32. Norman, P. M., Kjellbom, P., Bradley, D. J., Hahn, M. G., and Lamb, C. J. (1996) Immunoaffinity purification and biochemical characterization of plasma-membrane arabinogalactans-rich glycoproteins of *Nicotiana glutinosa*. *Planta* **181**, 365–373.
33. Yariv, M., Rapport, M. M., and Graf, L. (1962) The interaction of glycosides and saccharides with antibody to corresponding phenyl glycosides. *Biochem J* **85**, 383–388.
34. Willats, W. G. T., and Knox, J. P. (1996) A role for arabinogalactan-proteins in plant cell expansion: evidence from studies on the interaction of β-D-glucosyl Yariv reagent with seedlings of *Arabidopsis thaliana*. *Plant J* **9**, 919–925.
35. Anderson, R. L. , Clarke, A. E. , Jermyn, M. A., Knox, R .B. , and Stone, B. A. (1977) A carbohydrate binding arabinogalactan-protein from liquid suspension cultures of *Lolium multiflorum* endosperm. *Aust J Plant Physiol.* **4**, 143–158.
36. Clarke, A. E., Anderson, A. L., and Stone, B. A. (1979) Form and function of arabinogalactans and arabinogalactan proteins. *Phytochemistry* **18**, 521–540.
37. Gleeson, P. A., and Clarke, A. E. (1979) Structural studies on the major component of Gladiolus style mucilage, an arabinogalactan protein. *Biochem J* **181**, 607–621.
38. Jermyn, M. A., and Yeow, M. (1975) A class of lectins present in the tissues of seed plants. *Aust J Plant Physiol* **2**, 501–531.
39. Lamport, D. T. A., Kieliszewski, M. J., and Showalter, A. M. (2005) Salt stress upregulates periplasmic arabinogalactan proteins: using salt stress to analyse AGP function. *New Phytol* **169**, 479–492.
40. Sommer-Knudsen, J., Clarke, A. E., and Bacic, A. (1997) Proline- and hydroxyproline-rich gene products in the sexual tissues of flowers. *Sex Plant Reprod* **10**, 253–260.
41. Triplett, B. A., and Timpa, J. D. (1997) β-Glucosyl and α-galactosyl Yariv reagents bind to cellulose and other glucans. *J Agric Food Chem* **45**, 4650–4654.
42. Van Holst G. -J., and Clarke, A. E. (1985) Quantification of arabinogalactans-protein in plant extracts by single radial gel diffusion. *Anal Biochem* **148**, 446–450.
43. Osman, M., Menzies, A. R., Albo Martin, B., Williams, P. A., Phillips, G. O., and Baldwin, T.C. (1995) Characterization of gum arabic fractions obtained by anion-exchange chromatography. *Phytochemistry* **38**, 409–417.
44. Parveen, S., Gupta, A. D., and Prasad, R. (2006) Arabinogalactan protein from *Arachis hypogaea*: role as a carrier in drug formulations. *Int J Pharm* **333**, 78–86.
45. Yariv, J. H., Lis, E., Katchalshi, E. (1967) Precipitation of arabic acid and some seed polysaccharides by glycosyl phenylazo dyes. *Biochem J* **195**, 1c–2c.
46. Basile, D. V., and Ganjian, I. (2004) β-D-Glucosyl and α-D-galactosyl Yariv reagents: Syntheses from *p*-nitrophenyl-D-glycosides by transfer reduction using ammonium formate. *J Agr Food Chem* **52**, 7453–7456.
47. Blaukopf, C., Krol, M. Z., and Seifert, G. J. (2011) New insights into the control of cell growth. Zoë A. Popper (Ed.), *The Plant Cell Wall: Methods and Protocols.* Humana Press, New Jersey, USA, pp. 221–244.
48. Schultz, C. J., Johnson, K. L., Currie, G., and Bacic, A. (2000) The classical arabinogalactan protein gene family of Arabidopsis. *Plant Cel*l **12**, 1751–1768.
49. Fry, S. C. (2000). The Growing Plant Cell Wall: Chemical and Metabolic Analysis. Reprint Edition, Blackburn, Caldwell, NJ. [ISBN 1-930665-08-3].

Chapter 18

Characterization of the Plant Cell Wall Proteome Using High-Throughput Screens

Sang-Jik Lee and Jocelyn K.C. Rose

Abstract

Plant cell wall proteins play essential roles in many important biological processes, and yet there is still not a comprehensive catalogue of the cell wall proteome, or "secretome". Here, we describe three procedures, including a yeast secretion trap (YST), *Agrobacterium*-mediated transient expression using a necrosis-inducing protein (NIP) and protein localization assay using a fluorescent protein, to identify and confirm the localization of cell wall proteins. The approaches are orthogonal and collectively provide a powerful suite of approaches to complement more commonly used strategies to isolate plant cell wall-associated proteins.

Key words: Plant cell wall protein, Secreted protein, Secretome, Yeast secretion trap, Necrosis-inducing protein, Agroinfiltration, Confocal fluorescence, Extracellular matrix

1. Introduction

A large number of plant proteins are secreted to the plant cell wall, or apoplastic environment – where they contribute to reinforcement or restructuring of wall architecture, protection from pathogen attack and abiotic stresses, signalling and metabolism of apoplastic compounds (1, 2). However, there is still only a superficial understanding of the plant cell wall proteome, both in terms of the complement of secreted proteins and the dynamics of their expression. There is therefore considerable interest in better defining the composition of the plant cell wall proteome, or "secretome", either by non-targeted profiling of secreted protein populations or by examining the localization, accumulation, and structure of specific cell wall proteins.

Many proteomics projects target subcellular proteomes by extracting highly pure organelle extracts and then fractionating

Zoë A. Popper (ed.), *The Plant Cell Wall: Methods and Protocols*, Methods in Molecular Biology, vol. 715,
DOI 10.1007/978-1-61779-008-9_18,

and sequencing the constituent proteins, typically using advanced mass spectrometry methods. However, in this regard the cell wall proteome presents a number of conceptual and practical challenges (1). For example, unlike subcellular compartment such as the chloroplast or nucleus, the apoplast is a continuum, which limits the ability to isolate a more comprehensive and uncontaminated cell wall protein extract. In addition, many cell wall proteins can be covalently linked into the cell wall matrix and so highly resistant to extraction. Therefore, while there are many studies that have examined the protein content of apoplastic fluids, or cell wall associated extracts, such an approach inevitably involves both protein losses and contamination by intracellular proteins (3).

An alternative approach is to use computational prediction to search for canonical N-terminal signal peptides that target proteins to the classical secretory pathway (1). However, it is important to bear in mind that this only identified proteins that are targeted to the canonical secretory pathway, and the encoded proteins may be retained within that pathway or targeted to intracellular organelles or compartments. In other words, the presence of an ER-targeting N-terminal signal peptide does not indicate that the associated mature polypeptide is ultimately secreted to the cell wall. Additionally, there is growing evidence that a subset of cell wall/apoplastic proteins are secreted via non-classical secretion pathways, as has been reported in animals (4), and yeast (5).

A third option is to use so-called functional screens, where genes encoding secreted proteins are identified based on the ultimate localization of the encoded protein, utilizing protein markers whose activities confirm targeting to the cell surface.

In this chapter, we describe the use of two such approaches (the YST and NIP screens) to search cDNA libraries for secreted proteins, as well as subsequent confirmation of their localization using fluorescent protein markers (Fig. 1). Such functional approaches can be valuable complements to more traditional strategies involving the fractionation and sequencing of cell wall protein extracts and will provide important information for plant cell wall targeting and localisation of secreted proteins *in vivo* (Fig. 1).

2. Materials

2.1. Yeast Secretion Trap (YST)

1. Fresh or frozen tissues of interest.
2. cDNA Synthesis Kit (Stratagene) (see Note 1).
3. Oligotex mRNA Mini Kit (Qiagen) (see Note 1).
4. QIAquick Gel Extraction Kit (Qiagen) (see Note 1).

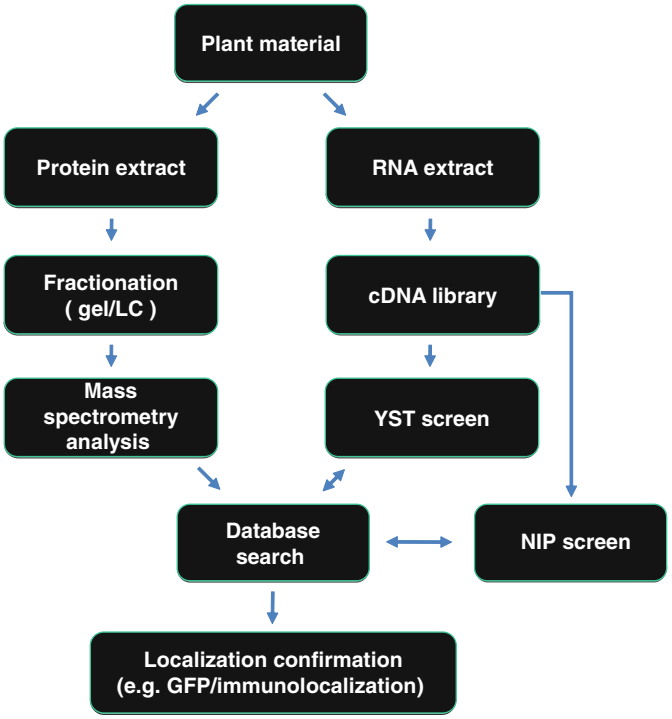

Fig. 1. Flow chart summarizing the steps for identification of plant cell wall proteins. *LC* liquid chromatography.

5. QIAquick PCR Purification Kit (Qiagen) (see Note 1).
6. QIAprep Spin Miniprep Kit (Qiagen) (see Note 1).
7. Cloning vector(s): pYST-0, -1, and -2 three vector set (6). These vectors contain alcohol dehydrogenase (*ADH1*) promoter, invertase (*SUC2*) gene lacking its signal peptide, and *ADH1* terminator.
8. One Shot® TOP10 Electrocomp™ *E. coli* cells (Invitrogen): Electrocompetent cells can be prepared manually (7, 8) or obtained from commercial sources.
9. Random hexamer linker primer: 5′-GAGAGAGAGAGAGA GAACCGCGCGGCCGCCNNNNNN-3′ (*Not* I restriction enzyme site, underlined).
10. Yeast (*Saccharomyces cerevisiae*) strain(s): DBYα2445 (Matα, *suc2Δ9, lys2-801, ura3-52, ade2-101*). The host yeast strain carries a mutation which ensures that the endogenous *SUC2* gene is not expressed (6).
11. Dimethyl sulfoxide (DMSO).
12. Glass beads 425–600 μm, acid-washed (Sigma).
13. Luria–Bertani (LB) medium (broth and agar plate): 10 g/L of tryptone, 5 g/L yeast extract, 10 g/L NaCl, 20 g/L agar

(for plates only). Adjust pH to 7.0 with NaOH solution. Add deionized H_2O to a final volume of 1 L. Autoclave.

14. LB-ampicillin medium (150×15 mm plates): 10 g/L tryptone, 5 g/L yeast extract, 10 g/L NaCl, 20 g/L agar, 100 mg/L ampicillin. Adjust pH to 7.0 with NaOH solution. Add deionized H_2O to a final volume of 1 L. Autoclave.
15. Microcentrifuge tubes and conical tubes.
16. MicroPulser Electroporator (Bio-Rad).
17. Petri dishes.
18. 3 M sodium acetate.
19. 70% (v/v) ethanol.
20. Restriction enzymes (Promega).
21. Sucrose selection medium: 20 g/L Difco peptone, 10 g/L yeast extract, 20 g/L agar (for plates only). Adjust the pH to 6.5 with HCl solution if necessary. Add deionised H_2O to a final volume of 950 mL. Autoclave. Cool to 55°C. Add sucrose (filter-sterilized) to 2% (v/v) by adding 50 mL of a 40% stock solution.
22. T4 DNA ligase (Promega).
23. TE-LiAc solution: Prepare fresh immediately prior to yeast transformation by combining 0.2 mL of 10× TE with 0.2 mL of 10× LiAc. Bring the total volume to 2 mL using sterile H_2O.
24. TE-LiAc-PEG solution: Prepare fresh immediately prior to yeast transformation by adding 1 mL of 10× TE, 1 mL of 10× LiAc and 8 mL of 50% (w/v) PEG 3350 to make the final volume of 10 mL.
25. Yeast lysis buffer: 2% (v/v) Triton X-100, 1% (w/v) SDS, 100 mM NaCl, 10 mM Tris-HCl (pH 8.0), 1 mM EDTA.
26. YEASTMAKER™ Yeast Transformation System 2 (BD Biosciences) contains components (10× LiAc, 10× TE, 50% PEG, and Herring testes carrier DNA, denatured (10 mg/mL)) for yeast transformation.
27. YPD medium: Dissolve 20 g/L peptone and 10 g/L yeast extract. Adjust the pH to 6.5 with HCl solution if necessary. Add deionized H_2O to a final volume of 950 mL. Autoclave and cool to 55°C. Add glucose (filter-sterilized with 0.2-μm membrane filter) to 2% (v/v) by adding 50 mL of a 40% stock solution.
28. Phenol/chloroform/isoamyl alcohol 25:24:1 (v/v/v).

2.2. In Planta Transient Expression of Secreted Protein Genes (NIP screen)

1. *Nicotiana benthamiana*.
2. *Agrobacterium tumefaciens* strains such as C58C1 (9) and GV3101 (10).

3. 20 mM $CaCl_2$
4. Buffer for storing *Agrobacterium* competent cells: 20 mM $CaCl_2$ containing 20% glycerol. Sterilize and reduce temperature to ice-cold before use.
5. Liquid nitrogen for rapid freezing.
6. Microcentrifuge tubes.
7. Conical tubes.
8. Infiltration medium: 10 mM MES pH 5.6, 10 mM $MgCl_2$ and 200 μM acetosyringone (11).
9. *Agrobacterium* culture medium: Luria–Bertani (LB) (see Subheading 2.1).
10. Cloning vectors: pART-NIP^F (see Note 2), pART-NIP^M (see Note 3), pART-$XTH2^{SP}$:NIP^M (see Note 4), and pBIN61S-CymRSV p19 (see Note 5).
11. 1-mL syringe without needle.

2.3. Confocal Fluorescence Imaging for Plant Cell Wall Localization

1. Onion (*Allium cepa* L.)
2. PDS-1000/He biolistic transformation system (Bio-Rad).
3. Confocal laser-scanning microscope equipped with helium/neon lasers.
4. Cloning vector(s): pART-GFP (see Note 6) and pART-PG^{SP}:tdTOMATO (see Note 7).
5. M-10 tungsten particles.
6. Forceps.
7. 50% Glycerol.
8. Isopropanol for soaking rupture disk.
9. Microcentrifuge tubes.
10. 70% ethanol.
11. 100% ethanol.
12. 0.8 M Sucrose.
13. Petri dishes, 100 × 15 mm.
14. Whatman 3MM chromatography paper.
15. 2.5 M $CaCl_2$.
16. 0.1 M Spermidine.

3. Methods

3.1. Yeast Secretion Trap Screen

This screen is based on the principal of generating a library of cDNAs fused to the N-terminus of invertase, and then transforming the library into an invertase-deficient yeast mutant (6). The

transformed yeast mutant collection is then spread on plates of sucrose, and any yeast colony that grows must have been transformed with a gene encoding a secreted protein, the fusion of which to invertase rescued the phenotype. This represents a rapid means to identify large number of genes encoding secreted proteins.

3.1.1. Construction of the YST cDNA Library

1. Isolate polyadenylated mRNA from total RNA using an Oligotex mRNA Mini Kit, according to the manufacturer's instructions.
2. Synthesize the first- and second-strand cDNAs from the mRNA (5 μg) using a random hexamer linker primer containing a *Not*I restriction site for a directional cloning using a cDNA Synthesis Kit (Stratagene) according to the manufacturer's instructions.
3. Ligate the *Eco*RI adapters (provided with the Stratagene cDNA Synthesis Kit) to the blunted cDNAs and phosphorylate the *Eco*RI ends according to the manufacturer's instructions.
4. Purify cDNA using a QIAquick PCR Purification Kit (Qiagen) (see Note 8).
5. Add 5 μL of 10× *Not*I buffer and 5 μL of *Not*I (10 U/μL) to digest 40 μL of the cDNAs. Incubate the reaction for 2 h at 37°C.
6. Run a 1% agarose gel to fractionate the cDNA fragments and excise a gel slice corresponding to the region from approximately 0.3–1.0 kb, as judged using DNA ladder molecular weight markers.
7. Purify the excised cDNAs with a QIAquick Gel Extraction Kit (Qiagen).
8. Ligate the cDNAs into the *Eco*RI and *Not*I sites of the YST vector(s) by adding the eluted cDNA (~20 ng), 1 μL of 10× ligase buffer, 1 μL of T4 DNA ligase and the pYST vectors digested with *Eco*RI and *Not*I (~200 ng, comprising equal quantities of the pYST-0, -1 and -2 vectors), to a final volume of 10 μL. Incubate the reaction overnight at 16°C (see Note 9).
9. Transform 2 μL of the ligation mix into 50 μL of a TOP10 electrocompetent *E. coli* strain (Invitrogen) by electroporation using a MicroPulser (Bio-Rad) according to the manufacturer's instructions. Immediately add 1 mL of SOC medium (provided with TOP10 electrocompetent cells) to the tube to recover the transformed cells. Incubate for 1 h at 37°C. Plate 1 μL of the transformation mixture onto an agar plate supplemented with ampicillin (100 mg/L). Incubate the plate for 16–18 h at 37°C. Count the colonies (see Note 10).

10. Transform the remaining 8 μL ligation mixture into *E. coli* in more electroporation reactions (see Note 11).
11. Plate 250 μL of the transformed *E. coli* cells onto each LB-ampicillin agar plate (150 × 15 mm) at a density of roughly 5×10^4 CFU/plate and incubate the plates for 16–18 h at 37°C.
12. Add 20 mL of LB liquid medium per plate to harvest the transformants from each plate and incubate at 37°C for 3 h with gentle shaking.
13. Pool the overlaying LB cultures in a sterile 250-mL flask (see Note 12).
14. Isolate the library plasmids from 30–50 mL of the bacterial LB cultures according to the manufacturer's instructions as described for the Perfectprep Plasmid Midi Kit.
15. Quantify the amount of the library plasmid DNA using an UV spectrophotometer and store at –20°C.

3.1.2. Yeast Transformation

1. Inoculate 1 mL of YPD liquid medium in a 1.5-mL micro-centrifuge tube with one or two 2–3 m yeast colonies and vortex the culture vigorously to disperse any clumps.
2. Transfer the cells to 50 mL of YPD in a 250-mL flask.
3. Incubate the culture at 30°C for 16–18 h with shaking at 250 rpm.
4. Check the OD at 600 nm using 1 mL of the culture every 30 min until OD at 600 nm reads 1.2.
5. Transfer the 50-mL culture into 300 mL of YPD in a 1-L flask to produce 0.2–0.3 OD at 600 nm.
6. Incubate the culture for 3 h at 30°C, shaking at 250 rpm until OD (600 nm) reaches 0.4–0.6.
7. Centrifuge the cells at 4,500 × *g* for 5 min at room temperature.
8. Discard the supernatant and resuspend the cells by vortexing in 50 mL of sterile H_2O.
9. Centrifuge the cells at 4,500 × *g* for 5 min at room temperature.
10. Discard the supernatant and resuspend cells in 1.5 mL of freshly prepared TE-LiAc solution.
11. In a 50-mL tube, add 50 μg of cDNA library plasmids and 2 mg of carrier DNA (herring testes DNA or salmon sperm DNA) and mix well.
12. In 1.5-mL tubes, add 100 ng of control plasmids (positive: a secreted protein gene in-frame with *suc2*; and negative: a *suc2* fusion construct lacking a signal peptide) and 0.1 mg of carrier

DNA (herring testes DNA or salmon sperm DNA) and mix well (see Note 13).

13. Add 1 mL of yeast competent cells to the tube containing the library plasmids (or 0.1 mL to control tubes) and mix well by vortexing.
14. Add 6 mL of TE-LiAc-PEG solution to the tube containing the library plasmids (or 0.6 mL to control tubes) and mix well by vortexing.
15. Incubate at 30°C for 30 min with shaking at 200 rpm.
16. Add 700 μL of DMSO to the tube containing the library plasmids (or 70 μL to control tubes) and mix well gently (see Note 14).
17. Heat-shock the samples by incubating for 15 min in a 42°C water bath and swirl gently every 5 min.
18. Place the tubes on ice for 5 min.
19. Centrifuge the cells at 4,500 × *g* for 5 min (or 15 s for controls) at room temperature.
20. Remove the supernatant and resuspend cells in 5 mL (or 0.5 mL for controls) of 1× TE buffer.
21. Spread 200 μL of the transformation mixture onto a 150 × 15 mm plate containing the sucrose selection medium (or 100 μL onto a 100 × 15 mm plate for controls).
22. Incubate plates at 30°C for 6–10 days (Fig. 2, see Note 15).

3.1.3. Identification of cDNA Clone Encoding a Putative Signal Peptide

1. Streak all the growing yeast transformants on the sucrose selection medium and incubate at 30°C for 2 days.
2. Inoculate yeast cells from the streaked plate with a sterile spatula into 2 mL of sucrose selection medium and incubate at 30°C for 16–18 h.

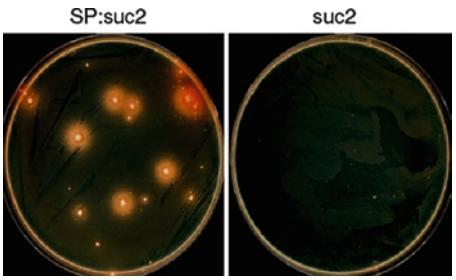

Fig. 2. Yeast secretion trap (YST) system to identify secreted proteins. The invertase-deficient yeast mutant can be rescued when the cDNA encodes a secreted protein fused with the invertase (SP:suc2, as shown at left), but the mutant yeast cells are unable to grow on a sucrose selection medium because the invertase is not secreted (suc2, as shown at *right*).

3. Transfer the culture into a 2.0-mL microcentrifuge tube and centrifuge the cells at 14,000×*g* for 2 min and discard the supernatant.
4. Resuspend the pellet in 0.2 mL of yeast lysis buffer with 0.2 g of glass beads by vortexing vigorously for 2 min.
5. Add 0.2 mL of phenol/chloroform/isoamyl alcohol (25:24:1 (v/v/v)) and vortex vigorously for 2 min (see Note 16).
6. Centrifuge at 14,000×*g* for 5 min and transfer the upper aqueous layer into a new tube.
7. Precipitate the DNA by adding 20 μL of 3 M sodium acetate and 500 μL of absolute ethanol and mix well by vortexing. Precipitate the DNA overnight at −20°C.
8. Centrifuge at 14,000×*g* for 10 min to pellet the DNA.
9. Wash the DNA pellet by adding 0.5 mL of 70% (v/v) ethanol and spin at 14,000×*g* for 2 min at room temperature.
10. Resuspend the DNA pellet in 35 μL of sterile H_2O or TE buffer (see Note 17).
11. Transform 1 μL of DNA into electrocompetent *E. coli* cells by electroporation and select transformants on LB plates supplemented with the ampicillin.
12. Identify colonies that contain the YST vector by preparing miniprep DNA from colonies on the LB-ampicillin agar plates with a QIAprep Spin Miniprep Kit (Qiagen) and by restriction enzyme digestion.
13. Perform DNA sequencing using a specific primer (5′-TCCT CGTCATTGTTCTCGTTCC-3′) derived from YST vector to confirm in-frame fusion between the cDNA and the *suc2* invertase gene.
14. Signal peptides of the translated amino acid sequences can be predicted computationally using publicly available signal peptide prediction programs such as SignalP version 3.0 (www.cbs.dtu.dk/services/SignalP)(12).

3.2. In Planta Transient Expression Screen of Secreted Protein Genes (NIP Screen)

This screen is somewhat similar to the YST screen described above, except that a "necrosis inducing protein" (NIP) is used as a marker, rather than invertase. NIP acts as a toxin and is known to induce rapid necrosis in compatible plant species when localized in the apoplast, but not in the cytosol (13). Briefly, the NIP screen works by fusing a cDNA population to the N-terminus of a NIP gene. The NIP-fusion library is then transformed into *A. tumefaciens* and a library spread among 96-well plates. Media containing the individual *A. tumefaciens* transformants is then flooded into the apoplast of *N. benthamiana* leaves. The presence of a secreted NIP fusion protein will then be evident by a rapid cell death/necrosis phenotype.

3.2.1. Preparation of Agrobacterium Competent Cells

1. Streak out *Agrobacterium* strain from glycerol stock stored at –80°C onto LB agar plate supplemented with the appropriate antibiotic and incubate the preculture for 3 days at 28°C.
2. Inoculate a single colony into 2 mL of LB liquid medium and incubate the culture overnight at 28°C under constant agitation at 250 rpm.
3. Transfer 1 mL of culture to inoculate 50 mL of LB liquid medium in a 250-mL flask.
4. Incubate the culture at 28°C under constant agitation at 250 rpm to an OD (600 nm) of 0.5–1.0.
5. Chill the culture on ice for 5 min and harvest cells in pre-chilled 50-mL tube by centrifugation for 10 min at 4,500 × *g* at 4°C.
6. Resuspend the cells in 1 volume of ice-cold, sterile 20 mM $CaCl_2$.
7. Repeat Step 5.
8. Resuspend the cells in 1 mL of ice-cold, sterile 20 mM $CaCl_2$/20% glycerol.
9. Freeze 50 μL aliquots in 1.5-mL microfuge tubes in liquid nitrogen and store at –80°C until use.

3.2.2. Agrobacterium Transformation

1. Thaw *Agrobacterium* competent cells on ice.
2. Add plasmid DNA (0.5–1.0 μg, 5 μL of standard *E. coli* miniprep DNA) in a 1.5-mL microfuge tube containing 50 μL of *Agrobacterium* competent cells.
3. Mix them together and place the tube on ice for 10 min.
4. Freeze the cells in liquid nitrogen for 5 min.
5. Place the tube on the benchtop at room temperature for 10 min.
6. Add 1 mL of LB to the tube.
7. Incubate for 2–4 h at 28°C with gentle agitation.
8. Plate the transformed cells (100–200 μL) on an LB agar plate containing the appropriate antibiotic.
9. Incubate the cells for 3 days at 28°C.
10. Restreak the colonies on a new LB agar plate and incubate for 2 days at 28°C.
11. Grow 2 mL of culture from a single colony overnight at 28°C under constant agitation at 250 rpm and confirm the presence of the introduced plasmid DNA by PCR and/or sequence analysis using miniprep DNA.
12. Store glycerol stocks at –80°C.

3.2.3. Agroinfiltration

1. Streak out *Agrobacterium* strain from glycerol stock stored at −80°C onto LB agar plate supplemented with the appropriate antibiotic and incubate the plate for 3 days at 28°C.
2. Inoculate a single colony into 2 mL of LB liquid medium and incubate the culture overnight at 28°C under constant agitation at 250 rpm.
3. Harvest cells by centrifugation at 4,500 × *g* for 15 min at room temperature.
4. Resuspend the cell pellets in 1 volume of infiltration medium (10 mM MES pH 5.6, 10 mM $MgCl_2$ and 200 μM acetosyringone) and incubate for 1 h at room temperature.
5. Dilute the culture for infiltration to an OD (600 nm) of 0.3 before infiltration.
6. Infiltrate *Agrobacterium* suspension into the abaxial side of the leaves of 4–6-week-old *N. benthamiana* plants using a 1-mL syringe without needle.
7. Incubate infiltrated plants in the growth chamber in constant light at 24°C for 3–5 days.
8. Photographs can be taken at 5 days post infiltration (Fig. 3, see Note 18).

3.3. Confocal Fluorescence Imaging for Plant Cell Wall Localization

Once a candidate cell wall protein has been identified, it may be advisable to confirm its extracellular localization using an orthogonal approach, such as examining the localization of a fluorescent protein marker fused to the candidate protein. A rapid approach using transient expression of the fusion protein in onion epidermal cells is described below, although stable transformation is another

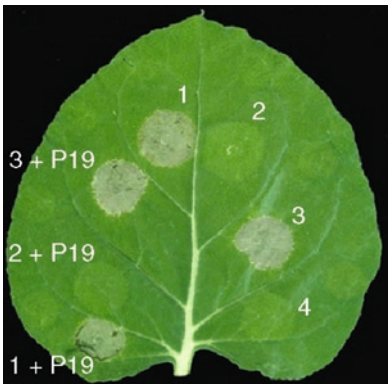

Fig. 3. Transient expression of the necrosis-inducing protein (NIP) in agroinfiltrated *Nicotiana benthamiana*. Leaves of *N. benthamiana* plants were infiltrated with *A. tumefaciens* carrying pART-NIP^F (1), pART-NIP^M (2), pART-$XTH2^{SP}$:NIP^M (3), and no plasmid DNA (4). The P19 protein can be co-expressed for high-level transient expression of a protein of interest in whole plants.

option that may, in some cases, be more robust. An example of this approach is previously described (14).

3.3.1. Preparation of Tungsten Particles

1. Weigh out tungsten particles (30 mg) and transfer to a microcentrifuge.
2. Add 1 mL of 70% ethanol.
3. Vortex for 10–15 min.
4. Centrifuge the particles at 14,000 × *g* for 10 s and remove supernatant.
5. Repeat 70% ethanol wash twice. Pellet the particles by brief centrifugation between washes.
6. Add 1 mL of sterile H_2O, vortex for 1 min, let settle for 1 min, and then spin briefly (~2 s).
7. Repeat sterile H_2O wash steps three times.
8. Remove supernatant. Add 500 µL of 50% glycerol. Vortex briefly.
9. Freeze at –20°C until use.

3.3.2. Preparation of Onion Tissues

1. Remove the outer papery layers of a yellow or white onion purchased at a local grocery store. Cut off the dry tips.
2. Split the onion lengthwise into quarters.
3. Discard two outermost layers of the leaves.
4. Cut the third outermost layer of leaves into slices of ~1.5 cm^2 and place on a piece of Whatman paper moisturized with 5 mL of sterile H_2O on the centre of a Petri dish. Bombardment will occur on the epidermal peel on the inner side of an onion piece.
5. Close the lid to keep from drying out.

3.3.3. Coating Microcarriers

1. Place plasmid DNA (0.5–1.0 µg, 5 µL of standard *E. coli* miniprep DNA) in a 1.5-mL microcentrifuge tube. Total volume should be 26 µL (see Note 19).
2. Add 10 µL of tungsten particles and mix well (see Note 20).
3. Add 30 µL of 2.5 M $CaCl_2$ and mix well.
4. Add 12.5 µL of 0.1 M spermidine and mix well.
5. Incubate for 20 min on ice with occasional vortexing.
6. Spin briefly (~10 s) and remove supernatant.
7. Add 300 µL of 70% ethanol and vortex.
8. Spin briefly (~10 s) and remove supernatant.
9. Add 300 µL of 100% ethanol and vortex.
10. Spin briefly (~10 s) and remove supernatant.
11. Resuspend the pellet in 30 µL of 100% ethanol and vortex (see Note 21).

12. Place 15 μL onto a macrocarrier by spreading out the particles uniformly. Allow the ethanol to evaporate.

3.3.4. Bombardment

1. Start vacuum pump.
2. Open helium tank.
3. Screw in adjustment handle until the pressure of the helium tank is set at 1,300 psi.
4. Switch on the gene gun (left switch of three red buttons).
5. Load a rupture disk (1,100 psi-rated, soaked in isopropanol) in the rupture disk retaining cap at the top of chamber (see Note 22).
6. Place a stopping screen (convex side up) in the bottom of macrocarrier assembly.
7. Invert a macrocarrier holder with DNA-coated macrocarrier (tungsten particles should be facing down) and place over the screen.
8. Screw the macrocarrier cover lid back on.
9. Slide the macrocarrier launch assembly into the second shelf from the top.
10. Place the Petri dish with onion sample on the target plate shelf and slide into the fourth shelf from the top.
11. Close the chamber door.
12. Pull vacuum (upper position on three-way middle switch of three red buttons) until the vacuum reaches 27.5 in. Hg. Hold the vacuum by quickly pressing the three-way switch all the way down.
13. Press the fire switch (right switch of three red buttons) and hold it down. Pressure will rise and the rupture disk will burst when pressure reaches 1,100 psi.
14. Release vacuum.
15. Open the chamber door and remove sample.
16. Seal Petri dish with Parafilm®. Incubate in the dark for 16–24 h at 24°C.
17. Shut down the particle bombardment system.
    (a) Close the helium tank valve.
    (b) Close the chamber.
    (c) Pull vacuum.
    (d) Press the fire switch until the pressure on helium regulator gauge reads zero.
    (e) Release vacuum.
    (f) Loosen pin until it turns freely.
    (g) Turn off gene gun and vacuum pump.

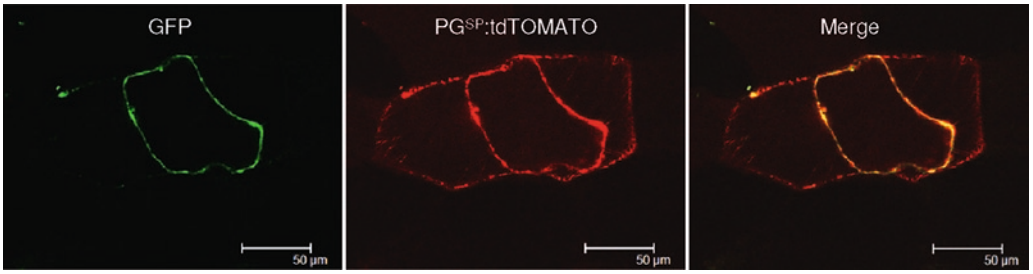

Fig. 4. Transient expression of a secreted tdTOMATO in onion epidermal cells. GFP (as shown on *left*) was co-expressed with the PG^{SP}:tdTOMATO (as shown in *middle*) in order to differentiate between cytoplasm and cell wall. A merged image (*right*) and the scale bar representing 50 μm are shown.

3.3.5. Confocal Imaging

1. Peel off the thin epidermis layer carefully with forceps.
2. Mount the epidermal cells in 0.8 M sucrose solution under a coverslip for plasmolysis (see Note 23).
3. Incubate for 10–20 min at room temperature.
4. Observe fluorescent signals using a confocal laser-microscope (Fig. 4, see Note 24).

4. Notes

1. Other similar commercial kits would be adequate and could be used as an alternative.
2. To construct pART-NIP^{F}, the full-length *Phytophthora sojae NIP* coding sequence (NCBI accession number AAM48170) (13) was amplified from *P. sojae* race 1 genomic DNA with primers NIP1K (5′-gcgcgcGGTACCCCATGAACCTCCG CCCTGCA-3′) and NIP3H (5′-gcgcgcAAGCTTTTAAG CGTAGTAGGCGTTGCC-3′). The plasmid pKANNIBAL1-NIP was constructed by ligating the *Kpn*I/*Hin*dIII-digested PCR product into *Kpn*I/*Hin*dIII-digested pKANNIBAL (15). The pKANNIBAL1-NIP construct was subcloned as *Not*I fragments into pART27 (16) to generate pART-NIP^{F}.
3. To construct pART-NIP^{M}, the coding sequence of the mature form of *P. sojae NIP* was PCR-amplified from the full-length *P. sojae NIP* clone with primers NIP2K (5′-gcgcgcGGTACC CCATGAGCGTTATCAACCACGAC-3′) and NIP3H. The plasmid pKANNIBAL2-NIP was constructed by ligating the *Kpn*I/*Hin*dIII-digested PCR product into *Kpn*I/*Hin*dIII-digested pKANNIBAL. The pKANNIBAL2-NIP construct was subcloned as *Not*I fragments into pART27. A new *Sgf*I restriction site was introduced into the cloning site upstream of the NIP coding sequence to generate pART-NIP^{M}.

4. To construct pART-XTH2^{SP}:NIP^{M}, the sequence encoding the signal peptide of tomato SlXTH2 (17), which is one of the xyloglucan endotransglycosylase/hydrolase genes (NCBI accession number AF176776), was amplified from the full-length *SlXTH2* cDNA with primers XTH2E (5′-gcgcgc GAATTCATGATCAAAACATCAAGT-3′) and XTH2S (5′-gcgcgcGCGATCGCCCAAAAGCCACCACTAC-GAA-3′). The *Eco*RI/*Sgf*I-digested PCR product was cloned into *Eco*RI/*Sgf*I-digested pART-NIP^{M} to generate pART-XTH2^{SP}:NIP^{M}.
5. The pBIN61S-CymRSV P19 vector was kindly provided by Dr. J. Burgyán (Hungary). Tombusvirus P19 has been shown to suppress posttranscriptional gene silencing (18–20). The P19 protein may be useful for high level of transient expression of proteins *in planta* (21).
6. To construct pART-GFP vector, the intron in pHANNIBAL (15) was excised by *Kpn*I/*Hind*III digestion and replaced with the *Kpn*I/*Hin*dIII-digested smGFP open reading frame from pSMGFP (22). The *Not*I fragment (containing the CaMV 35S promoter, GFP coding sequence and OCS terminator) of the pHANNIBAL-GFP vector was cloned into the *Not*I site of the binary vector pART27 to produce pART-GFP.
7. To construct pART-PG^{SP}:tdTOMATO, the GFP open reading frame of pART-GFP was firstly replaced with the *Kpn*I/*Xba*I-digested tdTOMATO (23) amplified using the primers TOM5 (5′-gcgcgcGGTACCATGGTTTCCAAG GGTGAG-3′) and TOM3 (5′-gcgcgcTCTAGAATTACTTG-TACAACTCGTC-3′) using the plasmid DNA (LAT52_ tdTOMATO_NOS in pLAT1 vector; kindly provided by Dr. B.A. McClure) as a template to generate pART-tdTO-MATO. Secondly, the sequence encoding the signal peptide of tomato PG-2a (NCBI accession number P05117) was amplified from the full-length PG-2a cDNA with primers PG1 (5′-gcgcgcCTCGAGATGGTTATCCAAAGGAAT-3′) and PG2 (5′-gcgcgcGGTACCGCTTCTACAAGTTGA AAT-3′). Then, the *Xho*I/*Kpn*I-digested PCR products of tomato PG-2a signal peptide-encoding region were cloned into *Xho*I/*Kpn*I-digested pART-tdTOMATO to produce pART-PG^{SP}:tdTOMATO.
8. We follow the protocol provided with the QIAquick PCR Purification Kit by adding 5 volumes of buffer PB (provided in the kit) to 1 volume of the reaction. Ensure that 40 μL of elution buffer are added to the column to elute the cDNAs for the subsequent reactions.
9. Shorter (<0.3 kb) or longer (>1.0 kb) cDNA fragments are likely to contain stop codons, which could disrupt the in-frame gene fusion with the invertase gene.

10. T4 DNA ligase buffer contains ATP, which degrades rapidly. Avoid multiple freeze-thaw cycles by making smaller aliquots of the buffer and storing them at −80°C.
11. We recommend commercially prepared electrocompetent cells as these typically provide a high transformation efficiency of $>1 \times 10^9$ colony forming units (CFU)/μg. Approximately 200 colonies should be obtained from 1 μL of the transformation mixture.
12. The majority (>70% recombinants) of clones in the cDNA library should contain cDNA inserts. Approximately 50 clones from the *E. coli* library should be selected at random to check the percentage of recombinant clones, and the average insert size of the cDNAs using the plasmid isolated according to the manufacturer's instructions as described for the QIAprep Spin Miniprep Kit.
13. Yeast competent cells should be used immediately after preparation.
14. Do not vortex as the yeast cells are more fragile.
15. Yeast transformants expressing the positive control (SP:suc2) should grow on the sucrose selection medium, while yeast expressing the same protein without the predicted SP should not grow. The first colonies should appear after approximately 4–5 days although the slow-growing transformants may continue to appear until 10 days.
16. This should be handled under a fume hood. Wear safety glasses, a lab coat, and gloves.
17. The DNA pellet should be briefly dried before adding sterile H_2O or TE buffer to remove residual ethanol.
18. The smaller size of the fusion protein can help maintain the activity of NIP protein, as the fusion protein may abolish the NIP activity.
19. This prepares enough particles for two shots.
20. Make sure that the tungsten particles are completely resuspended.
21. The DNA-coated tungsten particle suspension can be briefly sonicated.
22. Make sure that the rupture disk retaining cap should be firmly tightened.
23. Onion epidermal cells can be bathed in a range of sucrose solutions (e.g., 0.4–1.0 M).
24. It is important to note that onion epidermal cells should be co-bombarded with plasmids expressing GFP (or GFP-ER) and tdTOMATO for a dual-colour fluorescence imaging.

Acknowledgements

Research in this area was supported by grants from the NSF Plant Genome Program (DBI-0606595), the New York State Office of Science, Technology and Academic Research (NYSTAR) and Cornell Center for a Sustainable Future (CCSF).

References

1. Lee, S.-J., Saravanan, R. S., Damasceno, C. M. B., Yamane, H., Kim, B. -D. and Rose, J. K. C. (2004) Digging deeper into the plant cell wall proteome. *Plant Physiol Biochem* **42,** 979–988.
2. Jamet, E., Albenne, C., Boudart, G. Irshad, M., Canut H., and Pont-Lezica., R. (2008) Recent advances in plant cell wall proteomics. *Proteomics* **8,** 893–908.
3. Rose, J. K. C., Bashir, S., Giovannoni, J. J., Jahn, M. M., and Saravanan, R. S. (2004) Tackling the plant proteome: practical approaches, hurdles, and experimental tools. *Plant J* **39,** 715–733.
4. Nickel, W. (2005) Unconventional secretory routes: direct protein export across the plasma membrane of mammalian cells. *Traffic* **6,** 607–614.
5. Nombela, C., Gil, C., and Chaffin, W. L. (2006) Non-conventional protein secretion in yeast. *Trends Microbiol* **14,** 15–21.
6. Lee, S. -J., Kim, B. -D., and Rose, J. K. C. (2006) Identification of eukaryotic secreted and cell surface proteins using the yeast secretion trap (YST) screen. *Nat Protoc* **1,** 2439–2447.
7. Ausubel, F. M., Brent, R., Kingston, R. E., Moore, D. D., Seidman, J. G., Smith, J. A., and Struhl, K. (1987) (eds.) *Current Protocols in Molecular Biology*, Wiley, New York.
8. Miller, E. M. and Nickoloff, J. A. (1995) *Escherichia coli* electrotransformation, in *Methods in Molecular Biology* **47,** Nickoloff, J. A., ed., Humana, Totowa, NJ, 105.
9. Koncz, C. and Schell, J. (1986) The promoter of T_L-DNA gene 5 controls the tissue-specific expression of chimaeric genes carried by a novel type of *Agrobacterium* binary vector. *Mol Gen Genet* **204,** 383–396.
10. Koncz, C., Kreuzaler, F., Kalman, Z., and Schell, J. (1984) A simple method to transfer, integrate and study expression of foreign genes, such as chicken ovalbumin and α-actin in plant tumors. *EMBO J* **3,** 1029–1037.
11. Bendahmane, A., Querci, M., Kanyuka, K., and Baulcombe, D. C. (2000) *Agrobacterium* transient expression system as a tool for the isolation of disease resistance genes: application to the *Rx2* locus in potato. *Plant J* **21,** 73–81.
12. Bendtsen, J. D., Nielsen, H., von Heijne, G., and Brunak, S. (2004) Improved prediction of signal peptides: SignalP 3.0. *J Mol Biol* **340,** 783–795.
13. Qutob, D., Kamoun, S., and Gijzen, M. (2002) Expression of a *Phytophthora sojae* necrosis inducing protein occurs during transition from biotrophy to necrotrophy. *Plant J* **32,** 361–373.
14. Yamane, H., Lee, S. -J., Kim, B. -D., Tao, R., and Rose, J. K. C. (2005) A coupled yeast signal sequence trap and transient plant expression strategy to identify and confirm genes encoding extracellular proteins from peach pistils. *J Exp Bot* **56,** 2229–2238.
15. Wesley, V. S., Helliwell, C., Smith, N. A., Wang, M. B., Rouse, D., Liu, Q., Gooding, P.S., Singh, S.R., Abbott, D., Stoutjesdijk, A., Robinson, S.P., Gleave, A. P., Green, A. G., and Waterhouse, P. M. (2001) Construct design for efficient, effective and high-throughput gene silencing in plants. *Plant J* **27,** 581–590.
16. Gleave, A. P. (1992) A versatile binary vector system with a T-DNA organizational structure conducive to efficient integration of cloned DNA into the plant genome. *Plant Mol Biol* **20,** 1203–1207.
17. Catalá, C., Rose, J. K. C., York, W. S., Albersheim, P., Darvill, A. G., and Bennett, A. B. (2001) Characterization of a tomato xyloglucan endotransglycosylase gene that is down-regulated by auxin in etiolated hypocotyls. *Plant Physiol* **127,** 1180–1192.
18. Qiu, W., Park, J. -W., and Scholthof, H .B. (2002) Tombusvirus P19-mediated suppression of virus-induced gene silencing is

controlled by genetic and dosage features that influence pathogenicity. *Mol Plant Microbe Interact* **15,** 269–280.

19. Qu, F. and Morris, T. J. (2002) Efficient infection of *Nicotiana benthamiana* by *Tomato bushy stunt virus* is facilitated by the coat protein and maintained by p19 through suppression of gene silencing. *Mol Plant-Microbe Interact* **15**, 193–202.
20. Silhavy, D., Molnár, A., Lucioli, A., Szittya, G., Hornyik, C., Tavazza, M and Burgyán, J. (2002) A viral protein suppresses RNA silencing and binds silencing-generated, 21- to 25-nucleotide double-stranded RNAs. *EMBO J* **21,** 3070–3080.
21. Voinnet, O., Rivas, S., Mestre, P., and Baulcombe, D. C. (2003) An enhanced transient expression system in plants based on suppression of gene silencing by the p19 protein of tomato bushy stunt virus. *Plant J* **33,** 949–956.
22. Davis, S. J. and Vierstra, R. D. (1998) Soluble, highly fluorescent variants of green fluorescent protein (GFP) for use in higher plants. *Plant Mol Biol* **36,** 521–528.
23. Shaner, N. C., Campbell, R. E., Steinbach, P. A., Giepmans, B. N., Palmer, A. E., and Tsien, R. Y. (2004) Improved monomeric red, orange and yellow fluorescent proteins derived from *Discosoma* sp. red fluorescent protein. *Nat Biotechnol* **22,** 1567–1572.

Chapter 19

Knocking Out the Wall: Protocols for Gene Targeting in *Physcomitrella patens*

Alison W. Roberts, Christos S. Dimos, Michael J. Budziszek Jr., Chessa A. Goss, and Virginia Lai

Abstract

The moss *Physcomitrella patens* has become established as a model for investigating plant gene function due to the feasibility of gene targeting. The chemical composition of the *P. patens* cell wall is similar to that of vascular plants and phylogenetic analyses of glycosyltransferase sequences from the *P. patens* genome have identified genes that putatively encode cell wall biosynthetic enzymes, providing a basis for investigating the evolution of cell wall polysaccharides and the enzymes that synthesize them. The protocols described in this chapter provide methods for targeted gene knockout in *P. patens*, from constructing vectors and maintaining cultures to transforming protoplasts and analyzing the genotypes and phenotypes of the resulting transformed lines.

Key words: Gene targeting, Immunocytochemistry, *Physcomitrella patens*, Gateway® cloning

1. Introduction

The moss *Physcomitrella patens* has become established as a model for investigating plant gene function due to its uniquely high rate of homologous recombination, which enables targeted gene modification (1). Wild type alleles can be knocked out by targeting with vectors containing homologous sequences interrupted by a selection cassette (2). Targeted mutagenesis can be accomplished by replacing genes with vectors carrying insertions, deletions, or point mutations (3). Functional transgenes can be inserted using expression vectors targeted to intergenic regions (4). Translational fusions can also be created at the native locus by gene targeting (5). A further advantage of *P. patens* is that the dominant phase in its life-cycle is haploid, which enables

Zoë A. Popper (ed.), *The Plant Cell Wall: Methods and Protocols*, Methods in Molecular Biology, vol. 715,
DOI 10.1007/978-1-61779-008-9_19,

detection of mutant phenotypes in primary transformants and eliminates the need for backcrossing (6). Genomic resources for *P. patens* include EST sequences and their corresponding full-length cDNA clones (http://moss.nibb.ac.jp/), microarrays (7, 8), and the annotated genome sequence http://www.cosmoss.org/ (9). Methods for gene silencing by RNAi (10) and miRNA (11) and for producing temperature sensitive mutants (12) have also been developed.

Several aspects of *P. patens* morphology and development are advantageous for investigating cell wall biosynthesis and evolution. Development of *P. patens* from haploid spores, protoplasts, or fragmented tissue begins as photosynthetic chloronemal filaments that extend by apical division and tip growth (13). Growth of chloronemal filaments can be maintained for several weeks on medium containing ammonium tartrate. Thus, in contrast to vascular plants, it is possible to produce tissue consisting of a single cell type (chloronemal filaments) from *P. patens*. This greatly simplifies the task of assigning changes in cell wall composition to alterations in the expression of specific genes and the activity of specific enzymes. In the absence of ammonium tartrate, the apical cells of the chloronemal filaments increase their growth rate to begin producing caulonemal filaments (6). Caulonemal filaments produce buds that develop into the familiar leafy portion of the moss plant, the gametophore, which enlarges by diffuse growth. Zygotes derived from fusion of gametes, produced at the gametophore apex, develop into diploid sporophytes consisting of a short stalk and a sporangium (13).

Like those of vascular plants, *P. patens* cell walls contain cellulose, xyloglucan, mannan, pectins, and arabinogalactan proteins (14–18). Like other bryophytes, they lack lignin (19, 20). Phylogenetic analyses of glycosyltransferase sequences from the *P. patens* genome have identified orthologs of genes that encode cell wall biosynthetic enzymes in *Arabidopsis* and rice http://wiki.genomics.purdue.edu/index.php/Cell_wall_composition_and_glycosyltransferases_involved_in_cell_wall_formation (21) and provide a basis for investigating the evolution of cell wall polysaccharides and the enzymes that synthesize them. Various aspects of *P. patens* biology have been reviewed (1, 3, 6, 22–27) and protocols for culture and transformation have been described previously in print (28, 29) and online (http://moss.nibb.ac.jp/, http://www.plant-biotech.net/; http://biology4.wustl.edu/moss/methods.html). The following protocols provide a guide for targeted gene knock out in *P. patens*, from constructing a vector and maintaining cultures to transforming protoplasts and analyzing the genotypes and phenotypes of the resulting transformed lines.

2. Materials

2.1. Vector Construction

1. Sequence of interest as a query for searching the *P. patens* genome.
2. Multisite Gateway® Pro 3.0 three-fragment or Multisite Gateway® Pro Plus flexible cloning kit (Invitrogen, Carlsbad, CA, USA).
3. Reagents for PCR.
4. Destination vector (available upon request from the authors).
5. Commercial plasmid DNA midi- or maxi-prep kit.

2.2. Culture of P. patens

1. Incubator set to 25°C with constant illumination at 50–80 µmol/m^2/s.
2. Paint shaker (e.g., Tornado II, Blair Equipment Company, Flint, MI, USA), optional.
3. BCDAT or BCD medium (see Table 1, Note 1).
4. Unvented Petri plates, 95 mm (Greiner Bio-One, Frickenhausen, Germany, see Note 2).

Table 1
Media for culture and transformation of *P. patens* (29). Dry ingredients are added to purified water, q.s. to 1 L, and sterilized by autoclaving. Calcium chloride solution is added after autoclaving to prevent precipitation

	BCD (per L)	BCDAT (per L)	PRMB (per L)	PRMT (per L)	PRML (per L)
$MgSO_4$ heptahydrate	0.25 g	0.25 g	0.25 g	0.25 g	0.25 g
KH_2PO_4	0.25 g	0.25 g	0.25 g	0.25 g	0.25 g
KNO_3	1.0 g	1.0 g	1.0 g	1.0 g	1.0 g
$FeSO_4$ septahydrate	12.5 mg	12.5 mg	12.5 mg	12.5 mg	12.5 mg
Diammonium tartrate	–	0.92 g	0.92 g	0.92 g	0.92 g
Trace element solution[a]	1 mL	1 mL	1 mL	1 mL	1 mL
Mannitol	–	–	60 g	80 g	80 g
Agar	7 g	7 g	8 g	5 g	–
Calcium chloride solution 55.5 g/L $CaCl_2$ (sterile) Add after autoclaving	1 mL	1 mL	10 mL	10 mL	10 mL

[a]55 mg/L cupric sulfate pentahydrate; 55 mg/L zinc sufate heptahydrate; 614 mg/L boric acid; 389 mg/L manganous chloride tetrahydrate; 55 mg/L cobalt chloride hexahydrate; 28 mg/L potassium iodide; 25 mg/L sodium molybdate dehydrate (32)

5. Sterile cellophane disks (Type 325P, AA Packaging Ltd., Lancashire, UK) interleaved with circles of copy paper and autoclaved in glass Petri plates (see Note 3).
6. Inoculum of *P. patens* (Gransden, available from David Cove, Washington University, St. Louis, MO, USA).
7. Sterile 15 mL disposable centrifuge tubes (polystyrene or polypropylene).
8. Sterile 10 mL serological pipettes.
9. Sterile purified water.
10. Sterile stainless steel beads (3.2 mm, Biospec Products, Bartlesville, OK, USA).

2.3. Transformation and Selection

1. Materials for subculture of *P. patens* (see above).
2. Pipettors (20, 200, and 1,000 µL capacity) and sterile tips.
3. Heated water bath with thermometer.
4. Orbital shaker.
5. Hemocytometer.
6. 50 µg vector DNA: linearized, 1 µg/µL in sterile purified water or 5 mM Tris, pH 7.5.
7. 8.5% (w/v) D-mannitol (sterilized by autoclaving).
8. 3 M solution: the following are added to 40 mL purified water: 4.55 g D-mannitol, 750 µL of 1 M $MgCl_2$, 5 mL of 1% MES-KOH, pH 5.6; q.s. to 50 mL; filter sterilized; stored at 4°C for up to 6 months.
9. 2% Driselase solution: 1 g Driselase (Sigma, St. Louis, MO, USA) is dissolved in 50 mL 8.5% D-mannitol; stirred gently 30 min 21–25°C; chilled 30 min 4°C; stirred 5 min 21–25°C; centrifuged 2,500 × g 10 min; filter sterilized; stored as 3 mL aliquots in sterile 15 mL centrifuge tubes at –20°C).
10. PEG solution: To prepare part 1: 9 mL of 8.5% D-mannitol is combined with 1 mL of 1 M $Ca(NO_3)_2$ and 100 µL of 1 M Tris-HCl, pH 8.0, and filter sterilized; to prepare part 2: 4 g PEG 8000 (Sigma) is melted in a sterile 50 mL disposable centrifuge tube by microwaving; Part 1 is added to Part 2 and vortexed until completely mixed; kept at 21–25°C for 2 h before use; stored in 1 mL aliquots at –20°C).
11. PRMB and PRMT media (see Table 1).
12. Sterile nylon filters (Cell Strainer, BD Falcon, Franklin Lakes, NJ, USA).
13. Sterile 15 and 50 mL disposable conical centrifuge tubes and 15 mL round-bottom culture tubes.
14. Antibiotic stock: e.g., 15 mg/mL hygromycin in purified water.

2.4. Genotype Analysis by PCR

1. Vector primers (Vector F = TGACAGATAGCTGGGCAATG, Vector R = TCCGAGGGCAAAGAAATAGA) and flanking primers (gene specific, see below).
2. Kontes Pellet Pestle® Micro Grinder (Kimble/Kontes, Vineland, NJ, USA).
3. DNA extraction buffer for PCR: 0.2 M Tris-HCl, pH 9.0, 0.4 M LiCl, 25 mM EDTA, 1% SDS.
4. Isopropanol.
5. TE buffer: 10 mM Tris-HCl, pH 8, 1 mM EDTA.

2.5. Genotype Analysis by Southern Blotting

1. Transformed *P. patens* line cultured on BCDAT plate for 7 days (see Subheading 3.2).
2. DNA extraction buffer for Southern blotting: the following are combined in the order listed in a 15 mL disposable centrifuge tube: Solution 1: 350 mM sorbitol, 100 mM Tris–HCl, pH 7.5, 5 mM EDTA, sterilized by autoclaving (1 mL); 3.8 mg sodium bisulfite; Solution 2: 200 mM Tris-HCl, pH 7.5, 50 mM EDTA, 2% (w/v) CTAB, 2 M sodium chloride, sterilized by autoclaving (1 mL); 0.4 mL of 5% (w/v) *N*-lauroylsarcosine; 5 µL of 10 mg/mL RNaseA; prepared just before use.
3. Chloroform:octanol 24:1.
4. Cryocup Grinder (Research Products International, Mt. Prospect, IL, USA).
5. Liquid nitrogen.
6. DNA precipitation buffer: 80 mL ethanol, 20 mL 1 M sodium acetate, pH 7.0.
7. 70% ethanol.
8. Supplies and reagents for Southern blotting.

2.6. Immunofluorescent Cell Wall Labeling

1. 1 mL pipette tips, tips cut off with a razor blade at 1 cm, autoclaved.
2. Primary antibodies or carbohydrate binding modules (CBM) (see Plant Probes www.plantprobes.net; Biosupplies Australia www.biosupplies.com.au).
3. Secondary antibodies (ALEXA Fluor® 488 labeled goat anti-rat or antimouse as appropriate for primary antibody, Invitrogen).
4. FlexiPERM® 12 well chambers (ISC BioExpress, Kaysville, UT, USA).
5. Poly-L-lysine coated slides (Fisher Scientific).
6. Sterile nylon filters (see Subheading 2.3, step 12).
7. 15 and 50 mL disposable centrifuge tubes.

8. 2× fixative stock: 100 mM PIPES, pH 6.8, 5 mM magnesium sulfate, 10 mM EGTA.
9. Fixative: 500 µL 2× fixative stock, 270 µL purified water, 230 µL 16% formaldehyde (methanol-free, Polysciences Inc., Warrington, PA, USA), prepared just before use.
10. Phosphate-buffered saline (PBS): 137 mM NaCl, 2.7 mM KCl, 10 mM Na_2HPO_4, 1.4 mM KH_2PO_4, pH 7.4.
11. Blocking solution: 5% w/v nonfat dry milk in PBS, prepared just before use.
12. Coverslips (24 × 60 mm).
13. Antifade reagent (SlowFade® Gold, Invitrogen).

2.7. Morphological Analysis

(see Subheading 2.2)

3. Methods

3.1. Preparation of Knockout Vectors

Replacement vectors for deleting target genes include homologous sequences upstream and downstream of the target gene coding sequence, separated by a selection cassette (Fig. 1). The selection cassette replaces the target gene when the vector is integrated into the genome by homologous recombination. Vectors are constructed using Gateway Multisite® Cloning (Invitrogen). The following describes methods for cloning homologous sequences upstream and downstream of the target gene into the appropriate pDONR vectors for cloning into pBHSNRG (Fig. 1a, see Note 4).

1. *P. patens* homologs of genes of interest are identified using the BLAST function available at the Cosmoss homepage (http://www.cosmoss.org/, see Note 5). Choose "GENOME", then "BLAST" from the menu. Paste your peptide or nucleic acid sequence into the box, choose the appropriate molecule (i.e., peptide or nucleic acid) and click "Submit" at the bottom of the page. When your search is complete, click the "Click here …" link, then the "my query" link. The results of a search are reported as a list of gene models producing significant alignments. Clicking on a gene model will direct you to the alignment, where you can click on the "Genome Browser" icon to examine the gene model. To download the genomic and flanking sequences, zoom out to show at least 2 kb of flanking sequence on both ends of the coding sequence. From the "Report and Analysis" dropdown box, choose "Download sequence file" and click on "Configure". At the top of the

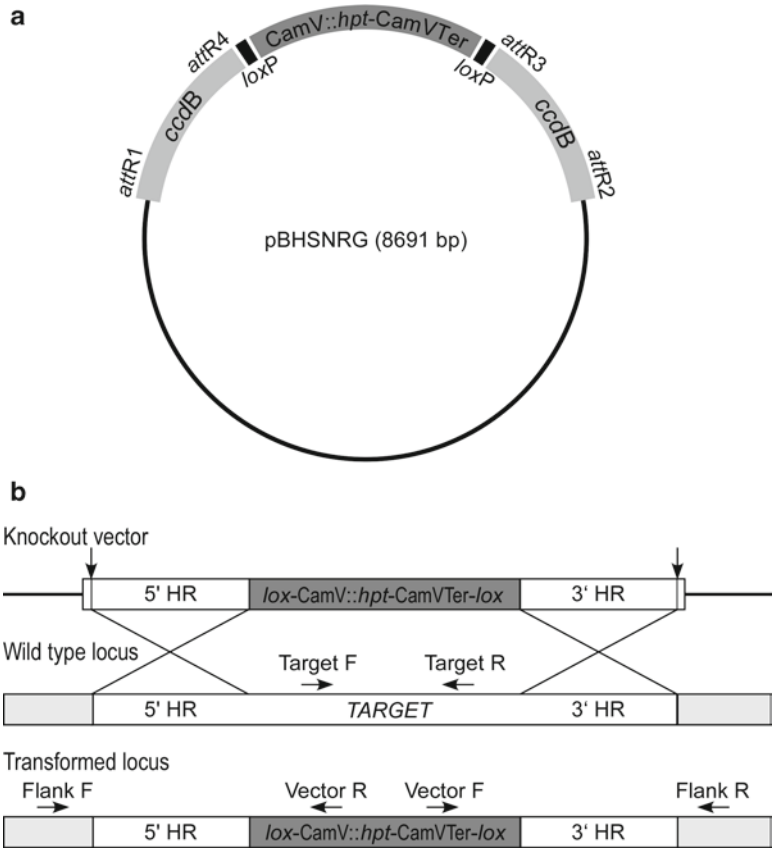

Fig. 1. (**a**) Multisite Gateway® destination vector pBHSNRG. Amplified 5′ and 3′ homologous regions cloned into pDONR 221 P1-P4 and pDONR 221 P3–P2, respectively, are inserted in the destination vector when the *att* R1/*att* R4 and *att* R3/*att* R2 sites of pBHSNRG recombine with the entry clone *att* L1/*att* L4 and *att* L3/*att* L2 sites to make the knockout vector. (**b**) Knockout vector, wild type target genomic locus and transformed target genomic locus. The vector is linearized using BsrGI or restriction enzymes chosen to cut near the ends of the homologous region (vertical arrows). The positions of primers used to test for targeted integration (Flank F/Vector R and Vector F/Flank R), deletion of the target gene (Target F/Target R), and absence of concatenated vector sequences (Vector F/Vector R) are shown.

"Configure" page, click the radio button for "Save to Disk" and then click the "Go" button at the bottom of the page to save the text file.

2. Open the sequence text file in any text editor. After the start and stop codons are identified, primers are designed to amplify about 1 kb of homologous sequence upstream and 1 kb of homologous sequence downstream of the gene of interest. Sequences for cloning into pDONR 221 P1-P4 (Element 1) are added to the upstream forward and reverse primers, and sequences for cloning into pDONR 221 P3-P2 (Element 3) are added to the downstream forward and reverse primers (see Gateway Multisite® instruction manual).

3. Primers are used to amplify genomic DNA isolated from wild type *P. patens* (see Subheading 3.5) and the amplified fragments are cloned into their respective pDONR vectors using the BP Clonase II recombination reaction as described in the Gateway Multisite® instruction manual to construct Element 1 and Element 3.
4. Element 1 and Element 3 are cloned into BHSNRG using the LR Clonase II Plus recombination reaction as described in the Gateway Multisite® instruction manual. Clones are verified by sequencing with the M13 Reverse primer supplied in the Gateway Multisite® kit and Vector R (see Subheading 2.4, step 1, Fig. 1b).
5. Plasmid DNA is prepared using a commercial midi- or maxiprep kit.
6. The vector is linearized using BsrGI or restriction enzymes chosen to cut near the ends of the homologous regions if BsrGI truncates the vector (Fig. 1b).

3.2. Subculture of P. patens Chloronemal Filaments

1. Plates are prepared by melting BCDAT medium and pouring about 25 mL into each unvented Petri plate. After the medium solidifies, plates are overlain with sterile cellophane disks using sterile forceps. Cellophane is allowed to relax and flatten out for 10 min, and then straightened, if necessary, with sterile forceps.
2. For each line to be subcultured, 2–4 stainless steel beads and sterile water (2 mL for each plate to be inoculated from a single line) are added to a sterile 15 mL centrifuge tube.
3. Sterile forceps are used to scrape the filaments from the starter culture into a mound and transfer them to the centrifuge tube. Up to ¼ of a confluent plate (about 50 mg of tissue) is used for each new plate to be inoculated. Alternatively, a pinch of tissue from a colony maintained on BCDAT medium may be used (see Subheading 3.3, step 18).
4. Tubes are capped tightly, clamped in a paint shaker, and shaken for several min until large clumps are broken up and small clumps of a few dozen cells remain (see Note 6). When older starter cultures are used, longer shaking is required.
5. Using a serological pipette, 2 mL of suspension are transferred to the surface of each plate and spread evenly.
6. Plates are incubated at 25°C with constant illumination at 50–80 μmol/m²/s (see Note 7). They are not sealed with Parafilm® or stacked.
7. After 1 week, tissue is subcultured or plates are sealed with Parafilm® and transferred to an incubator set to 10°C with a 2 h photoperiod at 20 μmol/m²/s for storage up to 1 year.

Clones can also be conserved for several years by suspending about 50 mg of tissue in 1 mL of sterile distilled water in a sterile microcentrifuge tube and storing at 4°C (see Note 8).

3.3. Transformation and Selection

1. 5–7 days before transformation, chloronemal tissue from the line to be transformed is subcultured from a fresh plate (see Note 9) on cellophane-overlain BCDAT plates and incubated as described in Subheading 3.2.
2. Protoplast regeneration plates (3 per transformation) are prepared with PRMB medium and overlain with sterile cellophane (Subheading 3.2, step 1).
3. Before beginning protoplast preparation, all materials are made ready: waterbath is equilibrated to 45°C for heat shock; a 500 mL beaker containing 300 mL of water is equilibrated to room temperature (21–25°C); PRMT medium is melted and equilibrated to 45°C in the water bath; linearized vector DNA is ethanol precipitated and dissolved in sterile water at 1 μg/μL; one aliquot of Driselase solution per line to be transformed and one aliquot of PEG solution per 1–3 vectors are thawed and completely redissolved.
4. Protoplast preparation is begun by pipetting 9 mL of 8.5% mannitol into a Petri plate and adding chloronemal filaments scraped from the plate using sterile forceps, followed by 3 mL of 2% Driselase solution. Petri plates are incubated for 60 min with shaking at 60 rpm on an orbital shaker at 21–25°C.
5. Using a serological pipette, protoplast suspension is gently drawn from the Petri plate and passed through a nylon filter placed on top of a 50 mL disposal centrifuge tube.
6. Filtrate is transferred to a 15 mL disposable conical centrifuge tube and centrifuged at speed 2–3 in a clinical centrifuge (see Note 10) for 7 min; supernatant is discarded.
7. Protoplasts are resuspended in 10 mL 8.5% mannitol pipetted directly onto the pellet from a serological pipette. It is important to resuspend protoplasts gently and to avoid aspirating protoplasts into the pipette. The suspension is centrifuged for 7 min, speed 2–3; supernatant is discarded. This step is repeated.
8. During step 7, 15–30 μL of each vector is pipetted into a labeled 15 mL disposable round-bottomed centrifuge tube.
9. Protoplasts are resuspended in 10 mL of 8.5% mannitol. After 10 μL of suspension are removed and loaded into a hemocytometer, the suspension is centrifuged for 7 min, speed 2–3.
10. Intact protoplasts (see Note 11) are counted and the density is estimated; use the instructions supplied with your hemocytometer; $2–4 \times 10^5$ protoplasts/mL is typical.

11. Supernatant is discarded and protoplasts are resuspended in 3 M solution at 2×10^6 protoplasts/mL; 2–4 mL of suspension is typical.
12. Protoplast suspension (0.3 mL) and PEG solution (0.3 mL) are added to each tube containing vector DNA. The suspension is mixed gently but thoroughly and incubated at 21–25°C for 10 min.
13. Protoplasts are heat-shocked for 3 min at 45°C and transferred immediately to a beaker of 21–25°C water for 10 min. Important – the water bath heater is turned off just before submerging the tubes containing the protoplasts to prevent overheating should the heater turn on during incubation.
14. Protoplasts are resuspended in 5 mL PRMT held at 45°C and 1.6 mL of suspension is spread on each of three cellophane-overlain PRMB plates. This should result in an inoculation rate of 2×10^5 protoplasts/plate (i.e., 2×10^6 protoplasts/mL × 0.3 mL/transformation ÷ 3 plates/transformation).
15. Plates are incubated for 5 days at 25°C with constant illumination at 50–80 μmol/m²/s.
16. The regeneration rate can be estimated on day 5 as follows: using a mm ruler, determine the field area of your dissecting microscope on high power. Using the same magnification, count the number of regenerated protoplasts in 3–5 fields and calculate the average. The area of a plate is about 6,400 mm². Estimate the number of regenerated protoplasts per plate by multiplying the average number per field by 6,400 mm² and dividing by the field area in mm². Expect about 30% regeneration (see Note 12).
17. Selection is initiated after 5 days. Selection plates are prepared by melting BCDAT medium, cooling slightly, adding antibiotic (e.g., 15 μg/mL hygromycin), and pouring about 25 mL each into unvented Petri plates. After medium solidifies, cellophane disks are lifted from PRMB plates with sterile forceps and transferred to BCDAT/antibiotic plates, taking care to avoid trapping air bubbles under the cellophane. Plates are incubated for 7 days at 25°C with constant illumination at 50–80 μmol/m²/s.
18. Clones surviving after 7 days on selection consist of stable and unstable transformants. To select for stable transformants, cellophane disks are transferred to BCDAT plates for 7 days, then back to BCDAT/antibiotic plates for 7 days. Typically, clones that grow vigorously during the second round of selection are stable. When large enough, they are split and arrayed on duplicate BCDAT plates without cellophane and incubated for 7 days at 25°C with constant illumination at 50–80 μmol/m²/s, and then stored at 10°C with a 2 h

photoperiod at 20 μmol/m^2/s. A small amount of tissue (about 25 mm^3) is collected for genotype analysis.

3.4. Genotype Analysis by PCR

1. Genomic DNA for PCR is prepared by homogenizing tissue (about 25 mm^3) in a 1.5 mL microcentrifuge tube using a Pellet Pestle® Micro Grinder and immediately adding 500 μL of DNA extraction buffer. Debris is pelleted in a microcentrifuge at high speed for 5 min and 350 μL of supernatant is transferred to a 1.5 mL microcentrifuge tube containing 350 μL of isopropanol. DNA is pelleted in a microcentrifuge at high speed for 15 min. The supernatant is poured off and the tube containing the pellet is dried upside down on a paper towel. The pellet is dissolved in 400 μL of TE buffer by shaking for 30 min at 21–25°C.
2. PCR primers oriented outward from the selection cassette (Vector R/Vector F; see Subheading 2.4, step 1) are paired with primers designed to amplify inward from the genomic regions flanking the homologous sequences contained within the knockout vector (Flank F/Flank R) to test for 5′ and 3′ integration of the vector. Forward and reverse primers designed to amplify the target sequence (Target F/Target R) are used to test for deletion of the target gene (Fig. 1b). Flank and target sequence primers are gene-specific.
3. DNA extracted from each stable line (2–4 μL) is amplified with primers Flank F/Vector R (Fig. 1b) in a 25 μL PCR reaction to test for integration of the 5′ end of the vector (see Note 13).
4. For stable lines testing positive for 5′ integration, genomic DNA (2–4 μL) is amplified with primers Vector F/Flank R (Fig. 1b) in a 25 μL PCR reaction to test for integration of the 3′ end of the vector.
5. For stable lines testing positive for both 5′ and 3′ integration, genomic DNA (2–4 μL) is amplified with primers Target F/Target R (Fig. 1b) in a 25 μL PCR reaction to test for deletion of the target sequence.
6. For stable lines testing positive for 5′ and 3′ integration, and negative for the target sequence, genomic DNA (2–4 μL) is amplified with primers Vector F/Vector R (Fig. 1b) in a 25 μL PCR reaction to test for insertion of concatenated vector.

3.5. Genotype Analysis by Southern Blotting

Southern blots are performed to test for nonhomologous integration of the vector. The probe is synthesized using the selection cassette (amplified or restriction fragment) as a template. Genomic DNA (about 2–3 μg each) is digested with 2–4 restriction enzymes, each chosen to excise a 3–10 kb fragment containing

the selection cassette and run on a 0.7% agarose gel at 1 V/cm for 18–24 h. DNA is transferred, hybridized, and developed using standard methods. Hybridization only to the expected fragments is evidence for integration of a single copy of the vector at the target locus. The following procedure yields about 20 µg of genomic DNA (enough for 6–8 digests) and requires only a microcentrifuge:

1. Seven-day old chloronemal tissue is scraped from a plate and squeezed firmly between layers of filter paper to remove excess liquid.
2. Up to 240 mg of squeeze-dried tissue is ground in a liquid nitrogen-cooled Cryocup grinder. The resulting powder is transferred to a 15 mL disposable centrifuge tube containing 2.4 mL extraction buffer for Southern blotting.
3. Homogenate is incubated at 65°C for 20 min with occasional mixing by inversion.
4. Homogenate is transferred to three microcentrifuge tubes (0.75 mL each). After adding 0.75 mL of chloroform:octanol, each tube is inverted 6 times to mix.
5. Phases are separated by microcentrifuging at high speed, 5 min. Upper aqueous phase is transferred into clean microcentrifuge tubes, 0.9 mL DNA precipitation buffer is added and each tube is inverted 6 times and chilled at 4°C for 15 min.
6. DNA is pelleted in a microcentrifuge at high speed, 15 min.
7. Pellets are washed with 1.5 mL of 70% ethanol and microcentrifuged at high speed, 5 min.
8. Supernatant is removed and remaining ethanol is evaporated at 21–25°C, 10 min. Pellets are dissolved in 100 µL TE buffer and combined.

3.6. Immunofluorescent Cell Wall Labeling

1. Protoplasts are prepared as described in Subheading 3.3, steps 1–7 and plated in PRML (1 mL per plate) on cellophane-overlain PRMB at a density of about 15,000 per plate. The cellophanes are transferred to BCDAT plates after 2 days (see Note 14) and cultured on BCDAT for 3–5 days.
2. To collect colonies, the plate is flooded with 3–5 mL of sterile H_2O and a cut-off 1 mL pipette tip is used to pipette the suspension through a nylon filter placed over a 50 mL disposable centrifuge tube. This removes dead protoplasts, which create undesirable background labeling. The filter is placed upside down in a clean Petri plate and colonies are washed into the plate with 3–5 mL of purified water before pipetting them into a 15 mL tube.
3. Colonies are centrifuged for 7 min at speed 3 in a clinical centrifuge (speed is adjusted as necessary to collect tissue

without damaging it). Water is removed and colonies are suspended in 1 mL of fixative for 20 min at 21–25°C or overnight at 4°C.

4. Colonies are centrifuged for 7 min at speed 3 in a clinical centrifuge. Supernatant is removed and colonies are suspended in 3 mL of PBS. This step is repeated two more times.
5. During the washes, the flexiPERM cell chamber is pressed onto a poly-L-lysine coated slide. The slide is incubated on a slide warmer at 80°C for 20 min to ensure adhesion, and then cooled to 21–25°C.
6. Colonies are centrifuged for 7 min at speed 3 in a clinical centrifuge. Supernatant is removed and colonies are suspended in 3 mL of purified water. This step is repeated two more times, resuspending in 1 mL of purified water after the final wash. All salts must be removed as they interfere with adhesion of the tissue to the poly-L-lysine coated slides.
7. A cut-off 1 mL pipette tip is used to pipette about 50 µL of suspension into each well (including an extra well for a negative control). Tissue sinks to the bottoms of the wells and should cover them completely. More suspension may be added, if necessary. After 20 min, water is carefully removed and the slide is allowed to sit for 20 min to maximize adhesion.
8. Following the schedule below, solutions are pipetted into each well, and then removed using care not to dislodge the tissue. A multichannel pipettor may be used, if available.
   (a) 200 µL of blocking solution, 10 min.
   (b) 50 µL of primary antibody or CBM (see Note 15) diluted to the recommended working concentration with blocking solution OR; 50 µL of blocking solution for negative control wells, 1.5 h at 21–25°C or overnight at 4°C.
   (c) 200 µL of PBS, 5 min. Repeat for a total of three washes.
   (d) 50 µL of secondary antibody diluted 1:100 in blocking solution, 1.5 h at 21–25°C in the dark.
   (e) 200 µL of PBS, 5 min. Repeat for a total of three washes.
   (f) After removal of the final PBS wash, the flexiPERM® is carefully removed, and slides are air dried, 5–10 min. A few drops of antifade reagent and a coverslip are added and the slide is left in a dark dry place overnight.

3.7. Morphological Analysis

Cell wall defects are often manifested as alterations in the morphology of specific cells or tissues. The following methods can be used to test for alterations in various stages of *P. patens* growth and development.

3.7.1. Tip Growth Assay

Protoplasts are prepared as described in Subheading 3.3, steps 1–7 and plated on cellophane-overlain PRMB at a density of about 5,000 per plate. The cellophanes are transferred to BCDAT plates after 4 days (see Note 14) and cultured on BCDAT for 3 days. Chlorophyll autofluorescence from the resulting colonies is photographed at 63 × using a fluorescence dissecting microscope with blue excitation (488 nm). An ImageJ macro for analyzing area, circularity, and solidity is available from Luis Vidali, Worcester Polytechnic Institute, Worcester, MA, USA (30).

3.7.2. Gametophore Development Assay

Protoplasts are prepared as described in Subheading 3.3, steps 1–7 and plated in PRML on cellophane-overlain PRMB at a density of about 1,000 per plate. The cellophanes are transferred to BCD plates after 2–4 days (see Note 14) and cultured for 10 days at 25°C with constant illumination at 50–80 μmol/m²/s. Gametophore buds appear 6 days after transfer to BCD and develop into leafy gametophores over the next 4 days.

3.7.3. Caulonemal Gravitropism Assay

Petri plates containing BCDAT with 1.2% agar and 350 mM sucrose are prepared. About 7 small clumps of fresh chloronemal tissue are plated along the diameter of each plate. After incubation at 25°C with constant illumination at 50–80 μmol/m²/s, the plates are positioned vertically and incubated in the dark at 25°C for 14 days. Pigmented caulonemal filaments are negatively gravitropic and may exceed 2 cm in length (31).

3.7.4. Rhizoid Development Assay

Chloronemal tissue is plated on BCD medium supplemented with 0.1–1.0 μM naphthylacetic acid and cultured at 25°C with constant illumination at 50–80 μmol/m²/s for 14 days. Gametophores develop numerous rhizoids (5).

4. Notes

1. Some media formulas for *P. patens* use $Ca(NO_3)_2$ as a nitrate source (32). However, calcium phosphate precipitates form during autoclaving and this is prevented by using KNO_3 as a nitrate source and adding $CaCl_2$ solution after autoclaving.
2. The use of unvented Petri plates reduces evaporation and contamination. Alternatively, vented Petri plates can be sealed with Micropore® tape (3 M Corporation, St. Paul, MN, USA).
3. We have also used roll cellophane (Research Products International) cut in 8.5 × 11 in. sheets, interleaved with copy paper, cut into 9 cm circles, and autoclaved in glass Petri

plates. However, growth inhibition has been noted with some lots of this product.

4. Multisite Gateway® is a rapid method for producing knockout vectors. A destination vector (pBHSNRG) was constructed by inserting R1–R4 and R3–R2 Gateway® cassettes into the multiple cloning sites of pBHSNR (gift of D. Schaefer, University of Lausanne, constructed by inserting the *hpt* gene driven by a double 35 S promoter (Sac1-NotI fragment from pCAMBIA) in reverse orientation between the two loxP sites of pBilox) (33). The Gateway® Reading Frame Cassette A (Invitrogen) was modified by PCR (converting R2–R4 or R1–R3) and cloned into pGEM-T Easy (Promega Corp., Madison, WI, USA). The R1–R4 and R3–R2 cassettes were excised from pGEM-T Easy with SphI/SpeI and AvrII/NsiI, respectively, and ligated into the SphI/XbaI and SpeI/NsiI sites, respectively, of pBHSNR. pBHSNRG is available upon request. Vector construction methods using standard restriction digestion and ligation are available in print (29) and online (http://moss.nibb.ac.jp/). Detailed treatments of the effects of various vector parameters on recombination efficiency are also available (34, 35).
5. The *P. patens* genome was sequenced by the U.S. Department of Energy Joint Genome Institute Community Sequencing Program http://www.jgi.doe.gov/. The annotated sequence is hosted at Cosmoss http://www.cosmoss.org/.
6. As an alternative to shaking, protonema can be blended for subculture using a Polytron® type homogenizer (36). We have noted a reduced contamination frequency using the shaking method. When subculturing fresh cultures, vortexing can be substituted for shaking. However, older cultures are often not sufficiently broken up by vortexing.
7. *P. patens* may be grown with continuous light or a long-day photoperiod (typically 18 h). The cell division cycle becomes synchronized to the long-day photoperiod (28).
8. Other methods for long-term storage, including cryopreservation have been reported (28).
9. Chloronemal tissue used to generate protoplasts must be in excellent condition. Dead filaments cause clumping of protoplasts and low transformation efficiency. Tissue should be subcultured every 5–7 days until no dead, brown filaments are visible with a dissecting microscope.
10. This protocol uses more gentle centrifugation (about $25 \times g$) compared to published protocols (28, 29) and the resulting pellet is easier to resuspend. The supernatant from the protoplast washes should be clear. A green tinge results from free chloroplasts, a sign of protoplast lysis.

11. Intact protoplasts are spherical and appear turgid with their chloroplasts pressed against the plasma membrane. Protoplasts with chloroplasts aggregated in the centre will not regenerate and should not be counted. Intact protoplasts should substantially outnumber damaged protoplasts.
12. The rate of protoplast regeneration after 5 days is an indicator of successful transformation. At this stage protoplasts should have divided several times and there should be more than 50,000 per plate. A good transformation yields hundreds of unstable transformants, after the first round of selection, and dozens of stable transformants, after the second round of selection.
13. The following should be considered when interpreting the PCR genotyping results. The percentage of stable transformants in which the vector is integrated by homologous recombination at both the 5′ and 3′ ends typically ranges from 25 to 100%. In some cases, several tandem and/or inverted copies of the vector may be integrated at the target locus. Protoplast fusion can occur during transformation, producing diploid clones carrying both the vector integrated by homologous recombination and the wild type gene. Refer to detailed treatments of integration mechanisms and resulting genotypes (34, 35) for more information.
14. Developing protoplasts can be transferred from PRMB to antibiotic-free BCDAT after 2 days. However, the protoplasts require 4 days to develop antibiotic resistance.
15. The same protocol with modifications is used to label with CBM. CBM is substituted for primary antibody in Subheading 3.6, step 8(b), and an antipolyhistidine incubation and three washes are added before the secondary antibody incubation.

Acknowledgements

We thank the members of the moss community for their collegiality and helpful suggestions. Magdalena Bezanilla and the members of her group provided invaluable advice and assistance. We thank Didier Schaefer for the gift of pBHSNR. This project was supported by the National Research Initiative Competitive Grant no. 2007-35318-18389 from the USDA National Institute of Food and Agriculture.

References

1. Schaefer, D. G. (2002) A new moss genetics: targeted mutagenesis in *Physcomitrella patens*. *Annu Rev Plant Biol* **53,** 477–501.
2. Strepp, R., Scholz, S., Kruse, S., Speth, V., and Reski, R. (1998) Plant nuclear gene knockout reveals a role in plastid division for the homolog of the bacterial cell division protein FtsZ, an ancestral tubulin. *Proc Natl Acad Sci USA* **95,** 4368–4373.
3. Schaefer, D. and Zrÿd, J. -P. (2004) Principles of targeted mutagenesis in the moss *Physcomitrella patens*. In: Wood, A.J., Oliver, M.J., and Cove, D.J., eds. New Frontiers in Bryology: Physiology, Molecular Biology and Functional Genomics. Dordrecht: Kluwer; 37–49.
4. Perroud, P. -F. and Quatrano, R .S. (2006) The role of ARPC4 in tip growth and alignment of the polar axis in filaments of *Physcomitrella patens*. *Cell Motil Cytoskeleton* **63,** 162–171.
5. Sakakibara, K., Nishiyama, T., Sumikawa, N., Kofuji, R., Murata, T. and Hasebe, M. (2003) Involvement of auxin and a homeodomain-leucine zipper I gene in rhizoid development of the moss *Physcomitrella patens*. *Development* **130,** 4835–4846.
6. Cove, D. (2005) The moss *Physcomitrella patens*. *Annu Rev Genet* **39,** 339–58.
7. Richardt, S., Timmerhaus, G., Lang, D., Qudeimat, E., Corrêa, L.G.G., Reski, R., Rensing, S. A., and Frank, W. (2010) Microarray analysis of the moss *Physcomitrella patens* reveals evolutionarily conserved transcriptional regulation of salt stress and abscisic acid signalling. *Plant Mol Biol* **72,** 27–45.
8. Cuming, A. C., Cho, S. H., Kamisugi, Y., Graham, H., and Quatrano, R. S. (2007) Microarray analysis of transcriptional responses to abscisic acid and osmotic, salt, and drought stress in the moss, *Physcomitrella patens*. *New Phytol* **176,** 275–287.
9. Rensing, S. A., Lang, D., Zimmer, A. D., *et al.* (2008) The *Physcomitrella* genome reveals evolutionary insights into the conquest of land by plants. *Science* **319,** 64–69.
10. Bezanilla, M., Perroud, P. -F., Pan, A., Klueh, P., and Quatrano, R. S. (2005) An RNAi system in *Physcomitrella patens* with an internal marker for silencing allows for rapid identification of loss of function phenotypes. *Plant Biol* **7,** 251–257.
11. Khraiwesh, B., Ossowski, S., Weigel, D., Reski, R., and Frank, W. (2008) Specific gene silencing by artificial MicroRNAs in *Physcomitrella patens*: an alternative to targeted gene knockouts. *Plant Physiol* **148,** 684–693.
12. Vidali, L., Augustine, R. C., Fay, S. N., Franco, P., Pattavina, K. A., and Bezanilla M. (2009) Rapid screening for temperature-sensitive alleles in plants. *Plant Physiol* **151,** 506–514.
13. Schumaker, K. S., and Dietrich, M. A. (1998) Hormone-induced signaling during moss development. *Annu Rev Plant Physiol Plant Mol Biol* **49,** 501–523.
14. Lee, K. J. D., Sakata, Y., Mau, S. -L., Pettolino, F., Bacic, A., Quatrano, R. S., Knight, C. D., Knox, J. P. (2005) Arabinogalactan proteins are required for apical cell extension in the moss *Physcomitrella patens*. *Plant Cell* **17,** 3051–3065.
15. Liepman, A. H., Nairn, C. J., Willats, W. G. T., Sørensen, I., Roberts, A. W., and Keegstra, K. (2007) Functional genomic analysis supports conservation of function among *Cellulose synthase like A* gene family members and suggests diverse roles of mannans in plants. *Plant Physiol* **143,** 1881–1893.
16. Fu, H., Yadav, M. P., and Nothnagel, E. A. (2007) *Physcomitrella patens* arabinogalactan proteins contain abundant terminal 3-*O*-methyl-L-rhamnosyl residues not found in angiosperms. *Planta* **226,** 1511–1524.
17. Moller, I., Sørensen, I., Bernal, A. J., Blaukopf, C., Lee, K., Øbro, J., Pettolino, F., Roberts, A., Mikkelsen, J. D., Knox, J. P., Bacic, A., and Willats,W. G. T. (2007) High-throughput mapping of cell-wall polymers within and between plants using novel microarrays. *Plant J* **50,** 1118–1128.
18. Peña, M. J., Darvill, A. G., Eberhard, S., York, W. S., and O'Neill, M. A. (2008) Moss and liverwort xyloglucans contain galacturonic acid and are structurally distinct from the xyloglucans synthesized by hornworts and vascular plants. *Glycobiology* **18,** 891–904.
19. Graham, L. E., Cook, M. E., and Busse, J. S. (2000) The origin of plants: Body plan changes contributing to a major evolutionary radiation. *Proc Natl Acad Sci USA* **97,** 4535–4540.
20. Niklas, K. J. (2004) The cell walls that bind the tree of life. *BioScience* **54,** 831–841.

21. Roberts, A. W., and Bushoven, J. T. (2007) The cellulose synthase (*CESA*) gene superfamily of the moss *Physcomitrella patens. Plant Mol Biol* **63,** 207–219.
22. Schaefer, D. G., and Zrÿd, J. -P. (2001) The moss *Physcomitrella patens*, now and then. *Plant Physiol* **127,** 1430–1438.
23. Lang, D., Zimmer, A. D., Rensing, S. A., and Reski, R. (2008) Exploring plant biodiversity: the *Physcomitrella* genome and beyond. *Trends Plant Sci* **13,** 542–9.
24. Schaefer, D. G. (2001) Gene targeting in *Physcomitrella patens. Curr Opin Plant Biol* **4,** 143–150.
25. Decker, E. L., Frank, W., Sarnighausen, E., and Reski, R. (2006) Moss systems biology en route: phytohormones in *Physcomitrella* development. *Plant Biol* **8,** 397–405.
26. Cove, D., Benzanilla, M., Harries, P., and Quatrano, R. (2006) Mosses as model systems for the study of metabolism and development. *Annu Rev Plant Biol* **57,** 497–520.
27. Frank, W., Decker, E. L., and Reski, R. (2005) Molecular tools to study *Physcomitrella patens. Plant Biol* **7,** 220–227.
28. Cove, D. J., Perroud, P. F., Charron, A. J., McDaniel, S. F., Khandelwal, A., and Quatrano, R. S. (2009) The moss *Physcomitrella patens.* A novel model system for plant development and genomic studies. In: Behringer, R.R., Johnson, A.D., Krumla\uf, R.E., eds. Emerging Model Organisms: A Laboratory Manual: Cold Spring Harbor Laboratory Press 69–104.
29. Knight, C. D., Cove, D. J., Cuming, A. C., and Quatrano, R. S. (2002) Moss gene technology. In: Gilmartin, P.M., C. B, eds. Molecular Plant Biology — A Practical Approach. Oxford, New York: Oxford Press; 285–301.
30. Vidali, L., Augustine, R. C., Kleinman, K. P., and Bezanilla, M. (2007) Profilin is essential for tip growth in the moss *Physcomitrella patens Plant Cell* **19,** 3705–3722.
31. Cove, D. J., and Quatrano, R. S. (2004) The use of mosses for the study of cell polarity. In: Wood, A. J., Oliver, M. J., and Cove, D. J., eds. New Frontiers in Bryology: Physiology, Molecular Biology and Functional Genomics. Dordrecht: Kluwer, 189–203.
32. Ashton, N. W., Grimsley, N. H., and Cove, D. J. (1979) Analysis of gametophytic development in the moss, *Physcomitrella patens*, using auxin and cytokinin resistant mutants *Planta* **144,** 427–435.
33. Thelander, M., Nilsson, A., Olsson, T., Johansson, M., Girod, P. -A., Schaefer D. G., Zrÿd J. -P., and Ronne, H. (2007) The moss genes *PpSKI1* and *PpSKI2* encode nuclear *SnRK1* interacting proteins with homologues in vascular plants. *Plant Mol Biol* **64,** 559–573.
34. Kamisugi, Y., Cuming, A. C., and Cove, D. J. (2005) Parameters determining the efficiency of gene targeting in the moss *Physcomitrella patens. Nucleic Acids Res* **33,** e173.
35. Kamisugi, Y., Schlink, K., Rensing, S. A., Schween, G., von Stackelberg, M., Cuming, A. C., Reski, R., and Cove, D. J. (2006) The mechanism of gene targeting in *Physcomitrella patens*: homologous recombination, concatenation and multiple integration. *Nucleic Acids Res* **34,** 6205–6214.
36. Nishiyama, T., Hiwatashi, Y., Sakakibara, I., Kato, M., and Hasebe, M. (2000) Tagged mutagenesis and gene-trap in the moss, *Physcomitrella patens* by shuttle mutagenesis. *DNA Res* **7,** 9–17.

Chapter 20

Measuring *In Vitro* Extensibility of Growing Plant Cell Walls

Daniel J. Cosgrove

Abstract

This article summarizes the theory and practical aspects of measuring cell wall properties by four different extensometer techniques and how the results of these methods relate to the concept and ideal measurement of cell wall extensibility in the context of cell growth. These *in vitro* techniques are particularly useful for studies of the molecular basis of cell wall extension. Measurements of breaking strength, elastic compliance, and plastic compliance may be informative about changes in cell wall structure, whereas measurements of wall stress relaxation and creep are sensitive to both changes in wall structure and wall-loosening processes, such as those mediated by expansins and some lytic enzymes. A combination of methods is needed to obtain a broader view of cell wall behavior and properties connected with the concept of cell wall extensibility.

Key words: Extensibility, Cell wall, Stress relaxation, Creep, Expansin

1. Introduction

Acting like a firm corset, the cell wall gives plant cells their specific shape and size by restraining the expansive tendency of the protoplast. In growing cells, this mechanical restraint is rather more subtle than a corset, as the cell wall not only resists turgor pressure but at the same time it also stretches slowly and irreversibly and often anisotropically (directionally), a controlled process in which the load-bearing network of wall matrix polymers and cellulose microfibrils yields to the turgor-generated tensile forces in the cell wall. As used here, the term "wall extensibility" refers to this ability to extend irreversibly, but a close reading of the literature reveals this to be a fuzzy concept, with various technical definitions (when defined at all) and a variety of methods for estimating its value. These concepts and methods were critically reviewed in (1). The current article presents an update focused on the utility and concepts underlying various measurements of wall properties

Zoë A. Popper (ed.), *The Plant Cell Wall: Methods and Protocols*, Methods in Molecular Biology, vol. 715,
DOI 10.1007/978-1-61779-008-9_20,

in vitro, specifically by use of extensometers in which a cell wall specimen is clamped and extended in various modes to measure cell wall behavior that one might relate to cell wall extensibility in the context of cell growth. Measurements at the single cell level are also possible, but technically more challenging and difficult to interpret, and are detailed elsewhere (2, 3).

As a hydrated composite of complex polysaccharides, the growing plant cell wall has elastic, viscoelastic, and plastic properties, which have been measured in the past half century by a variety of static and dynamic loading methods. These mechanical techniques, in which a physical force is put on the isolated wall and the resulting deformation is measured, assess something a bit different from what we mean by wall extensibility in the context of cell growth. In biophysical terms, wall extensibility is usually defined as the local slope of the curve relating growth rate to cell turgor pressure (1, 4). This discrepancy between concept and technical measurement stems from the fact that cell wall expansive growth is not a simple matter of inert polymer mechanics; additionally, it depends on dynamic wall-loosening processes that modify the matrix-cellulose network in a time-dependent way, enabling the polymeric network to yield to wall stresses. This results in cell wall creep (slow, time-dependent, irreversible extension), in which the cellulose microfibrils shift or separate from one another. We might call this "*chemorheological extensibility*" (5) to emphasize that the wall's flow (rheological) behavior depends not only on cell wall structure and tensile stress but also on dynamic processes of polymer creep catalyzed by cell wall-loosening agents, such as expansins and lytic enzymes whose activity may be rapidly modulated by changes in wall pH, redox potential, hydration, ion concentrations, the supply of cell wall materials, and other ephemeral conditions within the cell wall space. The biophysical and cellular bases of this process were recently reviewed (4). This turn of phrase, chemorheological extensibility, may more clearly denote the dynamic nature of wall extensibility, but it still leaves us with the problem of how to measure this subtle property. This issue is relevant to a variety of studies where walls become more, or less, extensible during cell development and in response to hormones, light, gravity, dehydration, and a variety of other environmental and biological stresses that influence plant growth. Measuring wall extensibility and understanding the molecular nature of its modulation are key aspects of understanding how plants control their cell growth by modifying their primary cell walls.

In vivo methods for measuring wall extensibility, summarized in (1), have the advantage of fitting nicely into the biophysical theory of plant growth in quantitatively meaningful ways, and they are sensitive to the cell's dynamic modification of the cell wall environment. Methods for measuring wall stress relaxation *in vivo,*

such as the pressure-block method (6) or the pressure-probe method (7, 8), have some advantages over other *in vivo* methods, but they require specialized equipment and moreover they have limited utility for investigating cell wall loosening by exogenous enzymes or for other studies where the molecular nature of wall extension is investigated. For such studies, isolated cell walls – i.e., where the living cells of the tissue have been removed or otherwise made inactive – have particular merit because the results are not compromised by complicated responses of the living cells during the measurement and because a wider variety of treatments and methods may be applied to the isolated cell walls without concern about complex responses (even death!) of the living cells. These *in vitro* methods are particularly well suited to studies of the biochemical underpinnings of cell wall enlargement and are the subject of this article.

One notable caveat with such *in vitro* studies, however, is that a negative result (no measurable change in isolated wall properties) does not necessarily mean that *in vivo* wall extensibility does not change during a particular growth response. For instant, cells may rapidly modulate cell wall pH and thereby affect expansin activity and increase wall extensibility, but such action would not be detected in the methods outlined below. Thus, the results of *in vivo* and *in vitro* methods may disagree, likely pointing to an ephemeral, rather than structural, change in the cell wall.

Several methods for assessing extensibility of isolated cell walls by use of extensometers have been devised, four of which are summarized below. Note that they neglect, by their very nature, the dynamic aspects of cellular modulation of cell wall yielding, but there is still a chemorheological aspect because expansins and other wall modifying enzymes may remain active in the isolated walls (assuming no protein-denaturing treatments).

2. Materials

1. Plant material of interest: stems, hypocotyls, or plant organs of similar geometry. Slices of tissues may also be used. The plant material must be pretreated to disrupt the protoplasts (see Notes 1 and 2).
2. Extensometer: can be commercial or custom-made (see Note 3).
3. Carborundum powder, prewashed.
4. Microscope slides or other suitable glass plates.
5. Weight.
6. Liquid nitrogen or –80°C freezer.

7. Adhesive tape or cyanoacrylate adhesive ("Superglue").
8. Buffer: 20 mM sodium acetate, pH 4.5.

3. Methods

3.1. Preparation of Plant Tissues to Remove Protoplasts

To disrupt the protoplasts and remove the bulk water and cellular fluids within the tissue, a simple procedure is as follows (see Note 4):

1. Freeze the sample in liquid nitrogen or in a –80°C freezer.
2. Thaw at room temperature or 4°C and cut to size suitable for the extensometer clamps.
3. Permeabilize the cuticle, e.g., by abrasion with a slurry of well-washed carborundum powder (see Note 5).
4. Treat the plant tissues to inactivate wall-bound enzyme activity, e.g., by boiling (see Note 6).
5. Press the sample between two glass plates (i.e., microscope slides) for ~5 min under a weight to flatten the tissue and express the cell sap.

3.2. Measuring Cell Wall Mechanics

Four methods are detailed below for measuring (1) breaking strength, (2) elastic and plastic compliances, (3) stress relaxation, and (4) cell wall creep. These techniques measure different aspects of the cell wall mechanics, with the creep method coming perhaps closest to the measurement desired for *in-vitro* wall extensibility. All of the methods are essentially described as follows:

1. Clamp the prepared cell walls in an extensometer.
2. Apply a tensile force to the walls.
3. Either extend the walls at a defined rate or measure their extension.

A visual demonstration of these procedures may be found in (9).

3.2.1. Breaking Strength

The principle here is simple, if not simple minded: measure the force need to break the cell wall. There are various geometrical means for causing breakage or mechanical failure of plant organs, with pulling (axial tension) or buckling (compression or bending) being the most straightforward for engineering analysis. For measurements of axial breaking strength, a suitable sample is clamped in an extensometer that can extend the distance between the clamps while measuring the force needed for the extension. It is important to clamp the sample in such a way that the clamp does not cause tearing of the sample. Sometimes adhesive tape or cyanoacrylate adhesive ("Superglue") is used to help fix the walls to the clamping device (10, 11). As the sample is extended, the

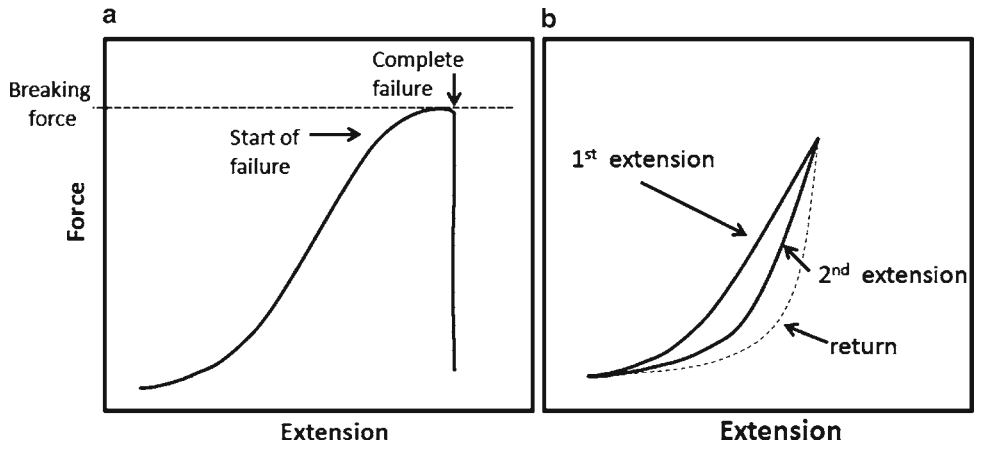

Fig. 1. Schematic diagrams of force-extension curves for cell walls measured in an extensometer for (**a**) tensile strength (breakage force) and (**b**) elastic and plastic moduli. For assessment of tensile strength the wall is extended until it fails, and the maximum force, the total extension, and the area under the curve may be useful metrics of changes in cell wall structure. For assessment of cell wall moduli, the wall is extended, then returned to its original size and extended a second time. The slope of the second extension, near the end of the extension, is taken as the elastic modulus; its reciprocal is the elastic compliance. The slope of the first extension is the total modulus and the total compliance is its reciprocal. The plastic compliance is the difference between the total compliance and the elastic compliance.

force increases and then levels off as the sample begins to fail and then drops quickly as the breakage is completed (Fig. 1). Typically, the maximum force is taken as the breaking strength, but one can also measure the percentage extension before failure and the area under the curve, which is the energy input for breakage (12). The breaking force of plant wall samples is often found to be a function of the extension rate, so this parameter needs to be the same for valid comparisons. Another important detail: be sure that the sample stays wet during the measurement, as wall dehydration greatly increases cell wall strength.

The breaking strength of hypocotyls or inflorescence stems has been used in recent times to characterize *Arabidopsis* mutants with defects in cell wall composition or in wall assembly (11, 13–15), thereby drawing inferences about the structural role of a particular wall polymer (Fig. 1a). What such measurements mean for wall extensibility in the context of growth is more difficult to say, as there is at best only an indirect connection between the two concepts. Organ breakage occurs at the weakest point in the sample, which may be the middle lamella, that is, the adhesive layer of matrix polysaccharides and structural proteins that cements adjacent cell walls together. Changes in organ anatomy could also affect breaking strength. In contrast, wall extensibility depends on rearrangements within the matrix-cellulose network. Thus, while breaking strength may be informative about aspects of cell wall structure or the glue that holds cells together, it is not a

reliable metric of wall extensibility. As a case in point, *Arabidopsis* hypocotyls from a xyloglucan-deficient mutant are weaker than wild type when assessed in mechanical tests of stiffness and breaking strength (14), yet they are stronger (less extensible) in assays of cell wall creep (Y.B. Park and D.J. Cosgrove, unpublished data). Thus, tensile breaking strength may be informative about structural changes in cell walls or tissue architecture, but is in general a poor measure of wall extensibility.

3.2.2. Elastic and Plastic Compliances: Axial Extension

The principle of this method is similar to that described above for breaking strength, except that the sample is not extended to the breaking point, but is extended a small amount in two cycles. In the first cycle, the sample is extended until a predetermined force is reached (well before the breakage point), then returned to the original length before a second extension is made. This second force-extension curve differs from the first one (Fig. 1b), but subsequent extensions cycles are reversible, at least to a first approximation, and so extension #2 is taken as an elastic extension. The difference between the first curve (total extension) and the second curve (elastic extension) gives the plastic, or irreversible, extension. The slope of the lines are estimated near the end of each extension cycle, to give Δforce/Δextension; this ratio is known as a *modulus*. The higher the modulus, the stiffer the material.

The modulus depends on many characteristics of the cell wall, but we do not have a comprehensive theory of this yet. Among the most important wall characteristics are the number and bundling of cellulose microfibrils in wall cross sectional area; the orientation of the microfibrils relative to the direction of extension; and the density, hydration, and cross linking of the matrix and its connection to the cellulose microfibrils. A recent theoretical study has attempted to explore the elastic modulus of cell walls by use of finite element analysis to calculate the elastic behavior of a virtual cellulose-hemicellulose network constructed to mimic aspects of real cell walls (16), while a very different type of model, based on the thermodynamics of hydrogen-bonded networks, was used to predict the plastic behavior of similar idealized cell walls (17). These and other theoretical models make significant steps toward gaining molecular-scale insights into cell wall mechanics, but they are still very simplified and limited compared to real cell walls.

The raw units for this modulus might be N/mm or g-force/mm. If the Δforce is divided by the cross-sectional area of the sample and the Δextension is calculated as fractional change in length, then the units can be readily converted to standard units of MPa (that is, stress divided by strain, or force per unit area divided by the fractional increase in length). Estimates of cross-sectional area, however, can be problematic (i.e., you cannot count cell lumens; the sample gets thinner as it extends, etc.),

introducing errors into the absolute values of the moduli. Hence, such values reported in the literature should be examined with a critical eye. As long as the cross sections are similar for all samples, then a comparison of values is valid for reaching conclusions about relative changes among groups. On the other hand, if different groups have different cross-sectional areas, then the interpretation of the values can be more challenging, as differences in organ anatomy can influence the results. Similarly, if wall thicknesses differ among comparison groups, then the interpretation of the values needs careful analysis. For instance, at equal force a thinner sample will have a larger stress than a thicker sample. The mechanical properties of cell walls are strongly nonlinear, so comparisons should be made at similar values of wall stress. This may mean one needs to apply a larger tensile force to a thicker tissue sample in order to equalize stress in the two measurements.

Because wall cross-sectional area in a sample is difficult to measure, a practical substitute is to use the cell wall mass per unit length of the sample. For many samples, this value can be estimated by cutting a sample to 1 cm length, freezing and thawing to disrupt the cells, then washing and pressing the sample to remove cell contents. What remains is mostly cell walls, which can be weighed after drying.

The reciprocal of the force/extension value is known as a *compliance*, which corresponds to a type of extensibility, with units of strain/stress (or Δextension/Δforce for practical measurements). The elastic or plastic compliances that one measures with this technique are sometimes called extensibilities, but keep in mind that these are purely mechanical extensibilities that depend primarily on cell wall structure and thickness and do not include the chemorheological aspects of cell wall extensibility. As an example, α-expansin does not affect elastic or plastic compliances of cucumber hypocotyl cell walls (18). These compliances are good reporters for changes in cell wall structure. For instance, treatment of cucumber cell walls with a family-12 endoglucanase caused large increases in both the elastic and plastic compliances of the cell walls (18).

3.2.3. Elastic and Plastic Compliances: Microindentation

A microscopic variant of the stress-strain method has been used for evaluating the mechanical properties of cell walls in single cells or parts of cells, such as at different parts of the apical dome of pollen tubes (19). The method does not separate out elastic and plastic components, as above, and the stiffness values obtained are useful for relative comparisons, but not for obtaining absolute values of wall modulus or compliance. The principle of the method is simple: a small probe is used to deform a local region of the cell wall and to measure the force on the wall. The resistance to such deformation is a complex function of cell wall stiffness, cell geometry, and turgor pressure (20). Wall stiffness depends on the

thickness of the wall and its modulus, which in turn depends on the arrangement of its structural elements (cellulose microfibril density, orientation, and interconnection by matrix polymers). The major advantage of the method is that it may be used at the single cell level and even to probe different parts of the cell (19), but this comes at the cost of some uncertainty about the physical interpretation of the measured values.

3.2.4. Stress Relaxation

A crucial biophysical difference between growing and nongrowing cell walls is that the former undergoes continuous stress relaxation (the physical face of cell wall loosening), which lowers cell turgor pressure and creates the water potential gradient necessary for sustained water uptake by the growing cell. Water uptake physically enlarges the cell and counter balances wall stress relaxation so that turgor pressure stabilizes. This theory of wall relaxation was first enunciated qualitatively by Ray *et al.* (21), elaborated in specific quantitative terms by Cosgrove (22), and demonstrated experimentally in a series of studies in which water uptake into the growing cells was prevented, thereby allowing stress relaxation to proceed unabated by water uptake, resulting in a decay in turgor pressure to the yield threshold (7, 8, 22).

These techniques for measuring *in vivo* wall stress relaxation have a counterpart for isolated cell walls (23–25), in which the isolated wall is clamped in an extensometer as above, rapidly extended until a predetermined force is attained, and then held to constant dimension while the holding force is monitored. The practical time scale for these measurements is from about 50 ms to 500 s. Longer times are possible if cell wall dehydration can be prevented. Shorter times are limited by the mechanics of the extensometer: it takes ~50 ms to extend the wall sample and to allow time for the induced vibrations (mechanical "ringing") in the sample to dampen out.

During the extension process, the cellulose-matrix network is elastically stretched; some of the wall polymers subsequently relax to lower energy states, resulting in wall stress relaxation. As a result, the holding force decays with time. The resulting decay in force, or stress relaxation, may be converted into a form known as a stress relaxation spectrum; a mathematically simpler operation, which approximates the relaxation spectrum, is to convert relaxation to log time scale and to plot the rate as a function of log time (Fig. 2), i.e., $-\Delta\text{force}/\Delta\log\text{ time}$ vs. log time (26). Much of this relaxation is the result of the viscoelastic nature of the cell wall material, that is, a passive physical response that depends on cell wall structure. This is the case for both growing and nongrowing walls, although the difference in wall structure in the two cases may result in different stress relaxation behavior.

Additionally, any wall-loosening processes that are still active in isolated cell walls may result in additional stress relaxation not

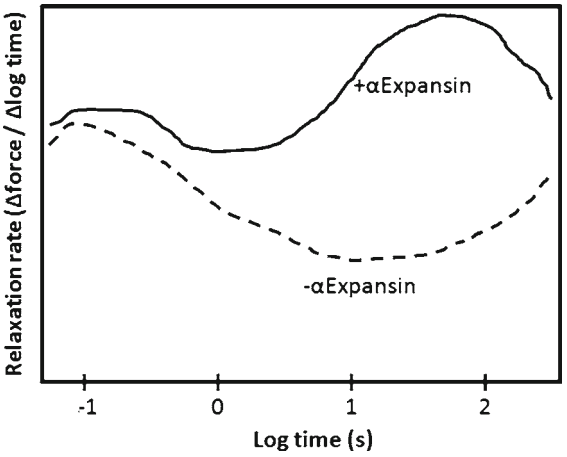

Fig. 2. Diagram illustrating stress relaxation spectra of heat-inactivated cucumber hypocotyl cell walls treated with buffer alone (–αExpansin) or with buffer containing α-expansins (+αExpansin) (18, 29).

found in the nongrowing cell wall. Expansin-induced stress relaxation is readily demonstrated in these assays (27); in acidic buffer, the cell walls exhibit faster stress relaxation than in neutral buffer. This difference is eliminated by brief heat treatment, showing that the difference is not simply due to a pH-dependence of pectin rigidity in the cell wall. It is restored by addition of expansins, showing them to be the major mediators of wall stress relaxation in such isolated cell walls. On the other hand, the family-12 endoglucanase that increased elastic and plastic compliances (mentioned above) had no effect on the stress relaxation spectrum at times >1 s; its action on wall plasticity could be seen as increased stress relaxation at times <0.2 s (18). Thus, stress relaxation assays are sensitive to changes in cell wall structure, expansin activity, and potentially lytic enzymes that promote cell wall extension.

3.2.5. Creep

The fourth extensometer method measures cell wall creep, which is the time-dependent, irreversible extension of wall samples held at constant force. Because wall creep is a slow process, the measurement period is typically in the range of 30–150 min and the wall samples are clamped in a buffer-filled cuvette to prevent dehydration. Wall samples are typically clamped at a constant force in a neutral buffer, and after 10–15 min the buffer is switched to an acid one, initiating rapid extension which gradually slows over 30–60 min to a constant or near constant rate (Fig. 3). A variant of this method is to clamp the walls in acidic buffer at low force which is insufficient to cause creep, then raise the force to a value high enough to cause wall creep.

Of the four *in vitro* methods described in this article, the creep method mimics the *in-vivo* wall extension process to the closest degree, and it readily distinguishes between growing and

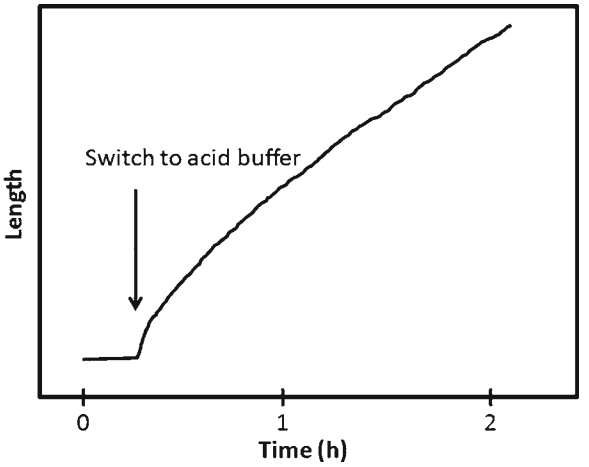

Fig. 3. Diagram illustrating the creep behavior of cucumber cell walls when clamped in a constant force extensometer at neutral pH and then switched to acidic buffer (26).

nongrowing cell walls for many plant tissues. The difference between growing and nongrowing walls, when measured with the creep method, is much larger than the other three extensometer techniques described above. Moreover, creep assays are more sensitive to the activity of both expansins and family-12 endoglucanases, making the creep assay more encompassing for detecting wall-loosening activities with different mechanisms of action and temporal signature.

There are two critical parameters for cell wall creep measurements. First, one must establish a suitable force, which should be large enough to cause cell wall creep, but not so large that breakage becomes a problem. This is a matter of trial and error. In our hands, single *Arabidopsis* hypocotyls (~0.1 mm diameter) give good creep curves with 0.5 g-force; cucumber hypocotyls (~2 mm diameter) creep well with 20 g-force. These axial forces are smaller than the calculated axial forces that are generated internally by cell turgor pressure in the living tissues.

The second parameter is the buffer: its pH, ionic strength, and chemical nature influence cell wall creep. Sodium acetate, at 20 mM and pH 4.5, works well for most tissues in our hands. At this pH endogenous expansins are active whereas pectin-methyl esterase, whose activity inhibits cell wall creep, is inactive. If enzymatic activities in the cell walls have not been inactivated (for instance with a brief heat treatment), then the activity of esterases and other enzymes attached to the cell wall may cause changes in the cell wall itself and also lead to pH drift. Buffer exchanges or higher buffer concentrations are potential solutions to this drift, but high buffer concentrations reduce the creep rate. We have tried a number of different buffers at the same pH and concentration and we found >2× differences in creep rates, evidently due to the anion effects on cell wall creep. Some buffer

anions, such as citrate, act as divalent chelators that can remove pectin-bound calcium from the cell wall and thereby affect wall physical properties.

Takahashi *et al.* (28) constructed a "programmable creep meter" in which the axial force starts at low values and gradually increases. In this way they were able to characterize creep rate as a function of applied force and to make estimates of the yield threshold for wall creep.

3.3. Conclusions

For reasons discussed in the text, it is unlikely that cell wall extensibility can be fully measured by *in-vitro* methods, as wall extensibility is based not only on wall mechanics but also depends on wall-loosening processes that are sensitive to ephemeral conditions in the cell wall space. Nevertheless, the methods outlined here can provide positive evidence for changes in wall structure (indicated by elastic and plastic compliances) and changes in wall-bound wall-loosening activities such as expansins and lytic enzymes. These methods are particularly useful for investigations of the molecular basis of cell wall extension and its dependence on cell wall structure.

4. Notes

1. For these methods to be interpreted in terms of cell wall properties, it is important that the protoplast be disrupted so that turgor pressure and mechanically driven water flows within the tissue do not complicate the measurement. Turgor pressure generates wall tension, making the cell wall stiffer, much as a pressurized tyre is stiffer than a flaccid one. As a result, the tensile properties of living tissues depend on both turgor pressure and cell wall structure. If protoplasts are intact, deformations can be partially limited by water flows from the protoplast, making for a more complicated interpretation of the results. For these reasons, these assays are simpler to interpret when the cell protoplasts are disrupted. On the other hand, there may be circumstances where these complications are not deemed important, for example see Abasolo *et al.* (10).
2. Sample variability typically requires 8–15 replicates to obtain adequate confidence limits of the measurements. The source of this variability is unknown but likely arises from differences in the plant materials. Therefore, care in growing, harvesting, selecting, and preparing the plant materials are important for limiting variability.
3. Trace levels of metal ions such as copper, iron, and aluminum are potent inhibitors of cell wall creep and stress relaxation. Therefore, metal clamps and other metallic parts of the

extensometer should be coated with epoxy, plastic, latex, or other material to avoid interactions with the cell walls. This is most important in methods entailing long measurement periods, e.g., the creep method and the stress relaxation method.

4. In some studies, researchers have boiled the cell walls in methanol, then rehydrated in buffer prior to measurement. This procedure disrupts the protoplast and inactivates most enzymes bound to the cell wall sample. However, the procedure does not inactivate expansins (26, 29) and also precipitates polysaccharides, potentially causing irreversible changes in wall mechanics. In most cases, this type of pretreatment is best avoided.
5. This step (cuticle abrasion) is only needed when buffers or other materials must be diffused into the wall samples or when the walls must be thoroughly washed. It is commonly omitted when measuring breaking strength and elastic and plastic compliances.
6. If wall-bound enzymes are not inactivated by heat or other treatment, care must be taken to limit enzymatic wall modification, most importantly pectin demethylation and polysaccharide hydrolysis, as such processes may modify the wall behaviors measured in these assays.

Acknowledgements

This material is based upon work supported as part of The Center for Lignocellulose Structure and Formation, an Energy Frontier Research Center funded by the U.S. Department of Energy, Office of Science, Office of Basic Energy Sciences under Award Number DE-SC0001090. The research on cell wall creep was supported by Award number DE-FG02-84ER13179 from the Department of Energy Office of Basic Energy Sciences.

References

1. Cosgrove, D. J. (1993) Wall extensibility: its nature, measurement, and relationship to plant cell growth. *New Phytol* **124,** 1–23.
2. Geitmann, A. (2006) Experimental approaches used to quantify physical parameters at cellular and subcellular levels. *Am J Bot* **93,** 1380–1390.
3. Burgert, I. (2006) Exploring the micromechanical design of plant cell walls. *Am J Bot* **93,** 1391–1401.
4. Geitmann, A., and Ortega, J. K. E. (2009) Mechanics and modeling of plant cell growth. *Trends Plant Sci* **14,** 467–478.
5. Ray, P. M. (1987) Principles of Plant Cell Growth. In Physiology of Cell Expansion during Plant Growth (Symposium in Plant Physiology, Penn State Univ), Cosgrove DJ, Knievel DJ, eds. (American Society of Plant Physiologists: Rockville), pp. 1–17.
6. Cosgrove, D. J. (1995) Measurements of wall stress relaxation in growing plant cells. *Methods Cell Biol* **49,** 229–241.
7. Cosgrove, D. J., Van Volkenburgh, E., and Cleland, R. E. (1984) Stress relaxation of cell walls and the yield threshold for growth: demonstration and measurement by micro-pressure

probe and psychrometer techniques. *Planta* **162,** 46–52.

8. Cosgrove, D. J. (1987) Wall relaxation in growing stems: comparison of four species and assessment of measurement techniques. *Planta* **171,** 266–278.
9. Durachko, D. M., and Cosgrove, D. J. (2009) Measuring plant cell wall extension (creep) induced by acidic pH and by alpha-expansin. *J Vis Exp* (25), 1263.
10. Abasolo, W., Eder, M., Yamauchi, K., Obel, N., Reinecke, A., Neumetzler, L., Dunlop, J. W. C., Mouille, G., Pauly, M., Höfte, H. et al. (2009) Pectin may hinder the unfolding of xyloglucan chains during cell deformation: Implications of the mechanical performance of Arabidopsis hypocotyls with pectin alterations. *Mol Plant* **2,** 990–999.
11. Reiter, W. D., Chapple, C. C., and Somerville, C. R. (1993) Altered growth and cell walls in a fucose-deficient mutant of *Arabidopsis*. *Science* **261,** 1032–1035.
12. Wainwright, S. A., Biggs, W. D., Currey, J. D., and Gosline, J. M. (1976). Mechanical Design in Organisms. (Edward Arnold: London), p. 423.
13. Ryden, P., Sugimoto-Shirasu, K., Smith, A. C., Findlay, K., Reiter, W. D., and McCann, M. C. (2003) Tensile properties of *Arabidopsis* cell walls depend on both a xyloglucan cross-linked microfibrillar network and rhamnogalacturonan II-borate complexes. *Plant Physiol* **132,** 1033–1040.
14. Cavalier, D. M., Lerouxel, O., Neumetzler, L., Yamauchi, K., Reinecke, A., Freshour, G., Zabotina, O. A., Hahn, M. G., Burgert, I., Pauly, M. et al. (2008) Disrupting two *Arabidopsis thaliana* xylosyltransferase genes results in plants deficient in xyloglucan, a major primary cell wall component. *Plant Cell* **20,** 1519–1537.
15. Zhong, R., Peña, M. J., Zhou, G. K., Nairn, C. J., Wood-Jones, A., Richardson, E. A., Morrison, W. H., III, Darvill, A. G., York, W. S., and Ye, Z. -H. (2005) *Arabidopsis* fragile fiber8, which encodes a putative glucuronyltransferase, is essential for normal secondary wall synthesis. *Plant Cell* **17,** 3390–3408.
16. Kha, H., Tuble, S. C., Kalyanasundaram, S., and Williamson, R. E. (2010) WallGen, software to construct layered cellulose-hemicellulose networks and predict their small deformation mechanics. *Plant Physiol* **152,** 774–786.
17. Veytsman, B. A., and Cosgrove, D. J. (1998) A model of cell wall expansion based on thermodynamics of polymer networks. *Biophys J* **75,** 2240–2250.
18. Yuan, S., Wu, Y., and Cosgrove, D. J. (2001) A fungal endoglucanase with plant cell wall extension activity. *Plant Physiol* **127,** 324–333.
19. Zerzour, R., Kroeger, J., and Geitmann, A. (2009) Polar growth in pollen tubes is associated with spatially confined dynamic changes in cell mechanical properties. *Dev Biol* **334,** 437–446.
20. Bolduc, J. F., Lewis, L. J., Aubin, C. E., and Geitmann, A. (2006) Finite-element analysis of geometrical factors in micro-indentation of pollen tubes. *Biomech Modeling Mechanobiol* **5,** 227–236.
21. Ray, P. M., Green, P. B., and Cleland, R. E. (1972) Role of turgor in plant cell growth. *Nature* **239,** 163–164.
22. Cosgrove, D. J. (1985) Cell wall yield properties of growing tissues. Evaluation by *in vivo* stress relaxation. *Plant Physiol* **78,** 347–356.
23. Yamamoto, R., Shinozaki, K., and Masuda, Y. (1970) Stress-relaxation properties of plant cell walls with special reference to auxin action. *Plant Cell Physiol* **11,** 947–956.
24. Yamamoto, R., Kawamura, H., and Masuda, Y. (1974) Stress relaxation properties of the cell wall of growing intact plants. *Plant Cell Physiol* **15,** 1073–1082.
25. Fujihara, S., Yamamoto, R., and Masuda, Y. (1978) Viscolelastic properties of plant cell walls II. Effect of pre-extension rate of stress relaxation. *Biorheology* **15,** 77–85.
26. Cosgrove, D. J. (1989) Characterization of long-term extension of isolated cell walls from growing cucumber hypocotyls. *Planta* **177,** 121–130.
27. McQueen-Mason, S. J., and Cosgrove, D. J. (1995) Expansin mode of action on cell walls. Analysis of wall hydrolysis, stress relaxation, and binding. *Plant Physiol* **107,** 87–100.
28. Takahashi, K., Hirata, S., Kido, N., and Katou, K. (2006) Wall-yielding properties of cell walls from elongating cucumber hypocotyls in relation to the action of expansin. *Plant Cell Physiol* **47,** 1520–1529.
29. McQueen-Mason, S., Durachko, D. M., and Cosgrove, D. J. (1992) Two endogenous proteins that induce cell wall expansion in plants. *Plant Cell* **4,** 1425–1433.

INDEX

Zoë A. Popper (ed.), *The Plant Cell Wall: Methods and Protocols*, Methods in Molecular Biology, vol. 715,
DOI 10.1007/978-1-61779-008-9, © Springer Science+Business Media, LLC 2011

D

E

N

O

P

Q

R

S

T

U

V

W

X

Y

Z